DOI: 10.31577/ahs-2020-0021.01.0001

ACTA HYDROLOGICA SLOVACA

Volume 21, No. 1, 2020, 3 – 8

CLM CLIMATE SCENARIO AND ITS IMPACT ON SEASONALITY CHANGES IN SHORT-TERM RAINFALL INTENSITIES IN MOUNTAINOUS REGIONS OF SLOVAKIA

Gabriel Földes*, Marija Mihaela Labat, Silvia Kohnová

The study is focusing on detecting changes in short-term rainfall at 4 selected climatological stations in the mountainous area in the northern part of Slovakia. The aim of the paper was to detect trends and seasonal changes in the future horizons using the outputs of the Community Land Model (CLM) scenario, which is a moderately pessimistic scenario that compares well to current processes in the atmosphere. The scenario was used to compare historical (1960–2000) and simulated future 2070–2100 periods. Finally, the results obtained for the stations from the high mountainous areas, were compared with the results from the southern parts of Slovakia. The results provide an overview of the predicted changes in the seasonality and trends of the short-term rainfall intensities in areas with mountainous climate in Slovakia.

KEY WORDS: short-term rainfall, seasonality, trends, CLM scenario, Slovakia

Introduction

Future changes in extreme precipitation may affect society more directly than variations in most other meteorological observable phenomena, but precipitation is difficult to characterize due to fluctuations in almost all temporal and spatial scales. Evidence for climate change and global warming can be seen as rising global air temperatures, ocean warming, glacier shrinkage, shrinking snow, sea level rise, ocean acidification and, last but not least, an increased number of extreme events (NASA, 2019).

In addition, the intensity of extreme precipitation increases significantly faster at a higher temperature than the rate of increasing the water retention capacity in the atmosphere, called Clausius-Clapeyron. The Clausius-Clapeyron relationship describes the rate of change in saturated vapor pressure, at approximately 7% increase to the degree of warming at typical surface temperatures, and thus sets the rate of increase in extreme precipitation (Trenberth et al., 2003). Climate models are largely used to assess past and forecast for the future, but given their unproven reliability at smaller scales (Tebaldi et al., 2006; Koutsoyiannis et al., 2008), we need more knowledge of the local effects of climate change in order to use long-term observation records to identify potential signals of precipitation changes (Vallebona et al., 2015). For the analysis mainly outputs from regional climate models are used, which are then compared with real observations. For example, the regional climate scenario RCP 8.5 analyzed the territory of northern Italy to northern Germany. Occurrences of intensive short-term daily and hourly rain show higher intensities and frequency (Ban et al., 2015).

Recent research shows that the increase is likely to occur in intensities of short-term rainfalls with durations less than one day, which may lead to more extreme rainfalls and flashfloods. Analysis of the evidence leading to an increase in extreme short-term rainfalls due to anthropogenic climate change, as well as a description of the current physical understanding of the association between extreme short-term rainfall intensity and atmospheric temperature, is needed to allow society to adapt to expected future changes in short-term rainfall intensity (Westra et al., 2014).

The Community Land Model (CLM) (CLM Community 2020) was created as a collaborative project between scientists from the Terrestrial Sciences Section (TSS) and the Climate and Global Dynamics Division (CGD) at the National Center for Atmospheric Research (NCAR) and the Community Earth System Model (CESM), the Land Model, and the Biogeochemistry Working Groups in the USA (Boulder, Colorado). The model formalizes and assesses ecological climatology concepts. Ecological climatology has a multidisciplinary structure. It is used to understand the impacts of changes in vegetation on the climate that are caused by humans and nature. It these studies physical, chemical, and biological processes by which terrestrial ecosystems influence and

are influenced by the climate on various spatial and temporal scales. The main theme is that terrestrial ecosystems are important determinants of the climate through their energy, water, chemical elements, and trace gases. The main parts of the CLM model are surface heterogeneity, bio-geophysics, the hydrological cycle, biogeochemistry, ecosystem dynamics, and the human dimension. The CLM addresses several aspects that allow for the study of two-way interactions between human activities in the countryside and the climate, changes in land cover/land use, agricultural practices, and urbanization (NCAR/UCAR, 2016; UCAR, 2019; Böhm et al., 2006).
This study is focused on an assessment of the predicted changes in seasonality and trends in the short-term rainfall intensities. The predicted changes are represented by data from the CLM scenario. The analysis of mountainous region is represented by four selected climatological station namely: Bardejov, Červený Kláštor, Javorina and Tatranská Lomnica. The periods analyzed for the future changes in short-term rainfall intensities are historical 1960–2000 and the simulated future 2070–2100.

Methods

Detection of changes in short-term rainfall characteristics was performed by using several methods. For the analysis of the seasonality changes the Burn´s vector method was used. For the detection of trend changes the Mann-Kendall trend test was used.

Burn´s Seasonality Analysis

Burn's vector method (Burn 1997) is used for the estimation of the seasonality of the occurrence of extreme seasonal phenomena. The variability of the date when the maximum rainfall occurs is described by this method, so that the direction of the vector corresponds to the expected day of the occurrence during the year, and its length describes the variability around the expected date of the occurrence.The date of occurrence D_i of the extreme event in the angular value θ_i is given by:

$$\theta_i = D_i \frac{2\pi}{365} \qquad (1)$$

The abscissa x and ordinate y of Burn's vector are calculated as:

$$x = \frac{1}{n}\sum_{i=1}^{n} \cos(\theta_i) \qquad (2)$$

$$y = \frac{1}{n}\sum_{i=1}^{n} \sin(\theta_i) \qquad (3)$$

The orientation of Burn's vector θ is calculated as:

$$\theta = \tan^{-1}\left(\frac{x}{y}\right) \qquad (4)$$

The seasonal concentration index r can be calculated as:

$$r = \sqrt{x^2 + y^2} \qquad (5)$$

The orientation of the vector can have a value from 0, which corresponds with the 1st of January to 2π, which corresponds with the 31st of December. The seasonal concentration index can have a value between 0 (the occurrences are uniformly distributed throughout the year) and 1 (the occurrence happens every year on the same date). The results are interpreted in Burn´s diagrams.

Mann-Kendall Trend Test

The Mann-Kendall (Mann, 1945; Kendall, 1975) Trend Test is used for the determination and assessing of the properties and significance of the trend of a selected quantity over time. The test is based on the correlation between the order of rows and their time order. The significance of a downward or upward trend is dependent on a steadily decreasing or increasing variable over time. The trend does not have to be linear. (Mann, 1945; Kendall 1975) The test for time series X={x1, x2, ..., xn} is given by:

$$S = \sum_{i<j} a_{ij} \qquad (6)$$

where
S – the testing statistic:

$$a_{ij} = sign\,(x_j - x_i) = sign\,(R_j - R_i) = \begin{cases} 1 & x_i < x_j \\ 0 & x_i = x_j \\ -1 & x_i > x_j \end{cases} \qquad (7)$$

where
$R_{j,i}$ – series of observations,
$x_{j,i}$ – time series.

The test depends on the order of the values as the actual value of the elements. The statistical test depends only on the order of the observation and not on their own values. This property is the result of statistics that do not depend on distribution. Variation of test statistics S is given by (Kendall, 1975):

$$Var(S) = \frac{1}{18}\left[n(n-1)(2n+5) - \sum_{j=1}^{m} t_j\,(t_j - 1)(2t_j + 5)\right] \qquad (8)$$

where
n – number of observations,
m – number of groups in the corresponding order and
t_j – appropriate observation.

The significance of the trend is determined using the standardized variable u at the required significance level α given by (Kendall, 1975):

$$u = \begin{cases} \frac{S-1}{\sqrt{Var(S)}} & S > 0 \\ 0 & S = 0 \\ \frac{S-1}{\sqrt{Var(S)}} & S > 0 \end{cases} \qquad (9)$$

Data analysis

The analysis of the future changes in short-term rainfall intensities was performed by the CLM scenario data. The data were provided by Martin Gera from Comenius University in Bratislava, Department of Astronomy, Physics of the Earth, and Meteorology (Lapin et al., 2012). The scenario used contains data of two time periods of a historical period (1960–2000) and for a future period (2070–2100). The analysis was made for the rainfall durations from 60 minutes up to 1440 minutes. The CLM scenario, which was selected relates well to the current processes in the atmosphere, it is a semi-pessimistic scenario with a predicted increase in the global temperature of about 2.9°C by the year 2100.

For the analysis four climatological station were selected: Bardejov, Červený Kláštor, Javorina and Tatranská Lomnica. The area is located in the north region of Slovakia and it belongs to a slightly warm climatic area with a mountain climate and low temperature inversions. The locations of the climatological stations are presented in Fig. 1.

Results and discussion

The first step in the study was to identify and analyze future changes in the seasonality in the short-term rainfall. The results were presented using the Burn´s diagram (Fig. 2–4). We can see that the rainfall maxima occurred in the month of July for all stations and each analyzed duration. The lowest differences between historical and future period were detected in the 240 and 1440 minutes rainfall durations. In all climatological stations the shift between the past and future period was less than 5 days to later period, except the Červený Kláštor climatological station, where the shift in the 240 duration was more than 20 days to later period. The highest shifts between the past and future periods were detected in the 120 and 180 minutes rainfall durations where the shifts were 10 days to later period. In the comparison of the analyzed stations the Bardejov climatological station has the lowest shift between past and future periods, where the shift is app. 5 days. The highest shifts in the occurrence of maximal rainfall events is in the Červený Kláštor climatological station where the shifts between the past and the future periods were between 2–3 weeks to late July. The results of the seasonality changes in the occurrence of rainfall maxima events are presented in the Figs 2–4.

The next step was to analyze the changes in trends of the rainfall intensities. For the past period the analysis of the rainfall intensities shows that there is a prevailing decreasing trend in all durations at all climatological station. Significant trends were detected in Bardejov and Červený Kláštor climatological stations in 180 and 1440 minutes rainfall durations at the 90% of significance level. The analysis show that there is an absence of significant trend changes for the future period at the 90% of significance level using Mann-Kendall methodology. For the future period the increasing trends were detected for all climatological stations and in all analyzed durations.

To analyze the differences between southern and northern parts of Slovakia, the results from climatological stations located in the southern part of Slovakia (Földes, 2018) were used. The seasonal extreme events in the southern region Slovakia show the occurrence in the late July or early August. The climatological stations in the southern part of Slovakia show the opposite trend in seasonality shift as at the northern region climatological stations. The shift in the northern region is from earlier period to later. In the southern part the shift is opposite from later time period in the month to the earlier period.

This is the significant difference between the climatological stations on the south and the north. In the properties of trends in the short-term rainfall intensities, there are not significant differences between the two regions, and it is different for each analyzed station. But the main result in all analyzed station is that there is a prevailing increasing trend not significant at 90% significance level in the short-term rainfall intensities.

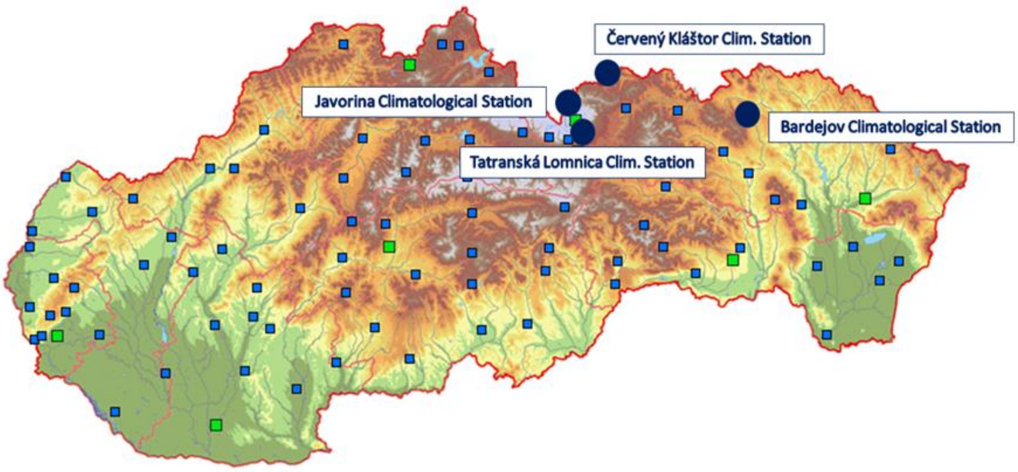

Fig. 1. Locations of the analyzed climatological stations in the Slovak Climatological Network.

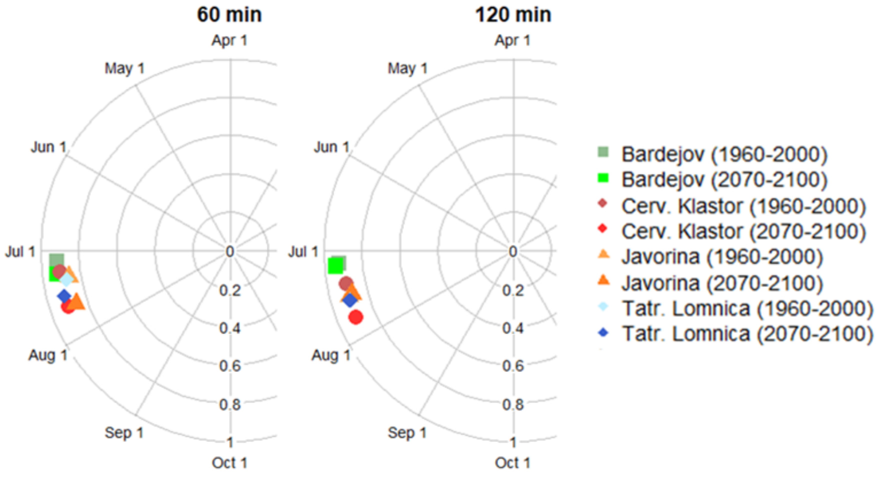

Fig. 2. Seasonality changes for the 60–120 min. rainfall durations.

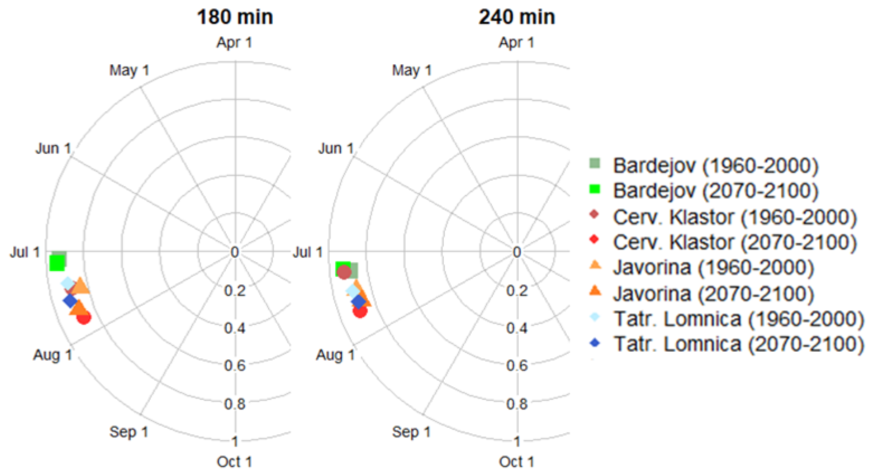

Fig. 3. Burn's diagram for 180–240 min. rainfall duration.

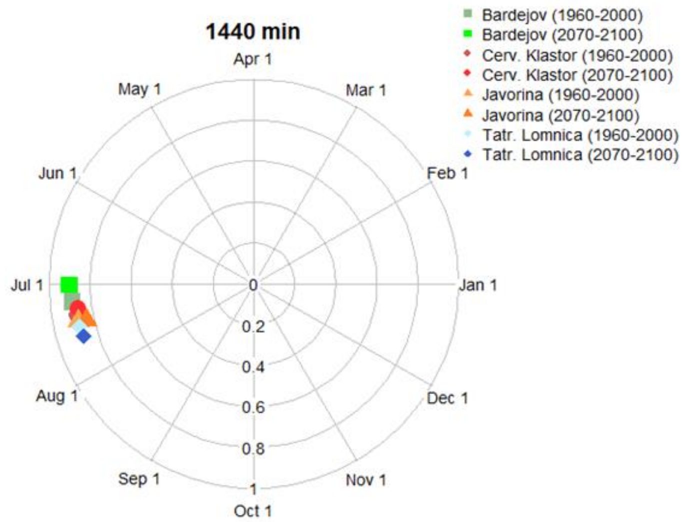

Fig. 4. Burn's diagram for 1440 min. rainfall duration.

Table 1. Trend analysis in the selected climatological stations

Station/Duration	60 min		120 min		180 min		240 min		1440 min	
	hist (1960-2000)	fut (2070-2100)	hist (1960-2000)	fut (2070-2100)	hist (1960-2000)	fut (2070-2100)	hist (1960-2000)	fut (2070-2100)	hist (1960-2000)	fut (2070-2100)
Bardejov	-	+	-	+	-	+	-	+	-	+
Červený Kláštor	-	+	-	+	-	+	-	+	-	+
Javorina	-	+	-	+	-	+	-	+	-	+
Tatranská Lomnica	-	+	-	+	-	+	-	+	-	+

orange – increasing trend, blue – decreasing trend, dark blue – significant decreasing trend (90% significance level)

Conclusion

This study presents results of the analysis of the predicted changes in seasonality and trends in the short-term rainfall intensities due to climate change represented by CLM scenario. The analyzed mountainous region is represented by four selected climatological station namely: Bardejov, Červený Kláštor, Javorina and Tatranská Lomnica.

The analysis was performed by using Burn´s vector method for the seasonality analysis and Mann-Kenndal trend test for the detection of trend changes. An analysis was performed for the historical (1960–2000) and future (2070–2100) time periods and for rainfall durations of 60, 120, 180, 240 and 1440 minutes of short-term rainfall. Results show that extreme rainfall events occurred in the month of July. The main findings can be summarized as follows:

– The seasonality of maximal rainfall intensities will be shifted by 5–10 days to later time period in the month of July.
– The lowest shifts are in 240–1440 minutes rainfall durations.
– The highest shifts are in the 120–180 minutes rainfall durations.
– The highest differences between past and future periods are in Červený Kláštor and Javorina climatological stations.
– There is an increasing trend tendency in short-term rainfall intensities. Trend is not significant at a 90% significance level.

These results confirm that short-term rainfall intensities will change in the future and water management measures in the area need to be re-evaluated.

Acknowledgement

This publication is the result of the project implementation: „ Scientific support of climate change adaptation in agriculture and mitigation of soil degradation" (ITMS2014+ 313011W580) supported by the Integrated Infrastructure Operational Programme funded by the ERDF. This work was supported by the Slovak Research and Development Agency under Contracts No. APVV-18-0347, APVV-15-0497 and the VEGA Grant Agency No. VEGA: 1/0632/19. Authors thanks the Agencies for their support.

References

Ban, N., Schmidli, J., Schär, CH. (2015): Heavy precipitation in a changing climate: Does short-term summer precipitation increase faster? *Geophysical Research Letters*, roč. 42, č. 4, 1165–1172, ISSN 00948276, doi:10.1002/2014GL062588.

Böhm, U., Kücken, M., Ahrens, W., Block, A., Hauffe, D., Keuler, K., Rockel, B., Will, A. (2006): CLM – the climate version of LM: brief description and long-term applications. *COSMO Newsl*, roč. 6, 225–235.

Burn, D. H. (1997): Catchments Similarity for Regional Flood Frequency Analysis Using Seasonality Measures FloodNet View project Catchment similarity for regional flood frequency analysis using seasonality measures. *Article in Journal of Hydrol.*, doi:10.1016/S0022-1694(97)00068-1.

Földes, G., Kohnová, S., Hlavčová, K. (2018) Analysis of future changes in the trends and scaling coefficients for short-term rainfall in southwestern Slovakia. In Pollack Periodica. Vol. 13, no. 3, 163–174. ISSN 1788-1994, doi: 10.1556/606.2018.13.3.16.

Kendall, M. G. (1975): *Rank Correlation Methods*.

Koutsoyiannis, D., Efstratiadis, A., Mamassis, N., Christofides, A. (2008): On the credibility of climate predictions. *Hydrological Sciences Journal*, roč. 53, č. 4, 671–684, ISSN 2150-3435, doi:10.1623/hysj.53.4.671.

Lapin, M., Bašták-Ďurán, I., Gera, M., Hrvoľ, J., Kremler, M., Melo M. (2012): New climate change scenarios for Slovakia based on global and regional general circulation models. *Acta Met. Univ. Comen*, roč. 37, 25–74.

Mann, H. B. (1945): Nonparametric Tests Against Trend. *Econometrica*, roč. 13, č. 3, 245 p., ISSN 00129682, doi:10.2307/1907187.

NASA, (2019): Climate Change: How Do We Know? *NASA GLOBAL CLIMATE CHANGE*, https://climate.nasa.gov/evidence/.

NCAR/UCAR, (2016): *Community Land Model*. http://www.cesm.ucar.edu/models/clm/.

Tebaldi, C., Hayhoe, K., Arblaster, J. M., Meehl, G. A. (2006): *Going to the extremes: An intercomparison of model-*

simulated historical and future changes in extreme events. B.m.: Springer Netherlands. doi:10.1007/s10584-006-9051-4.

Trenberth, K. E., Dai, A., Rasmussen, R. M., Parsons, D. B. (2003): *The changing character of precipitation* doi: 10.1175/BAMS-84-9-1205.

UCAR, University Corporation for Atmospheric Research, (2019): *CLM Home,* http://www.cgd.ucar.edu/tss/clm/.

Vallebona, Ch., Pellegrino, E., Frumento, P., Bonari, E. (2015): Temporal trends in extreme rainfall intensity and erosivity in the Mediterranean region: a case study in southern Tuscany, Italy. *Climatic Chang,* 2. roč. 128, č. 1–2, 139–151, ISSN 0165-0009, doi:10.1007/s10584-014-1287-9.

Westra, S., Fowler, H. J., Evans, J. P., Alexander, L. V., Berg, P., Johnson, F., Kendon, E. J., Lenderink, G., Roberts, N. M. (2014): Future changes to the intensity and frequency of short-duration extreme rainfall. *Reviews of Geophysics*, roč. 52, č. 3, 522–555, ISSN 87551209, doi:10.1002/ 2014RG 000464.

Ing. Gabriel Földes (*corresponding author, e-mail: gabriel.foldes@stuba.sk)
Prof. Ing. Silvia Kohnová, PhD.
Ing. Marija Mihaela Labat
Department of Land and Water Resources Management
Faculty of Civil Engineering
Slovak University of Technology
Radlinského 11
810 05 Bratislava
Slovak Republic

DOI: 10.31577/ahs-2020-0021.01.0002

ACTA HYDROLOGICA SLOVACA

Volume 21, No. 1, 2020, 9 – 18

RUNOFF REGIME CHANGES IN THE SLOVAK DANUBE RIVER TRIBUTARIES

Dana Halmová*, Pavla Pekárová

This paper deals with a statistical analysis of changes in the hydrological regime of Slovak tributaries of the Danube River at 11 stations over two 30-year periods: 1931–1960 and 1986–2015. We analyzed changes in monthly discharges using the Pardé coefficient method, as well as changes in average daily discharges.
The monthly Pardé coefficients may be used to plot so-called regime curves. Their course is essentially determined by the monthly water balances in the catchments, as well as by intra-annual storage effects like snow accumulation and snowmelt. Changes in the course of Pardé coefficients for water stations of Slovak tributaries of the Danube River do not show any major changes, except for the Ipeľ-Holiša and Topľa-Hanušovce stations. From the results of the daily flow rate analysis it is clear that the course of daily flow rates in the monitored stations remains unchanged during the year and in the most of the monitored Slovak stations the daily flow rates decrease, except for the water stations Belá-Podbanské and Váh-Liptovský Mikuláš.

KEY WORDS: intra-annual flow regime, PARDÉ coefficient, daily and monthly discharge, Slovak Danube tributaries

Introduction

The change in water level during the year characterizes the runoff regime. In the annual cycle, the long-term variability of flow rates has a typical regime depending on the geographical location and height division of the river basin.
In the specific case of the Hron River territory, the distribution of water in the year has the form of a single wave with a maximum in spring months (March-June) and with a minimum in autumn (September). In addition to the main low in September, there is also a minor winter low in January (Poórová, 2013). In river basins with a higher height segmentation and with a higher mean basin height, the winter secondary minimum is changed to the main minimum and autumn minimum to the secondary minimum (Parajka et al., 2008; 2009; Kohnová et al., 2019).
The Danube River with a total length of 2857 km and a long-term daily mean discharge of about 6500 $m^3 s^{-1}$ is listed as the second biggest river in Europe. In terms of length it is listed as the 21st biggest river in the world, in terms of drainage area it ranks as 25th with a drainage area of 817000 km^2. The Danube basin extends from the central Europe to the Black Sea. The extreme points of the basin are 8º 09' and 29º 45' of the Eastern longitude, and 42º 05' and 50º 15' of the Northern latitude (Stančík and Jovanovic, 1988). Out of the whole Danube basin area, 36% are covered with mountains: very tall (over 4000 m in the Alps), and tall (1000–2000 m in the Carpathians, the Balkans and the Dinaric Alps); 64% represent medium-high and low areas (tablelands, hills and plains) (Bondar and Iordache, 2017). In the case of the Danube River Basin, its landscape geomorphology is characterised by a diversity of morphological patterns and the river channel itself can be divided into 6 sections according to the river slope (Lászlóffy, 1965; Stănescu et al., 2004). The longitudinal profile of the Danube and its tributaries, subbasins area and long term discharge is illustrated on the Fig. 1.
In terms of physical-geographical conditions (position, relief and vegetation), a specific continental-temperate climate has developed in the course of time, its characteristic parametric values according Bondar and Iordache (2017) are given below:

- The annual mean air temperature stands between 8°C in the upper part of the basin and 12°C in its lower part; absolute air extremes of +37°C in summer and –36°C in winter. Values of +43° and of –33°C are recorded in the plain-area of the Lower Danube sector.
- A major climatic factor of the Danube basin, namely precipitation, is basically involved in the formation of water discharge and the river's water-regime. In view of the diversity of atmospheric circulation and of landform-types within the basin area, precipitations are unevenly distributed. Thus, in the lowlands, the annual mean stands at some 400–600 mm, with 800–1200 mm in the Carpathians and 1800–2500 and over in the Alps.

The main objective of this study is to analyse the runoff regime of selected Slovak rivers in the Danube Basin and its change during the time period 1931–2015.

Material

For studying of the natural runoff variability in any of the river gauging stations, existence of the long term reliable river discharge observations is inevitable. Detailed daily discharges are available at Slovak water gauging stations, but the size of the river basins is different. The characteristics of selected Slovak water gauging stations at Danube tributaries are listed in the Table 1 (Q_a – mean annual discharge, V – annual runoff volume, R – runoff depth, time period 1931–2005). The scheme of the Slovak Danube tributaries is on Fig. 2.

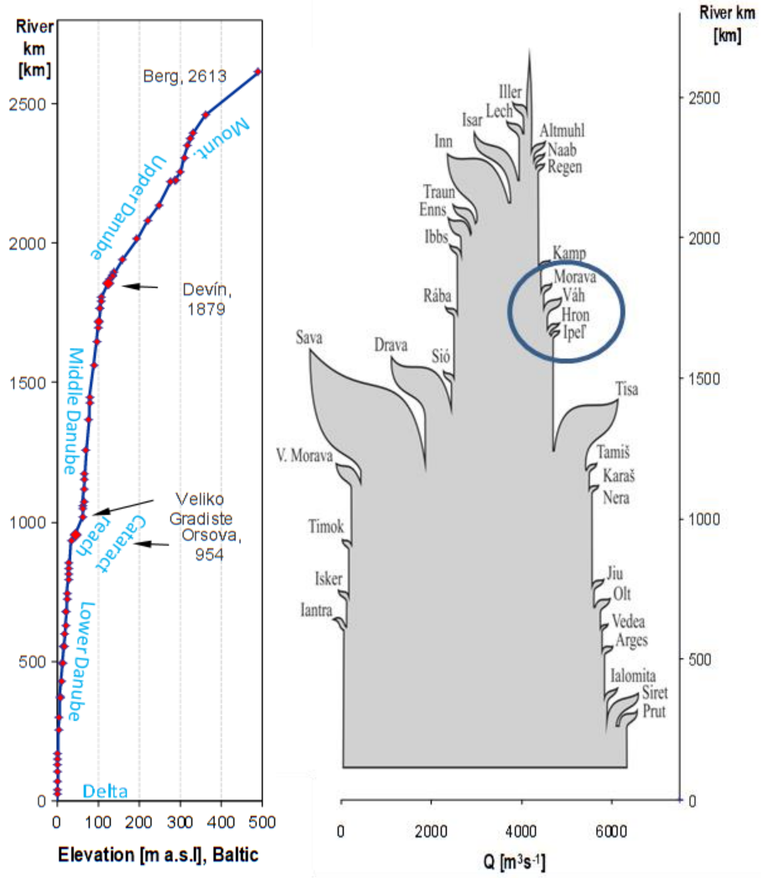

Fig. 1. Longitudinal profile of the Danube and its tributaries, long-term discharge (in detail there are Slovak tributaries); (right figure: values 0–6500 m^3.s^{-1} represent a range of discharges).

Table 1. Characteristics of Slovak water gauging stations

RIVER	WATER GAUGING STATION	AREA [km^2]	LAT	LONG	ALTITUDE [m a.s.l.]	Q_a [m^3 s^{-1}]	V 10^9 [m^3 y^{-1}]	R [mm y^{-1}]
Morava	Mor. Sv. Jan	24129	48.60	16.94	146.0	107.6	3.39	141
Bela	Podbanske	93.49	49.14	19.19	922.7	3.53	0.11	1190
Vah	L. Mikulas	1107	49.09	19.61	568.0	20.6	0.65	586
Vah	Sala	11218	48.16	17.88	109.0	145.7	4.60	410
Hron	B. Bystrica	1766	48.73	19.13	334.0	24.5	0.77	437
Hron	Brehy	3821	48.41	18.65	195.0	47.2	1.49	390
Kysuca	Kysucke N. Mesto	955	49.30	18.79	346.0	16.4	0.52	542
Topla	Hanusovce	1050	49.03	21.50	160.4	8.0	0.25	239
Krupinica	Plastovce	303	48.16	18.96	139.5	2.0	0.06	208
Ipel	Holisa	686	48.30	19.74	172.0	3.1	0.10	144
Nitra	Nitrianska Streda	2094	48.30	18.10	158.3	14.7	0.46	221

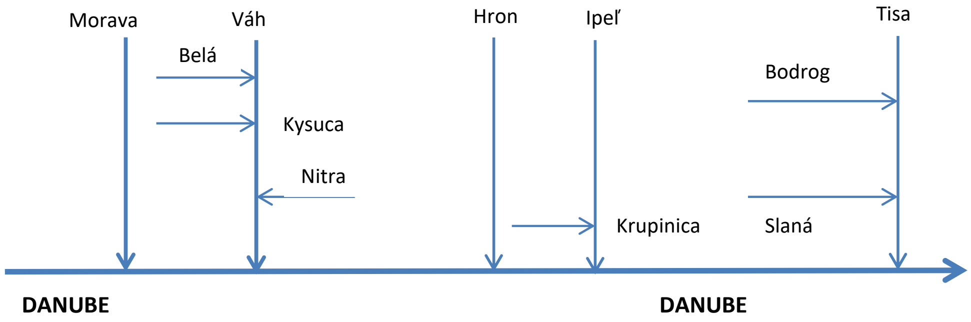

Fig. 2. Scheme of the Slovak tributaries of the Danube River.

Methods

Analysis of the mean annual runoff variability and its change in time are typically performed, applying the common classification method by Pardé (Pardé; 1964; Weingartner and Aschwanden, 1992; Belz et al., 2004; Bormann, 2010; Rössler et al., 2019). This analysis is based on the ratio of each of the twelve long-term monthly MQ_s with the associated long-term annual MQ making up the so-called Pardé coefficient. The calculation of Pardé coefficients has always the effect of a standardization that facilitates the direct comparison between different annual flow hydrographs.

The Pardé flow coefficient $Pk_{(i)}$ is defined as:

$$Pk_i = \overline{Qm_i} / \overline{Q} \tag{1}$$

where

$\overline{Qm}_i$ – long-term mean monthly streamflow in the single month *i*, *(i=I, XII)* [m³ s⁻¹],

$\overline{Q}$ – being the long-term annual streamflow [m³ s⁻¹].

Results

Runoff changes according to PARDÉ method

First, intra-annual flow-regime at selected gauges according to PARDÉ was analysed. The analysis of the mean annual runoff variability and its change in time are typically performed, applying the common classification method by PARDÉ. In Fig. 3 there are presented Pardé coefficients, course of moving averages of seasonal discharges and 2D picture of the monthly discharges for two 30-years periods 1931–1960 and 1986–2015 for Belá River at Podbanské water station. Partial figures at the Fig. 3. give us information about Pardé coefficient at two different time periods 1931–1960 and 1986–2015; about the course of moving averages of seasonal discharges and monthly discharges at Belá-Podbanské station at the whole time period 1931–2015. In Fig. 3 (part 2D), changes in monthly flow rates in magnitude and occurrence during the year and over the reference period are evident.

The monthly Pardé coefficients may be used to plot so-called regime curves. Their course is essentially determined by the monthly water balances in the catchments, as well as by intra-annual storage effects like snow accumulation and melt. Pardé originally distinguishes a multitude of types of flow regimes that shall not be discussed in detail here.

The distinction is made according to the number and position of monthly maxima and minima in the course of the year, the feeding/origin of flow (see below), and the variability range of the coefficient values. Simple types (one-peak) can be separated from complex ones that appear as multi-peak regimes. The latter results from a superposition of several processes which make up the annual course. The flow maxima are typically fed either by glacier-meltwater (glacial regime), snow-melt-water (nival regime) or by rainfall (pluvial regime), or weighted combination of these.

Major types of the Pardé flow regime (acc. to Pardé) we can define as:

- **the nival** (= snow-dominated) runoff regime of mountainous areas, displaying a very wide amplitude of coefficient values, single-peak with a maximum in early summer due to snowmelt and a minimum in winter when the water is retained in form of ice and snow;
- **the pluvial** (= rain dominated) oceanic regime, with a wide range of amplitude, single-peak, with a maximum in the mild rainy winter months and a minimum in summer resulting from intensive evapotranspiration;
- **a balanced pluvial mixed regime** („complex regime 2nd order") of the rain-snow type, two-peaks, with the main maximum in late autumn and a minimum in summer.

Summarizing Table 2 presents long-term characteristics (top two panels) like Q_m – long-term average monthly, annual and seasonal discharge in m³ s⁻¹; Q_{min}/Q_{max} – minimal/maximal monthly discharge, V_m – long-term monthly runoff volume in 10⁶ m³; R_m – long-term monthly runoff depth in mm, V_m/V_a – long-term monthly share on yearly runoff in %, t_r – trend slope of monthly discharges, c_s – coefficient of asymmetry, and c_v is coefficient of variability of the monthly discharges, $Pk_{1931–1960}$ and $Pk_{1986–2015}$ – Pardé coefficients.

For the following analysis we focus on the time period 1931–2015 for practical reasons. As discharge characteristics often change over time, a classification of this relatively short time period into the longer time periods is appropriate to avoid misinterpretations. However, on shorter time period changes in the discharge regime become apparent.

Fig. 4a–j present the same pictures for other Slovak Rivers.

The change in daily flow regime in selected tributary profiles

This part of the paper analyses the changes in daily flow rates for two different 30-year periods: 1931–1960 and 1986–2015. From the results it is clear that the course of daily flows during the year remains unchanged and in most of the monitored Slovak gauging stations there is a decrease in daily flows (Fig. 5).

At the stations Belá-Podbanské and Váh-Liptovský Mikuláš in the period 1986–2015 there is a slight increase in average daily flows in the months of April and May. (Fig. 6)

On the other hand, the most significant decrease in daily flows occurs at the stations Krupinica-Plášťovce and Ipeľ-Holiša, especially in spring and winter. (Fig. 7)

Conclusion

Regime types based on Pardé coefficients are regularly used to detect changes in the regime-defining processes by comparing coefficients of two (or more) time slices.

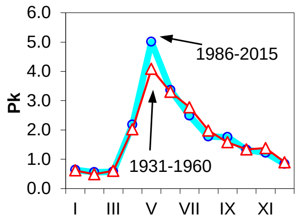

Pardé coefficient - two periods

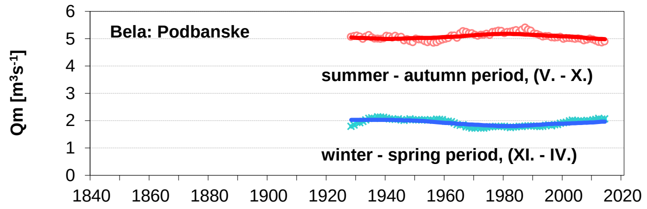

Course of moving averages of seasonal discharge

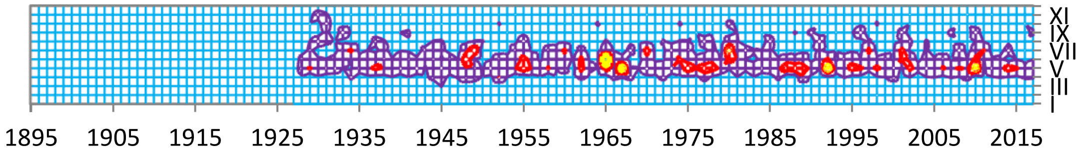

Monthly discharge, 2D plot.

Fig. 3. Partial figures: Pardé coefficient, course of moving averages of seasonal discharges, 2D picture of the monthly discharges, Belá-Podbanské station.

Table 2. Basic statistical characteristics of monthly and seasonal discharges at Belá-Podbanské, Q_m – long term mean monthly/seasonal discharge, Q_{min} – minimum monthly/seasonal discharge, Q_{max} – maximum monthly/seasonal discharge [$m^3\ s^{-1}$], V_m – monthly/seasonal runoff volume [$10^6\ m^3\ month^{-1}$], R_m – monthly/seasonal runoff depth [$mm\ month^{-1}$], t_r – long term trends slope, c_s – coefficient of symmetry, c_v – coefficient of variation, $Pk_{1931–1960}$ and $Pk_{1986–2015}$ – Pardé coefficients

	I	II	III	IV	V	VI	VII	VIII	IX	X	XI	XII	Year	XI-IV	V-X
Q_{ma}	1.22	1.01	1.12	3.99	8.87	6.66	5.31	3.83	3.11	2.67	2.45	1.67	3.50	1.91	5.08
Q_{min}	0.50	0.47	0.40	0.59	2.88	2.64	1.90	1.10	0.86	0.92	0.79	0.59	1.98	0.74	2.35
Q_{max}	2.45	3.19	5.26	10.01	16.52	20.25	15.15	9.82	8.69	7.86	6.81	3.91	5.16	3.56	8.41
V_m	3.3	2.4	3.0	10.3	23.8	17.5	14.2	10.4	8.2	7.2	6.4	4.5	111.2	29.8	81.4
R_m	35.1	26.0	32.0	110.6	254.2	184.8	152.2	109.6	86.3	76.5	67.8	48.0	1182.9	319.4	863.5
V_m/V_a	2.97	2.20	2.70	9.35	21.49	15.62	12.86	9.27	7.29	6.47	5.73	4.05	100.0	27.0	73.0
t_r	3.16	11.40	0.78	0.81	1.64	-0.37	-0.26	-2.13	0.15	-2.16	-6.48	-6.93	-1.23	-2.95	-0.16
c_s	0.61	2.58	3.64	0.55	0.37	1.98	1.40	0.94	1.41	1.39	1.09	0.89	0.30	0.73	0.50
c_v	0.30	0.38	0.57	0.50	0.31	0.40	0.53	0.45	0.52	0.49	0.47	0.36	0.20	0.29	0.24
$Pk_{1931-1960}$	0.62	0.49	0.60	2.02	4.09	3.30	2.77	1.98	1.58	1.33	1.38	0.90	1.00	2.51	2.51
$Pk_{1986-2015}$	0.64	0.55	0.57	2.18	5.02	3.33	2.44	1.74	1.72	1.32	1.23	0.84	1.00	2.60	2.60

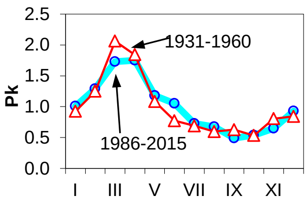

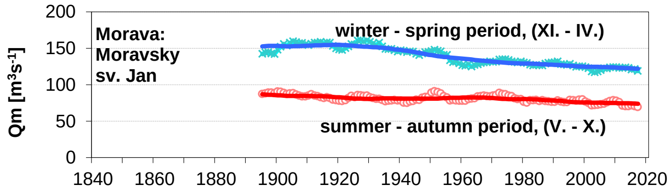

Pardé coefficient - two periods *Course of moving averages of seasonal discharge*

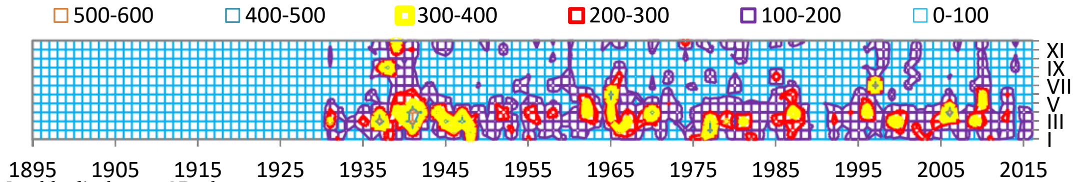

Monthly discharge, 2D plot.

a)

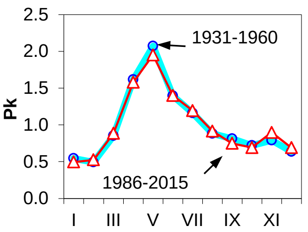

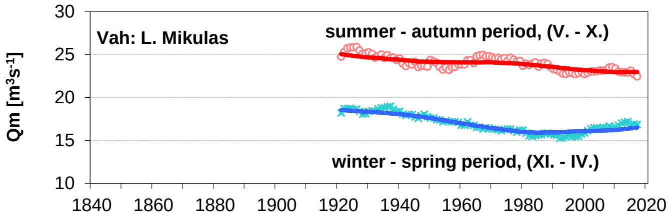

Pardé coefficient - two periods *Course of moving averages of seasonal discharge*

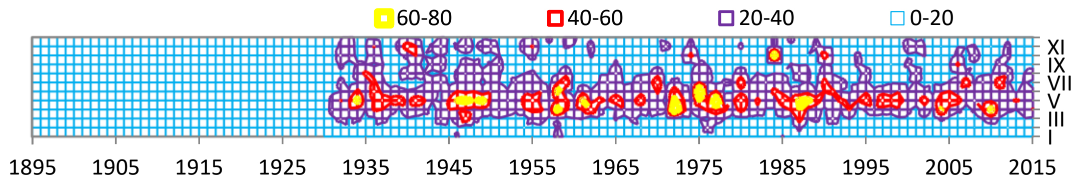

Monthly discharge, 2D plot.

b)

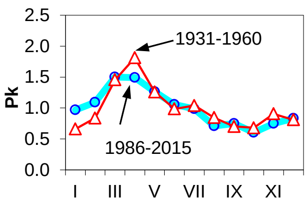

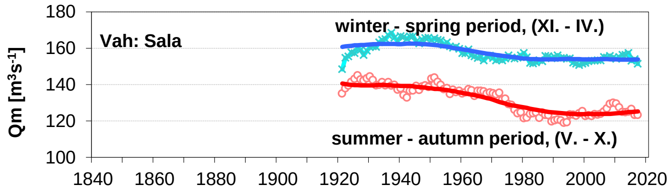

Pardé coefficient - two periods *Course of moving averages of seasonal discharge*

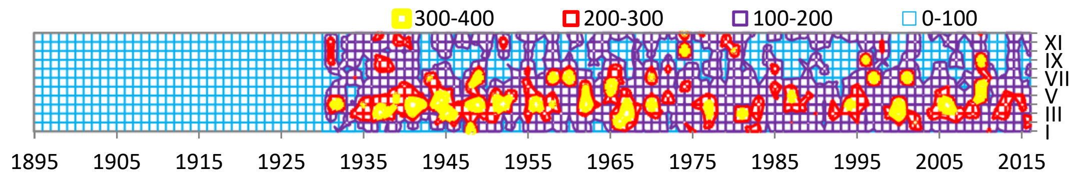

Monthly discharge, 2D plot.

c)

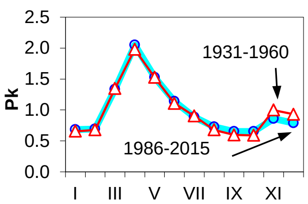

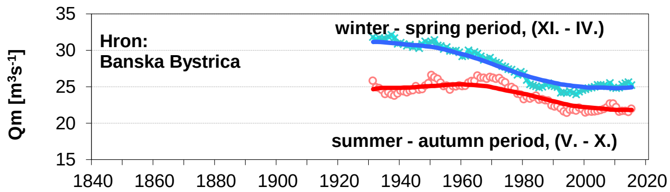

Pardé coefficient - two periods *Course of moving averages of seasonal discharge*

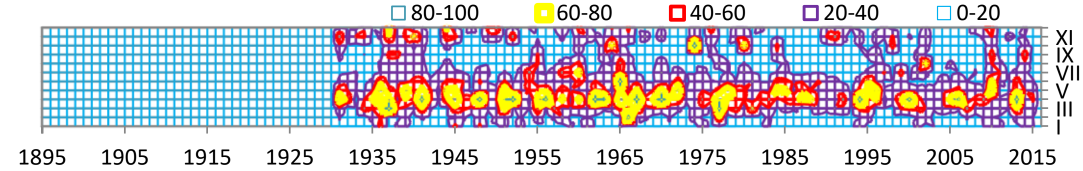

Monthly discharge, 2D plot.

d)

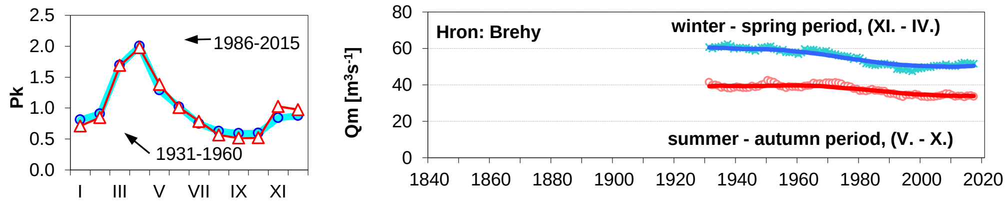

Pardé coefficient - two periods *Course of moving averages of seasonal discharge*

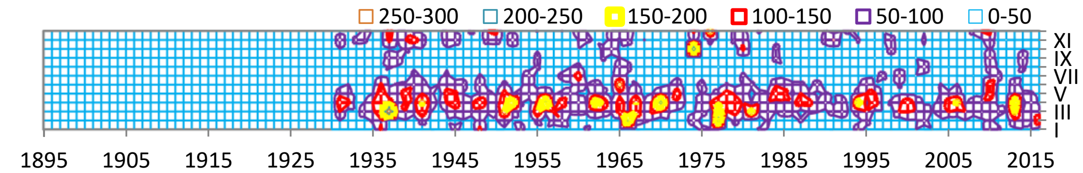

Monthly discharge, 2D plot.

e)

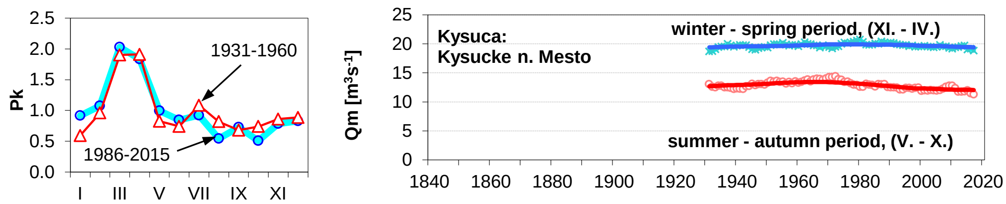

Pardé coefficient - two periods *Course of moving averages of seasonal discharge*

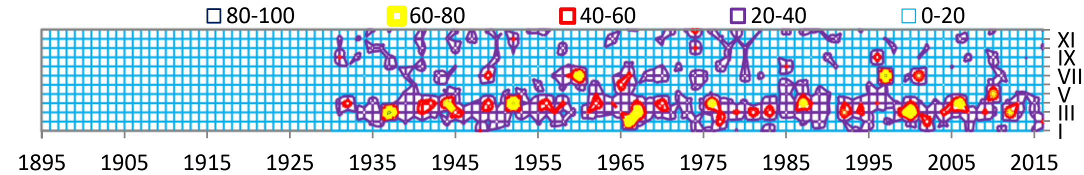

Monthly discharge, 2D plot.

f)

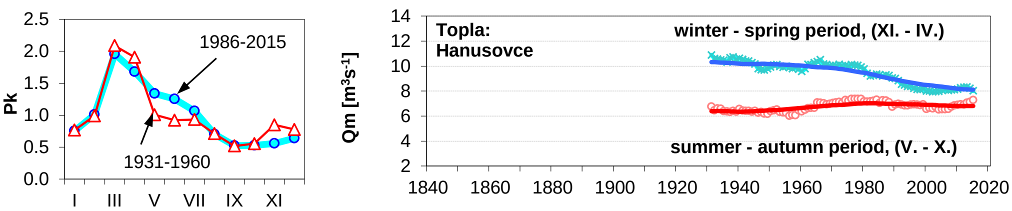

Pardé coefficient - two periods *Course of moving averages of seasonal discharge*

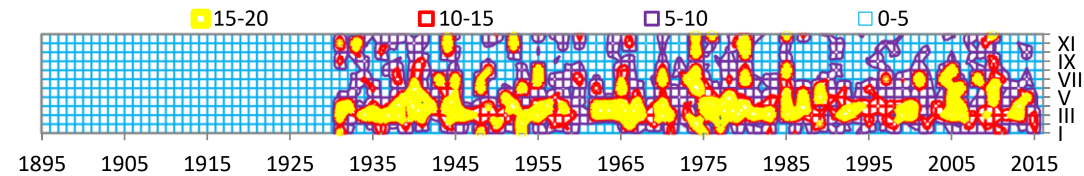

Monthly discharge, 2D plot.

g)

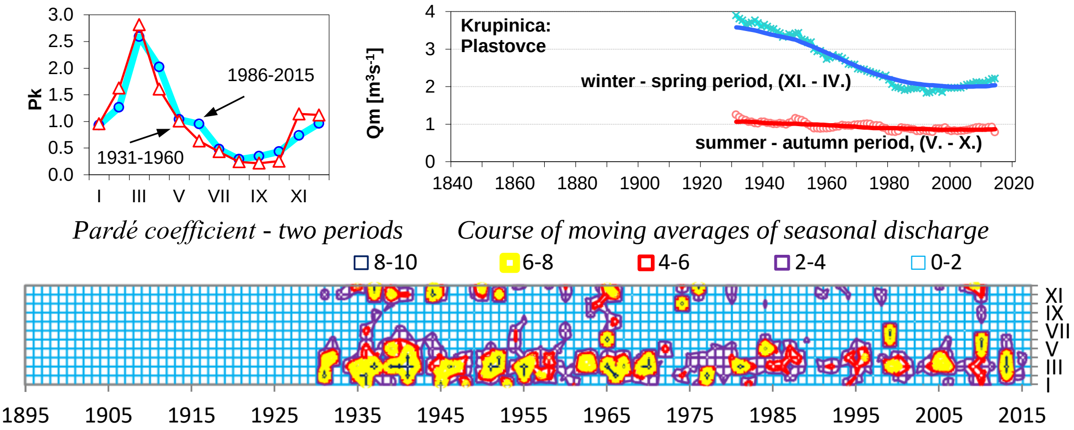

Monthly discharge, 2D plot.

h)

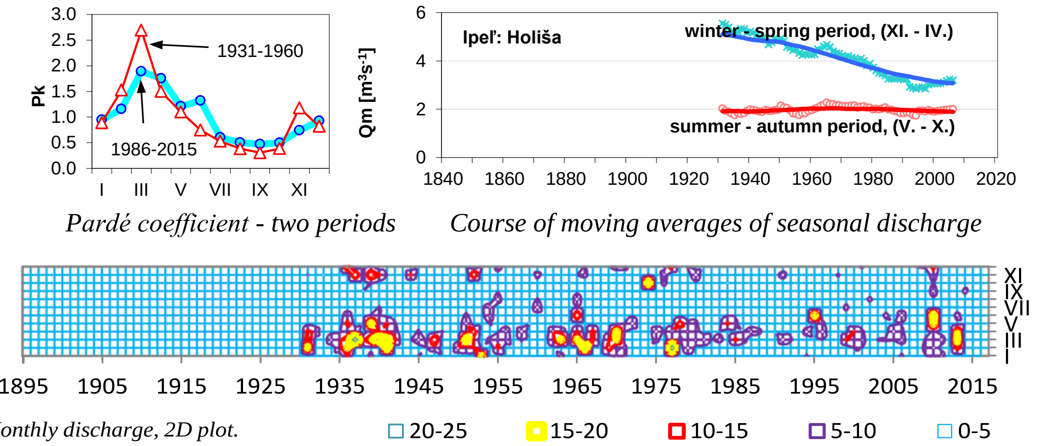

Monthly discharge, 2D plot.

i)

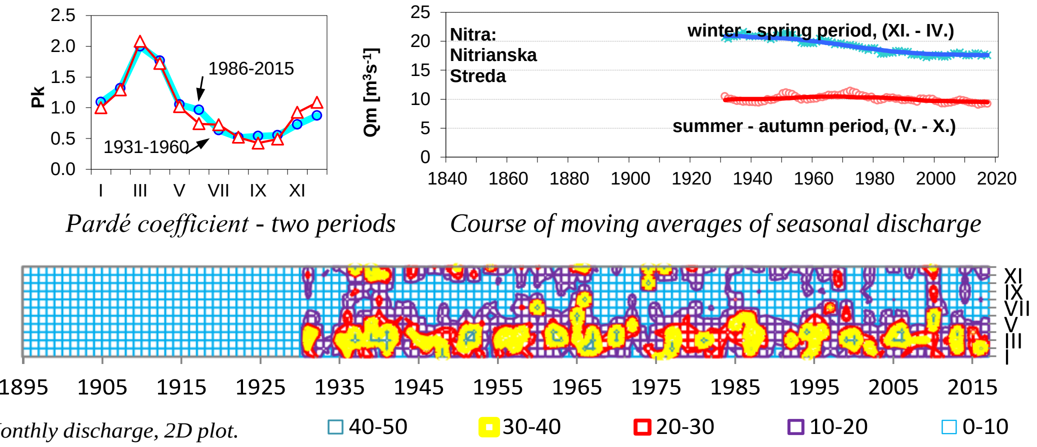

Monthly discharge, 2D plot.

j)

Fig. 4. Pardé coefficient, Course of moving averages of seasonal discharges and 2D picture of the monthly discharges, time period 1931–2015, Slovak tributaries (a–j).

Increase (or decrease) of the extreme values of monthly Pardé coefficients is investigated as well as a consequential impact on the seasonal variability of runoff and a potential temporal shift of the occurrence of the extremes of monthly Pardé coefficients. This might happen due to earlier snow melt caused by regional warming. In order to account for the term "climate", 30 year time periods are investigated. Here, we compared two 30-years periods 1931–1960 and 1986–2015. The Pardé method is a very illustrative way to show monthly discharge developments by comparing different runoff periods. The gauges Ipeľ-Holiša and Belá-Podbanské are taken here as an example (Fig. 8a, b) with 2 periods of 30 years each. The Fig. 8a don´t shows a shift of the discharge peak or minimum discharge. However, in the period 1986–2015 there is a decrease in daily (right side

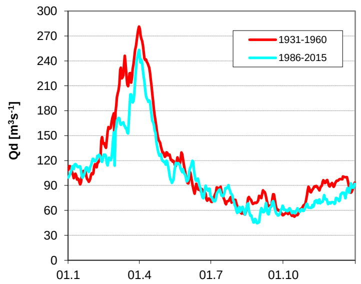

a) Morava-Moravský sv. Ján

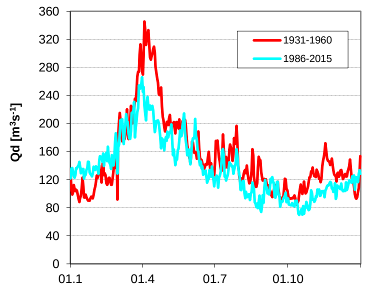

b) Váh-Šaľa

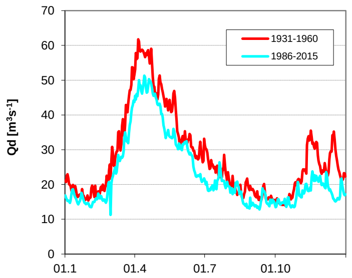

c) Hron-B. Bystrica

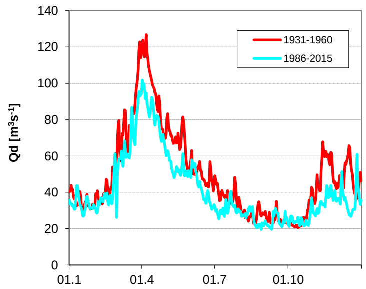

d) Hron-Brehy

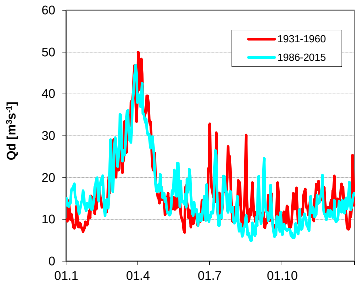

e) Kysuca-Kysucké n. Mesto

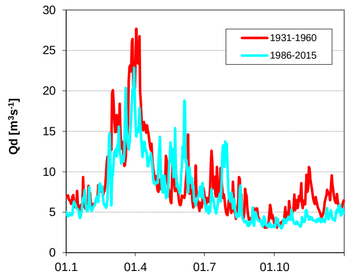

f) Topľa-Hanušovce

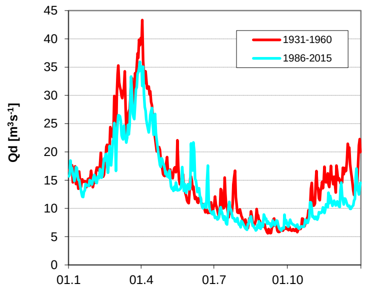

g) Nitra-Nitrianska Streda

Fig. 5. Changes in the flow regime of daily discharges in the 1931–1960 and 1986–2015 periods (a–g).

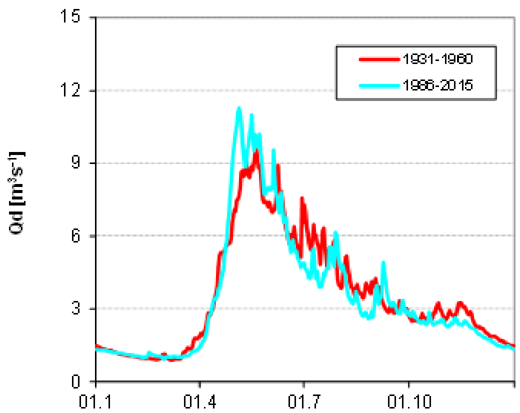

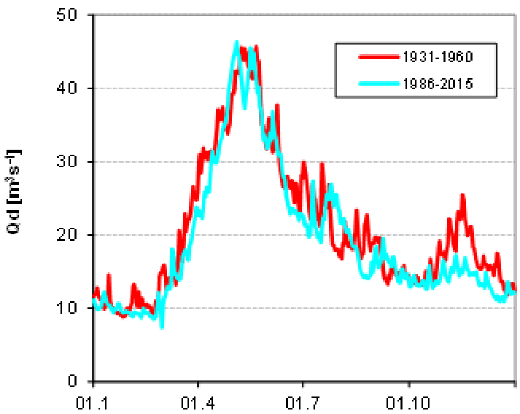

Belá-Podbanské

Váh-Liptovský Mikuláš

Fig. 6. Gauges Belá-Podbanské and Váh-Liptovský Mikuláš: Changes in the flow regime of daily discharges in the 1931–1960 and 1986–2015 periods.

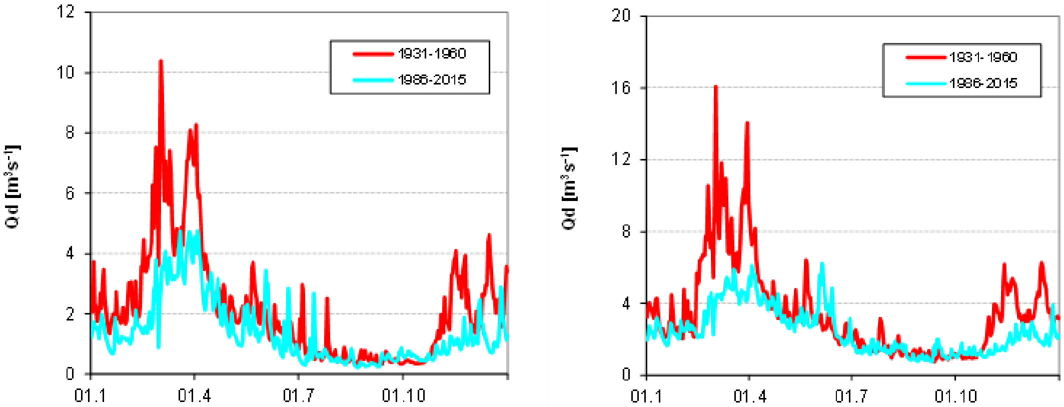

Krupinica-Plášťovce *Ipeľ-Holiša*

Fig. 7. Gauges Krupinica-Plášťovce and Ipeľ-Holiša: Changes in the flow regime of daily discharges in the 1931–1960 and 1986–2015 periods.

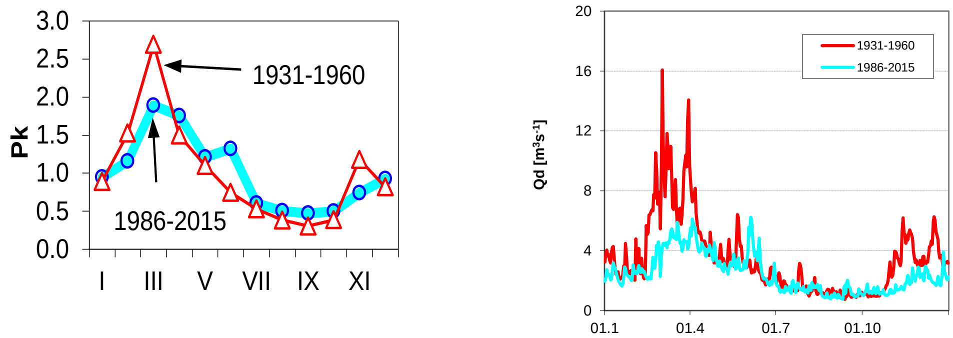

a) Ipeľ-Holiša

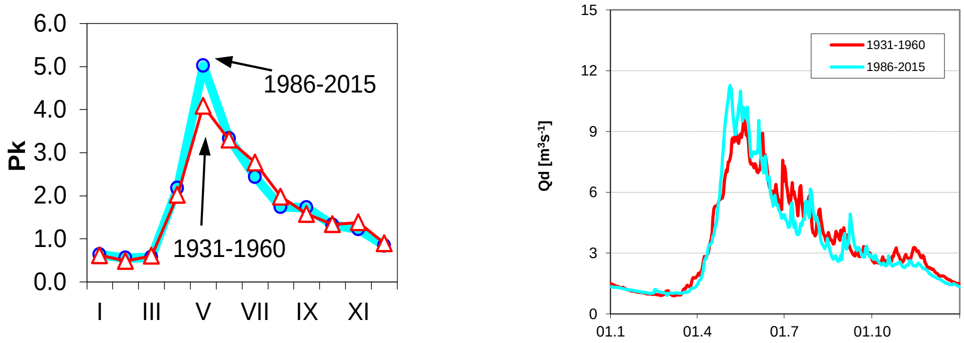

b) Belá-Podbanské

Fig. 8. Changes in the runoff regime shown by the intra-annual variations of streamflow in the 1931–1960 and 1986–2015 periods (left side pictures, Padré coefficient) and changes in the flow regime of daily discharges in the 1931–1960 and 1986–2015 periods (right side pictures), a) gauging station Ipeľ-Holiša, b) Belá-Podbanské.

figure) and subsequently monthly flows, which will be reflected in the change in the size of the Pardé coefficient. The Fig. 8b don´t shows a shift of the discharge peak or minimum discharge. However, in the period 1986–2015 there is slight increase in daily (right side figure) and subsequently monthly flows, which will be reflected in the change in the size of the Pardé coefficient.

From the results it is obvious that similar changes in daily flow rates in these periods (1931–1960 and 1986–2015) can be inferred from the calculation of this coefficient and the graphical output of the comparison of the two time periods. Changes in Ipeľ flows at the Holiša gauging station are very significant. It would be necessary to pay more attention to the development of flows in this station, to check the historical measurement curves by comparison with the flows in neighboring stations. If long-term flows have a similar downward trend, attention will need to be paid to the development of precipitation totals in the river basin. If there is no decrease in precipitation, this decrease in flows can be attributed to an air temperature increase and higher evaporation.

Defining temporal change in river discharge is a fundamental part of establishing hydrological variability, and crucially important for identifying climate–streamflow linkages, water resource planning, flood and drought management and for assessing geomorphological and hydro-ecological responses. Also detection of trends in hydrological data is a complex issue. The results could show that the trend analysis is dependent on the chosen period: in particular, it can have significant influence on both trend magnitude and the direction.

The implications of analytical decisions on the interpretations of hydrological change are important and impact on planning and development in many fields including water resources, flood defence, hydro-ecology and climate-flow analysis.

Acknowledgements:

This work was supported by the project VEGA 2/0004/19.

References

Belz, J. U., Goda, L., Buzás, Z., Domokos, M., Engel, H., Weber, J. (2004): Runoff Regimes in the Danube Basin. The Danube and its catchment – A hydrological monograph, Follow-up volume VIII/2, Regional Cooperation of the Danube Countries, Koblenz & Baja, 152 p.

Bondar, C., Iordache, C. (2017): Sediment transport on the Danube River in the Romanian border area – characteristics. Rev. Roum. Géogr./Rom. Journ. Geogr., București, 61, 1, 3–17.

Bormann, H. (2010): Runoff Regime Changes in German Rivers due to Climate Change. In. Erdkunde, Vol. 64, No. 3, pp. 257–279. DOI: 10.3112/erdkunde.2010.03.04. ISSN 0014-0015 http://www.erdkunde.uni-bonn.de.

Kohnová, S., Rončák, P., Hlavčová, K., Szolgay, J., Rutkowska, A. (2019): Future impacts of land use and climate change on extreme runoff values in selected catchments of Slovakia. Meteorology Hydrology and Water Management, 7(1), 47–55. DOI: https://doi.org/10.26491/mhwm/97254

Lászlóffy, W. (1965): Die Hydrographie der Donau. Der Fluss als Lebensraum. In: Liepolt, R. (ed.): Limnologie der Donau – Eine monographische Darstellung. II. Kapitel, Schweizerbart, Stuttgart. P. 16–57.

Parajka, J., Merz, R., Szolgay, J., Blöschl, G., Kohnová, S., Hlavčová, K. (2008): A comparison of precipitation and runoff seasonality in Slovakia and Austria. Meteorologický časopis, 11, 2008, 9–14.

Parajka, J. Kohnová, S., Merz, R., Szolgay, J., Hlavčová, K. Blöschl, G. (2009): Comparative analysis of the seasonality of hydrological characteristics in Slovakia and Austria. Hydrological Sciences–Journal–des Sciences Hydrologiques, 54, 3, 456–473.

Pardé, M. (1964): Fleuves et riviéres. Armand Colin, no 155, 4ème édition, 223 p.

Poórová, J., Škoda, P., Danáčová, Z., Šimor, V. (2013): Evolution of Hydrological Regime of Slovak Rivers, (in Slovak) Životné prostredie. 47, 3, 144–147.

Rössler, O., Belz, J., U., Mürlebach, M., Larina-Pooth, M., Halmová, D., Garaj, M., Pekárová, P. (2019): Analysis of the intra-annual regime of flood flow and its changes in the Danube basin. In: Pekárová, P., Miklánek, P. (eds.) Flood regime of rivers in the Danube River basin. Follow-up volume IX of the Regional Co-operation of the Danube Countries in IHP UNESCO. IH SAS, Bratislava, p. 101–122. DOI: https://doi.org/10.31577/2019.9788089139460

Stančík, A., Jovanovic, S. (1988): Hydrology of the River Danube. Publishing House Príroda, Bratislava, 272 pp + 4 maps.

Stănescu, V. A. (2004): Regional analysis of the annual peak discharges in the Danube catchment. The Danube and its catchment – A hydrological monograph, Follow-up volume No. VII, Regional Cooperation of the Danube Countries, Bucharest, 64 p.

Weingartner R., Aschwanden H. 1992. Discharge regime— the basis for the estimation of average flows. In: Hydrological Atlas of Switzerland, Plate 5.2, Department of Geography, Bern University – Hydrology & Swiss Federal Office for Water and Geology, Bern, Switzerland (in German, French and Italian).

Ing. Dana Halmová, PhD. (*corresponding author, e-mail: halmova@uh.savba.sk)
RNDr. Pavla Pekárová, DrSc.
Institute of Hydrology SAS
Dúbravská cesta č. 9
841 04 Bratislava
Slovak Republic

DOI: 10.31577/ahs-2020-0021.01.0003

ACTA HYDROLOGICA SLOVACA

Volume 21, No. 1, 2020, 19–28

ESTIMATION OF DISCHARGE WITH LONG RETURN PERIOD USING HISTORICAL FLOOD RECORDS

Jakub Mészáros*, Pavla Pekárová, Ján Pekár

Records of historical catastrophic floods provide extremely valuable knowledge about the frequency of occurrence of such events on the rivers that do not have a series of discharge observations long enough, or observations are completely absent. In this paper we present knowledge about historical floods on the Teplica River in Sobotište and its catchment. Based on statistical processing of the series of maximum annual discharge from the water gauge Sobotište-Teplica, we present the impact of the inclusion of historical floods on the estimation of the *T-year* design discharge values.

KEY WORDS: historical floods, *T-year* values, LP3 distribution, Teplica River

Introduction

One of the most important tasks of hydrology is to determine the values of a certain hydrological phenomenon (precipitation, discharge, etc.) that are exceeded with a certain preselected probability. With increasing length of observed hydrological series and with development of statistical stochastic methods it is possible to refine estimates of design values for very low probabilities of occurrence (200- to 1000-years values).
The design discharge values are generally determined for *T=1-, 2-, 5-, 10-, 20-, 50-, 100-* years according to Technical Standard 3112–1:03 (MŽP, 2003). The Technical Standard does not include methods for the determination of the *200-, 500-* and *1000*-year discharge. It is very complicated to determine discharge that occur every 200 or 1000 years.
Several methods (statistical methods, rainfall-runoff models, etc.) can be used to extrapolate the measured series over several decades for the *200-, 500-* or *1000-*year period.
It is up to the investigator's experience and knowledge, which method will be used to determine *T*-year discharge (Kohnová and Szolgay, 2003; Stănescu, 2004; Kohnová et al., 2006a, b, 2016; Šipikalová et al., 2006; Pekár et al., 2012; Pekárová et al., 2013; Gaál et al., 2010a, b; Merz and Blöschl, 2008a, b; Dysarz, 2019).
The aim of this paper is to analyze the impact of the inclusion of historical floods in the series of annual maximum discharge on the example of the Teplica River at the water gauge Sobotište. Their inclusion results in more precise *T*-year values with a long return period as determined by the statistical method. This work follows the work of Mészáros et al. (2019).

Description of the Teplica River Basin

Teplica (formerly also Vrbovčianka, or Malina) springs in the Czech Republic in the village of Kuželov in the Biele Karpaty Mountains under the pass U Tři Kamenů at an altitude of 440 m a. s. l. The length of the stream is 26.78 km and the catchment area is 152.83 km^2 (Fig. 1). The river flows through villages Vrbovce, Sobotište, Kunov and town Senica, where is the mouth to the Myjava River at an altitude 183 m a. s. l. Between the villages Sobotište and Kunov is water reservoir, but water gauge in Sobotište is uninfluenced by this water structure.
In Sobotište, the level of the river at the time of normal discharge is 237 m a. s. l. The slope of the stream bed is relatively small and therefore meanders are formed. In the Sobotiše cadastral territory the banks of the stream are natural, only partially modified.
The most part of Teplica River Basin belongs to Biele Karpaty Mountains created by flysh rocks and covered by cambisols. The southwestern part belongs to Chvojnícka pahorkatina Upland covered by loess sediments and with luvisol soli type. To the Sobotište water gauge is 20% of area covered by forest. Mean annual rainfall total is from cca 850 mm in highest locations in the northern part of the basin to cca 600 mm in the southern part of the basin.

Data

In the basin of the Teplica River, there are located four water gauges of the state hydrological network of Slovak Hydrometeorological Institute (SHMI) – namely, in Vrbovce (Fig. 2 on the left), in Sobotište (Fig. 2 on

the right), under the Kunov reservoir and in Senica. We used the annual maximum discharge from the Sobotište-Teplica water gauge provided by the SHMI. This gauge has the longest observation period and there are records of the historical floods on the Teplica River in Sobotište. To calculate the regional skew coefficient, we used a series of annual maximum discharge from water gauges that are in neighbouring river basins with similar physical-geographical characteristics, are unaffected and have an observation period longer than 40 years (Table 1).
The annual maximum discharge has been measured in the Sobotište water gauge since 1974 (Fig. 3). The series was supplemented with data from records of historical floods from 1902 and 1939. Sources of data about historical floods are in the chapter 5.2.

Methods

When determining *T*-year discharge by statistical methods from the series of maximum annual discharge Q_{max}, we can proceed in two ways:

1. Either we use different types of distribution functions and determine *T*-year discharge for each compliant distribution, or
2. We choose one type of distribution, use historical observations and try to regionalize the distribution parameters for the region.

Determination of T-year discharge based on different distribution functions

We consider the observed values of the investigated hydrological series to be a realization of a random variable. The basic task in determining *T*-year discharge is to find suitable distribution functions that accurately describe the random variable. Today various software can be used to find a suitable distribution function, e.g. Easy Fit software that includes over 50 types of distribution functions. Since the discharge are bounded by zero from the bottom, it is necessary to use the bottom bounded distributions. In Fig. 4. the histogram and 15

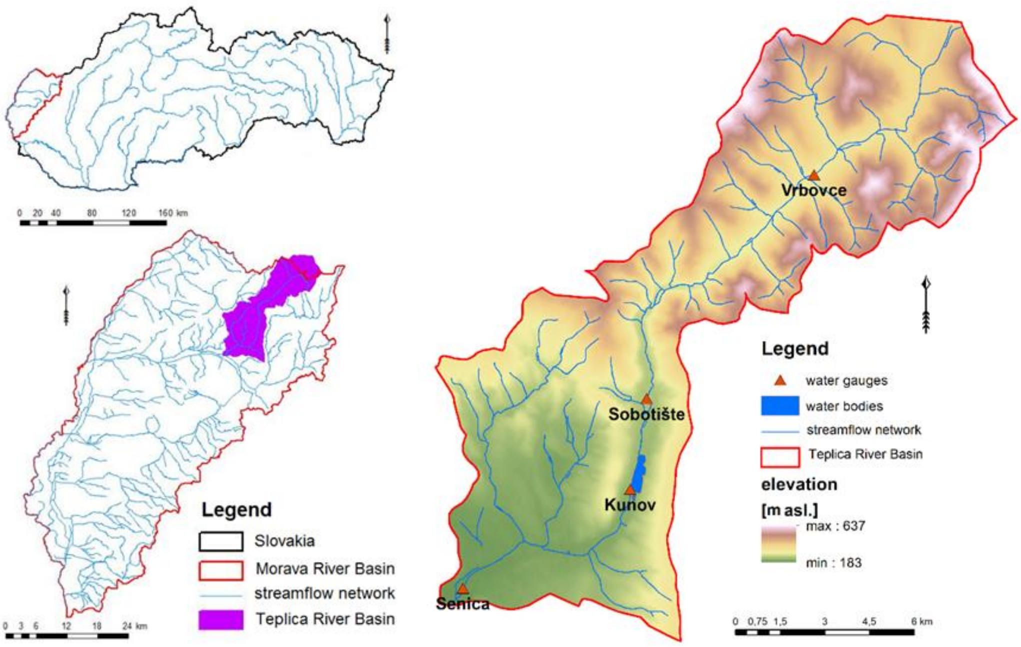

Fig. 1. Left up: Location of the Morava River Basin in Slovakia. Left down: The Teplica River Basin within the Morava River Basin and its streamflow network. Right: SHMI water gauge network and relief of the Teplica River Basin.

Table 1. Used water gauges with specified year of discharge measurement beginning and selected physical-geographical characteristics (Zítek et al., 1967; SHMI, 2017)

ID	gauge	river	discharge since	altitude [m a.s.l.]	forest cover [%]	basin shape	catchment area [km^2]	basin slope [°]
5010	Lopašov	Chvojnica	1969	272.70	40	0.25	31.13	2.27
5025	Sobotište	Teplica	1974	236.29	20	0.16	85.58	0.93
5020	Myjava	Myjava	1974	324.34	50	0.28	32.02	2.89
5030	Šaštín-Stráže	Myjava	1932	164.25	30	0.16	644.89	0.78

Fig. 2. Left: SHMI Vrbovce-Teplica water gauge in the valley of the Biele Karpaty Mountains. Source: Mészáros, January 2017. Right: SHMI Sobotište-Teplica water gauge. Source: Pekárová, February 2019.

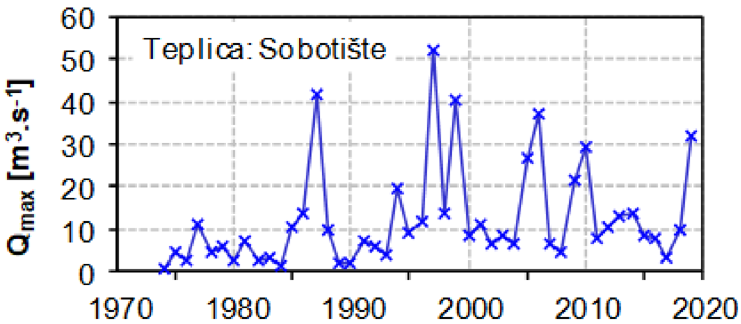

Fig. 3. Measured series of maximum annual discharge for hydrological years 1974–2018, deviations from moving averages in Sobotište-Teplica water gauge.

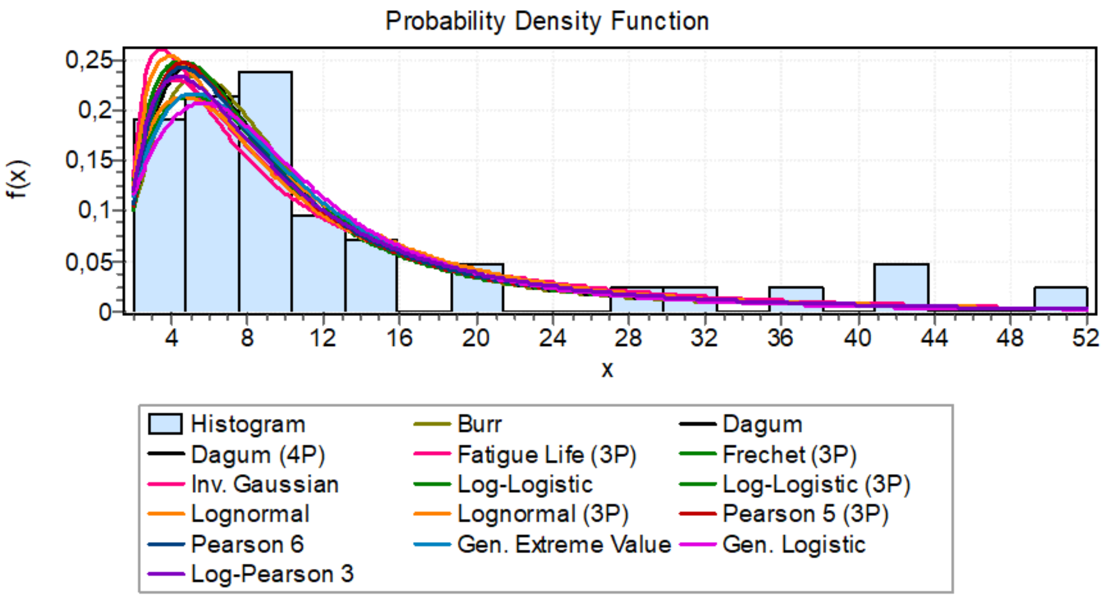

Fig. 4. Histogram and 15 probability functions of the annual maximum discharge of the Teplica River at the Sobotište water gauge.

probability functions of the maximum annual discharge Q_{max} of the Teplica River in the Sobotište water gauge for the period 1974–2018 are plotted. Using e. g. the fifteen best distribution functions calculate *T*-year discharge values. From these 15 values, the average, upper and lower estimates for each design discharge (e.g., *100-*, *200-* to *1000-*year discharge) are determined in the next step.

Determination of T-year discharge based on regionalization of parameters from one distribution function

In this work we use the methodology described in Bulletin 17B, which was published in the USA in 1981 and modified in 1982 at the Water Research Center of the University of Texas at Austin (IACWD, 1982).

According to this methodology, we test only one type of distribution, Log-Pearson III. type distribution (LP3), which is used to estimate extremes in many natural processes and is one of the most commonly used distributions in hydrology (Phien and Jivajirajah, 1984; Pilon and Adamowski, 1993; Griffis and Stendinger, 2009; Millington et al., 2011). The LP3 distribution has been used since 1976 in the USA (Koutsoyiannis, 2008). LP3 is also recommended by Stănescu (2004) to use this distribution to extrapolate regional curves in the Danube River Basin.

From the measured series of maximum annual discharge with a length about 80 years, we can afford to more accurately determine about *120*-year discharge. The author brings his own experience and estimates to the determination of *200-* or more year discharge. In any case, we must be aware that the determination of *1000*-year discharge is burdened by great uncertainty. While in determining the uncertainty of estimating design values based on the use of several types of distributions, essentially the error between estimates is determined, using one type of distribution determines the error resulting from the shortness and variance of the measured series.

The LP3 distribution is very flexible, it is a generalization of log-normal distribution and Pearson distribution. The use of one type of distribution makes it possible to estimate *T*-year discharge even in location without observation based solely on the parameters of distribution functions from neighbouring water gauge. It is possible to find the relationship of the skew coefficient on the water gauge altitude, or the catchment area, or the forest cover, or the runoff depth in the gauge. If we can find such a relationship, we can use the regional skew coefficient to refine this coefficient in gauges with short series of observations and thus improve the estimated *T*-year discharge value. We have found such a relationship along the Danube River and another in the Bela River Basin (Pekárová et al., 2018).

Historical floods

It is well known that extrapolation of data is very sensitive not only to the length of observations, but also to the inclusion of historical floods in the data series. Correct estimation of potential *T*-year discharge requires the inclusion of measured data series into the calculations, as well as the inclusion of historical data in the statistical processing of the series analyzed (Gaál et al., 2010a). Brazdil et al. (2006) studied historic hydrological materials to assess the threat of flooding in Europe. The estimation of uncertainty at the design discharge was examined for example by Merz and Thieken (2009), Merz et al. (2008a, b), or Rogger et al. (2012). Historical floods complement estimates the frequency of major floods and should therefore be included in the statistical analysis. Historical floods can also be used to assess the correctness of estimated *T*-year discharge, especially for long repetition times. If historical data are available, we can add them to the Q_{max} input set with the appropriate probability and specify the new distribution parameters.

Log-Pearson III. type distribution

The LP3 distribution is a three-parameter Gamma distribution with a logarithmic transformation of a random variable (Naghavi et al., 1990). Pearson distribution probability density function III. type is:

$$f(X|\tau,\alpha,\beta) = \frac{\left(\frac{X-\tau}{\beta}\right)^{\alpha-1}\exp\left(-\frac{X-\tau}{\beta}\right)}{|\beta|\Gamma(\alpha)} \quad (1)$$

$$\frac{X-\tau}{\beta} \geq 0,$$

where:
τ – location parameter;
α – slope parameter;
β – scaling parameter;
$\Gamma(\alpha)$ – Gamma function, given by:

$$\Gamma(\alpha) = \int_0^\infty t^{\alpha-1}\exp(-t)dt. \quad (2)$$

Random variable Q_{max} has LP3 distribution, if random variable X

$$X = \ln Q_{max}, \text{ or } X = \log Q_{max} \quad (3)$$

has Pearson III. type distribution (Decadal logarithm will be used in this paper).

Q_{max} input data requirements

The basic assumptions for the application of frequency analysis of the maximum annual Q_{max} series are as follows:

1. The series of maximum annual discharge shall be statistically independent and random;
2. Q_{max} measurements are stationary with respect to time (data series homogeneity);
3. Statistical characteristics of the measured data Q_{max} represent past, present and future.

Estimation of parameters of theoretical Log-Pearson III. type distribution

The method of moments uses the logarithms of flood flows to estimate the distribution parameters. The first three sample moments are used to estimate the LP3 parameters. These include the mean ($\hat{\mu}$), standard deviation ($\hat{\sigma}$), and skewness coefficient ($\hat{\gamma}$). If only systematic data are available, with no historical information, the mean, standard deviation and skewness coefficient of station data may be computed using the following equations:

$$\hat{\mu} = \frac{1}{n}\sum_{i=1}^{n} X_i \tag{4}$$

$$\hat{\sigma} = \sqrt{\frac{1}{n-1}\sum_{i=1}^{n}(X_i - \hat{\mu})^2} \tag{5}$$

$$\hat{\gamma} = \frac{n}{(n-1)(n-2)\hat{\sigma}^3}\sum_{i=1}^{n}(X_i - \hat{\mu})^3, \tag{6}$$

where:
n – number of flood observations Q_{max} series
(ˆ) – represents a sample estimate.

Regional skew coefficient Gr

There is a relatively large uncertainty when estimating the skew coefficient *G* from one water gauge. In series with short observation times, this moment is extremely sensitive to extreme events. In order to better estimate this coefficient for a given river basin, the skew coefficient *G* calculated from one gauge can be combined with the regional coefficient G_r.
If the regional skew coefficient G_r and the skew coefficient *G* from one gauge differ by more than 0.5; the input data and the physical-geographical characterristics of the river basin shall be carefully examined. Depending on the length of the observation, the greater weight can be given by the coefficient *G* calculated from the water gauge. Large deviations between regional coefficients and gauge coefficient may indicate that the characteristics at a given water gauge differ from those of the region.
On the basis of parameters of distribution functions, it is possible to estimate discharge in neighbouring river basins without observation. The estimated skew coefficient *G* of this distribution can be used for regionalization and can then be correlated with the physical-geographical characteristics of the river basin (Pekárová et al., 2018).

Results

Series of maximum annual discharge at Sobotište-Teplica water gauge.

In the first step we estimated the parameters of LP3 distribution line from the short series 2002–2018 for Sobotište-Teplica water gauge (Fig. 5 up). The skew coefficient G_s was 0.12 In the second step, we estimated the distribution curve for the series of whole observation period (Fig. 5 middle). The skew coefficient *G* was 0.07. A comparison of the graphs in Figure 5 up and in the middle shows that the extension of the range slightly increased the estimate of the *1000*-year discharge while at the same time substantially approaching the limits of 5 and 95% of the confidence limits. In Figure 5 in the middle, we can also notice two outlying values of low maximum annual discharge. In the third step we removed outliers from the series of observations as we are interested in the most accurate estimation of the upper extremes (Fig. 5 down). This step leads to *G* with value 0.27.
The regional skew coefficient G_r=0.18 was determined as the arithmetic mean of the coefficients *G* from the Lopašov-Chvojnica, Myjava-Myjava, Šaštín-Stráže-Myjava and Sobotište-Teplica water gauges. These gauges are located in the region based on similar physical-geographical characteristics *M.2 Basins of the left-sided tributaries of Moravia above Myjava* (MŽE, 2003).

Historical floods on the Teplica River

Since the historical floods in the Morava River Basin in the summer of 1997 and 1999, several extreme flood situations have occurred in the Slovak part of the Morava River Basin. These are linked to climate change. But in the history of the region, extreme floods with catastrophic consequences have also occurred in the past.

- The publication of P. Brezina (2017) lists the historical floods in Sobotište from 1630 on page 71. The three largest floods occurred in August 1672, in 1820 and in June 1902. From the flood of 5 June 1902 the house no. 310 retained the flood mark (Fig. 6).
- In the History of the Catholic Parishes of Myjava and Turá Luka, there is a mention of the catastrophic flood of 8 June 1775: "During his time in Myjava, after a storm June 8, 1775, a tragic flood came. For this reason, in December 1784 Myjava received support for the regulation of the river, thanks to which a river bed in the area of today's city was excavated".
- In the chronicle of the town Senica for the years 1936–1954 we found information about the floods on the Teplica River (there Vrbovčianka), 15 May 1939 (p. 169), 9 July 1943 (p. 202) and 30 April 1953 (p. 373).

River bed changes in the center of Sobotište village can be seen in Figure 7.

Supplementing historical floods in the skew coefficient estimation on the example on Teplica in Sobotište

Based on the field survey of the height of the flood mark from 1902 in Sobotište (the level in 1902 was 84.5 cm higher than the level of the 1997 flood), we estimated the maximum discharge from the 1902 flood on 80 $m^3 s^{-1}$ (Fig. 8).
We estimated the discharge for the flood in 1939 on the basis of historical records at 40 $m^3 s^{-1}$. We added these values to the calculation when estimating the skew coefficient G_h of theLP3 distribution including historical floods (Fig. 9).
The skew coefficient changed to 0.33. The resulting *T*-year discharge is shown in Table 2. From the values in the table, we can see that the uncertainty of the determination of 2*00*- to *1000*-year discharge values is still very high despite a thorough statistical analysis.

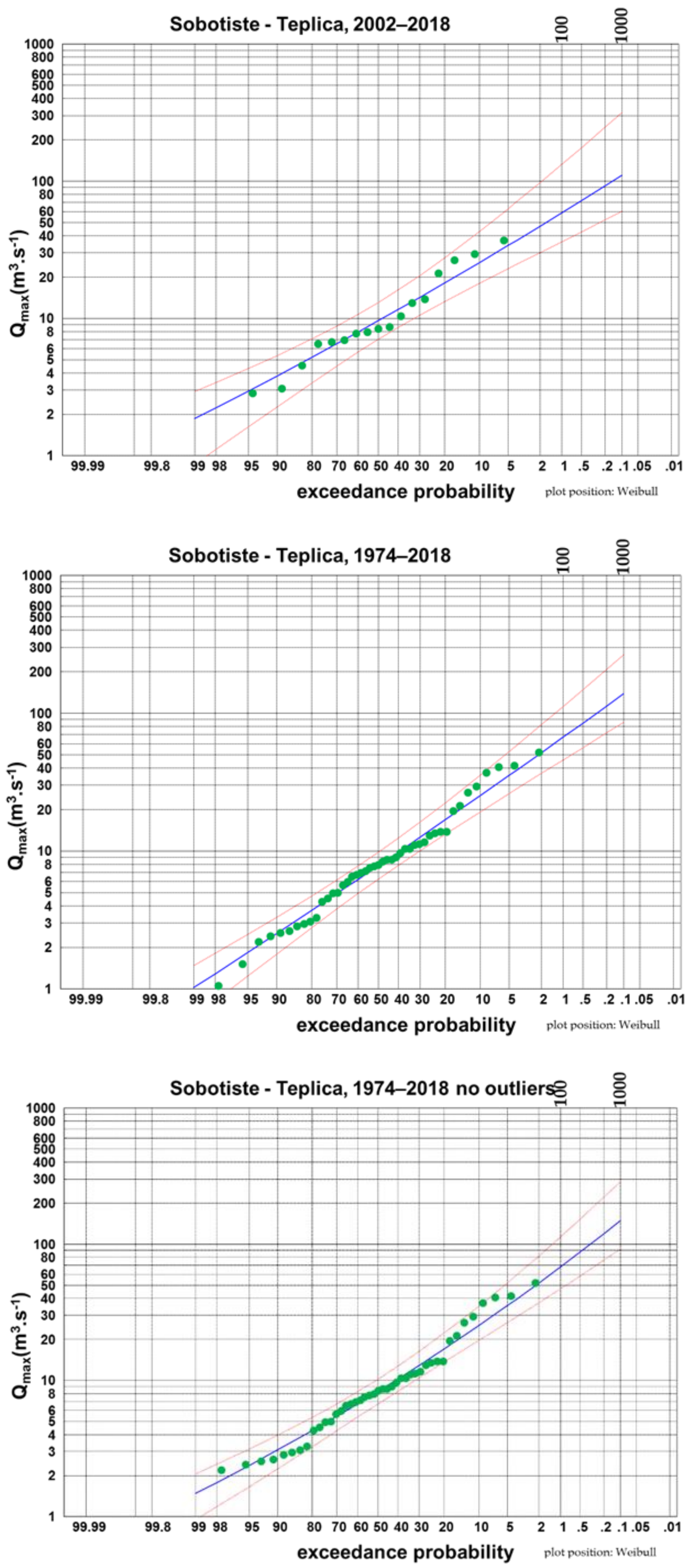

Fig. 5. Theoretical Log-Pearson III. type distribution curve of maximum annual discharge series from the water gauge Sobotište-Teplica, 5% and 95% confidence intervals, short period 2002–2018 – up; whole period 1974–2018 – middle; period 1974–2018 without outliers – down.

Fig. 6. *Location of the flood mark from June 5, 1902 in Sobotište, level of flood in 1902 and 1997.*

Fig. 7. *Development of built-up area and bed of the Teplica River in the centre of the Sobotište village and historical floods. Source: Brezina (2017), author.*

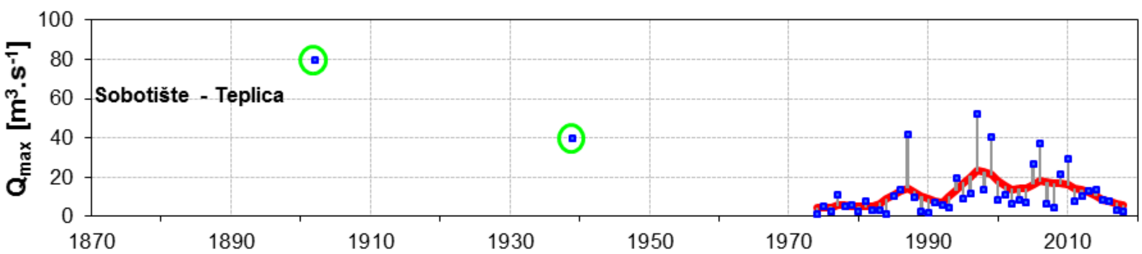

Fig. 8. *Example of measured series of the maximum annual discharge (per hydrological year), deviations from moving averages, historical floods 1902 and 1939 on Teplica at Sobotište water gauge.*

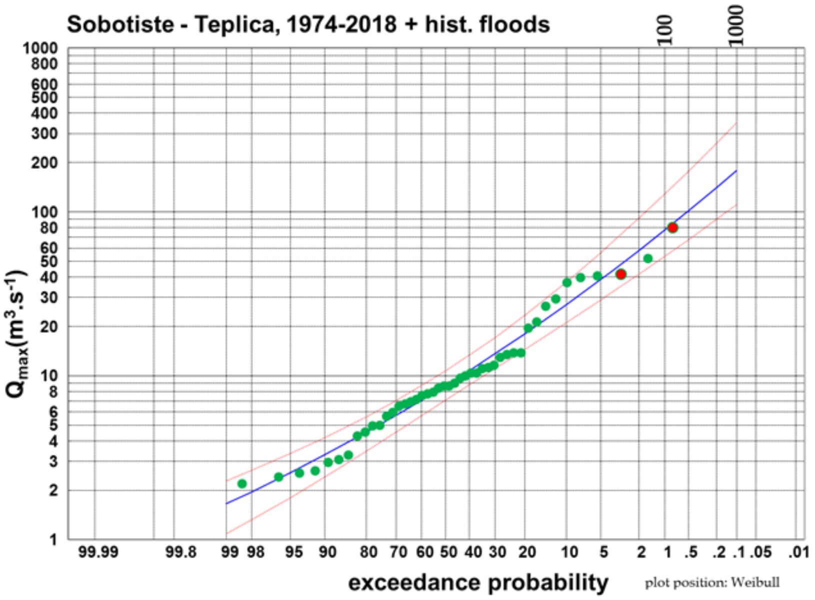

Fig. 9. Theoretical Log-Pearson III. type distribution line of maximum annual discharge series including historical floods from the water gauge Sobotište-Teplica, 5% and 95% confidence intervals.

Table 2. Estimated *T*-year discharge *Q* [m^3 s^{-1}] and specific runoff q [l s^{-1} m^2] at the water gauge Sobotište-Teplica with inclusion of historical floods, 5% and 95% confidence intervals

ID	gauge		*Q100*	*Q200*	*Q500*	*Q1000*	*q100*	*q200*	*q500*	*q1000*
5025	Sobotište	*T*-year	77	101	141	179	897	1176	1642	2085
		5%	128	176	263	350	1491	2050	3063	4077
		95%	53	67	90	111	617	780	1048	1293

Conclusion

In this paper we presented one of the methods for estimation of discharge with long return period. We used Log-Pearson III. type distribution, which contain parameter skewness coefficient. This parameter is related to physical-geographical characteristics of catchment and could be regionalised. So it is possible to use regional skewness coefficient to refine distribution and reduce uncertainty in discharge design values.

Estimation of discharge design values with long return period (*200-*, *500- to 1000-year*) from short series of observations (cca 50 years) is burdened by high uncertainty. That is the reason why it is necessary to search as much information about historical floods in individual locations. An important role in reducing the uncertainty of the determination of these design values by statistical methods is played by flood marks installed directly on historical buildings near rivers. Assuming there were no significant changes in the terrain (bed regulation, new buildings near the river), it is possible to estimate the maximum discharge based on the flood mark height.

Based on the historical flood mark in the Sobotište village dated June 5, 1902, we estimated the maximum discharge of this flood on the Teplica River at 80 m^3 s^{-1}. This value and the estimated value of the 1939 flood were entered into the calculation of the design values using the theoretical LP3 distribution. After prolonging the series of observations, removing outliers, recalculating according to the regional skewness coefficient and then including historical floods, we achieved a narrowing of the design values range. On the Teplica River at water gauge Sobotište we estimated discharge with return period 1000 years in range between 111 and 350 m^3 s^{-1} with mean value 179 m^3 s^{-1}.

Acknowledgements:

This work was supported by the projects Doktogrant and VEGA 2/0004/19.

References

Brazdil, R., Kundzewicz, Z. W., Benito, G. (2006): Historical hydrology for studying flood risk in Europe. Hydrological Science J., 51(5), 739–764, DOI:10.1623/hysj.51.5. 739.

Brezina, P. (2017): Sobotište na pohľadniciach a fotografiách. Obecný úrad Sobotište, 248 s.

Dysarz, T., Wicher – Dysarz, J., Sojka, M., Jaskuła, J. (2019): Analysis of extreme flow uncertainty impact on size of flood hazard zones for the Wronki gauge station in the Warta river. Acta Geophysica https://doi.org/10.1007/s11600-019-00264-8, 16 pp.

Gaal, L., Szolgay, J., Kohnova, S., Hlavcova, K., Viglione, A. (2010a): Inclusion of historical information in flood frequency analysis using a Bayesian MCMC technique: A case study for the power dam Orlik, Czech Republic, Contributions to Geophysics and Geodesy, 40, 2, 121–147.

Gaál, L., Szolgay, J., Kohnová, S. (2010b): Zohľadnenie historických povodní pri štatistickom určovaní návrhových maximálnych prietokov. Povodne 2010: Príčiny, priebeh a skúsenosti. Štrbské Pleso, VÚVH, 7 s.

Griffis, V. W., Stedinger, J. R. (2009): Log-Pearson type 3 distribution and its application in flood frequency analysis, III–sample skew and weighted skew estimators, Journal of Hydrology, 14, 2, 121–130.

IACWD (1982): Guidelines for determining flood flow frequency, Bulletin 17-B. Technical report, Interagency Committee on Water Data, Hydrology Subcommittee. 194 s.

Kohnová, S., Gaál, L., Bacigál, T., Szolgay, J., Hlavčová, K., Valent, P., Parajka, J., Blöschl, G. (2016): Process-based selection of copula types for flood peak-volume relationships in Northwest Austria: a case study. In Contributions to Geophysics and Geodesy. 46, 4, 245–268.

Kohnová, S., Szolgay, J. (2003): Regional estimation of the index flood and the standard deviation of the summer floods in the Tatry mountains. J. Hydrol. Hydromech., 51, 4, 241–255.

Kohnová, S., Szolgay, J., Hlavčová, K. (2006a): Hydroinformatika – Nové štatistické metódy odhadu návrhových prietokov a zrážok pre dimenzovanie hydrotechnických stavieb. STU Bratislava.

Kohnová, S., Szolgay, J., Solín, Ľ., Hlavčová, K. (2006b): Regional methods for prediction in ungauged basins. Key Publishing, Ostrava, 113 s.

Koutsoyiannis, D. (2008): Probability and statistics for geophysical processes, National Technical University of Athens, Athens.

Merz, B., Thieken, A., H. (2009): Flood risk curves and uncertainty bounds. Natural Hazards, 51, 3, 437–458.

Merz, R., Blöschl, G. (2008a): Flood frequency hydrology: 1. Temporal, spatial, and causal expansion of information. Water Resources Research, 44, 8, article number W08432, 17 pp.

Merz, R., Blöschl, G. (2008b): Flood frequency hydrology: 1. Temporal, spatial, and causal expansion of information, Water Resources Research, 44, W08432.

Mészáros, J., Pekárová, P., Pekár, J., Melová, K. (2019): Odhad N-ročných prietokov použitím regionálneho koeficientu šikmosti Log-Pearsonovho rozdelenia III. typu. Acta Hydrologica Slovaca, 20/1, 22–31.

Millington, N., Das, S., Simonovic, S. P. (2011): The Comparison of GEV, Log-Pearson Type 3 and Gumbel Distributions in the Upper Thames River Watershed under Global Climate Models. Water Resources Research Report. Department of Civil and Environmental Engineering, The University of Western Ontario London, Ontario, Canada, September 2011, 1–54.

MŽP (2003): Kvantita povrchových a podzemných vôd. Hydrologické údaje povrchových vôd. Kvantifikácia povodňového režimu. Časť1: Stanovenie N-ročných prietokov a N-ročných prietokových vĺn na väčších tokoch. Odvetvová technická norma OTN ŽP 3112–1:03, MŽP SR, Bratislava, 31 s.

Naghavi, B., Cruise, J. F., Arora, K. (1990): Comparative evaluation of three estimators of log Pearson type 3 distribution. Transportation Research Record, 1279, 103–112.

Pekár, J., Pekárová, P., Bačová Mitková, V., Holko, L., Kostka, Z. (2012): Historické povodne, regionalizácia a návrhové hodnoty N-ročných prietokov s krátkou dobou pozorovania v regióne Západných Tatier. Acta Hydrologica Slovaca, 13/1, 153–164.

Pekárová, P., Bačová Mitková, V., Pekár, J., Miklánek, P., Halmová, D., Liová, S. (2018): Historické povodne na území Slovenska a ich význam v hydrológii. Veda, vydavateľstvo Slovenskej akadémie vied, 135 s. ISBN 978 -80-224-1684-9.

Pekárová, P., Halmová, D., Bačová Mitková, V., Miklánek, P., Pekár, J., Škoda, P. (2013). Historic flood marks and flood frequency analysis of the Danube River at Bratislava, Slovakia. J. Hydrol. Hydromech., 61, 4, 326–333.

Phien, H. N., Jivajirajah, T. (1984): Applications of the log Pearson type-3 distribution in hydrology, Journal of Hydrology, 73, 359–372.

Pilon, P. J., Adamowski, K. (1993): Asymptotic variance of flood quantile in log Pearson type III distribution with historical information, J. of Hydrol., 143, 3-4, 481–503.

Rogger, M., Kohl, B., Pirkl, H., Viglione, A., Komma, J., Kirnbauer, R., Merz, R., Blöschl, G. (2012): Runoff models and flood frequency statistics for design flood estimation in Austria – Do they tell a consistent story? J. Hydrol., 456–457.

SHMÚ (2017): Hydrologická ročenka. Povrchové vody 2017. SHMÚ, Bratislava. 225 s.

Šipikalová, H. (ed.) (2006): Spracovanie hydrologických charakteristík – *N*-ročné maximálne prietoky. SHMÚ, Záverečná správa čiastkovej úlohy 5303-00. 90 s.

Stănescu, V. A. (2004): Regional analysis of annual peak discharges in the Danube Catchment. The Danube and its catchment–A hydrological Monograph, Followup volume VII. Regional Co-operation of the Danube Countries in the Frame of the International Hydrological Programme of UNESCO, Bucharest.

Zítek, J. (1967): Hydrologické poměry Československé socialistické republiky. Díl II. Hydrometeorologický ústav, Praha. 557 s.

Internet sources

Dejiny katolíckych farností v Myjave a Turej Lúke [online]. [cit. 2020-02-21]. Available on the Internet: http://www.rkmyj.szm.com/historia.htm

Kronika mesta Senica [online]. [cit. 2020-02-23]. Available on the Internet: http://kronika.senica.sk/1936-1954/#172

RNDr. Jakub Mészáros (*corresponding author, e-mail: hydrjaku@uh.savba.sk)
RNDr. Pavla Pekárová, DrSc.
Institute of Hydrology SAS
Dúbravská cesta č. 9
841 04 Bratislava
Slovak Republic

Doc. RNDr. Ján Pekár, CSc.
Comenius University in Bratislava
Faculty of Mathematics, Physics, and Informatics
Department of Applied Mathematics and Statistics
Mlynská dolina,
842 48 Bratislava
Slovak Republic

DOI: 10.31577/ahs-2020-0021.01.0004

ACTA HYDROLOGICA SLOVACA

Volume 21, No. 1, 2020, 29 – 38

BIVARIATE JOINT PROBABILITY ANALYSIS OF FLOOD HAZARD AT RIVER CONFLUENCE

Veronika Bačová Mitková*

Assessing the statistical significance of floods in the complex hydrological conditions that exist at the confluence of the main river and its tributaries, as well as the choice of hydrological design parameters for flood protection in these areas is one of the main tasks in the current hydrology. The main aim of this paper is a joint bivariate frequency analysis of annual peak discharges and synchronously occurred maximum discharges at the main river and its tributary. The annual maximum and daily maximum discharges of the Morava River, as main river, and its tributary Myjava River were analysed. We selected the most appropriate copula function for our bivariate analysis. Selected copulas were used to illustrate the joint occurrence probabilities and joint return periods of the discharge pairs and consequently to determine the joint probabilities of measured discharges. Results of such analyses provide comprehensive information about flood situations where a devastating effect may be increased in the case were floods occur at the same time on the main river and its tributary. And at the same time, the results obtained by the bivariate analysis of the variables which characterize the hydrological regime can contribute to a more reliable assessment of the flood risks.

KEY WORDS: maximal mean daily discharge, annual peak discharges, corresponding discharge, joint probability distribution, copula function.

Introduction

Flood wave is the result of the numerous natural processes, such as rainfall distribution and intensity, catchment characteristics and its area, land use, water reservoirs, etc. The determining of the flood wave significance for design of the water management project is based on adequate mathematical technique such as statistical theory of probability. The basic mathematical technique is based on the evaluation of the selected one dimensional variable, which characterizes some extreme event. It is established that, during the flood wave occurrence there is correlation between some hydrological characteristics (discharge, duration, volume) which may have an impact on the design of flood control measures. Therefore, a multidimensional approach to analysing hydrological characteristics is increasingly preferred in many studies (e.g. Yue, 2000; Hawkes et. al., 2002; Favre et al., 2004; De Michele et al., 2005; Szolgay et al., 2016; etc.).
Regulation of rivers as well as adjustments of the river basins often brings changes in concentration of basins drainage as well as increasing of the speed of flood wave. One of a result of such interventions, it may be coincidence of the waves on the main river and its tributary. Therefore, the one dimensional approach gives satisfactory results in the case of simple systems, for example, where the main river does not capture major tributaries. One dimensional approach may not give satisfactory results for the evaluation of flood risk in situations where floods occur on two or more rivers and join together at the same time. The bivariate statistical approach to analysis of flood events should be further developed and defined at neighbouring profiles on the main river and its tributaries.
Prohaska et al. (1999) dealt with synchronously occurring flood waves on the Danube and its tributaries. Their analysis was based on the theory of bivariate variable statistics and results confirmed that flood wave genesis is very complex within the Danube basin. In Slovak territory the coincidence of multiple flood waves caused the flood with time return period of 100-year on Tisa and Bodrog River in year 2000. For example the flood occurred in August, 2002 in Czech Republic on the Vltava River and Dyje River showed an increase in return period of the discharges with an increase in area of the basin. It was caused by coincidence of the flood waves in profiles of the river network (Report of T. G. Masaryk Water Research Institute, 2002). Chen et al. (2012) dealt with analysing the flood risk due to the correspondence of flood discharges at the main river and its tributaries using selected marginal probability distributions and multidimensional (4D) copula functions. Authors evaluated X-Gumbel copula function as appropriate for joint conditional distribution function and

return periods of joint discharges. Espinoza et al. (2013) analysed formation of the floods on the Amazonia River and its tributary. They focused on the flood occurred in 2012, when coincidence of two large flood waves has occurred. The coincidence of flood peaks from the Changjiang River and four other rivers, and the highest precipitation disaster drivers for Dongting Lake region flood vulnerability was study in Li et al. (2013). Joint probability of two random variables in contrast to the conditional probability reflects the probability with which the two random variables occur simultaneously. Gupta et al. (1976) dealt the using of the joint distribution function in estimating relationship of the large floods and their return period taking into account the seasonal influences. Bender et al. (2016) analysed flood peaks of two streams where was unlikely that all block maxima values occurred simultaneously. They concluded that in the majority of cases four marginal distributions and two distinct joint distribution functions are required to fully describe the stochastic behaviour of the system. Gilja et al. (2018) dealt with joint frequency analysis at the river confluences. The research conducted that flood hazards at the Sava River could be underestimated by traditional univariate analysis. Tadić et al. (2016) analysed the joint occurrence probability of floods on the Rivers Danube and Drava near Osijek. Their results showed that the probability of such situation is low (0.79%) but they reminded that such a situation occurred in 1966 and it was one of the biggest floods. Therefore, the results obtained by the bivariate analysis of the variables which characterize the hydrological regime can contribute to a more reliable assessment of the flood risks.

The main aim of this research is to analyse the floods occurred at the Morava River and its tributary Myjava and provide a practical approach for the designed flood estimation in areas of the rivers confluence. In the context of climatic extreme events, statistical techniques such as event coincidence analysis will be relevant for investigating the impacts of anthropogenic climate change on human societies and ecosystems globally. The results obtained by the bivariate (as well as threevariate) analysis of the variables which characterize the hydrological regime can contribute to a more reliable assessment of the flood risks.

In this research we focus upon an:

- description of the methodological approach;
- preparing of the data and identification of the variable pair combination for analysing the relationship between flood wave discharges on the main river and its tributary;
- identify univariate distribution function of the variables (discharges) of the main river and tributary;
- identify bivariate joint distribution function of the selected pair;
- compare joint exceedance probability with univariate flood frequency analysis based on the measured values on downstream of the confluence.

Methodology

Copula functions were used as a mathematical tool for determining a joint cumulative distribution of two dependent variables. According the Sklar (1959) theory for two dimensional (bivariate) distribution function $H_{(x,y)}$, we can write:

$$H_{(x,y)}=C(F_{(x)},F_{(y)}) \tag{1}$$

where $F_{(x)}=u$ and $F_{(y)}=v$ are marginal distribution functions. If $F_{(x)}$ and $F_{(y)}$ are continuous, then the copula function C is unique.

The identification of the univariate (marginal) distribution is the first step of the bivariate analysis. The random variables may have different properties and thus need to be converted to variables having interval of [0, 1] by scaling the data. Knowing the marginal distribution, we are able to separate marginal behaviour and dependence structure. The dependence structure is fully described by the joint distribution of uniform variables obtained from marginal distribution. To determine univariate parametric distribution functions (marginal distributions), standard MLM (maximum likelihood method) method was used. According to the goodness-of-fit tests (Kolmogorov-Smirnov and $\chi 2$) the marginal distributions can be selected.

In our study we used the Archimedean class of copula functions. Among existing types of copulas, the Archimedean one is the very popular class used in hydrological application (Zhang and Sing, 2006; Favre et al., 2004; De Michele et al., 2005; Gargouri-Ellouze and Eslamian, 2014; Dehghani, 2019 etc.). This class of copulas is popular in empirical applications for flexibility, easy construction and includes a whole suite of closed-form copulas that covers a wide range of dependency structures, including comprehensive and non-comprehensive copulas, radial symmetry and asymmetry, and asymptotic tail dependence and independence. The Clayton, Gumbel-Hougaard and Frank copulas were selected for this study (Table 1). The copula parameter θ was estimated using a mathematical relationship between the Kendall`s coefficient of rank correlation and the generating function $\varphi(t)$ (Nelsen, 2006).

Testing how well a statistical model (copula in this case) describes a set of observations is discussed as a topic in literature (e.g. Kojadinovic and Yan, 2011; Karmakar and Simonovic, 2009; Shiau et al., 2010; Chowdhary et al., 2011; Genest et al., 2009; Bender 2016). According to Meylan et al. (2012) we can divide these tests into three groups: a) based on probability integral transformation; b) based on the kernel estimation of the copula density and c) based on the empirical process of copulas. The first implies conditioning on successive components of the random vector and has the drawback of depending on the order in which this conditioning is done. The second category of tests depends on various arbitrary choices, such as the kernel, the window size and the weight function, which make their application cumbersome. Several goodness-of-fit tests can be used for comparison of the empirical joint probability population and the probability population derived by parametric copulas (e.g. Kolmogorov-Smirnov, Ci-square,

Table 1. **Probability functions, parameter space, generating function and relationship of non-parametric dependence measure with association parameter for the selected Archimedean copulas**

Copula function	*C (u, v, θ)*	parameter θ	Kendall's τ	Generator *φ(t)*
Clayton	$(u^{-\theta}+v^{-\theta}-1)^{-1/\theta}$	$[-1,\infty)$ /{0}	$\frac{\theta}{\theta+2}$	$\frac{1}{\theta}(t^{-\theta}-1)$
Gumbel-Hougaard	$\exp\left[-((-\ln u)^{\theta}+(-\ln v)^{\theta})^{1/\theta}\right]$	$[1,\infty)$	$\frac{\theta-1}{\theta}$	$(-\ln t)^{\theta}$
Frank	$-\frac{1}{\theta}\ln[1+\frac{(e^{-\theta u}-1)(e^{-\theta v}-1)}{(e^{-\theta}-1)}]$	$(-\infty,\infty)$/{0}	$1+\frac{4}{\theta}[D_1(\theta^*)-1]$	$-\ln\frac{e^{-\theta t}-1}{e^{-\theta}-1}$

Anderson-Darling or Cramér-von-Mises).
The empirical probability (Gringorten, 1963; Cunnane, 1978; Yue et al., 1999; Zhang and Singh, 2006) represents Equation (2).

$$F(x,y)=P(X\le x_i, Y\le y_j=\frac{\sum_{m=1}^{i}\sum_{l}^{i}n_{ml-0.44}}{N+0.12} \qquad (2)$$

where N is the total number of the variables, j and i ascending ranks of x_i and y_i , n_{ml} is the number of occurrence of the combinations of x_i and y_j.

In hydrological frequency analysis, the return period of the hydrological variable that occurs once in a year can be defined as:

$$T=\frac{1}{P(X\le x)}=\frac{1}{\lambda\,(1-F(x))}. \qquad (3)$$

where T is the return period in years and $F_{(x)}$ is univariate cumulative distribution function and λ represents average number of events per year. In frequency analysis of annual maximum value of λ is equal (1).

In multivariate statistical analysis, we can determine the return period of the phenomenon in two ways. The first is a joint return period, while the second is a conditional return period. The first one defines joint return periods as: the return periods using one random variable equalling or exceeding a certain magnitude and/or using another random variable equalling or exceeding another certain magnitude. The second one is conditional return period for one random variable, given that another random variable equals or exceeds a specific magnitude.
Joint return period for two variables defined by more authors (Shiau, 2003; Salvadori and De Michele, 2006) and it can be written in the form of:

$$T^{and}{}_{x,y}=\frac{1}{\lambda(1-F(x)-F(y)+H(x,y))} \qquad (4)$$

or

$$T^{or}{}_{x,y}=\frac{1}{\lambda(1-H(x,y))} \qquad (5)$$

Equation (4) represents the joint return period of $X\ge x$ *and* $Y\ge y$. Equation (5) represents joint return period of $X\ge x$ *or* $Y\ge y$. These relationships indicate, that different combinations of the numbers x and y, can take same return period (relation 8). $H(_{x,\,y})$ is the joint cumulative distribution function (can be expressed as copula function).

$$T^{or}(x,y)\le\min\left[T_x,T_y\right]\le\max\left[T_x,T_y\right]\le T^{and}(x,y) \qquad (6)$$

Conditional return period for X, given $Y\ge y$ may be expressed as (Shiau, 2003):

$$T_{(x|Y\ge y)}=\frac{1}{\lambda(1-F(y))(1-F(x)-F(y)+H(x,y))} \qquad (7)$$

where x and y are random variables and $H_{(x,\,y)}$ is the joint cumulative distribution function. Conditional cumulative distribution function of X, given $Y\ge y$ may be expressed as:

$$F_{(x|Y\ge y)}=\frac{F(y)-H(x,y)}{1-F(y)} \qquad (8)$$

where $H_{(x,\,y)}$ is the joint cumulative distribution function of the random variables X and Y, and $F_{(y)}$ is cumulative distribution function of the variable Y. An equivalent formula for conditional return period of $Y\ge y$, given $X\le x$ can be obtained.

Study area

The paper is focused on the bivariate analysis of the floods occurred at the main river and its tributary for the designed flood estimation in areas of the rivers confluence.
The Morava is a left tributary of the Danube River in Central Europe. The length of the Morava River is 329 km and its basin area covers 26 579.7 km^2. The river originates on the Králický Sněžník mountain near the border between the Czech Republic and Poland and has a vaguely southward trajectory. The lower part of the river's course forms the border between the Czech Republic and Slovakia and then between Austria and Slovakia.

The Myjava River is a river in western Slovakia and for a small part in the Czech Republic and left tributary of the Morava River. The length of the Myjava River is 79 km and its basin area is 806 km^2. It rises in the White Carpathians near the village of Nová Lhota in Moravia, but crosses the Czech-Slovak border shortly afterwards and flows in a southern direction until the town of Myjava, where it enters the Myjava Hills and turns west. Near Sobotište it flows into the Záhorie Lowland and turns south until the village of Jablonica, turning north-west and from Senica it flows west, passing through Šaštín-Stráže and finally flowing into the Morava River near Kúty. Table 2 lists selected main river, tributary, gauging stations and measurement period. The first year of the analysed period is the beginning of data measurements in current stations. The scheme of the selected rivers confluence is presented in Fig.1.

Preparing of the data

With regard to flood coincidence analysis, it is necessary to consider gauging stations immediately downstream and upstream from the tributary. In our work we investigated combination of the first pairs of Q_{amaxup} –Q_{amaxtr} and second pairs of Q_{maxup} – Q_{cor1tr}.
Where:
Q_{amaxup}, $Q_{amaxdwn}$, Q_{amaxtr} – are annual peak discharges on upstream and downstream on main river and the annual maximum discharges on tributary;
Q_{maxdwn} – is maximum daily discharge on the main river downstream from the confluence (same event like in upstream station);
Q_{maxup} – is maximum daily discharge on the main river upstream from the confluence;
Q_{cor1tr} – is corresponding discharge on the tributary in the moment of occurrence of the maximum daily discharge on the main river upstream from the confluence (may be moved one or two days).

Discharges time series of the annual peak discharges Morava and Myjava reveal that high annual peaks at the Myjava River do not frequently coincide with high annual peaks at Morava River (Fig. 2).
The analysis of flood hazard is based on the continuous record of discharges on a gauging station that reflects water regime in particular section. As the first we analysed pairs of annual peak discharges Q_{amaxup} – Q_{amaxtr}. In this study only the combination of the values of annual peak discharge were analysed not they occurrence within the year. Selected and analysed pairs of annual peak discharges Morava – Myjava confluence are presented in Fig. 3a. The linear Pearson correlation coefficient of this pairs is R=0.63 and Kendall rank correlation coefficient is τ=0.42.
The annual maximum (AM) series approach is the most frequently used in probabilistic hydrology. But this data series are limited by two factors: 1) the length of the series of annual maxima can be very short and 2) the annual maxima time-series may be interrupted and thus they may not allow us to infer the antecedent conditions in the basin preceding a given peak. The first limiting factor produces uncertainties in interpreting statistical analyses, while the latter constrain implies that statistical models built on a phenomenological basis must rely on ancillary data in order to validate the underling hypotheses (Claps and Lio, 2003). This situation is avoided in the Peaks Over Threshold method (POT). Data series of the POT method consider all values exceeding a certain predefi-

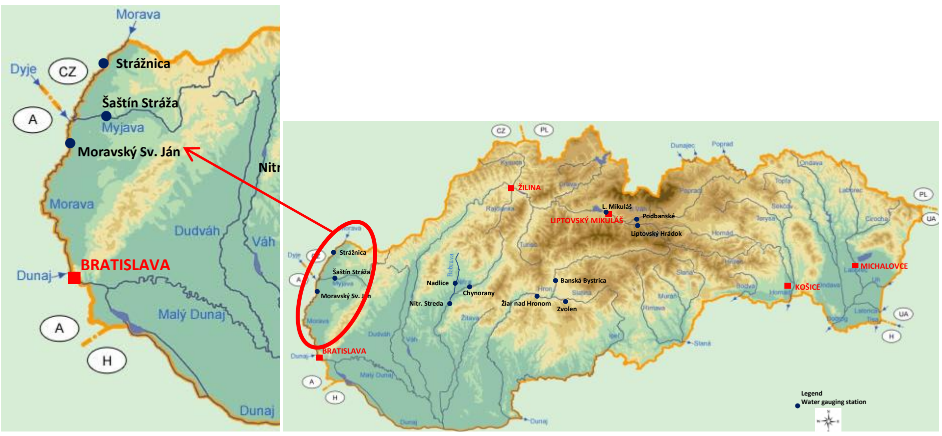

Fig. 1. The map of the Morava and Myjava confluence.

Table 2. Selected main river and tributary, gauging stations and analysed periods

River	Gauge station	River kilometer [km]	Q_{amax} [m^3 s^{-1}]	period
Morava	Strážnica (CZ)	133.5	901	1968–2011
	Moravský Svätý Ján (SK)	67.15	1502	1968–2011
Myjava	Šaštín Stráža (SK)	15.18	82	1968–2011

ned threshold (Bayliss, 1999; Rao and Hamed, 2000). The POT method has been proposed as an alternative analytical tool to the AM approach in analysis of extreme hydrological events. This method was discussed in a number of papers (Langbein, 1949; Todorovic, 1970; Cunnane, 1973; Rosbjerg, 1977; Madsen at al., 1997a; Madsen at al., 1997b; Lang at al., 1999; Bača and Bačová Mitkova, 2007; Bačová Mitková and Onderka, 2010). Therefore, in practice it seems to be more meaningful to consider not only the annual discharge maxima but also flood events that exceed safety limits. The first threshold can be chosen near the long-term mean discharge. This value is rather low; POT series can have high diffusion and can include some insignificant maxims. Therefore, a threshold value is usually chosen so that POT data series includes in average 4 maximum values per year and flood events must be independent (Bayliss, 1999). The threshold value in our calculations was appointed at the level of 40–50% of the long-term maximum annual discharge in order to ensure the independence of the waves and to include all significant events in the analysed year. On the basis of daily discharges and POT method the flood waves were selected for bivariate statistical analysis. The maximum mean daily discharges and synchronous discharges according to the above mentioned scheme were selected.

The pairs of maximum daily discharges and correspondding daily tributary discharges of the Morava – Myjava confluence based on POT method are presented in Fig. 3b. The linear the Pearson correlation coefficient of this pairs are R=0.57 and Kendall rank correlation coefficient is τ=0.37.

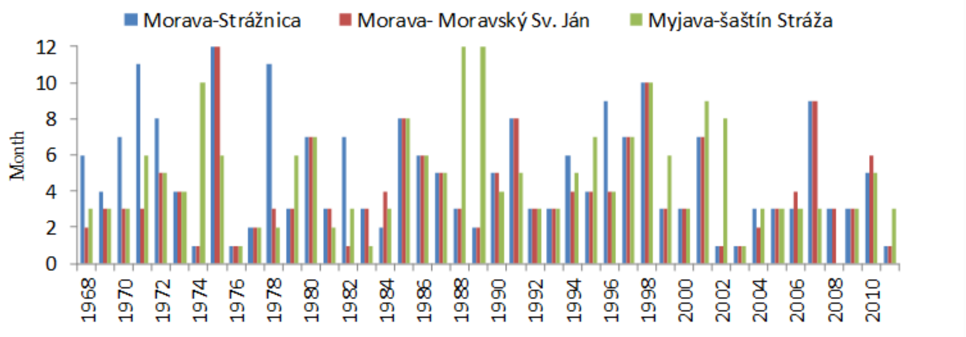

Fig. 2. Occurrence of the annual peak discharges during within the year (1968–2011).

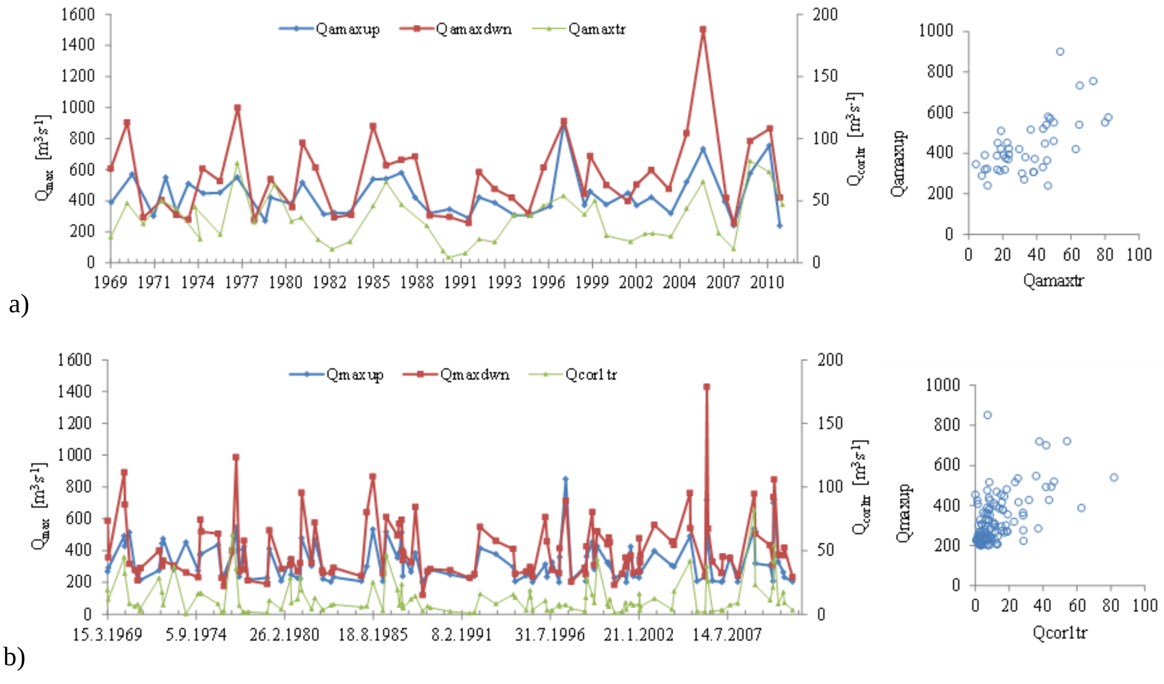

Fig. 3. Selected and analysed pairs of a) annual peak discharges Morava – Myjava confluence and b) maximum daily discharges and corresponding daily discharge Morava – Myjava confluence (based on POT method).

The results of the correlation analysis of different combinations of the variables (discharge) show a statistically significant correlation. All of the combinations of the variables can be used on the following bivariate joint frequency analysis to investigate, how the relationship of the hydrological characteristics may affect the size and course of extreme hydrological situations.

Univariate Analysis

In order to determine univariate parametric distribution functions (marginal distributions), standard MLM (maximum likelihood method) method was used. According to the goodness-of-fit test (Kolmogorov-Smirnov) the marginal distributions where selected.
The variables of the annual maximum (AM) approach were preferable fitted with Gumbel, Gamma and LogPearson III. The Gumbel distribution is asymmetric, extreme value distribution (EVD) and is used to model the distribution of the maximum (or the minimum). The Gamma two-parametric distribution is a very important model in statistical hydrology. It is a flexible function capable taking many different shapes and has been widely used in many countries for flood series modelling. The Pearson type III distribution is sometimes called three-parameter Gamma distribution, since it can be obtained from the two-parameter Gamma distribution by introducing location parameter τ. It is very flexible since it has three parameters which can produce a wide variety of shapes of density function.
The variables derived by POT method was preferably fitted with distributions JohnsonSB, Gamma and LogPearson III. The JohnsonSB distribution is a continuous four-parametric distribution defined on bounded range, and the distribution can be symmetric or asymmetric. The Kolmogorov-Smirnov test was performed to test the assumption that the discharge magnitudes follow the theoretical distributions. The *p*-value ($p \geq 0.05$) was used as a criterion for rejection of the proposed distribution hypothesis. The fitted distributions, *p*-value of the goodness-of-fit test and calculated designed discharges are presented in Table 3. We cannot reject the hypothesis that selected distributions fit well to the observed data at a 5% significance level. Comparison of the AM and POT approaches shows significant differences (in average 13%) for discharges with return period of 50 and 100 years on tributary. The lower estimated values of designed discharges may be result of the creation of the analysed POT data series, especially for tributary where are corresponding discharges with Q_{maxup} and not only Q_{maxtr}. It effects the estimation of Q_N.

Joint bivariate analysis of the discharges at the rivers confluence using copulas

The joint probability distribution of two hydrologic variables at the confluence was evaluated by copulas to calculate the joint exceedance probability for the analysation of the flood hazard occurred at the confluence of the main river and its tributary. Results of the correlation show that there is a strong positive dependence between the discharges at river confluence with values of Kendall`s coefficient of rank correlation ranked over 0.3. The values of the estimated parameters of selected Archimedean copula functions are listed in Table 4.
Results of the comparison of the joint empirical probabilities with fitted parametric copula showed that computed errors of the estimation reached relatively small differences between all three tested Archimedean copula functions (Fig. 4). The Kolmogorov-Smirnov test was performed to test the assumption that the joint pair magnitudes follow the theoretical joint distributions (copula). The *p*-value ($p \geq 0.05$) was used as a criterion for rejection of the proposed distribution hypothesis. The fitted joint distributions (copula) and *p*-value of the goodness-of-fit test are presented in Table 4. We cannot reject the hypothesis that selected joint distributions fit well to the observed data at a 5% significance level. Based on the results of non-parametric test the all three Archimedean copula functions were used to determine the joint probability distribution of the pair variables.
Subsequently, the all selected copula functions were used for simulation of 3000 pairs for all combination of variables on selected river (Fig. 5). The figures show the scatter plot of measured data pairs and simulated values generated from copula models for the discharge pairs at the confluence. Simulated pairs were performed to determine the joint probability distribution using copulas and consequently to determine the joint occurrence probability of the variables. For traditional method, the resulting discharge for the selected return period is

Table 3. Best fitted parametric univariate distributions of the variables and *p*-values of the Kolmogorov-Smirnov test (α=0.05)

Confluence	Q [m^3 s^{-1}]	λ	Distr.	*p*-value	Estimated Q_N [m^3 s^{-1}]					Measured Q_{max} [m^3 s^{-1}]	
					Q_{50}	Q_{100}	Q_{200}	Q_{500}	Q_{1000}	Q_{amax} Q_{max}	T [year]
Morava Myjava	Q_{amaxup}	1	Gumbel	0.96	791	867	942	1041	1116	901	137
	Q_{amaxtr}	1	Gamma	0.8	87	97	107	119	129	82	37
	$Q_{amaxdwn}$	1	LogPear III.	0.51	1293	1489	1699	1999	2246	1506	106
	Q_{maxup}	2.6	Jon SB	0.48	798	863	920	983	1025	850	96
	Q_{cor1tr}	2.6	Gamma	0.51	77	86	98	112	119	82	74
	Q_{maxdwn}	2.6	LogPear III.	0.55	1223	1416	1624	1942	2190	1430	105

Table 4. Copula parameters (C – Clayton, G-H – Gumbel-Hougaard, F – Frank), selected combinations of the variables

Confluence	pair	R_{meas}	τ_{meas}		Clayton	Gumbel-Hougaard	Frank
						parameter	
Morava – Myjava	$Q_{amaxup} - Q_{amaxtr}$				*1.45*	*1.7*	*4.4*
		0.63		R_{sim}	0.46	0.68	0.54
			0.42	τ_{sim}	0.42	0.43	0.42
	$Q_{maxup} - Q_{cor1tr}$				*1.2*	*1.6*	*3.9*
		0.57		R_{sim}	0.35	0.62	0.42
			0.37	τ_{sim}	0.36	0.38	0.36

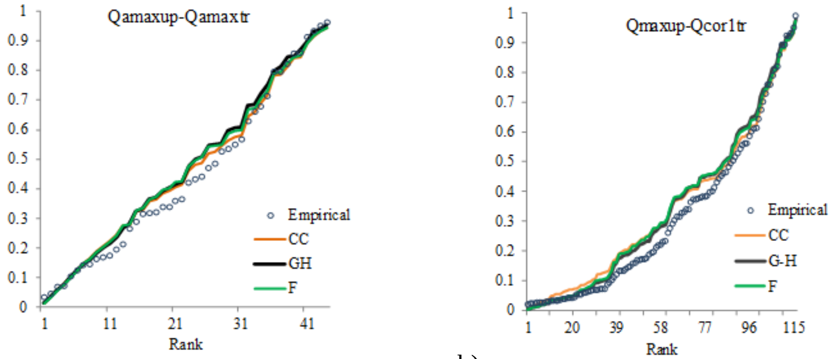

a) b)

Fig. 4. Comparison of the joint empirical with fitted parametric copula probabilities Morava – Myjava confluence a) annual peak pairs and b) daily maximum and corresponded pairs.

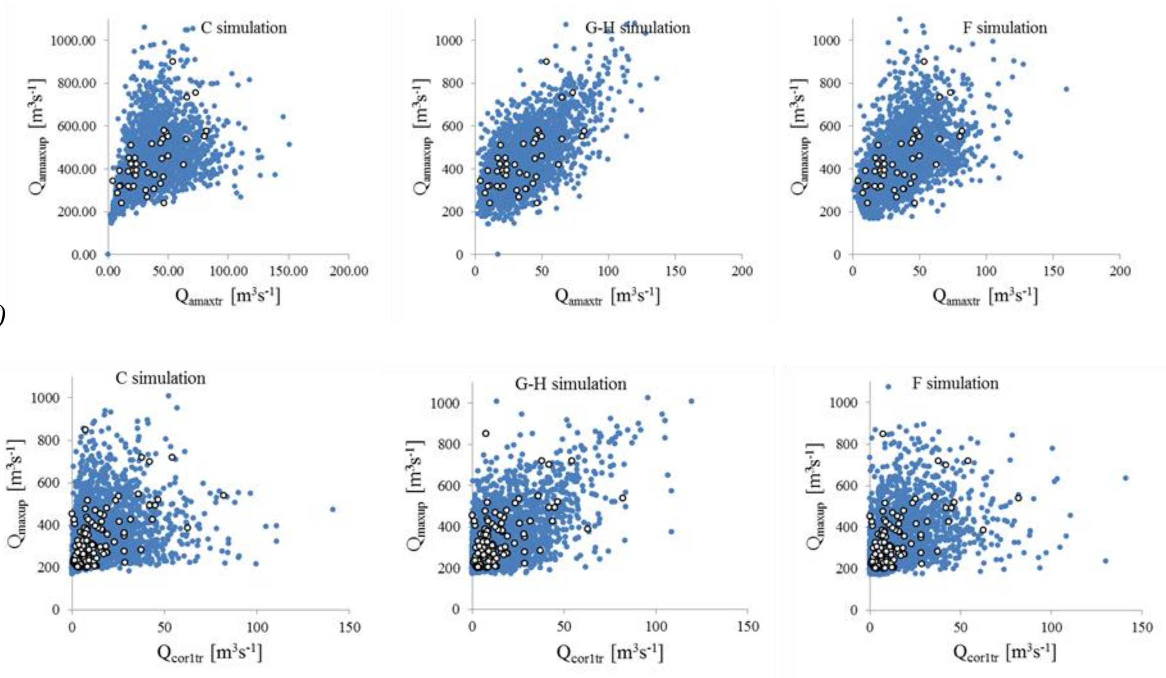

a)

b)

Fig. 5. Scatter plots of 3000 data pairs generated from copulas (C – Clayton, G-H – Gumbel-Hougaard and F – Frank) and measured data of for selected combinations a) $Q_{amaxup} - Q_{amaxtr}$ Morava – Myjava, b) $Q_{maxup} - Q_{cor1tr}$ Morava – Myjava.

calculated as reciprocal of the probability of exceedance. The discharge calculated using the copulas can lie anywhere on the isoline representing return period and can have infinite combinations. Since the worst-case scenario is regarding flood hazard at confluences, the extreme value of combined discharges was calculated, i.e. the maximum discharge resulting from infinite combinations of discharges at the Morava River and its tributary Myjava River. The comparison of the characteristic designed discharges (Q_N) calculated using traditional univariate distribution and bivariate copula distribution at annual peak discharges and maximum daily discharges are presented in Table 6.

Conclusions

The paper presents the bivariate joint frequency analysis of the discharges at the main river and its tributary. The annual peak discharges and mean daily discharges of the Morava and Myjava confluence were analysed (period of 1968–2011). For analysis the two statistical approaches were used. The first was traditional univariate approach and the second one was the bivariate joint distribution approach using the copulas.
The results in this paper show that:

- The type of theoretical probability distribution as well as the type of used input data series significantly affects the estimated Q_N.
- Comparison of the AM and POT approaches shows significant differences (in average 13%) for discharges with return period of 50 and 100 years on tributary.
- Comparison of the AM and POT univariate approaches with selected marginal distributions didn't show significant differences for estimated maximum discharges with return period up to 100 years.
- All tested Archimedes copula function achieved relatively small differences between calculated errors of estimation.
- According to the KS test we cannot reject any of tested Archimedean copula function that the joint pair magnitudes follow the theoretical joint distributions.
- Discharges estimated from Gumbel-Hougaard copula are higher than the ones calculated using the univariate method about 12%. Gumbel-Hougaard copula can well describe the multivariate relationship and improve the abnormal crossing phenomena, so it can give more reasonable results and be further applied to hydrological extreme analysis.

In conclusion, we can say, that the selection of the distribution function to estimate *T*-year discharges and also the processing of the statistical data series affects the results of the estimation. Determining the specific value of a 500- or 1000-year flood for engineering practice is extremely complex and in interpreting the results, it should be kept in mind that estimated values with very high return periods are extrapolated values. Each statistical method includes some uncertainty that may be caused by the method but also the data may be affected by certain measurement error therefore, is also necessary to specify confidence intervals in which the flow of a given 100-, 500-, or 1000-year flood may occur with probability, for example, 90%. Results of the bivariate analysis showed that bivariate copula model can be successfully applied at locations where significant change in flow regime is present, or flood intensity is governed by several variables, such as at river confluen-

Table 5. Evaluation of Archimedean copula functions for computing the joint distribution function by Kolmogorov-Smirnov test (α = 0.05)

Confluence	pair	Clayton	Gumbel-Hougaard	Frank
		p-value	*p*-value	*p*-value
Morava – Myjava	$Q_{amaxup} - Q_{amaxtr}$	0.93	0.81	0.8
	Q_{maxup} - Q_{cor1tr}	0.37	0.56	0.46

Table 6. Comparison of the characteristic discharges based on univariate and copula method for gauging station Moravský Svätý Ján of the Morava River

Confluence	Q [m^3 s^{-1}]		Univariate Q_{Ndwn}	Copula Estimated Q_N [m^3 s^{-1}]			Differences [%]		
				C	G-H	F	C	G-H	F
Morava – Myjava	$Q_{amaxdwn}$	Q_{50}	**1293**	1310	**1496**	1315	1.3	**+13.6**	1.7
		Q_{100}	**1489**	1496	**1704**	1502	0.5	**+12.6**	0.9
		Q_{500}	**1999**	2003	**2251**	2004	0.2	**+11.2**	0.2
		Q_{1000}	**2246**	2248	**2513**	2248	0.1	**+10.6**	0.1
	Q_{maxdwn}	Q_{50}	**1223**	1229	**1386**	1229	0.5	**+11.8**	0.5
		Q_{100}	**1416**	1419	**1600**	1419	0.2	**+11.5**	0.2
		Q_{500}	**1924**	1942	**2170**	1942	0.9	**+11.3**	0.9
		Q_{1000}	**2190**	2192	**2462**	2210	0.1	**+11.0**	0.9

ces. At river confluences, marginal distributions of inflow discharges rarely follow similar distribution, making copula model especially suitable for flood hazard assessment. When analysing the complex stochastic character of a river system on streams where the extreme event does not occur nearly simultaneous and where the tributary contributes significantly to the main river is necessary to analyse also pairs $Q_{maxtr} - Q_{corup}$ (Bender et al., 2016).

Acknowledgements:

This work was supported by the project VEGA No. 2/0004/19 and it results from the project implementation of the ITMS 26210120009 Infrastructure completion of hydrological research stations, supported by the Research & Development Operational Programme funded by the ERDF.

References

Bača, P., Bačová Mitková, V. (2007): Analysis of seasonal extreme flows using Peaks Over Threshold method. Journal of Hydrol. and Hydromech. Vol.55, No.1, 16–22.

Bačová Mitková, V., Onderka, M. (2010): Analysis of extreme hydrological events on the Danube using the Peak Over Threshold method. In Journal of Hydrology and Hydromechanics, Vol. 58, no. 2, 88–101.

Bayliss, A. C. (1999): Deriving flood peak data. Flood estimation: Hanbook. Vol.3, 273–283.

Bender, J., Wahl, T., Müller, A., Jensen, J. (2016): A multivariate design framework for river confluences. Hydrologica. Science Journal-Journal des Sciences Hydrologiques., 61(2016) 4, 367–381

Claps, P., Lio, F. (2003): Can continuous stream flow data support flood frequency analysis? An alternative to the partial duration series approach. Water Resour. Res., 39 (8), p. 1216.

Cunnane, C. (1973): A particular comparison of annual maximum and partial duration series methods of flood frequency prediction. Journal of Hydrology, 18, 257–271.

Cunnane, C. (1978): Methods and merits of regional flood frequency analysis. J. Hydrol., 100, 269–290.

Dehghani, M.; Saghafian, B.; Zargar, M. (2019): Probabilistic hydrological drought index forecasting based on meteorological drought index using Archimedean copulas Hydrology Research (2019) 50 (5): 1230–1250. https://doi.org/10.2166/nh.2019.051

De Michele, C. et al. (2005): Bivariate statistical approach to check adequacy of dam spillway. J. Hydrol. Eng., 10 (1), 50–57.

Espinoza, J. C. et al. (2013): The Major Floods in the Amazonas River and Tributaries (Western Amazon Basin) during the 1970–2012 Period: A Focus on the 2012 Flood. Journal of Meteorology, Vol. 14, 1000–1008. doi: 10.1175/JHM-D-12-0100.1.

Favre, A. C. et al. (2004): Multivariate hydrological frequency analysis using copulas. Water Resour. Res., 40, W01101, 1–12.

Gargouri-Ellouze, E., Eslamian, S. (2014): Application of Copulas in Hydrology: Geomorphological Instantaneous Unit Hydrograph and Intensity Index of Infiltration Frequency, in Handbook of Engineering Hydrology, Ch. 1, Vol. 2: Modelling, Climate Changes and Variability, Ed. By Eslamian, S., Francis and Taylor, CRC Group, USA, 1–18.

Genest, C. et al. (2009): Goodness-of-fit tests for copulas: A review and a power study. Insurance: Mathematics and Economics, 44, 199–213. doi:10.1016/j.insmatheco.2007.10.005.

Gilja, G., Ocvirk, E., Kuspilić, N. (2018): Joint probability analysis of flood hazard at river confluences using bivariate copulas. Journal of the Croatian Association of Civil Engineers (0350-2465). 70. 267–275. Doi:10.14256/jce.2173.2017.

Gringorten, I. I. (1963): A plotting rule for extreme probability paper. J. Geophys. Res., 68(3), 813–814.

Gupta, V. K. et al. (1976): On the joint distribution of the largest flood and its time of occurrence, Water Resour. Res., 12(2), 295–304, doi:10.1029/WR012i002p00295.

Hawkes P. J. et al. (2002): The joint probability of waves and water levels in coastal engineering design. Journal of Hydraulic Research, 40(3), 241–251.

Chen, L. et al. (2012): Flood Coincidence Risk Analysis Using Multivariate Copula Functions. J. Hydrol. Eng., 10.1061/(ASCE)HE.1943-5584.0000504, 742–755.

Chowdhary, H. et al. (2011): Identification of suitable copulas for bivariate frequency analysis of flood peak and flood volume data. Hydrol. Res., 42(2-3), 193–215.

Karmakar, S., Simonovic, S. P. (2009): Bivariate flood frequency analysis. Part 1: Determination of marginals by parametric and nonparametric techniques. J. Flood Risk Manag., 1, 190–200.

Kojadinovic, I., Yan, J. (2011): A Goodness-of-Fit Test for Multivariate Multiparameter Copulas Based on Multiplier Central Limit Theorems. Statistics and Computing, 21(1), 1–26.

Lang, M., et al. (1999): Towards operational quidlines for over threshold modelling. J. Hydrol., 225, 103–117.

Langbein, W. B. (1949): Annual floods and the partial-duration flood series. Transactions, AGU 30 (6), 879–881.

Li, C. H., Li1, N. et al. (2013): A relative vulnerability estimation of flood disaster using data envelopment analysis in the Dongting Lake region of Hunan. Nat. Hazards Earth Syst. Sci., 13, 1723–1734. doi:10.5194/nhess-13-1723-2013

Madsen, H. et al. (1997a): Comparison of annual maximum series and partial duration series methods for modelling extreme hydrologic events: 1. At-sit modelling, Water Resour. Res., 33(4), 747–757.

Madsen, H. et al. (1997b): Comparison of annual maximum series and partial duration series methods for modelling extreme hydrologic events: 2. Regional modelling, Water Resour. Res., 33(4), 759–769.

Meylan, P. et al. (2012): Predictive hydrology: a Frequency Analysis Approach. Boca Raton, FL: CRC Press; 212 p.

Nelsen, R. B. (2006): An introduction to Copula. The 2nd edition. Springer, New York.

Prohaska, S. et al. (1999): Coincidence of flood flow of the Danube River and its tributaries. A Hydrological monograph of the Danube River Basin. Belgrade University.

Rao, A. R., Hamed, K. H. (2000): Flood frequency analysis. CRC Press LLC, N. W. Corporate Blvd., Boca Raton, Florida.

Report of T. G. MASARYK WATER RESEARCH INSTITUTE (2002): Assessment of the catastrophic floods in August 2002 and proposal for adaptation of the flood prevention system, Final report on the 2002 project, Prague, pp. 174. (In Czech)

Rosbjerg, D. (1977): Returns periods of hydrological events. Nordic Hydrol., 8, 57–61.

Salvadori, G., De Michele, C. (2006): Frequency analysis via copulas: theoretical aspects and applications to hydrological events. Water Resour Res. 40, W12511.

Shiau, J. T. (2003): Return period of bivariate distributed extreme hydrological events. Stoch. Envir. Res. Risk Assess., 17, 42–57.

Shiau, J. T. et al. (2010): Copula-based depth-duration-frequency analysis of thyphoons in Taiwan. Hydrol. Res., 41(5), 414–422.

Sklar, A. (1959): Fonction de re'partition a'n dimensions et leurs marges. Publications de L'Institute de Statistique, Université' de Paris, 229–231.

Szolgay, J. et al. (2016): A regional comparative analysis of empirical and theoretical flood peak-volume relationships. J. Hydrol. Hydromech. Vol. 64(4), 367–381. doi: 10.1515/johh-2016-0042.

Todorovic, P. (1970): On some problems involving random number of random variables. Ann. Math. Statistics, Vol. 41(3), 1059–1063.

Tadić, L. et al. (2016): Analysis of the Drava and Danube rivers floods in Osijek (Croatia) and possibility of their coincidence. Environ Earth Sci, 75:1238, p. 12. https://doi.org/10.1007/s12665-016-6052-0

Yue, S. et al. (1999): The Gumbel mixed model for flood frequency analysis. J. Hydrol. 226(1–2), 88–100.

Yue, S. (2000): Joint probability distribution of annual maximum storm peaks and amounts as represented by daily rainfalls. Hydrological Science Journal, Vol. 45 (2), 315–326.

Zhang, L., Singh, V. P. (2006): Bivariate flood frequency analysis using the copula method. J. Hydrol. Eng. ASCE, 11(2), 150–164.

Ing. Veronika Bačová Mitková, PhD. (*corresponding author, e-mail: mitkova@uh.savba.sk)
Institute of Hydrology SAS
Dúbravská cesta 9
84104 Bratislava
Slovak Republic

DOI: 10.31577/ahs-2020-0021.01.0005

ACTA HYDROLOGICA SLOVACA

Volume 21, No. 1, 2020, 39 – 47

THE DETECTION OF CHANGES IN THE UPPER VÁH RIVER BASIN ACCORDING TO A DECADAL ANALYSIS

Mária Ďurigová*, Kamila Hlavčová

In changing climate conditions, hydrometeorological data analysis is an option for determining identifiers for changes in runoff. Various methods are used for the analysis of hydrometeorological elements, e.g., statistical tests or various hydrological analysis. The aim of the article is to analyse hydrological time data series by comparing their averages over decades. The time data series used were mean monthly, seasonal, and annual discharges; the average total monthly rainfall in a river basin, and the average air temperatures in the river basin. The decadal analysis was applied at 16 stage-discharge gauging stations that are located in the upper section of the Váh river basin in Slovakia. The total monthly rainfall and air temperatures were calculated as the average values for the various catchments. The results show the lowest discharge occurred in the 1980s and the highest in the 2000s. Comparing the winter and summer season discharges, stations located in the eastern part of the area have a higher summer season discharges, while other stations have higher discharges in the winter season. The results of the air temperature analysis indicate an apparent upward trend in all the stations. Between the warmest and the coldest decades, the average difference in each river basin is 1.5°C. The precipitation regime in the earlier decades had a variable or decreasing character. Since the 1980s, there has been a slight increase. The increase in air temperature appears to affect the decreasing flow rate due to increasing evapotranspiration. The increase in precipitation in recent decades has been reflected in some stations by an increase in discharges.

KEY WORDS: analysis of decades, Váh river basin, climate change

Introduction

Flood Analysing the hydrological data of an instrumental period and identifying identifiers of changes in a runoff regime allow for determining changes in the statistical properties of the data. This can be used in models of a hydrological regime´s evolution under climate change conditions (Szolgay et al., 2004). Foreign and Slovak authors dealing with the issue of change detection, especially in hydrological data, can detect changes using various methods.

Škoda et al. (2008) examined minimum annual discharges and the frequency of their occurrence in Slovakia. Halmová and Pekárová (2013) evaluated minimum and maximum daily discharges from 1929 to 2011 using IHA hydrological software. Jeneiová et al. (2015) focused on detecting changes in long-term data series. The annual peak discharges from nine stations in southern Slovakia were used for the analysis. Changes in the flood regime of the Danube River in Slovakia were analysed by Pramuk et al. (2013). They evaluated changes in the amount, time of occurrence, and size of flood waves. Frequency analysis and long-term trend analysis were used. The results contained in the papers by the various Slovak authors above show a reduction in the runoff coefficient (Pramuk et al., 2016), following by an increase in the frequency of floods but a reduction their duration (Pramuk et al., 2013).

Various German papers point to an upward trend in discharges on the Rhine River, which were caused by an increase in winter precipitation (Bronstert et al., 2002; Schönwiese and Rapp, 1997). Petrow and Merz (2009) dealt with the frequency of floods in Germany, where increasing trends were also detected.

Bawden et al. (2014) dealt with an analysis of the trends and variability of the hydrological regime in the Athabasca catchment and surrounding catchments in Canada. The study showed a decreasing tendency in the trends.

Wong et al. (2006) identified the change points in a hydrological time series using the grey relational method. The method was applied at several stations on the Shunde River in China. Gautier et al. (2018) investigated the hydrological response to climate change at the Lena River in eastern Siberia. The locality is the coldest area of the northern hemisphere, and the authors focused on the development of the floods. They found an increase in spring floods and peak discharges and also determined the beginning of a flood is less predictable. Summer floods are more frequent and intense.

Material and methods

The decadal analysis was applied at 16 stage-discharge gauging stations that are located in the upper section of the Váh river basin (Fig. 1, Table 1). The selected stations and their catchment areas are small areas. The largest is the Váh river basin with Liptovský Mikuláš station, with an area of 1107.21 km^2. The smallest is the Ipoltica river basin with the Čierny Váh station, with a catchment area of 87.07 km^2.
The discharge was provided by the Slovak Hydrometeorological Institute. The total rainfall and air temperature coming from the CarpatClim database (CarpatClim, 2013).
Some of the catchments are nested. There are smaller basins with identification number (ID) 5310, 5311, 5330 and 5400 belongs to the Váh catchment to the Liptovský Mikuláš station (5550). Then, there is the Kysuce catchment to the Čadca station (6180), which is nested in the Kysuca catchment to the Kysucké Nové Mesto (6200).
A decadal analysis was used in Sleziak, 2017. The work

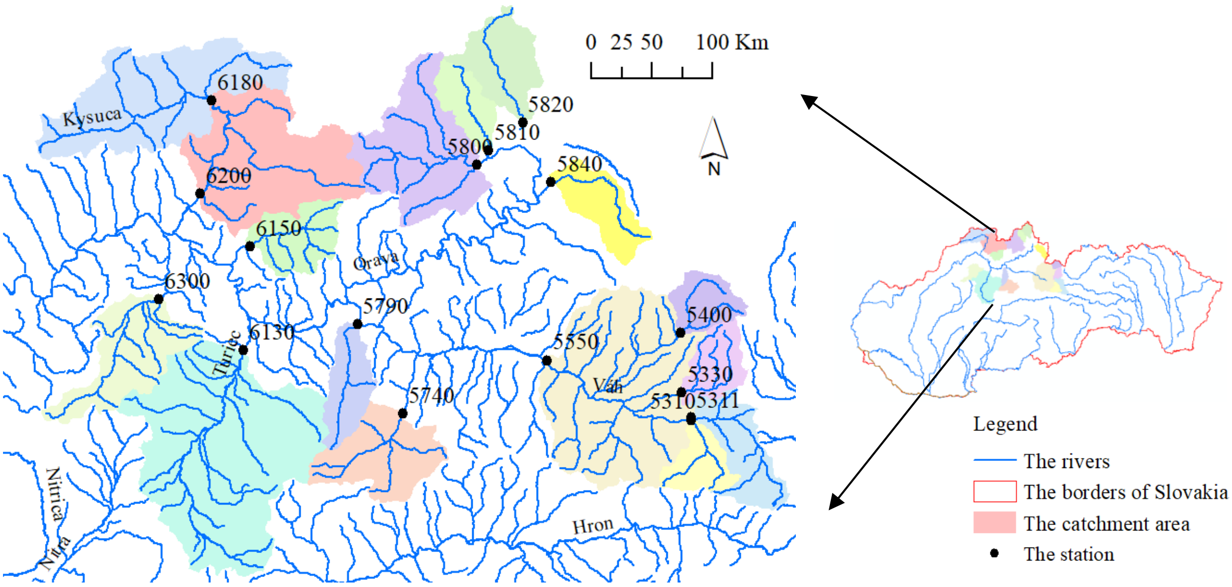

Fig. 1. The localization of the selected stage-discharge gauging stations with their catchments.

Table 1. The list of stage-discharge gauging stations used

ID	Station	River	River Km	Catchment area [km^2]	Altitude of station [m a.s.l]
5310	Čierny Váh	Ipoltica	0.08	87.07	736.36
5311	Čierny Váh	Čierny Váh	11.70	243.06	733.31
5330	Východná	Biely Váh	10.20	105.64	731.64
5400	Podbanské	Belá	21.35	93.49	922.72
5550	Lip. Mikuláš	Váh	346.60	1107.21	567.68
5740	Podsuchá	Revúca	11.20	217.95	558.21
5790	Ľubochňa	Ľubochnianka	0.30	118.39	442.00
5800	Lokca	Biela Orava	4.20	359.96	619.06
5810	Orav. Jasenica	Veselianka	1.00	90.10	618.09
5820	Zubrohlava	Polhoranka	1.60	158.67	605.69
5840	Trstená	Oravica	3.55	129.95	585.49
6130	Martin	Turiec	6.90	827.00	389.90
6150	Stráža	Varínka	5.10	139.70	399.87
6180	Čadca	Kysuca	29.20	492.54	408.36
6200	Kys. N. Mesto	Kysuca	8.00	955.09	346.09
6300	Poluvsie	Rajčianka	13.30	243.60	393.06

was focused on the modelling of rainfall-runoff processes. In this case, a decadal analysis was used to compare changes in model parameter values over three decades. The values were selected according to rain and snow seasons, within which the differences were evaluated.
In our case, three hydrometeorological elements were evaluated over five decades, i.e., the 1960s (from 1961 to 1970), 1970s (from 1971 to 1980), 1980s (from 1981 to 1990), 1990s (from 1991 to 2000), and 2000s (from 2001 to 2010) by a decadal analysis. The following hydrometeorological elements were used:

- the discharges measured at stations,
- the total precipitation per river basin,
- the air temperatures per river basin.

The data from CarpatClim have the form of grid points. The Theissen polygon method was chosen to calculate the total average rainfall and air temperature for the catchments. The total average rainfall and air temperature were calculated as a weighted average of the data from the individual grid points of the CarpatClim database. The weight of the area assigned to the relevant point within the river basin was considered as the weight (Keszeliová, 2019). The range of the CarpatClim data is from 1961 to 2010, which is also the range of the data used in this paper. The form of the data series was as follows:

- average annual data series,
- average seasonal data series for the winter season (November–April) and summer season (May–October),
- average monthly data series (from November to October, i.e., the hydrological year).

The selected data were further averaged for the individual decades. The average values of the decades were thus calculated as the average values for single months, seasons, and years. The results were evaluated using multiple graphs.

Results and discussion

The results of the decadal analysis show a comparison of two river basins, namely, the Čierny Váh river basin to the Čierny Váh station and Rajčianka river basin to the Poluvsie station. There are detailed assessments of the discharges, air temperature, and precipitation for each decade. Subsequently, all the stations were evaluated together. In this case, the winter and summer season time data series were plotted using box charts.

Results from the Čierny Váh and Poluvsie stations

The Čierny Váh river basin to the Čierny Váh station (5311) and the Rajčianka river basin to the Poluvsie station (6300) have the same catchment area, i.e., 243 km^2. The altitude of the Čierny Váh station is 733.31m a.s.l. The second station is situated at a lower altitude, i.e., 393.06 m a.s.l. The long-term mean discharge of Čierny Váh station is Q_a=3.52 m^3.s^{-1} and Q_a=3.42 m^3.s^{-1} for the Poluvsie station.
The results of these stations are shown in the graphs in Figs. 2 and 3. In both graphs, the left Y-axis shows the precipitation scale (green); the right is the air temperature scale (blue, black, and red lines) and the discharge (yellow). The black, blue, and red column borders represent the yearly (*year*) and seasonal averages (*winter, summer*) for the decades. The decades of the stations are plotted on the primary X-axis.

The discharge regime

The mean annual discharge over the decades at the Čierny Váh station (Fig. 2, yellow) and the Poluvsie station (Fig. 3, yellow) are similar. The highest mean annual discharge was in the 1970s. At the Čierny Váh station, the discharge for the recent decades have been slightly rising, but at the Poluvsie station, the discharge has been falling. The slightly increasing discharge at the Čierny Váh station in the last two decades is probably due to higher precipitation. In the Poluvsie station, despite slightly increasing precipitation, the discharge has continued to decrease, which is probably due to the increased evapotranspiration caused by the increasing air temperature.
The courses of the average discharges of the winter and summer seasons are different. The discharge of the summer season at the first station is higher than the discharge of the winter season. It is the other way around in the second station, so the discharge of the winter season is always higher than the discharge of the summer season.
A closer look at the discharge during each month (Fig. 4) allows one to see the maximum discharge in April and May at the Čierny Váh station. The Poluvsie station has the discharge peaks in March and April. This regime was probably reflected in the course of the discharges of the winter and summer seasons. The winter season is defined from November to April; therefore, the highest discharge of the winter season is at the Poluvsie station. The maximum values at the Čierny Váh station belong more to the summer season.

The air temperature regime

The air temperature in the Čierny Váh catchment has a clear upward trend (Fig. 2). The differences in the air temperature appear in comparison to the summer and winter seasons. The average air temperature in the 1970s in the summer season is the lowest, but in the winter season, it is higher than in the 1980s and the same as in the 1990s. Thus, the 1970s seem to be the mildest decade in both seasons. In the Rajčianka catchment to the Poluvsie station, there is a similar course for the air temperature, but it is about 2 ˚C warmer in each decade. The reason for the difference is the various altitudes of the basin.
The air temperature cycle according to months is expected to be higher in the Rajčianka catchment (Fig. 5, green colour). The maximum and the minimum values are found in both basins in the same months. The highest

air temperature is in July and August, and the lowest air temperature is in January. The 1960s had the lowest air temperature, while the warmest decade was the 2000s.

The precipitation regime

The course of the total rainfall in the Čierny Váh catchment (Fig. 2, green colour) show variable behaviour until the 1980s. Since the 1980s, the volume of precipitation has been gradually increasing. This applies to the winter and summer seasons of any year. In the Rajčianka catchment (Fig. 3, yellow colour), the total rainfall was slightly decreasing to the 1980s and then was slightly increasing.
The monthly total rainfall in the hydrological year by months are varied at both stations (Fig. 6). Both catchments have similar volumes of total rainfall. The lowest values of the total rainfall at both stations are mostly found in the winter months, especially in February. The maximum total rainfall are in June and July with a significant peak in the 2000s in the Čierny Váh catchment.

Evaluation of all the stations

The box graphs (Figs. 7, 8, and 9) were used to evaluate all the stations collectively. Each box contains a value from each station from the winter and summer seasons. These seasons are chronologically organized from the 1960s to the 2000s.

The discharge regime

In the evaluation of all the stations, a higher discharge in the summer season is found in the eastern catchments. These stations are the Čierny Váh stations (5310, 5311), the Východná station (5330), the Podbanské station

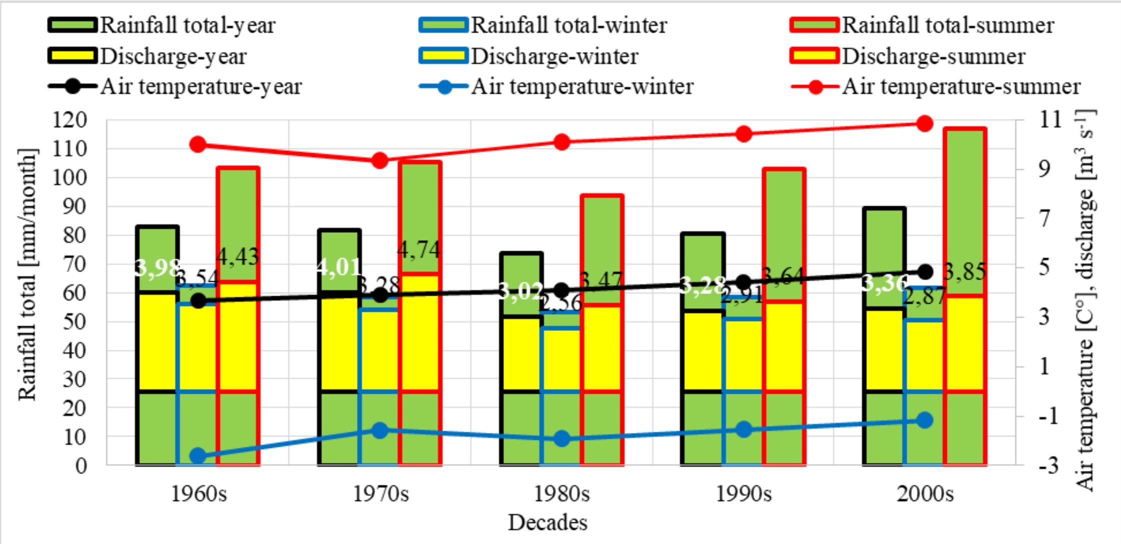

Fig. 2. The results of the decadal analysis at the Čierny Váh station (ID 5311).

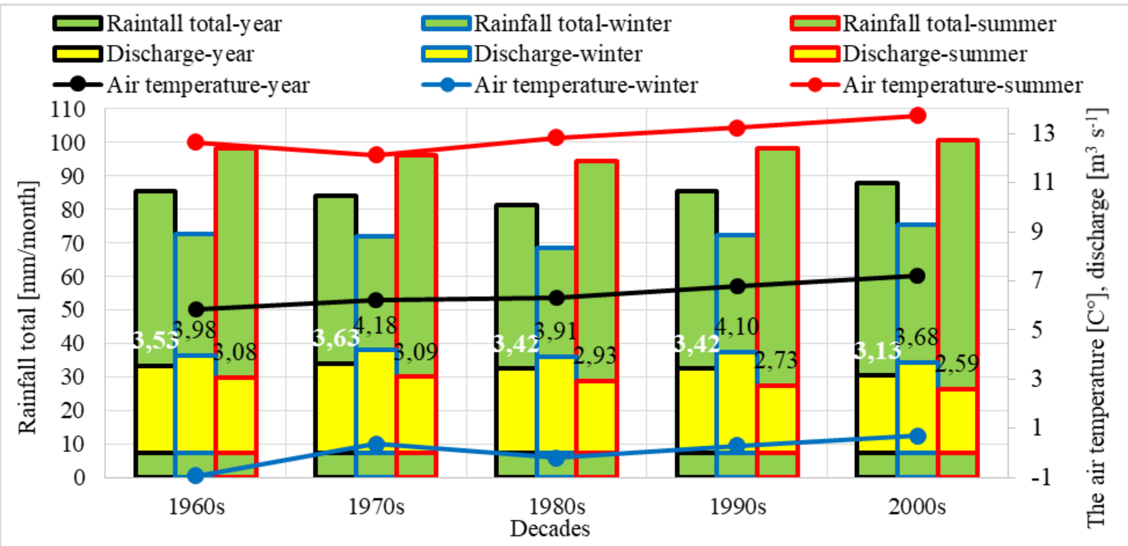

Fig. 3. The results of the decadal analysis at the Poluvsie station (ID 6300).

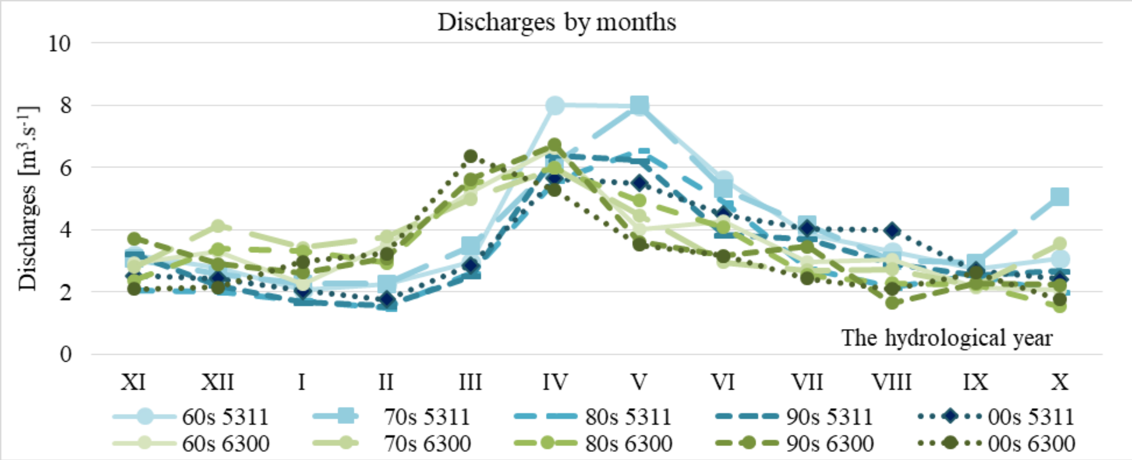

Fig. 4. Comparison of the discharges by the months of the hydrological year at the Čierny Váh station – 5311 (blue colour) and the Poluvsie station – 6300 (green colour).

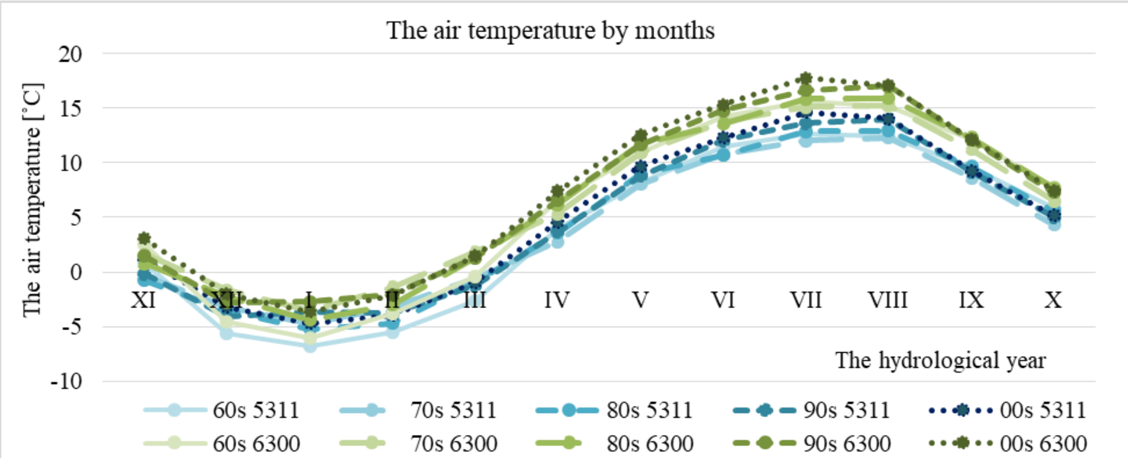

Fig. 5. Comparison of the air temperature by months of the hydrological year at the Čierny Váh station – 5311 (blue colour) and the Poluvsie station – 6300 (green colour).

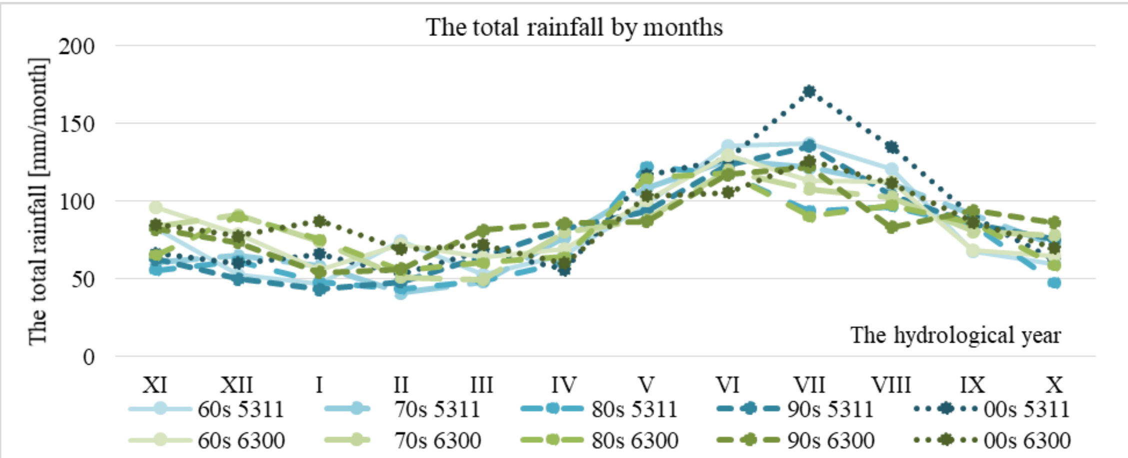

Fig. 6. Comparison of the total rainfall by months of the hydrological year at the Čierny Váh station – 5311 (blue colour) and the Poluvsie station – 6300 (green colour).

(5400), the Liptovský Mikuláš station (5550) and the Trstená station (5840). The reason for the differences is the maximum discharge in May, which belongs to the discharge of the summer season. All the other stations show higher discharges of the winter season than discharges of the summer season. This can be seen in Fig. 4, which show the courses of the discharge by months for the Čierny Váh station and the Poluvsie station.
The differences between the winter and summer seasons are also possible to see in the box graph (Fig. 7). All the winter seasons have a larger range of values at the 0.25 and 0.75 percentiles. The variance between the 0.25 and 0.75 percentiles in the summer season is smaller, but the outliers are more pronounced than in the winter season. This phenomenon is probably due to intense summer floods. The differences between the medians and arithmetic means are small.

The air temperature regime

The coldest catchment is the Belá river basin (the Podbanské station – 5400), and the warmest is the Turiec river basin (the Martin station – 6130). The difference between the coldest and the warmest decade in the winter season is 1.59°C on average for all the stations. The coldest decade is the 1960s, and the warmest decade is the 2000s. In the summer season, the coldest decade is the 1970s, and the warmest is the 2000s. The difference between these decades is 1.56°C on average for all the stations.
The box graph in Fig. 8 shows the course of the air temperature in the winter and summer seasons chronologically. The course of the air temperature in all the stations is generally similar to that described in comparison to the Čierny Váh catchment and the Rajčianka catchment. The outliers are caused by the Belá catchment, which has the lowest air temperature of all the catchments. The mildest decade is the 1970s (Fig. 8, *T winter 1970s* – light grey colour; *T summer 1970s* – yellow colour).

The precipitation regime

The largest amount of precipitation in the winter season fell in the Belá catchment, i.e., about 100 mm/month in each decade. The lowest amount of precipitation in the winter season fell in the Oravica catchment and the Ipoltica catchment, i.e., 50 to 57 mm/month.
The largest amount of precipitation in the summer season fell in the Belá catchment, i.e., an average of 141 mm/month. The lowest amount of precipitation fell in the Turiec catchment during the summer season, an average of 94 mm/month.
When comparing to the decades, the decade with the least rainfall decade is the 1980s in the winter and summer seasons. The 1980s in the winter season had a total rainfall of 64.1 mm/month on average for all the stations and 98.4 mm/month on average in the summer season. The 2000s represent the decade with the highest total rainfall on average. The 2000s in the winter season had total rainfall of 69.5 mm/month on average, and in the summer season it was 114.9 mm/month on average. The difference between the total rainfall of the 1980s and 2000s in the winter season is 5.4 mm/month for all the catchments on average. In the summer season, the difference between the 1980s and 2000s is 16.5 mm/month on average.
The course of the average total seasonal rainfall was decreasing until the 1980s (Fig. 9). Subsequently, the volume of precipitation has been increasing. The Belá catchment is the cause of the outlying values; it has the highest precipitation totals from all the catchments.
The results mentioned above with the average values for all the stations were summarized in Table 2. The summa-

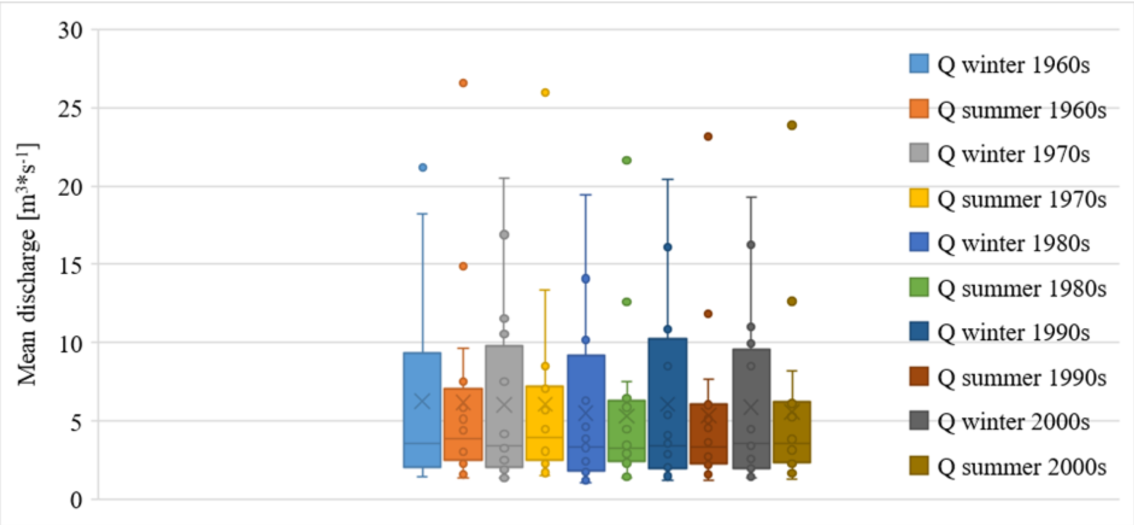

Fig. 7. The results of the discharge for the winter and summer seasons for all the stations in the form of box graph.

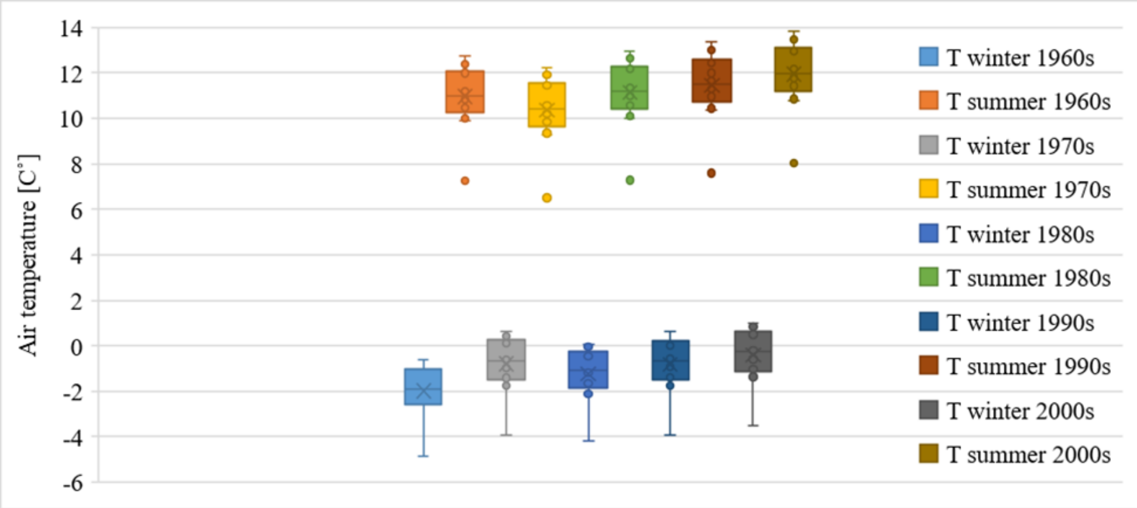

Fig. 8. The results of the air temperature for the winter and summer seasons for all the stations in the form of a box graph.

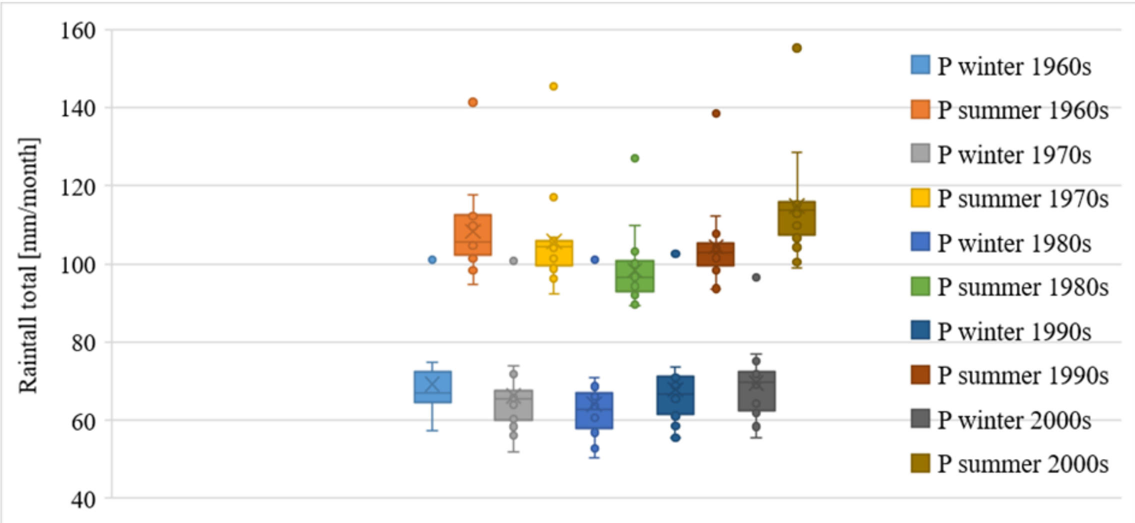

Fig. 9. The results of the total rainfall for the winter and summer seasons for all the stations in the form of a box graph.

Table 2. The summary results of the average values from all the stations with their maximums, minima and the differences between them (Q – discharge, T – air temperature, P – total rainfall)

Decade	Q winter [$m^3 s^{-1}$]	Q summer [$m^3 s^{-1}$]	T winter [°C]	T summer [°C]	P winter [mm/month]	P summer [mm/month]
1960s	**6.3**	**6.2**	**-2.0**	11.0	69.2	108.4
1970s	6.1	6.1	-0.8	**10.4**	66.3	105.8
1980s	**5.5**	**5.3**	-1.2	11.1	**64.1**	**98.4**
1990s	6.1	5.4	-0.8	11.5	68.0	104.5
2000s	5.9	5.6	**-0.4**	**11.9**	**69.5**	**114.9**
Maximum	6.3	6.2	-0.4	11.9	69.5	114.9
Minimum	5.5	5.3	-2.0	10.4	64.1	98.4
Differ. (max-min)	0.8	0.9	1.6	1.6	5.4	16.5

ry shows the largest changes in discharge occurred in the first decades. The air temperature over all the decades and changes in precipitation have become more apparent in recent decades.

Conclusions

The comparison of the Čierny Váh station and the Poluvsie station, which have the same catchment area but are at different altitudes, showed the different courses of discharges in the winter and summer seasons. The Čierny Váh catchment is 2°C colder than the Rajčianka catchment. The precipitation regime showed the highest total rainfall in the 2000s.

The results of the evaluation of all the stations showed the lowest discharge in the 1980s and the highest discharge in the 2000s. In comparison to the discharges of the winter and summer seasons, the stations located in the east part have a higher discharge in the summer season than in the winter season. This phenomenon is probably due to different discharge peaks in the winter and summer months. Either the peaks appear in April, which belongs to the winter season, or the peaks appear in May, which belongs to the summer season.

The results of the decadal analysis in the air temperature pointed to an apparent upward trend in all the stations. The difference between the warmest and coldest decades is 1.5°C. The air temperature curve is similar in all the catchments. The coldest month is January, and the warmest months are July and August.

The precipitation regime in the earliest decades has a variable or decreasing character. There has been a slight increase since the 1980s. The 2000s was the decade with the highest precipitation totals. The least amount of rainfall fell in the 1980s. The difference between the 2000s and 1980s in the winter season is on average 5.4 mm/month for all the stations. In the summer season, the difference is 16.5 mm/month. The influence of the increase in rainfall growth in recent decades has shown a slight increase in discharges in some stations. Nevertheless, the discharges have decreased in some stations. This decreasing discharge is caused by increased evapotranspiration due to the increase in air temperature.

Acknowledgement

This work was supported by the Science Grant Agency (Slovakia) under VEGA Contract No. 1/0891/17 and APVV-15-0497.

References

Bawden, A., Linton, H., Burn, D., Prowse, T. (2014): A spatio-temporal analysis of hydrological trends and variability in the Athabasca River region, Canada. Journal of Hydrology 509, 333–342.

Bronstert, A., Niehoff, D., Bürger, L. (2002): Effects of climate and land-use change on storm runoff generation: Present knowledge and modelling capabilities. Hydrological Processes, 16 (2), 509–529, DOI: 10.1002/hyp.326.

CarpatClim Database © European Commission – JRC (2013): Szalai, S., Auer, I., Hiebl, J., Milkovich, J., Radim, T. Stepanek, P., Zahradnicek, P., Bihari, Z., Lakatos, M., Szentimrey, T., Limanowka, D., Kilar, P., Cheval, S., Deak, Gy., Mihic, D., Antolovic, I., Mihajlovic, V., Nejedlik, P., Stastny, P., Mikulova, K., Nabyvanets, I., Skyryk, O., Krakovskaya, S.,Vogt, J., Antofie, T., Spinoni, J.: Climate of the Greater Carpathian Region. Final Technical Report, www.carpatclim-eu.org.

Gautier, E., Dépret, T., Costard, F., Virmoux, C., Federov, A., Grancher, D., Konstantinov, P., Brunstein, D. (2018): Going with the flow: Hydrologic response of middle Lena River (Siberia) to the climate variability and change. Journal of Hydrology 557, 475–488.

Halmová, D., Pekárová, P. (2013): The trend analysis of monthly and extreme discharges in the Belá-Podbanské station. Acta Hydrolog. Slovaca, vol. 14, no. 1, 193–203.

Jeneiová, K., Kohnová, S., Parajka, J., Szolgay, J. (2015): The detection of changes in the time data series of peak flows in southern Slovakia. Acta Hydrologica Slovaca, vol. 16, 2015, 53–58.

Keszeliová, A. (2019): Comparison of territorial evapotranspiration in selected catchments of Slovakia. Blahová, A. – Matoková, K. Proceedings of Young Scientists´ Conference 2019. Bratislava: The Slovak Hydrometeorological Institute, 2019, ISBN 978-80-99929-03-7.

Petrow, T., Merz, B. (2009): Trends in flood magnitude, frequency, and seasonality in Germany in the period 1951–2002. Journal of Hydrology 371, 129–141.

Pramuk, B., Pekárová, P., Halmová, D. (2013): The identification of changes in the Danube flood discharges at the Bratislava station in the period 1876–1943 and 1944–2010. Acta Hydrologica Slovaca, vol. 14, no. 2, 327–336.

Pramuk, B., Pekárová, P., Škoda, P., Halmová, D., Bačová Mitková, V. (2016): The identification of changes in the regime of daily discharges in Slovakia. Acta Hydrologica Slovaca, vol. 17, no. 1, 2016, 65–77.

Schönwiese CD., Rapp J. (1997): Climate Trend Atlas of Europe-Based on Observations 1891–1990. Kluwer Academic Publishers; Dordrecht, 224 p.

Sleziak, P. (2017): The modelling rainfall-runoff processes in the climate change condition. The Slovak University of Technology in Bratislava, Faculty of Civil Engineering, Dissertation thesis, 135–144.

Szolgay, J., Dzubák, M., Hlavčová, K., Kohnová, S. (2004): The hydrology, the runoff process, and the surface water hydrology. The Slovak University of Technology in Bratislava, Faculty of Civil Engineering, 198, 63 p.

Škoda, P., Majerčáková, O., Demeterová, B, Danáčová, Z. (2008): The evaluation of minimum discharges in Slovakia, National Climate Program of the Slovak Republic, NKP 12/08, Consequences of the climate change and the adaptation measures, 49–60.

Wong, H., Hu, B. Q., Ip, W. C., Xia, J. (2006): Change point analysis of hydrological time series using grey relational method. Journal of Hydrology 324, 323–338.

Ing. Mária Ďurigová (*corresponding author, e-mail: maria.durigova@stuba.sk)
prof. Ing. Kamila Hlavčová, PhD.
Department of Land and Water Resources Management
Faculty of Civil Engineering,
Slovak University of Technology in Bratislava
Radlinského 11
810 05 Bratislava
Slovak Republic

DOI: 10.31577/ahs-2020-0021.01.0006

ACTA HYDROLOGICA SLOVACA

Volume 21, No. 1, 2020, 48 – 55

LONG-TERM DEVELOPMENT OF DISCHARGE AND NITRATE CONCENTRATIONS IN THE LITTLE CARPATHIANS HEADWATERS

Pavla Pekárová*, Pavol Miklánek, Ján Pekár, Zuzana Danáčová

One of the requirements imposed by the Water Framework Directive 2000/60/EC (WFD, 2000) is to analyze and predict long-term evolution of surface water quality parameters. During 28-years period (1991–2018), the concentrations of selected pollutants were monitored in the Little Carpathians headwater basins by the Institute of Hydrology, SAS. In this study we analyse the long-term development of runoff and nitrates nitrogen concentrations in the Parná River at Horné Orešany water gauge station during the period 1991–2018. Discharges in the Parná River decreased slightly, but the trend is not statistically significant. In the case of nitrate nitrogen concentrations the marked decrease occurred in this river basin from the value of 5.11 mg l^{-1} during the years 1991–1995 to the value of 2.49 mg l^{-1} in the years 2015–2018. The relation between discharge and nitrate concentration was used to derive exponential empirical relations for estimation of the nitrate nitrogen concentrations in the stream based on mean daily discharge during the sampling day. These equations can be used for indirect estimation of nitrate nitrogen concentrations when they were not measured directly.

KEY WORDS: runoff, discharge variability, nitrate, long term trends

Introduction

One of the negative consequences of the expected global warming will be the increase of stream water temperature and runoff decrease during summer season, which will result in stream water quality worsening. The intensification of the agricultural mass production and increase of the inorganic nitrate fertilization doses worldwide (also in Slovakia) after the Second World War influenced the increase of nitrate concentrations in the stream water. Nitrate loading from an agricultural basin is generally strongly related to the amount of fertilizers applied. On Fig. 1 there is presented the annual development of average consumption of industrial nitrogen fertilizers applied to 1 ha of agricultural soils in Slovakia during the period 1960–2015 (upper). The lower part of the figure shows the monthly nitrate concentrations in three streams with long monitoring (Pekárová and Miklánek, 2013). In the plot we can see the direct influence of the increased nitrate doses upon the nitrate concentrations in the rivers. The fertilizer consumption per hectare arable land in 2012 in other EU countries published by the World Bank (WB, 2020) is plotted in Fig. 2 for comparison. This figure equates to 151 kg of fertilizers consumed per ha arable land on average for the EU countries.

Influence of agricultural activity on the nitrate content in drinking water sources in Slovakia was studied by Hyánková et al (1995). Pavelková (2000) assessed the water quality in drainage channels in the Eastern Slovakian Lowland in 1994–1996. She demonstrated the insufficient water quality, mainly due to nitrites nitrogen concentrations. The long-term development of nitrate in house wells in the villages of Michalovce and Sobrance District was analysed by Pavelková and Babinec (2017). The intensive daily monitoring of nitrate concentrations was managed by IH SAS in 1986–1993 in order to make detailed analysis of nitrate development at the inflow to water reservoir Veľká Domaša. Five sampling sites were established in the Ondava basin, and some other also in the Little Carpathians and Strážov Highland. It was proved by the study that the lowering of fertilisation doses and of the agricultural production resulted in lowering of nitrate concentrations in surface streams (Pekárová and Velísková, 1998; Pekárová and Pekár, 1996; Pekárová and Miklánek, 2013; Velískova et al., 2012). The influence of the forested and arable basin on nitrate concentrations was studied at experimental microbasins of IH SAS near to Kúnovec in the Strážov highland in 1986–2006 (Pekárová et al., 2008). The nitrate concentrations in the small forested Vydrica basin near to Bratislava were studied by Pekárová and Pekár (1998), Pekárová and Onderka (2005), and Sebíň et al. (2007).

The application of fertilizers was at low level in Slovakia in 2012 compared to other EU countries (Fig. 2), but due to increasing fertilization in Slovakia it is necessary to continue in evaluation of the nitrate content in the streams.

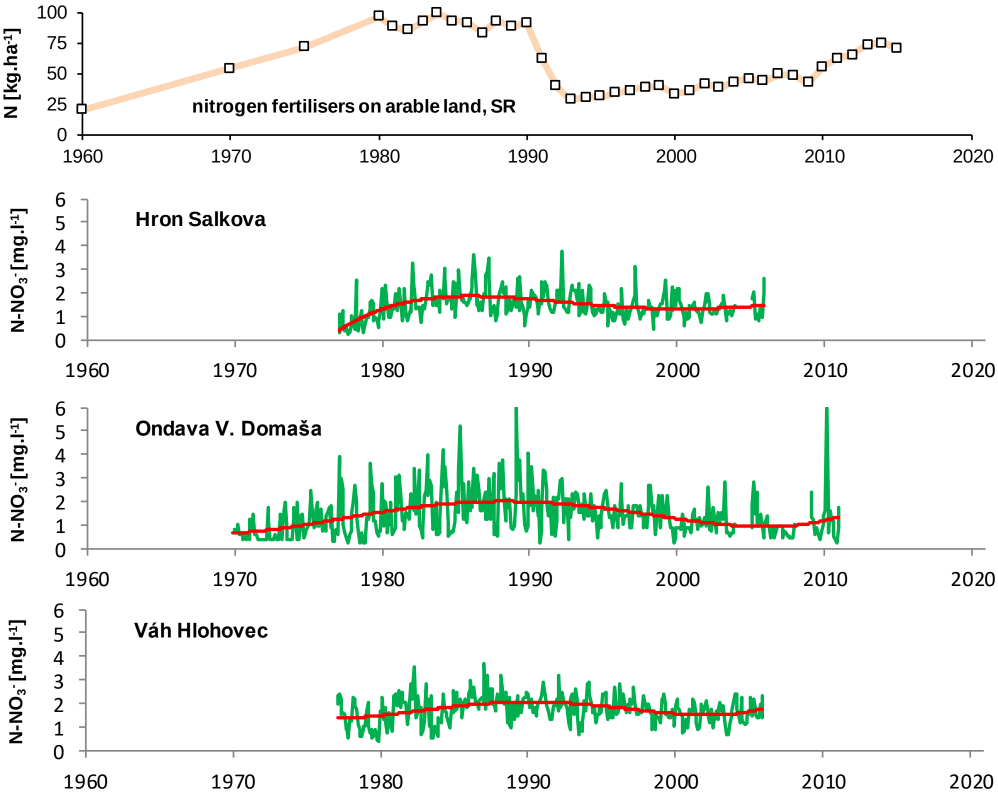

Fig. 1. Annual development of average consumption of industrial nitrogen fertilizers applied to 1 ha of agricultural soils in Slovakia during the period 1960–2015 (upper) in kg per 1 ha of agricultural land. Monthly nitrate nitrogen concentrations of the Hron, Ondava, and Váh rivers (SHMI data, according to Pekárová and Miklánek, 2013).

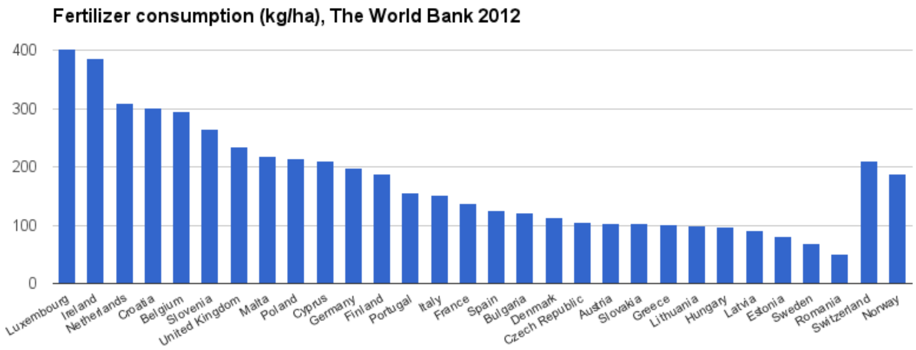

Fig. 2. Fertilizer consumption per hectare arable land in 2012 for the EU countries (the World Bank).

In this study we pay attention to the long-term development of the nitrate concentrations in the Little Carpathians headwater – in the stream Parná during 1991–2018.

The aims of this study are as follows:

1. Detailed analysis of the hydrological regime of the Parná stream at Horné Orešany during 1961–2018;
2. Analysis of the nitrate concentrations observed in the Parná stream at Horné Orešany sampling site in the 28–years period (1991–2018).

Material

The Little Carpathians lie in the Northeast of Bratislava between 17°–17°50' Eastern Longitude and 48°10'–48°40' Northern Latitude. The Little Carpathians are affected by air streams from the agriculturally polluted part of the Western Slovakia and Southern Moravia, which are densely populated areas. Both, the intensive industry and agriculture have a negative influence on water quality in this region. For example, the total volume of waste water discharged from Chemolak Smolenice was 477.3 thousand m^3 in 1991, with BOD_5 of 12.5 t.y^{-1} (tons per year), COD of 38.1 t.y^{-1} and 150.3 t.y^{-1} of insoluble substances (Molnár et al., 1993). The intensive agriculture in the lowland area has great negative impact on high nitrates content in surface water. Most local settlements (incl. Trnava) are exclusively supplied by drinking water from local groundwater sources. Because these sources are irreplaceable, it was necessary to give attention to the water quality problem.

Surface and groundwater quality in the basin of Trnávka River has been studied by several authors in the past. Gálik (1990) was interested in the impact of human activities on groundwater quality. He found that chloride, sulphate, and especially nitrate concentrations increase permanently in the groundwater. Guliš et al. (1994) evaluated drinking water quality. Lehotský and Tóth (1992) assessed the water quality of 96 forest springs and wells on the ridge of the Little Carpathians. Slaninka et al. (2005) monitored precipitation, surface runoff, and spring water runoff, for the sake of mass balance in the Vydrica catchment up to the Spariska section.

The analysis of surface water quality in this study was based on the data obtained by IH SAS at four sampling sites (Fig. 3):

1. Gidra River at water gauge Píla;
2. Parná River at Horné Orešany water gauge;
3. Hlboča brook in Smolenice;
4. Trnávka River at Buková water gauge.

Brief physical and geographical description of these catchments is presented in Table 1.

During last twenty years, surface water samples were taken by Institute of Hydrology, SAS (IH SAS) during three sub-periods: VI 1991–VIII 1995, XI 2004–XII 2006, and IV 2015–XII 2019. During the first period nitrate, nitrite, ammonium, sulphate, phosphate, chloride, and pH were analysed in the chemical laboratory of IH SAS in Michalovce. During second period the samples were analysed in accredited laboratory in Bratislava, and

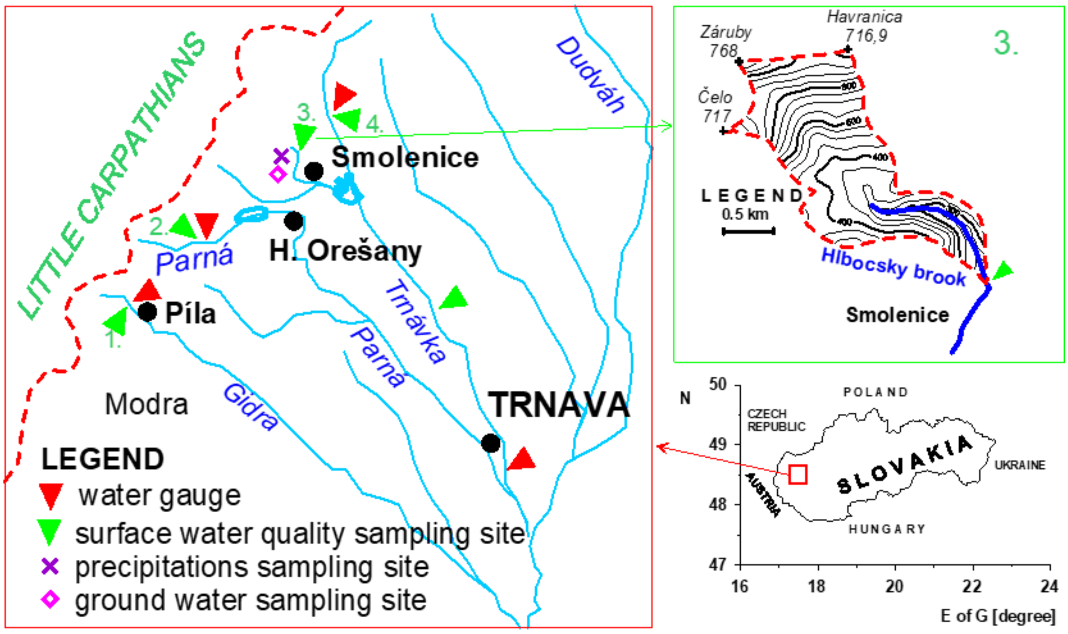

Fig. 3. Location of surface water gauges (SHMI stations) and water quality sampling sites (IH SAS sampling sites) in the Little Carpathians, Hlboča brook basin in details.

Table 1. Basic morphometrical, vegetation, and hydrological characteristics of experimental basins

river - cross-section	area [km^2]	agric. [%]	forest [%]	elev. a.s.l. min	elev. a.s.l. max	G	vegetation
Gidra – Píla	32.95	0	80	280	695	1	beech, oak, hornbeam
Parná – H. Orešany	37.86	10	90	235	661	2	beech, oak, hornbeam
Hlbočský b. – Smolenice	2.31	0	95	240	768	2	beech, oak, hornbeam
Trnávka – Buková	21.88	20	70	220	768	1	beech, oak, hornbeam

G – Characteristics of the geological substrate permeability
1 – good (river sediments), 2 – very good (karst, limestone)

during third period in laboratory of IH SAS in Bratislava. The selected sampling sites of IH SAS represent a headwater quality (forested area). The sampling sites Gidra: Píla, Parná: Majdán and Trnávka: Buková are identical with the water gauge of the Slovak Hydrometeorological Institute (SHMI).

The temporal variability of the nitrate nitrogen concentrations was very similar in all 4 stations in the period 1991–1994 (Fig. 4). Therefore we decided to focus on variability of the pollution concentrations only in Parná River at sampling site Horné Orešany water gauge (upstream the small reservoir Horné Orešany) and the sampling program was completed by another sampling site below the water reservoir in Horné Orešany village.

Methods

The statistical analysis of daily discharge series included the testing of homogeneity, stationarity, autocorrelation, multiannual cyclicity and long-term trends in measured data series. For testing we have used the autocorrelation and spectral analysis with application of the AnClim software (Štepánek, 2010).

At the trend analysis of the time series, the parametric and non-parametric tests can be used (Procházka et al., 2001). The parametric test considers the linear regression of the random variable x_i on time. The parameters of the trend line are calculated by using standard method for estimation of the parameters of a simple linear regression model, i.e. by using least square method. To identification of the long-term trends we used Mann-Kendall nonparametric trend test. The Mann-Kendall nonparametric test (M-K test) is one of the most widely used non-parametric tests for significant trends detection in time series. By M-K test, we want to test the null hypothesis H_0 of no trend, i.e. the observations x_i are randomly ordered in time, against the alternative hypothesis H_1, where there is an increasing or decreasing monotonic trend.

The maximum concentrations of nitrates in surface water usually occur during the high discharges period (see Fig. 4) and therefore the impact of discharge cannot be omitted when analysing the mean (monthly, annual) nitrate concentrations. In order to assess the mean nitrate concentrations we have to calculate the weighted mean with respect to discharge, it means to calculate the mean concentration of nitrates in the stream according to the relation (Pekárová et al., 1995; Pekárová and Pekár, 1996):

$$C_q = \frac{\sum_{i=1}^{m} C_i . Q_i}{\sum_{i=1}^{m} Q_i .} \qquad (1)$$

where

C_i – measured nitrate concentrations, [mg l^{-1}];
Q_i – measured discharge, [m^3 s^{-1}];
C_q – weighted mean of nitrate concentrations, [mg l^{-1}];
m – number of measured data.

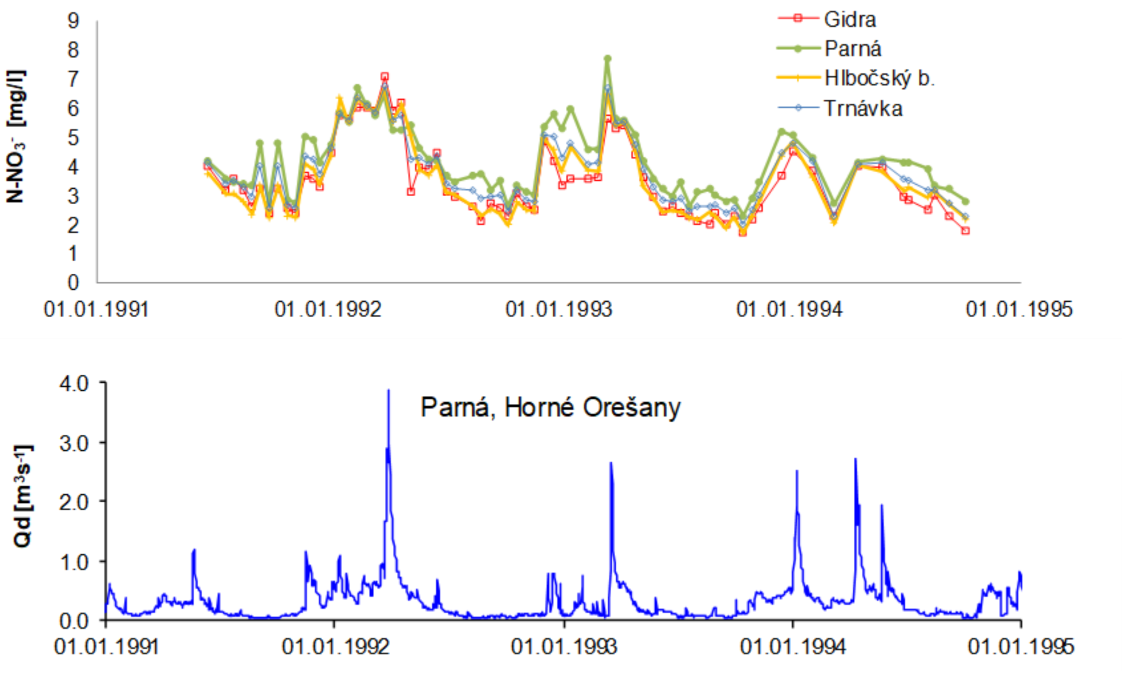

Fig. 4. The temporal variability of observed nitrate nitrogen concentrations in stream water, the Little Carpathians sampling sites, June 1991–October 1994 and daily discharge at Parná River: H. Orešany.

Results

Discharge analysis

The water gauge of Parná: Horné Orešany (Number 5250, river km 26.8) is situated above the water reservoir Horné Orešany (Výleta et al., 2017). The average annual discharge of the Parná River at the station of Horné Orešany for the period of 1961–2018 was 0.351 $m^3 s^{-1}$. The minimum and maximum flow observed during this period was 0.025 $m^3 s^{-1}$ and 7.653 $m^3 s^{-1}$, respectively. Other statistical characteristics can be found in Table 2.
On Fig. 5a, we can observe the variability of dry and humid periods. Periods 1971–1974, 1989–1991, 2001–2003, and 2017–2018 were extremely dry. The regularity of changing the dry and humid years was studied by the autocorrelation and spectral analyses of mean annual discharge time series (Fig. 5b). Autocorrelogram shows significant autocorrelation near the 14th year. This period was proved by the spectral analysis as well. The spectral analysis identified also other multiannual cycles: 4.5–5.5 years; 3.6 years, and 2.4 years. With respect to this more or less regular variability we can expect the more humid years to come.
The intraannual variability of mean, maximum, and minimum daily discharge did not change significantly (Fig. 5c).
On the other hand, the discharges are decreasing from the long-term point of view. With respect to the multi-annual cycles of low and high discharges, we recommend to estimate the long-term trend since low period around year 1971 to low period around year 2018, (see results in the Table 3). Flows decreased slightly during this period, but the trend is not statistically significant.

Nitrate concentrations in surface water

Nitrates are of significant seasonal variability. Higher nitrate values occur during snow-melting in spring (Mendel, Halmová, 1993; Pekárová et al., 1994; Hyánková et al, 1995; Pekárová, Pekár, 1996). Incorrect application of fertilizers during the vegetation period leads to a rapid increase of nitrate concentration in stream waters. The time variation of measured nitrate concentrations is shown in Fig. 4.
In Table 4 there are summarised the estimated means of nitrate nitrogen in three different periods and calculated by two different approaches:

1. Arithmetic average of measured data,
2. Weighted average with respect to discharge according to Eq. (1).

The highest nitrate pollution was found at the Parná River, above Horné Orešany in the first period 1991–1994, where average nitrate concentrations reached 4.2 mg l^{-1}, and weighted average 5.11 mg l^{-1}. After 1993 nitrate concentration in Parná headwater decreased.

Hydrological regime and estimation of nitrate nitrogen concentrations in the stream

As already mentioned, the water quality has a strong seasonal dependency, especially for some matters. Nitrate concentrations reach their maximum values during the wet periods, mainly during the spring snow melting. In Parná River, the minimum concentrations occur in summer-autumn (June–November), while the maximum concentrations are measured between December and May (Fig. 6a). Rain water washes nitrates off from the surface into a river. Generally, in the rivers of the Little Carpathian headwater region, an increased discharge leads to an increase in the nitrate concentration. But, during big floods, the nitrates concentration starts to be diluted by increasing discharge. We have derived exponential empirical relations for estimation of the nitrate nitrogen concentrations in the Parná River stream (Fig. 6b) based on mean daily discharge Q_d during the sampling day.
In period 1991–1994:

$$N\text{-}NO_3^- = 5.5176.Q_d^{0.1984} \quad \text{for } Q_d < 2 \tag{2}$$

$$N\text{-}NO_3^- = 15.785.\exp(-0.375.Q_d) \quad \text{for } Q_d \le 2 \tag{3}$$

In period 2004–2018:

$$N\text{-}NO_3^- = 4.5315.Q_d^{0.4001} \quad \text{for } Q_d < 2 \tag{4}$$

$$N\text{-}NO_3^- = 15.785.\exp(-0.375.Q_d) \quad \text{for } Q_d \le 2 \tag{3}$$

Conclusions

In Slovakia, the application of industrial fertilizers decreased significantly due to decrease of the agricultural mass production 30 years ago after 1989. The decrease in production impacted positively the decrease of nitrogen content in surface waters in Slovakia. After 20 years, since 2010, the fertilization dozes have increased to values close to the original ones before 1989. It can be expected that the nitrate concentrations will increase as well in our streams. Moreover, due to increasing air temperature (global warming) the evaporation increases as well and river runoff is decreasing slowly. The most

Table 2. Basic discharge statistical characteristics of the Parná: H. Orešany River, 1961–2018 period. *Q* – discharge, *q* – specific runoff, *R* – runoff depth

	mean	min	max	330-day	30-day	c_s	c_v
Q [$m^3 s^{-1}$]	0.351	0.025	7.653	0.078	0.810	5.209	1.264
q [$l\ s^{-1} km^{-2}$]	9.284	0.660	202.14	2.060	21.395		
R [mm]	292.8						

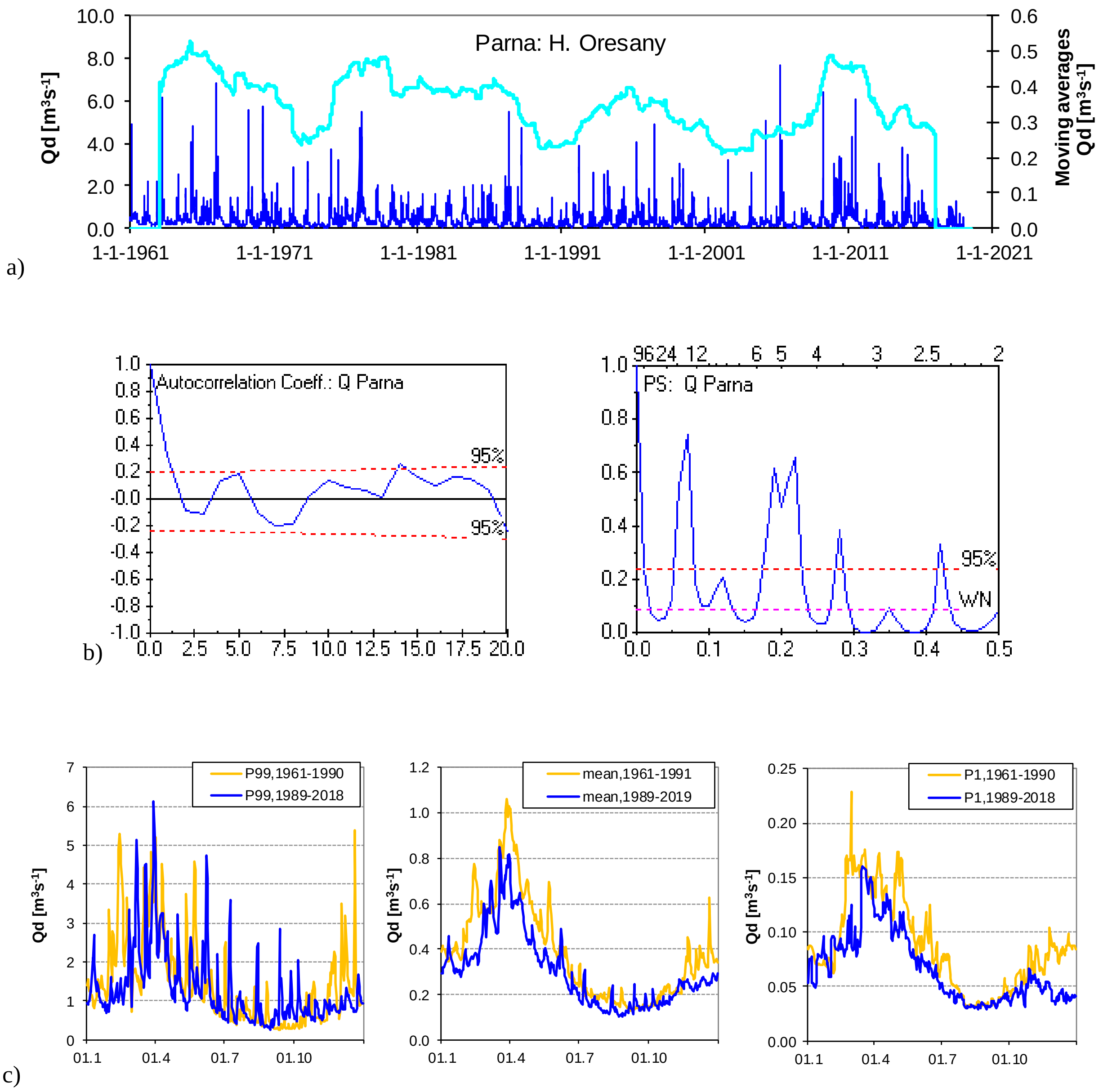

Fig. 5. a) Daily discharge and 4-years moving averages. Parná: H. Orešany; b) Plots of the autocorrelogram and power spectrum (MESA method), annual discharge. c) Long-term daily discharge for two periods, P99 – 99th percentiles, long-term mean daily discharge, and P01 – 1st percentiles.

Table 3. Results of annual discharge M-K trend tests for selected time periods, gauging station Parná: H. Orešany *(– level of significance α=0.01; * – level of significance α=0.05;)***

				Mann-Kendall trend			Sen's slope estimate				
Time series	**First year**	**Last year**	***n***	**Test Z**	**Signific.**	***A***	***A**min 95*	***A**max 95*	***B***	***B**min 95*	***B**max 95*
Qa	1961	2018	58	-2.80	**	-0.0030	-0.0050	-0.0010	0.4351	0.4814	0.3765
Qa	1971	2018	48	-1.38		-0.0020	-0.0046	0.0007	0.3998	0.4736	0.3126
Qa	1961	2011	51	-2.18	*	-0.0030	-0.0053	-0.0003	0.4341	0.4828	0.3692

Table 4. Basic statistical characteristics of estimated nitrate nitrogen concentrations in Parná stream [mg l^{-1}], at Horné Orešany sampling site, three periods

River	Parná	Parná	Parná
Period	1991–1994	2004–2006	2015–2018
Average	4.20	2.34	2.30
Weighted average according Eq.(1)	**5.11**	**2.69**	**2.49**
Min	2.27	1.08	1.08
Max	7.70	4.19	3.60
Std. deviation	1.16	0.79	0.81

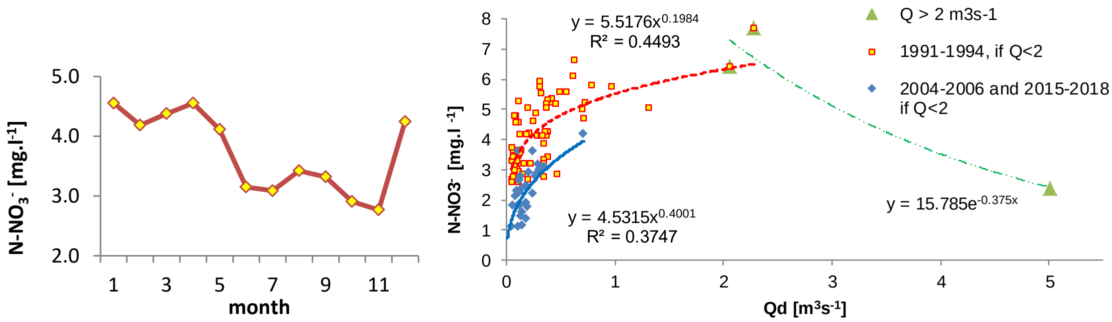

a *b*

Fig. 6. a) Monthly regime of the nitrate nitrogen concentrations;b)Relationships between N-NO_3^- concentrations and daily discharge, in the Parná River

endangered are the lowland streams in agricultural areas. The aim of this study was to assess the long-term development of the hydrological regime of the Parná River at Horné Orešany gauge during the period 1961–2018 and to assess the development of the nitrate nitrogen concentrations at this sampling site during the period 1991–2018.

The analysis of the hydrological regime proved the changing of wet and humid periods in approximately 14-years cycles in the Parná River series. In the main the discharge is decreasing slightly.

In the case of nitrate nitrogen concentrations the marked decrease occurred in this river basin from the value of 5.11 mg l^{-1} during the years 1991–1995 to the value of 2.49 mg l^{-1} in the years 2015–2018.

It was shown that the nitrate concentrations in surface streams are increasing with increasing discharge in the Little Carpathians headwaters, but there exists a threshold value of discharge when the nitrates concentration starts to be diluted by increasing discharge. The relation between discharge and nitrate concentration was used to derive exponential empirical relations for estimation of the nitrate nitrogen concentrations in the stream (Fig. 6b) based on mean daily discharge during the sampling day. These equations can be used for indirect estimation of nitrate nitrogen concentrations when they were not measured directly.

Acknowledgements:

This work was supported by the project VEGA 2/0004/19.

References

Gálik, M. (1990): The Causes of Undesirable Effects of Anthropogenic Activities on the Quality of Groundwater (In Slovak.) PhD Thesis, SVŠT, Bratislava.

Guliš, G., Wittgruber, J., Dubrovčáková, E. (1994): The Development of Drinking Water Quality Sources on Trnavka River Drainage Area (In Slovak.) Vodní hosp., 2, 5–8.

Hyánková, K., Ženišová, Z., Janský, L., Fendeková, M., Flaková, R. (1995): Influence of Agricultural Activity on the Nitrate Content in Drinking Water Sources in Slovakia. Hrvatske vode, Vol. 3, 12, 293–300.

Lehotský, J., Tóth, P. (1992): Springs in the Low Carpathians: Comparison of Two Classifying Criteria. Ecology (Slovakia), Vol. 11, 2, 167–180.

Mendel, O., Halmová, D. (1993): Analysis of the Runoff and Nitrate Loads in Two Small Microbasins. Proc. Abstracts Biogeomon and Workshop on Integrated Monitoring CzGS, Prague, 202–203.

Molnár, L., Miklánek, P., Mészároš, I. (eds.) (1993): International Environmental Programme for the Danube Basin - National Review of Danube Basins in Slovak Republic. Bratislava, ME SR, 476 pp.

Pavelková, D. (2000): Water Quality Characteristics Monitoring in the Drainage Channels in the East Slovakian Lowland. Acta Hydrologica Slovaca Vol. 1, 1, 197–205.

Pavelková, D., Babinec, K. (2017): Nitrate in House Wells in the Villages of Michalovce and Sobrance District (In Slovak). In XXI. Okresné dni vody. ÚH SAV, Výskumná hydrologická základňa, Východoslovenská vodárenská spoločnosť, a.s. Košice, 77–80.

Pekárová, P., Mendel, O., Koníček, A., Halmová, D. (1994): Analysis of the Selected Pollutants in Forested Catchments in the Carpathian Region. Proc. Developments in Hydrology of Mountainous Areas, Stará Lesná, 97–98.

Pekárová, P., Miklánek, P., Rončák, P. (1995): Stream Load and Specific Yield of Nitrogen and Phosphates from Slovakia. J. Hydrol. Hydromech., Vol. 43, 4–5, 233–248.
Pekárová, P., Miklánek, P. (2013): Surface and Ground Water Pollution by Nitrates in Eastern Slovakia. The 13th International Multidisciplinary Scientific GeoConference SGEM 2013: Hydrology and Water Resources, Soil, Forest Ecosystems, Marine and Ocean Ecosystems, Sofia: STEF 92, 341–348.
Pekárová, P., Onderka, M. (2005): Nitrate Concentration Modeling in Vydrica Stream by an Empirical Model. Acta Hydrologica Slovaca, Vol. 6, 1, 141–148.
Pekárová, P., Pekár, J. (1996): The Impact of Land Use on Stream Water Quality in Slovakia, Journal of Hydrology, Vol. 180, 333–350.
Pekárová, P., Pekár, J. (1998): The Chemical Regime and Interaction of Surface and Groundwater in Small Carpathian Region, Ekologia-Bratislava, Vol. 17, 4, 391–401.
Pekárová, P., Sebíň, M., Pekár, J., Onderka, M., Miklánek., P. (2008): Simulation of the Impact of Fertilizer Dozes on Nitrate Concentrations in the Stream. Cereal Research Communications, ISSN 0133-3720, Vol. 36, 1051–1054.
Pekárová, P., Velísková, Y. (1998): Water Quality Modeling in the Ondava Catchment Area, VEDA, Bratislava, 256 p.
Procházka, M, Deyl, M, Novický, O. (2001): Technology for Detecting Trends and Changes in Time Series of Hydrological and Meteorological Variables - Change and Trend Problem Analysis (CTPA). User's Guide. CHMI, Prague; 25 p.
Sebíň, P., Pekárová, P., Miklánek, P. (2007): Nitrate Wash Off from the Bratislava Forest Park Basin Vydrica in Years 1986–2005, J. Hydrol. Hydromech., Vol. 55, 3, 145–155.
Slaninka, I., Dlapa, P., Kordik, J. (2005): Cycle of Selected Substances in Natural Waters of Forest Ecosystem in Upper Vydrica Brook. (In Slovak.) In: Hydrologie maleho povodi, Institute of Hydrodynamics AS CR, Praha, 261–268.
Štěpánek, P. (2010): AnClim – software for time series analysis. Department of Geography, Faculty of Natural Science, MU, Brno. [on-line.] Accessible on www: http://www.climahom.eu/software-solution/anclim
Velísková, Y., Sokáč, M., Halaj, P. (2012): Simulation of Pollution Transport at Upper Part of Ondava River (In Slovak). In Proc. XVI. Okresné dni vody, Michalovce, ÚH SAV, 93–96.
Výleta R., Škrinár A., Danáčová M., Valent P. (2017): Optimizing use of water management systems during changes of hydrological conditions. IOP Conf. Series: Materials Science and Engineering, vol. 245, 10 pp.
WB (2020): http://data.worldbank.org/indicator/AG.CON.FERT.ZS/countries?order=wbapi_data_value_2007%20wbapi_data_value&sort=desc&display=default.
WFD (2000): Directive 2000/60/EC of the European Parliament and of the Council of the 23 October 2000, establishing a framework for Community action in the field of water policy, EU.

RNDr. Pavla Pekárová, DrSc. (*corresponding author, e-mail: pekarova@uh.savba.sk)
RNDr. Pavol Miklánek, CSc.
Institute of Hydrology SAS
Dúbravská cesta č. 9
841 04 Bratislava
Slovak Republic

Doc. RNDr. Ján Pekár, CSc.
Comenius University in Bratislava
Faculty of Mathematics, Physics, and Informatics
Department of Applied Mathematics and Statistics
Mlynská dolina
842 48 Bratislava
Slovak Republic

Ing. Zuzana Danáčová, PhD.
Slovak Hydrometeorological Institute
Jeséniova 17
833 15 Bratislava
Slovak Republic

DOI: 10.31577/ahs-2020-0021.01.0007

ACTA HYDROLOGICA SLOVACA

Volume 21, No. 1, 2020, 56 – 64

IMPACT OF DIFFERENT PROPORTION OF AGRICULTURAL LAND IN RIVER CATCHMENTS ON NITROGEN SURFACE STREAMS POLLUTION

Cyril Siman*, Yvetta Velísková

Water quality is threatened particularly in regions where the agricultural landscape is prevailing. This study presents results of the comparison of yearly total nitrogen emissions and contribution of different emission pathways on this emissions into surface streams for three river catchments in Slovakia territory with the contrasting proportion of agricultural land to the total area of the river catchment. For nitrogen yearly emissions and pathways detection, the numerical model MONERIS has been used. Results indicate that in river catchments with a higher proportion of agricultural land higher contribution of nitrogen emission carried out mainly via groundwater (especially in lowland), but also via agricultural erosion and drainage system.

KEY WORDS: water quality, surface stream, nitrogen emission, MONERIS, river catchment

Introduction

The Water Framework Directive (European Community, 2000), that rules the current European water policy, defines water quality as the level of deviation from the type-specific 'reference conditions'. Water quality in surface streams can be expressed by physical, chemical and biological indicators and most often is affected by a combination of anthropogenic as well as natural factors, the relative influences of which change with temporal and spatial scale. Many studies refer that the water pollution problem is caused by changes in the composition of land use within a catchment as human activities increase (Amiri and Nakane, 2009; Boskidis et al., 2010).

Understanding the influence of river catchment parameters on time and spatial variability of nutrients concentrations is the basic requirement for effective water quality management, especially in regions where the agricultural landscape is prevailing (Hill, 1981; Sliva and Williams, 2001; Foley et al., 2011).

Agriculture is considered to be one of the most representative examples of a non-point source of surface streams pollution (Lam et al., 2010). The non-point source emissions that end up in surface waters have many different pathways: overland flow, groundwater flow, tile drainage, erosion, urban systems and atmospheric deposition, etc. Surface streams are polluted during more intensive rainfall mainly and in snowmelt period, thus during significant runoff events (Julínek and Říha, 2017; Halmová et al., 2019). The heightened amount of nitrogen in surface streams can result environmental issues such as eutrophication of waters, growth of periphyton, etc. (Weitzel, 1979) and decrease of biodiversity (Di and Cameron, 2002).

To effectively target pollution mitigation and remediation actions in regions with impaired water quality, a number of models have been developed (Rothwell et al., 2010). One of them is the MONERIS (MOdelling Nutrient Emissions into RIver Systems) model. This model calculates the emissions of nutrients (e. g. nitrogen) to the surface water by different pathways (Behrendt et al., 2007).

We used this model to calculate and compare yearly total nitrogen emission in tonnes per year [t y^{-1}] as well as in kg per hectare per year [kg ha^{-1} y^{-1}] among three middle-sized river catchments from different parts of Slovak territory with different proportion of agricultural land to the total area of the river catchment. Results of the model were used also for determination of the pathways with the most important contribution to the nitrogen emission in these catchments.

Material and methods

In order to fulfill the objectives of this contribution, there was necessary to handle several datasets from different sources and in diverse quality, as well. All these data were necessary as the input data to the MONERIS model in order to calculate yearly total nitrogen emissions (YTNE) and also to determine the proportion of different pathways on YTNE into surface streams in three river catchments.

MONERIS model is a semi-empirical conceptual model which allows quantification of nutrient emissions from point and diffuse pollution sources into surface streams (Behrendt et al., 2002; 2007; Schreiber et al., 2005). While the wastewater from municipal wastewater treatment plants and from industry is directly discharged into the rivers and is not difficult to identify them, diffuse emissions of pollutants into surface waters are caused by the sum of different pathways, which are realized by separate flow components. They can be divided to these main groups (Behrendt et al., 2007):

- input into surface water via atmospheric deposition,
- input into surface water via groundwater,
- input into surface water via tile drainage,
- input into surface water via paved urban areas,
- input into surface water by erosion,
- input into surface water via surface runoff (dissolved nutrients).

Basis of the spatial resolution is the analytical unit, thus sub-catchments in a river basin. It is possible to run the model in a spatial resolution of 1 km^2 (Behrendt et al., 2007), but due to the calibration needs, a minimum spatial level depends on accessible input data resolution. Water quality data in three river catchments were collected for the years 2008–2017. These catchments were selected from different parts of Slovakia territory and they represent different proportion of agricultural land to the total area of the river catchment. Data that changes dynamically in time and space such as precipitation, runoff or nitrogen balance we collected and processed for 2017. More detailed information about data used for this analysis is possible to find either in Table 1 or in the next paragraphs.

All data was distinguished into several categories as follows:

- data on physical geography, where we included mainly data on relief, land cover, soil, geology and climatology:
  - digital elevation model (NASA JPL, 2013) that has spatial resolution approximately 30x30 m; from this data also average angle of slope and average elevation were derived,
  - data on land cover derived from the CORINE Land Cover 2012 (CLC) (EEA and SAZP, 2012),
  - the additional dataset consists mainly on data about agricultural land use available from the Land Parcel Identification System layer (LPIS) (Ministry of Agriculture of the SR, 2017),
  - data on soil texture, soil losses, and nitrogen top soil content available from the European Soil Data Centre (European Commission, 2009, 2015, 2016a),
  - data on rocks permeability taken from the Global Hydrogeology Maps of Permeability and Porosity (Gleeson et al., 2018),
  - bonitized Soil-Ecological Units layer (BPEJ) (NAFC, 2017),
- data on precipitation, evapotranspiration, river discharge and the water temperature was provided by the Slovak Hydrometeorological Institute (SHMI),
- data on non-point pollution sources:
  - data on the consumption of industrial and organic fertilizers at the district level of Slovakia territory provided by the Central Testing and Control Institute of Agriculture,
  - data on gross nutrient balance at the district level of Slovakia territory according to Directive No. 151/2016 (the Ministry of Agriculture of the SR, 2016) provided by the Central Control and Testing Institute in Agriculture in Bratislava,
  - modeled data on wet and dry atmospheric deposition, reduced as well as oxidized, was provided by the European Monitoring and Evaluation Programme (MET Norway, 2019),
  - data on crops grown at district level of Slovakia (harvest area in hectares, total harvest in tonnes, harvest from one hectare in tonnes), data on livestock at district level provided by the Statistical Office of the Slovak Republic,
- data on point pollution sources:
  - data on important point pollution sources (The Ministry of Environment of the Slovak Republic, 2009) in Slovakia,
  - data on wastewater treatment plants in Slovakia territory (European Commission, 2016b),
  - data on the number of inhabitants connected to the sewer system and number of inhabitants connected to sewer system via wastewater treatment plants provided by the Water Research Institute in Bratislava,
- data on water quality: monthly data consist of concentrations in total nitrogen water quality indicator in the period 2008–2017 provided by SHMI (for the long term and seasonal statistic processing the whole dataset was used, for MONERIS model only data from 2017 was used),
- other data:
  - detailed boundaries of river catchments provided by the SHMI,
  - data on the number of inhabitants of Slovak municipalities and towns provided by the Statistical Office of the Slovak Republic,
  - data on drainage channels provided by the Hydromelioration state-owned enterprise.

Total nitrogen concentrations values lower than the limit of quantification were set to the half value of the quantification limit according to Government Regulation No. 201/2011 Coll (Government of the Slovak Republic, 2011). Fig. 1 shows localization of monitoring places for water sampling as well as boundaries of river catchments where analysis of river catchment parameters was done. Table 1 shows selected parameters of the river catchments that were also used as inputs in the MONERIS model.

For identification of land cover, we used datasets from EEA and SAZP (2012) and Ministry of Agriculture of the SR (2017). Based on these two data sources, we divided individual land cover categories into four groups as follows:

- agricultural areas: arable land and pastures,
- forest and seminatural areas,
- urbanized and technique areas,
- uncategorized: open pit mine, open land, glaciers, wetland, water surface area.

Group of agricultural areas consist only of two land cover categories – arable land and pastures – for two main reasons: in these areas the application of industrial and organic fertilizers is the highest one and therefore in catchments with a higher proportion of mainly these two land cover categories there is also a higher potential for nitrogen surface streams pollution; another reason is that Land Parcel Identification System (LPIS) layer, that we used mainly for identification of arable land and pastures, has higher spatial accuracy and reliability in comparison with CORINE Land Cover.

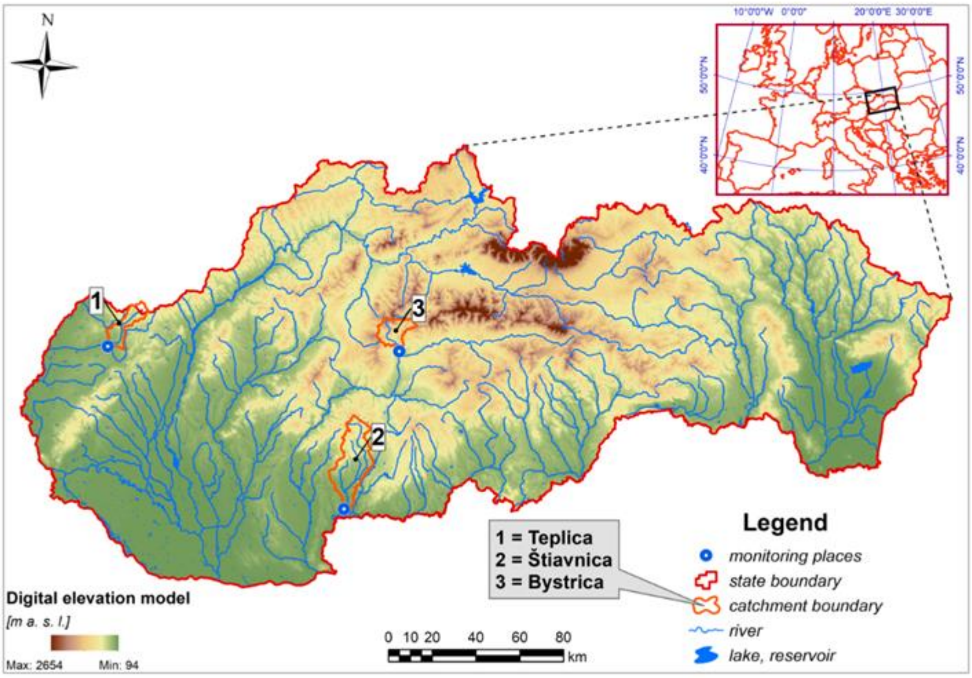

Fig. 1. Situation of evaluated river catchments in Slovakia territory and localities of water quality measurements.

Table 1. Summary of investigated catchments parameters

catchment parameter	unit	Teplica catchment	Štiavnica catchment	Bystrica catchment
size	km^2	152.6	445.7	158.9
average slope	%	12.4	15.9	46.9
agricultural land (AgL.)	km^2	94.9	186.5	11.8
proportion of AgL. to the total area of catchment	%	62.2	41.9	7.4
drained AgL	km^2	6.9	7.0	0.0
proportion of drained AgL to the total area of AgL	%	7.3	3.8	0.0
forest and seminatural area	km^2	46.5	236.7	142.6
urban area	km^2	10.6	20.1	3.7
uncategorized area	km^2	0.7	2.3	0.9
yearly precipitation	$mm\ y^{-1}$	559.9	706.0	957.2
average annual discharge	$m^3\ s^{-1}$	0.2	1.2	2.5
average annual water temperature	°C	12.7	10.5	8.6
nitrogen balance on AgL. land	$kg\ ha^{-1}\ y^{-1}$	49.3	70.4	72.9
population	inhabitants	25 310	24 034	2 134
population connected to WWTP´s via sewer system	inhabitants	20 489	12 585	0.0

The basis for modeling of nitrogen emission pathways in the MONERIS model

In this paper, we focused mainly on differences in nitrogen emissions that entry surface streams via emission pathways that relate to the area of agricultural land: agricultural erosion and drainage systems. However, as it has been already mentioned, in the MONERIS model more than only these two emission pathways are present. Therefore, in the results of this work we present emissions from all emission pathways as they are available in the MONERIS model. A more detailed investigation of the contribution of other emission pathways will be performed in future work. Nevertheless, in this section, we will briefly explain which data are most relevant for the calculation of emissions via other emission pathways that are also important in regard to overall nitrogen emissions.

To calculate nitrogen emission via point sources, data on important point pollution sources and wastewater treatment plants has been used. Statistical data such as number of inhabitants and mainly number of inhabitants connected to a sewer system and connected to a sewer system with wastewater treatment plants are important for the calculation of nutrient emissions from paved urban areas. To calculate emission via groundwater, data on rock permeability, data on soils, and also data on nitrogen balance on the agricultural area was necessary to process. Geology or rock types are in the MONERIS model discriminate according to consolidation and groundwater level (Behrendt et al., 2007). It is an important parameter for the calculation of nitrogen retention in the unsaturated and saturated zone and then for calculation of nitrogen concentration in groundwater. Inevitable inputs for calculation of the contribution of surface runoff on overall total nitrogen emissions are land cover categories, river discharge, and precipitation. Surface runoff is calculated separately for different land cover categories. The basis for the surface runoff calculation is the specific runoff from these areas (Venohr et al., 2011). The basis for the calculation of emissions via natural and agricultural erosion creates data on soil losses, land cover, digital elevation model (slope), and N-content of topsoils. Emissions via drainage systems are calculated using data on drained agricultural area, data on precipitation, and nitrogen balance on agricultural land.

Results and discussion

Nitrogen concentrations, yearly emissions in t y^{-1} and kg ha^{-1} y^{-1} to the surface streams and proportion of emission pathways on YTNE in three river catchments with different proportion of agricultural land to the total area of the river catchment were analyzed. Table 1 gives a summary of the selected river catchment parameters.

Fig. 2 shows area of arable land and pasture (agricultural land) and also localization of till-drainage channels. Arable land is prevailed land cover category mainly in the Teplica river catchment and also in the south part of the Štiavnica river catchment. On the other hand, we can see only minimal area of arable land and just small area of pasture in the Bystrica river catchment.

We should notice that the Štiavnica river catchment area is approximately three times larger than the areas of rest two catchments. On the other hand, average elevation and average slope were the highest in the Bystrica river catchment.

In Fig. 3 is possible to see that total nitrogen concentrations in two out of three investigated river catchments are decreasing during 10-year period. It is noticeable mainly in the Teplica river catchment (nitrogen concentration have decreased from approximately 8 mg l^{-1} at the beginning of the period (2008) to around 4 mg l^{-1} at the end of period in 2017). In the Štiavnica river catchment, a decrease of about mg l^{-1} in the 10-year period was recorded. On the other side, in the Bystrica river catchment no trend in total nitrogen concentrations was detected.

Total nitrogen emissions into surface streams were calculated using the MONERIS model that simulated surface streams nitrogen emissions along 11 emission pathways as follows:

- atmospheric deposition,
- surface runoff,
- snowmelt,
- agricultural erosion,
- natural erosion,
- drainage systems / tile drainage,
- groundwater,
- urban areas connected to a separated sewage system,
- urban areas connected to a combined sewagesystem,
- urban areas not connected to a sewage system,
- point sources of nitrogen.

It is possible to display total emissions in tonnes per year as well as in kg per hectare per year and the proportion of each pathway on yearly total nitrogen emissions. Fig. 4 shows the total nitrogen emission in tonnes per year divided into above-mentioned 11 pathways. On the other hand in Fig. 5 it is possible to see area-specific nitrogen emission also divided into eleven pathways, but in kg per hectare per year. This kind of analysis is independent on the catchment size. The MONERIS model results show that the highest contribution on total nitrogen emission in all three catchments has groundwater pathway. Second important pathway in the Teplica and the Štiavnica river catchment is a drainage system and in all catchments also the contribution of nitrogen emissions from point sources. The contribution of surface runoff is not negligible mainly in the Bystrica river catchment. In the context of the proportion of agricultural land to the total area of the river catchment, we are focused to differences in nitrogen emissions originating from agricultural erosion. In case of a flat territory (lowland) also the existing drainage channels determine significantly the proportion of nitrogen emission to surface streams, what was confirmed also by the results of this study. Till-drainage network in the Teplica river catchment drains approximately 6.9 km^2, thus only slightly more than 7% of the total area of the river catchment. In the Štiavnica

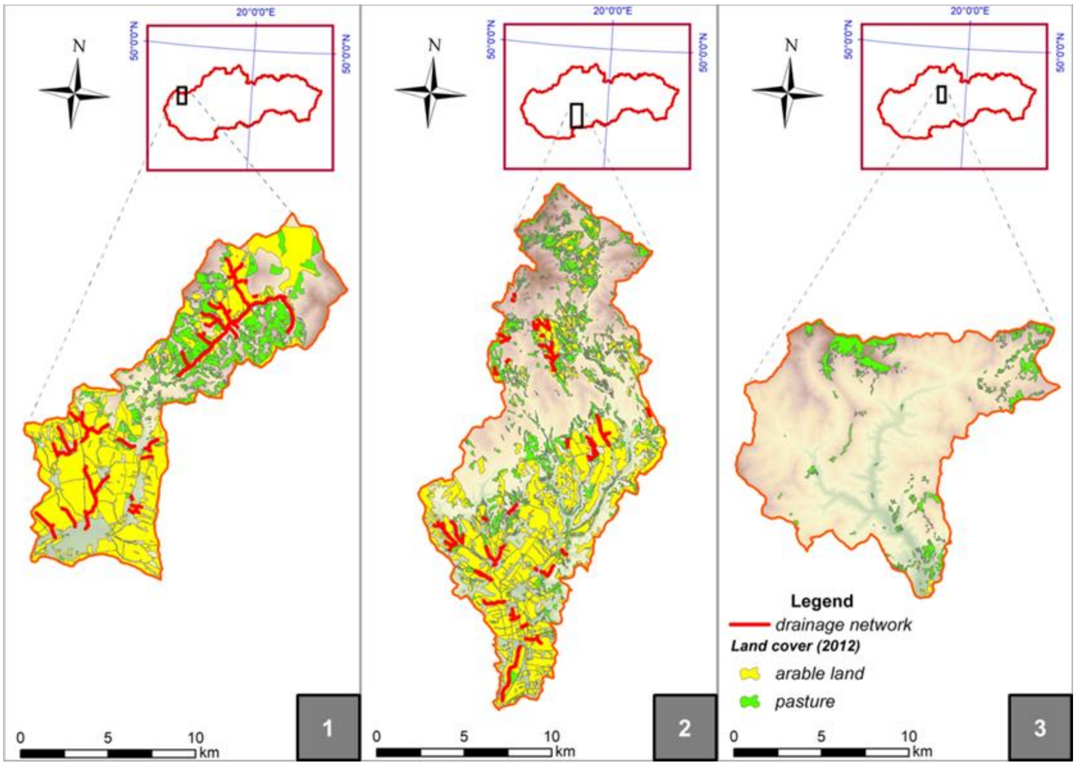

Fig. 2. Agricultural land cover categories and tile-drainage network in evaluated river catchments (numbers correspond with Fig. 1) on the background of digital elevation model (legend valid for all three maps).

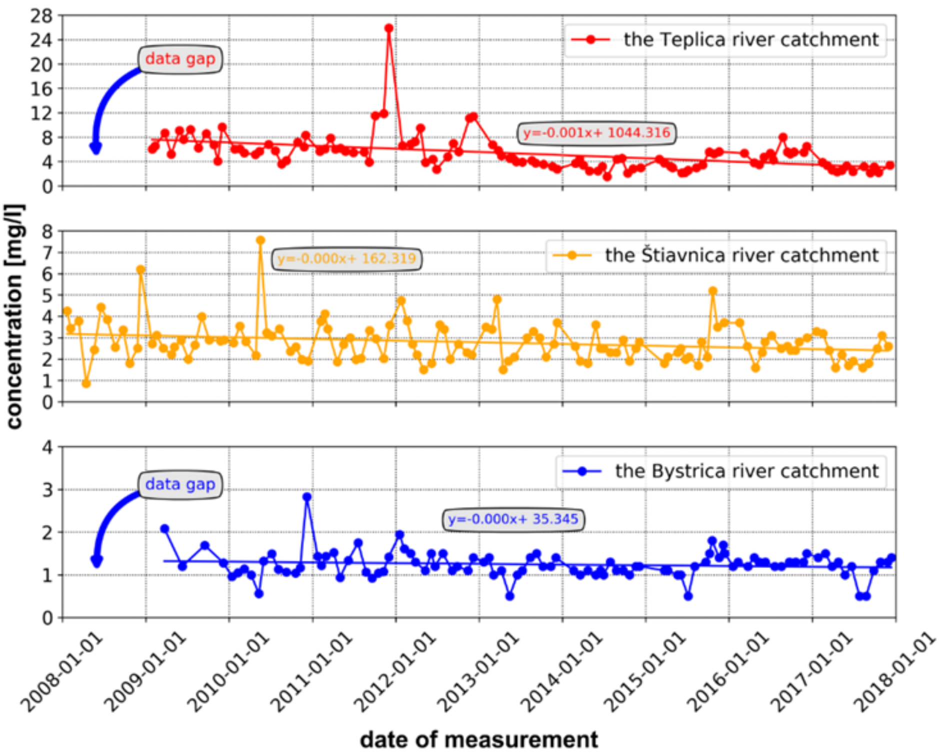

Fig. 3. Time series of total nitrogen concentrations in three investigated catchments in the period 2008–2017 (data with monthly time step collected from one location at the catchment outlet).

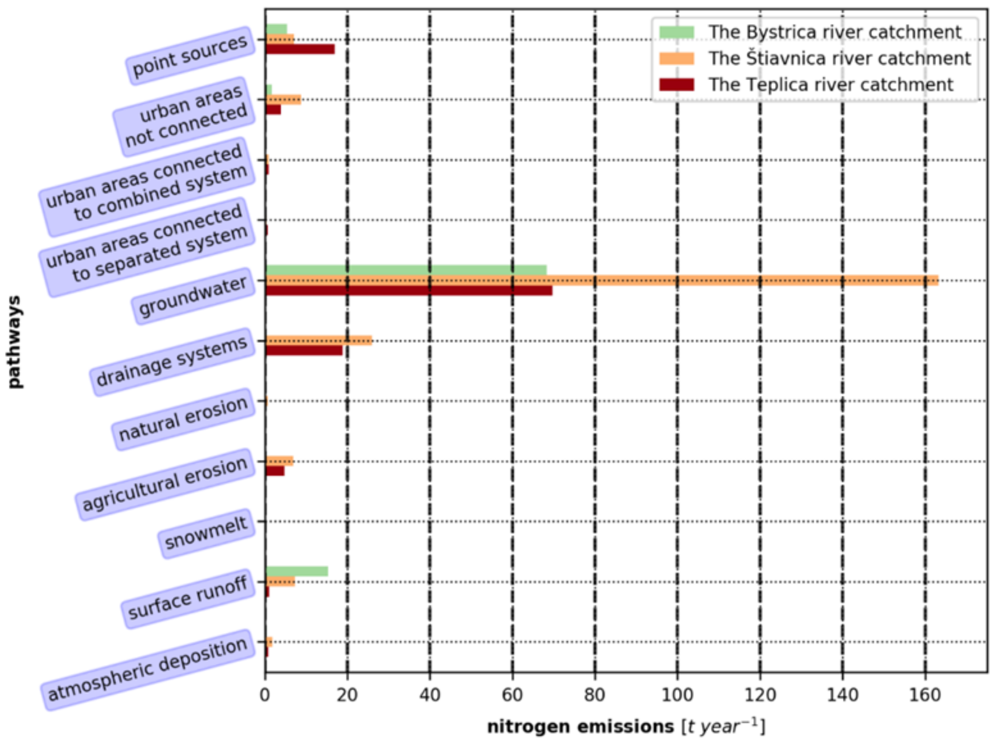

Fig. 4. *Emissions of total nitrogen in three evaluated catchments via different pathways in tonnes per year by MONERIS model results.*

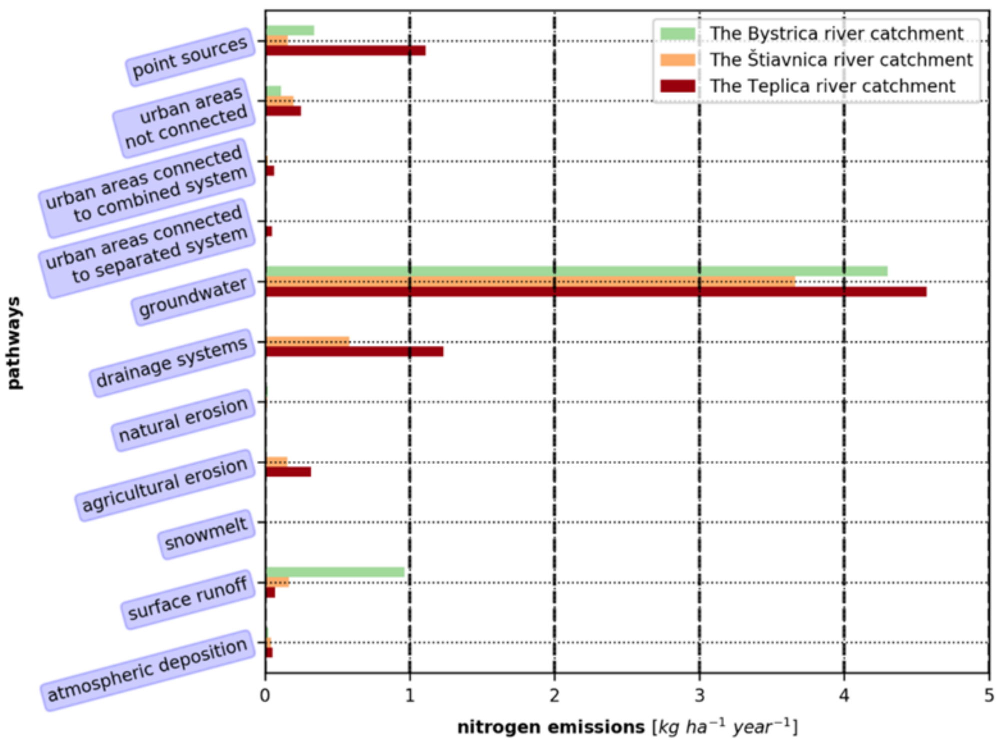

Fig. 5. *Emissions of total nitrogen in three evaluated catchments via different pathways in kg per hectare per year by MONERIS model results.*

river catchment proportion of drained agricultural land to the total area of agricultural land is only 3.8%. The highest contribution of drainage network on YTNE in tonnes per year was in the Štiavnica river catchment (26 t y^{-1}) (Fig. 4). On the other hand, area-specific nitrogen emission, which considering or eliminate river catchment size impact, was the highest in the Teplica river catchment (1.2 kg ha^{-1} y^{-1}) via the drainage system pathway (Fig. 5).

Another important pathway for nitrogen is erosion of nitrogen in particulate soil organic matter or sorbed on clays. It was confirmed that by soil erosion there are transported soil particles and also nitrogen which contributes to surface water contamination (Follett and Delgado, 2002). In the MONERIS model this process is represented by agricultural erosion pathway. Since the catchments have not the same size, graph that show proportion of agricultural erosion and drainage system pathway (in percentages) on YTNE was plotted and it shows detailed comparison of nitrogen emission carried out via these pathways in investigated catchments (Fig. 6).

In the Štiavnica and the Teplica catchments, contributions of nitrogen emissions via drainage network and agricultural erosion pathway have higher importance than in the Bystrica river catchment. At first, we focused on differences in yearly nitrogen emission via agriculture erosion as well as via the drainage system in t y^{-1} and kg ha^{-1} y^{-1} (Fig. 4 and 5) that were observed between the Štiavnica and the Teplica river catchments. Results in t y^{-1} are influenced with the fact that the Štiavnica river catchment is three times larger than the Teplica river catchment and therefore there is more total area of agricultural land, thus also more nitrogen sources (e. g. application of fertilizers). Comparison of emission in kg ha^{-1} y^{-1} allows us to compare differences in nitrogen emission more objectively (Fig. 5). This is also the case in Fig. 6 where is possible to see that the highest contribution on YTNE in agricultural erosion and drainage system pathways is in the Teplica river catchment (16%), thus in the catchment with the highest proportion of agricultural land to the total area of the catchment. On the other side, there is practically no contribution to the YTNE from these pathways in the Bystrica river catchment. In the Bystrica catchment there is no drainage network and only a small proportion of agricultural land, thus agricultural erosion and drainage system have only negligible contribution on overall total nitrogen emission into surface streams in this catchment. However, in this catchment surface runoff has a non-negligible (second highest one after groundwater pathway) contribution to overall YTNE (Fig. 5). It is probably results of high slopes in this river catchment and also a higher amount of yearly precipitation.

Summary of YTNE in all three investigated catchments offers Table 2. It is possible to see that nitrogen emission in t y^{-1} is the highest in the Štiavnica river catchment, thus in the largest river catchment in our study. On the other hand, area-specific emission in kg ha^{-1} y^{-1} is the highest in the Teplica river catchment, thus in the catchment with a higher proportion of agricultural land to the total area of the river catchment. In the Teplica river catchment, we can see also the highest contribution of agricultural erosion (4.1%) and drainage system (16%) pathways to the YTNE in comparison with the rest two catchments. These two emission pathways are related to the proportion of agricultural land in investigated areas. As was already mentioned, there is only small contribution from agricultural erosion and no contribution via drainage system pathway on YTNE in the Bystrica river catchment since there is no drainage network and only small area of agricultural land there.

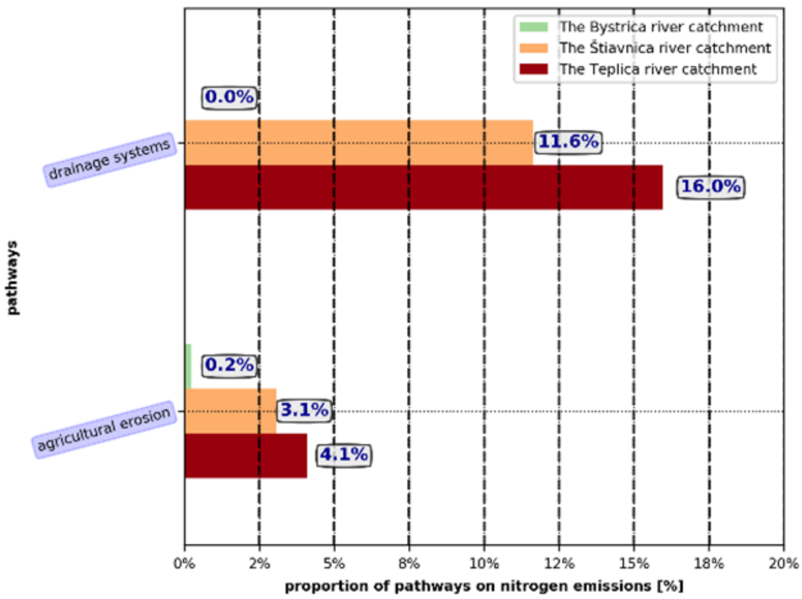

Fig. 6. Proportion of agricultural erosion and drainage system emission pathways on YTNE into surface streams in three evaluated river catchments by MONERIS model results.

Table 2. **Yearly total nitrogen emissions (YTNE) via different pathways and proportion of each pathway on total emission in three investigated catchments**

pathway	Teplica river catchment			Štiavnica river catchment			Bystrica river catchment		
	*	**	***	*	**	***	*	**	***
atmospheric deposition	0.1	0.8	0.7	0.0	1.9	0.8	0.0	0.4	0.4
surface runoff	0.1	1.1	0.9	0.2	7.3	3.3	1.0	15.3	16.7
snowmelt	0.0	0.0	0.0	0.0	0.0	0.0	0.0	0.0	0.0
agricultural erosion	0.3	4.8	4.1	0.2	6.9	3.1	0.0	0.2	0.2
natural erosion	0.0	0.1	0.1	0.0	0.7	0.3	0.0	0.3	0.3
drainage systems	1.2	18.8	16.0	0.6	26.0	11.6	0.0	0.0	0.0
groundwater	4.6	69.7	59.2	3.7	163.2	73.1	4.3	68.3	74.5
u. a.(1) connected to separated system	0.0	0.8	0.6	0.0	0.5	0.2	0.0	0.0	0.0
u. a.(1) connected to combined system	0.1	1.0	0.8	0.0	0.9	0.4	0.0	0.0	0.0
urban areas not connected	0.3	3.8	3.2	0.2	8.9	4.0	0.1	1.8	1.9
point sources	1.1	16.9	14.4	0.2	7.1	3.2	0.3	5.4	5.9
TOTAL	7.7	117.9	100	5.0	223.3	100	5.8	91.7	100

(1) *u. a. – urban areas; * kg ha^{-1} y^{-1}; ** t y^{-1}; *** proportion in %*

Conclusion

In this contribution, we used the MONERIS model to simulate the nitrogen loads to surface streams in three river catchments with different proportion of agricultural land to the total area of them. There was determined also proportion of emission pathways on this emission. In the Teplica river catchment where around 62 % of catchment area is covered by agricultural land, long term median concentration of total nitrogen was four times higher than in the Bystrica river catchment where the proportion of agricultural land is only around 7%. Furthermore, emission of total nitrogen via the drainage system pathway in the Teplica river catchment was 16% of overall yearly total nitrogen emission. Drainage system pathway contributed 4.1% of YTNE. On the other hand, there was practically no contribution from above-mentioned emission pathways in the Bystrica river catchment. In the Štiavnica catchment (41.9% of the catchment area is covered by agricultural land), 11.6% of overall nitrogen emission carried out via drainage system and 3.1% via agricultural erosion. Most important nitrogen emission pathway in all three catchments was groundwater.
The MONERIS model is helpful tool for evaluation of proportion of emission pathways on total nitrogen emission in catchments, but it is very demanding to input data.

Acknowledgement

The paper was created with support from VEGA project no. 2/0085/20 and the project no. APVV–18–0205.

References

Amiri, B. J., Nakane, K. (2009): Modeling the Linkage Between River Water Quality and Landscape Metrics in the Chugoku District of Japan, Water Resources Management. Springer Netherlands, 23(5), 931–956. doi: 10.1007/s11269-008-9307-z.

Behrendt, H., Kornmilch, M., Opitz, D., Schmoll, O., Scholz, G. (2002): Estimation of the nutrient inputs into river systems – experiences from German rivers, Journal of Material Cycles and Waste Management. Springer-Verlag, 107–117. doi: 10.1007/s10113-002-0042-3.

Behrendt, H., Venohr, M., Hirt, U., Hofmann, J., Opitz, D., Gericke, A. (2007): The model system MONERIS Version 2.0 User's Manual.

Boskidis, I., Gikas, G. D., Pisinaras, V., Tsihrintzis, V. A. (2010): Spatial and temporal changes of water quality, and SWAT modeling of Vosvozis river basin, North Greece, Journal of Environmental Science and Health Part A, 45, 1421–1440. doi: 10.1080/10934529.2010.500936.

Di, H. J., Cameron, K. C. (2002): Nitrate leaching in temperate agroecosystems: sources, factors and mitigating strategies, Nutrient Cycling in Agroecosystems, 64(3), 237–256. doi: 10.1023/A:1021471531188.

EEA and SAZP (2012): CORINE Land Cover (CLC). European Environmental Agency. Slovak Environment Agency. COPERNICUS PROGRAMME – Copernicus Land Monitoring Service. Available at: <http://copernicus.sazp.sk/>.[Online: 15th-March-2020].

European Commission (2009): LUCAS 2009 TOPSOIL data. European Soil Data Centre (ESDAC), European Commission, Joint Research Centre. Available at: <https://lnk.sk/eE24>. [Online: 15th-March-2020].

European Commission (2015): SOIL EROSION BY WATER (RUSLE2015). European Soil Data Centre (ESDAC), European Commission, Joint Research Centre. Available at: <https://lnk.sk/bpLW>. [Online: 15th-March-2020].

European Commission (2016a): TOPSOIL PHYSICAL PROPERTIES FOR EUROPE (based on LUCAS topsoil data). European Soil Data Centre (ESDAC), esdac.jrc.ec.europa.eu, European Commission, Joint Research Centre. Available at: <https://lnk.sk/pFX6>. [Online: 15th-March-2020].

European Commission (2016b): Urban Wastewater Treatment Plant. URBAN WASTEWATER TREATMENT PLANT REPORTED DATA – EUROPEAN COMMISSION urban wastewater website. Available at: <https://lnk.sk/vCH1>. [Online: 15th-March-2020].

European Community (2000): Directive 2000/60/EC of the European Parliament and of the Council of 23 October 2000 establishing a framework for Community action in the field of water policy, Official Journal of the European Parliament. Brussels, Belgium, Official Journal of the European Parliament. doi: 10.1039/ap9842100196.

Foley, J. A. et al. (2011): Solutions for a cultivated planet, Nature. Nature Publishing Group, 478(7369), 337–342. doi: 10.1038/nature10452.

Follett, R. F., Delgado, J. A. (2002): Nitrogen fate and transport in agricultural systems, Journal of Soil and Water Conservation, 57(6), 402–408. Available at: <https://lnk.sk/cioL>. [Online: 15th-March-2020].

Gleeson, T. (2018): GLobal HYdrogeology MaPS (GLHYMPS) of permeability and porosity. Scholars Portal Dataverse. doi: doi/10.5683/SP2/DLGXYO.

Government of the Slovak Republic (2011): Govermment Regulation SR No. 201/2011 Coll., that rules technical specifications for chemical analysis and monitoring of water status. Available at: <https://lnk.sk/nyLT>.[Online: 15th-March-2020].

Halmová, D., Pekárová, P., Bačová Mitková, V. (2019): Long-term trend changes of monthly and extreme discharges for different time periods, Acta Hydr. Slov., 20(2), 122–130.

Hill, A. R. (1981): Stream Phosphorus Exports From Watersheds with Contrasting Land Uses in Southern Ontario, Journal of the American Water Resources Association. John Wiley & Sons, Ltd (10.1111), 17(4), 627–634. doi: 10.1111/j.1752-1688.1981.tb01269.x.

Julínek, T., Říha, J. (2017): Assessing stream water quality influenced by storm overflows from sewers., Pollack Periodica, 12(2), 117–128.

Lam, Q. D., Schmalz, B., Fohrer, N. (2010): Modelling point and diffuse source pollution of nitrate in a rural lowland catchment using the SWAT model, Agricultural Water Management. Elsevier, 97(2), 317–325. doi: 10.1016/J.AGWAT.2009.10.004.

MET Norway (2019): Modelled air concentrations and depositions. The Norwegian Meteorological institute and the European Monitoring and Evaluation Programme (EMEP). Available at: <https://lnk.sk/FT57>. [Online: 15th-March-2020].

Ministry of Agriculture of the SR (2017): LPIS - LAND PARCEL IDENTIFICATION SYSTEM. Ministry of Agriculture and Rural Development of the Slovak Republic. Available at: <https://lnk.sk/uTZ9>. [Online: 15th-March-2020].

NAFC (2017): BONITIZED SOIL-ECOLOGICAL UNITS. National Agricultural and Food Centre Lužianky. Available at: <https://lnk.sk/imF4>. [Online: 15th-March-2020].

NASA JPL (2013): NASA Shuttle Radar Topography Mission Global 1 arc second, distributed by NASA EOSDIS Land Processes DAAC. Available at: <https://lnk.sk/iD03>. [Online: 15th-March-2020].

Rothwell, J. J., Dise, N. B., Taylor, K. G., Allott, T. E. H., Scholefield, P., Davies, H., Neal, C. (2010): Predicting river water quality across North West England using catchment characteristics, Journal of Hydrol., 395 (3–4), 153–162. doi: 10.1016/j.jhydrol.2010.10.015.

Schreiber, H. et al. (2005): Nutrient emissions from diffuse and point sources into the River Danube and its main tributaries for the period of 1998–2000 – results and problems, Water Science and Technology. IWA Publishing, 51(3–4), pp. 283–290. doi: 10.2166/wst.2005.0602.

Sliva, L. and Williams, D. D. (2001): Buffer zone versus whole catchment approaches to studying land use impact on river water quality, Water Research. Pergamon, 35(14), 3462–3472. doi: 10.1016/S0043-1354(01)00062-8.

The Ministry of Environment of the Slovak Republic (2009): Water Plan of Slovakia. Available at: <https://lnk.sk/lpsX>.[Online: 15th-March-2020].

The Ministry of Agriculture of the SR (2016): Decree no. 151/2016 Coll. Decree of the Ministry of Agriculture and Rural Development of the Slovak Republic laying down details on agrochemical testing of soils and on the storage and use of fertilizers (In Slovak).

Venohr, M. et al. (2011): Modelling of Nutrient Emissions in River Systems - MONERIS – Methods and Background, International Review of Hydrobiology, 96(5), pp. 435–483. doi: 10.1002/iroh.201111331.

Weitzel, L. R. (1979): Periphyton measurements and applications, in Weitzel, L. R. (ed.) Methods and measurements of periphyton communities: A Review. American Society for Testing and Materials, 3–33. Available at: <https://lnk.sk/boHM>. [Online: 15th-March-2020].

Mgr. Cyril Siman (*corresponding author, e-mail: siman@uh.savba.sk)
Ing. Yvetta Velísková, PhD.
Institute of Hydrology, SAS
Dúbravská cesta 9
841 04 Bratislava
Slovak Republic

DOI: 10.31577/ahs-2020-0021.01.0008

ACTA HYDROLOGICA SLOVACA

Volume 21, No. 1, 2020, 65 – 73

ASSESSMENT OF SURFACE WATER EUTROPHICATION AT ŽITNÝ OSTROV REGION

Viera Kováčová*

The purpose of this report is to review the role of nitrogen (N) and phosphorus (P) in the eutrophication of surface water. The work was required by Water Framework Directive 2000/60/ES as part of investigating excessive nutrient enrichment. This report reviews nutrient inputs to surface water; the role of nutrients in the eutrophication of surface water; the response of biota to nutrient enrichment; monitoring of changes due to eutrophication and the management of eutrophication. Monitoring of surface water bodies has been provided in terms of requirements of the Water Framework Directive. With regards of international and national legislative for the ecological status assessment ecological potential, chemical status, biological quality elements, supporting physical-chemical and hydro-morphological quality elements as well as the specific substances have been investigated. The aim of this contribution was to analyse eutrophication problem, factors affecting this process, its consequences and possibilities of prevention. The partial aim was to evaluate eutrophication state of surface water in Žitný ostrov channel network following the assessment physical-chemical and microbiological indicators in monitored period.

KEY WORDS: surface water, eutrophication, nutrients, nitrogen, phosphorus

Introduction

Eutrophication is the term applied to the observable effects of increased nutrients on an aquatic system. The nutrients of primary concern are nitrogen (N) compounds and phosphorus (P) compounds. Eutrophication is a process not a state, requiring factors external to a system to act in order to bring about change within the system. This is especially so in rivers where plant communities respond to flow, sediment type, and underlying geology more than any transient changes in dissolved nutrient status derived from external inputs. Flushing in flowing systems tends to reduce exposure times to enhanced nutrient loads, thereby reducing the scale of any change. Increases in both N and P cause changes in plant communities (Jickells, 2005).
The majority of observable effects of eutrophication are due to enrichment of running waters by P, or a combination of N and P. Enrichment by N tends to be associated with dissolved nutrients in the water column, whereas enrichment by P is associated with both sediment-bound and water column nutrients. It is therefore theoretically possible to reduce the effects of N-enrichment relatively easily over a relatively short timeframe if inputs are controlled, while the effects of P will be less easily resolved over short timescales. Assuming that the major observable effects are P-driven, and exacerbated by N enrichment, then the observable effects of a reduction in N may not be detectable until P is also reduced (Nedwell et al., 2001; Newman et al., 2005; Pärn et al., 2012; 2018).
Eutrophication of rivers is best managed by reducing inputs to the river system, rather than any in situ remedial action. Point source pollutants are easily managed, but diffuse pollution from agriculture, industry, urbanisation and others is less easily controlled. Diffuse pollution may be caused by leaching of nutrients from soil over a long period. Significant reductions in nutrients are those that have the capacity to change plant community, population structure and to improve the water quality (Devlin et al., 2011; Harper, 1992).
The effects of an eutrophication process on submerged macrophyte species will be more easily characterised in large, slow-flowing, sediment-retaining rivers, rather than in fast flowing smaller river systems. The speed of change due to eutrophication will be more rapid in large, slow-flowing rivers because plant communities are able to adapt within the timeframe of exposure to increased nutrients. Monitoring of eutrophication rates and effects needs to be adapted to the type of river system under investigation. Groundwater nutrient concentrations and their variability by region and over time are less well documented and this needs further work. There are clear ecological effects of raised nutrient concentrations in both lakes and rivers, including (Dzuro and Králiková, 2016; Pavlidou et al., 2015).

The external supplies of N and P to aquatic ecosystems are derived from a wide variety of sources, including groundwater, fluvial, and atmospheric inputs. The sum of these three sources can be termed the external load. The external supplies of nutrients to a water body can originate both as point sources, which are localized and more easily monitored and controlled, and as nonpoint sources, which are diffuse and much more difficult to monitor and regulate. The relative contributions of these two types of sources can differ substantially from watershed to watershed, depending upon local human population densities and land use (Fiala, 2016).

N and P exports from point and nonpoint sources can have profound effects upon the quality of receiving waters. The most common effects of increased N and P supplies on aquatic ecosystems are perceived as increases in the abundance of algae and aquatic plants. However, the environmental consequences of excessive nutrient enrichment are more serious and far-reaching than nuisance increases in plant growth alone. The degradation of water resources by eutrophication can result in worsening of water quality (Hessen, 1999; Smith et al., 1999; Wang et al., 2001).

Eutrophication in freshwaters is primarily driven by increases in N and P compounds. In terms of N, nitrate concentrations in rivers (and groundwaters) have increased substantially during the last decades and have been linked to changing agricultural practices (increased levels of fertilisation and the move to growing crops with higher N demand). There has also been an increasing input from atmospheric N-deposition, but this is probably a relatively insignificant contribution apart from in upland catchments with little agricultural influence. For phosphorus the main period for the transport of diffuse, agricultural sources of P is during the winter and particularly the autumn rains and the P concentration from these sources will be at its highest during the low summer flows.

Changes in freshwater biological communities as a response to pollution have long been recognised. Mostly research has focused on impairment to water quality resulting from pollution of either a physical, chemical or organic nature. Gradually there has been recognition of the role of both point – and non-point (or diffuse) sources of nutrient enrichment of surface waters. Studies of this eutrophication have historically concentrated on lentic and transitional waters of estuaries and coasts, but since the 1960's interest has also turned to the importance of nutrient enrichment from increasing levels of nitrogen and phosphorus in lotic systems or flowing waters.

The impact of nutrient enrichment on rivers is complicated by their dynamic nature, but symptoms such as excessive phytoplankton and filamentous algae development, weed growth and changes in macrophyte communities have clearly impacted water supply, fisheries and conservation value.

The eutrophication of several water bodies leads to significant changes in the structure and function of the aquatic ecosystem. Some profiles in this region have recently been found to be highly eutrophic. Most of the surface water bodies are surrounded with densely populated human settlement areas and agricultural fields. The size of smaller water bodies in human settlement areas is on the decrease with rise in population. After treatment, some quantity of sewage from the households is regularly discharged into the water bodies. The runoff brings down fertilizers and other chemicals from agricultural fields. The nitrogen and phosphorus containned in these effluents is known to promote excessive growth of plants (Khan et al., 2005; Harper, 1992).

Continuous point sources of phosphorus, dominated by sewage treatment works, have a highly important influence on levels of bioavailable phosphorus in the water column through the growing season. It is important to tackle point sources comprehensively so that reductions in phosphorus concentrations are maximised during this critical time of year. Diffuse sources of phosphorus, particularly from agriculture, are a major contributor to phosphorus levels in riverine sediments, where it can be utilised by benthic algae and rooted plants. This phosphorus can also be released into the water column by a variety of processes. As point sources are brought under control, the relative contribution from diffuse sources becomes increasingly important (Mainstone et al., 2002).

It is generally recognised that an increase in nutrient loading is a prerequisite of increased eutrophication in rivers (Schneider and Melzer, 2003). However, it has still not been unequivocally established which of the main nutrients, if any, is generally limiting in rivers. There is some evidence suggesting that phosphorus has a significant effect on macrophyte community structure. Although raised concentrations of nutrients in the water column (and pore water) are required to induce hyper-eutrophic conditions. Schneider and Melzer (2004) noted that all requirements for plant growth, such as light levels, trace nutrient concentrations, etc., must be in excess for plants to achieve their full growth potential, i.e. the maximum amount of growth which could be achieved at a given temperature if a specific nutrient were limiting and all other factors were in excess. Hence, if the river flows through a shaded area, such as a forest, then that growth potential will not be achieved due to light limitation and the river may not show any apparent signs of hyper-eutrophication. At low to medium productivity, nutrients probably limit macrophyte biomass but at high concentrations they are probably not limiting.

Impact of vegetation on flow in a lowland stream during the growing season investigated Velísková et al. (2017), Dulovičová et al. (2016), Schügerl et al. (2018). Vegetation growing in the water along watercourses has been the subject of several studies since it was recognized that it could have a significant impact on the water flow. It may increase resistance to flow and cause higher water levels. Also, it has an effect on the velocity profiles. Previous investigations on the flow of water through emergent vegetation have shown different results. The purpose of these studies was determine how aquatic vegetation influences flow resistance, water depth and discharge in the Chotárny channel at the Žitný Ostrov area. The Chotarny channel is one of three main channels of this network. Measurements performed during six years at this channel were used for an evaluation of vegetation impact on flow conditions. The roughness coefficient was used as one way of quantifying this impact. The results show variation of this parameter during the growing season. Vegetation causes resistance to flow; it reduces flow velocities, discharge and increases water depth. How the sprouting of stream bed vegetation influences channel`s flow conditions and its capacity was demonstrate.

The present state of surface water eutrophication in Slovakia indicate, that there was a change of water quality in 90`s in accordance with as consequence of social changes. Many practices result in point and non-point source of surface water pollution, include fertilizers and manure applications, dissolved nitrogen and phosphorus in precipitation, irrigation flows, and dry atmospheric deposition were reduced Phosphorus and nitrogen fertilizers were reduced very significantly, phosphorus fertilizers for 80% lower and nitrogen fertilizers for 51% lower than before 1989 (Kobza et al., 2008).

Mechanisms and assessment of water eutrophication investigated Yang et al. (2008). Water eutrophication has become a worldwide environmental problem in recent years, and understanding the mechanisms of water eutrophication will help for prevention and remediation of water eutrophication. Recent advances in current status and major mechanisms of water eutrophication, assessment and evaluation criteria, and the influencing factors were reviewed. Water eutrophication in lakes, reservoirs, estuaries and rivers is widespread all over the world and the severity is increasing, especially in the developing countries. The assessment of water eutrophication has been advanced from simple individual parameters like total phosphorus, total nitrogen, etc., to comprehensive indexes like total nutrient status index. The major influencing factors on water eutrophication include nutrient enrichment, hydrodynamics, environmental factors such as temperature, salinity, carbon dioxide, element balance, etc., and microbial and biodiversity. The occurrence of water eutrophication is actually a complex function of all the possible influencing factors. The mechanisms of algal blooming are not fully understood and need to be further investigated. The mechanisms of water eutrophication are not fully understood, but excessive nutrient loading into surface water system is considered to be one of the major factors. The nutrient level of many rivers and lakes has increased over the past several years in response to increased discharge of domestic wastes and non-point pollution from agricultural practices and urban development (Mainstone and Parr, 2002; Cheng et al., 2006).

Eutrophication can be defined as the sum of the effects of the excessive growth of phytoplanktons leading to imbalanced primary and secondary productivity and a faster rate of succession from existence to higher serial stage, as caused by nutrient enrichment through runoffs that carry down overused fertilizers from agroecosystems and/or discharged human waste from settlements (Khan and Ansari, 2005). Water eutrophication can be greatly accelerated by human activities that increase the rate of nutrient input in a water body, due to rapid urbanization, industrialization and intensifying agricultural production. Because the influence of the human activities, excessive nitrogen, phosphorus and other nutrients are loaded into water bodies, which could cause negative ecological consequences on aquatic ecosystem structures, processes and functions, result in the fast growth of algae and other plankton, and deteriorate water quality (Western, 2001).

Material and methods

Factors influencing water eutrophication

Water eutrophication is mainly caused by excessive loading of nutrients into water bodies like N and P. Excessive nutrients come from both point pollution such as waste water from industry and municipal sewage, and non-point pollution like irrigation water, surface run water containing fertilizer from farmland, etc. Increased nutrient load to water body is now recognized as a major threat of water quality degradation.

At present, excessive total nitrogen (TN) and total phosphorus (TP) in water are considered as the only factors inducing water eutrophication, but nutrient enrichment is only the necessary but not the sufficient condition for algal boom. Eutrophication is not likely to occur if both TN and TP in water are low, but eutrophication may not occur in water high in TN and TP if other conditions such as temperature and current speed are not favorable. The influencing factors of water eutrophication include: (1) excessive TN and TP, (2) slow current velocity, (3) adequate temperature and favorable other environmental factors, and (4) microbial activity and biodiversity.

(1) Nutrient enrichment
(2) Hydrodynamics
(3) Environmental factors
(4) Microbial and biodiversity

(1) The relationship of nutrient enrichment to water eutrophication and algal bloom: (a) When P concentration in water is low, it may be the limiting factor for inducing water eutrophication and algal bloom; (b) When P concentration in water increases rapidly, other may become a new limiting factor, such as pH, water depth, temperature, light, wave, wind or other biological factors; N and P input and enrichment in water are the most primary factors to induce water eutrophication.

(2) Hydrodynamics is not related to disturbing water itself but is influenced indirectly by changing light and nutrient status. In shallow water, increased frequency of disturbance could increased the P release from the sediment, especially at high temperature.

(3) Temperature and salinity are the two important factors to induce algal bloom. Algal bloom always occurs at temperature between 23°C and 28°C, salinity between 23% and 28%. The variation of temperature and salinity also affect algal bloom, and an important condition for algal bloom is that temperature increases and salinity decreases faster than ever in short time. Statistical analysis shows that the influence of temperature on algal growth rate is the largest, followed by salinity and their interaction. Change of salinity is also influenced by the concentration of nutrition. Research shows that salinity is negatively related with $N\text{-}NO_3^-$ and $P\text{-}PO_4^{3-}$, but positively related with $N\text{-}NH_4^+$ and however, it is not very related with $N\text{-}NO_2^-$. Light plays an important role in the growth, diversity and density of aquatic flora.

Algal growth has been reported to increase with light intensity, and luminescence of 4000 lux was found most favorable. There are other factors like pH and dissolved oxygen affecting water eutrophication. The direct relationship between phytoplankton and dissolved oxygen content has been observed by a number of researchers. The change in pH is directly related to the availability and absorption of nutrients from solution. Ionization of electrolytes or the valence numbers of different ion species are influenced by changes in pH. High pH values promote the growth of phytoplankton and result in bloom.
It must be pointed out that many factors influencing eutrophication are relative and affect each other.

Methods of monitoring and assessment of surface water

Historically are important year 1991, when was passed Directive 91/271/EHS regard cleaning urban waste-water and Directive 91/676 EHS regard nitrate agricultural source pollution and year 2000, when was passed Water Framework Directive (WFD) 2000/60/ES. The ecological status, ecological potential and chemical status assessment the biological quality elements (phytoplankton, phytobenthos and water macrophytes, benthic invertebrates), supporting physical-chemical and hydromorphological quality elements as well as the specific substances have been investigated. Ecological status/ potential assessment has been type specific, it has reflected reference conditions, the species diversity, quantity (abundance or biomass) and sensitive species have been included as well. The classification schemes have been already harmonized in the process of European intercalibration.
With regards of international legislative was in national legislative proposed assessment of the trophic state of water bodies according to following metodics (Makovinská et al., 2015; Hucko et al., 2013; Tlučáková et al., 2016):

a) Assessment of the trophic state of surface water with regards of the Supplement No.1 Directive of Government SR No. 269/2010 – monitored indicators are: total nitrogen, total phosphorus, ammonia nitrogen, nitrite nitrogen, nitrate nitrogen concentrations and phytoplankton biomass (chlorophyll-a) (Table 1).
b) Assessment of the trophic state of surface water with „France metodic“ – for the assessment is necessary to use average summer concentrations of nitrates, phosphates and total phosphorus and maximum summer concentration for chlorophyll-a (summer period means months april–september) (Table 2).
c) Assessment of the trophic state of backwaters with regards of OECD metodic (annual average of total phosphorus concentrations, chlorophyll-a concentrations a Secchi depth).

Monitoring of surface water in Žitný ostrov channel network (Danube Lowland, Slovakia) has been provided in terms of requirements Supplement No.1 Directive of Government SR No. 269/2010, Part A (general indicators) and Part E (hydrogeological and microbiological indicators) in the period of 1987–2019. For assessment of sensitive localities and identification of eutrophication endangered places the Supplement No. 12 and No. 13 are used.
Monitoring and assessment of following indicators were performed – total nitrogen (N_{TOT}), nitrate nitrogen ($N\text{-} NO_3^-$), nitrite nitrogen ($N\text{-}NO_2^-$), ammonia nitrogen ($N\text{-} NH_4^+$), total phosphorus (P_{TOT}), phosphate phosphorus ($P\text{-}PO_4^{3-}$) according the Supplement No.1 Directive of Government SR No. 269/2010, Part A and biomas of phytoplankton (CHL_a) according Part E.

Results and discussion

The Žitný ostrov is one of the most productive agricultural areas of Slovakia, situated on the Danube Lowland. Under its surface is the richest water reservoir of Slovakia. For this reason, it is very important to deal

Table 1. Evaluation of trophic state of surface water according to Supplement No.1 Directive of Government SR No. 269/2010

Indicator	Symbol	Unit	Value
Ammonia nitrogen	$N\text{-}NH_4^+$	$mg\ l^{-1}$	1
Nitrite nitrogen	$N\text{-}NO_2^-$	$mg\ l^{-1}$	0.02
Nitrate nitrogen	$N\text{-}NO_3^-$	$mg\ l^{-1}$	5
Nitrogen total	N_{TOT}	$mg\ l^{-1}$	9
Phosphorus total	P_{TOT}	$mg\ l^{-1}$	0.4
Phytoplankton biomass (chlorophyll-a)	CHL_a	$\mu g\ l^{-1}$	50

Table 2. Evaluation of trophic state – Directive 91/676/CEE – Surface water – rivers (France metodic)

Indicator	Unit	State				
		I Ultraoligotrophic	II Oligotrophic	III Mezotrophic	IV Eutrophic	V Hypereutrophic
Nitrates (average summer concentration)	mg l^{-1}	< 2	< 10	< 25	< 50	> 50
Phosphates (average summer concentration)	mg l^{-1}	< 0.1	< 0.5	< 1	< 2	> 2
Phosphorus tot. (average summer concentration)	mg l^{-1}	< 0.05	< 0.2	< 0.5	< 1	> 1
Chlorophyll-a (max. summer concentration)	μg l^{-1}	< 2.5	< 8	< 25	< 75	> 75

with quantity and quality of water resources in this region. The channel network at the Žitný Ostrov area was built up for drainage and also to provide irrigation water. There are three main channels of this network: Chotárny channel, Gabčíkovo-Topoľníky channel and Komárňanský channel. Chotárny channel – is the P1M water body type (partial river-basin Váh, code SKW0029), Gabčíkovo-Topoľníky channel – is the P1M water body type (partial river-basin Váh, code SKW0023), Komárňanský channel – is the P1M water body type (partial river-basin Váh, code SKV0226). For the evaluation the water quality we went out from the data obtained on Institute of Hydrology SAS during the 1987–2019. Monitored localities was chosen so that they be the most representative area-covering.
The main purpose of this paper is to provide a brief review on recent state of eutrophication in Žitný ostrov channel network and understanding the mechanisms of water eutrophication and progresses in identifying the influence factors inducing water eutrophication.
The nutrient level in surface water has decreased after 1990^{th} in response to decreased discharge of domestic wastes and non-point pollution from agricultural practices and urban development (Fig. 1–4). However we observe slight increasing in Komárňanský kanál (Fig. 5, 6, 7) during last few years. Excessive nutrient inputs (have been gone over the limit values not only in some months, but average annual values for nitrates and phosphates, too) and other conditions, such as high temperature, decreased dissolved oxygen content, higher pH and increased light intensity in summer period induced enhanced water eutrophication.

Conclusion

The present review deals with the studies conducted on the impact of nitrogen and phosphorus amount on eutrophication in surface water on the Žitný ostrov channel network. The review covers the definition and concept of eutrophication and the adverse effects on quality and ecosystem functioning. The eutrophication of several water bodies leads to significant changes in the structure and function of the aquatic ecosystem. Some profiles in this region have recently been found to be highly eutrophic. Most of the surface water bodies are surrounded with densely populated human settlement areas and agricultural fields. The size of smaller water bodies in human settlement areas is on the decrease with rise in population. After treatment, a some quantity of sewage from the households is regularly discharged into the water bodies. The runoff brings down fertilizers and other chemicals from agricultural fields. The nitrogen and phosphorus contained in these effluents is known to promote excessive growth of plants.
The detergents that are the major source of phosphorus inputs into water bodies (through sewage and drainage systems) have been thoroughly discussed. The major part of detergents comprises builders containing polyphosphate salts. An environment-friendly and effective synthetic builder is yet to be developed to replace existing phosphorus containing builders of detergents. The utility of the alternative builders available has been reviewed. Nitrogen has also been reported to affect the phytoplankton production in eutrophic waters in temperate regions. This review is an account of the role, sources, and monitoring of nitrogen and phosphorus, as well as its influence on surface water eutrophication. Several environmental factors have also been found to add to the problem of eutrophication in addition to nutrients. The limiting factors - namely temperature, pH, light, dissolved oxygen and CO_2 level are known to affect eutrophic water bodies. The results of nitrogen and phosphorus amounts reported in this study are the best indicators of the level of eutrophication.
Continuous point sources of nitrogen and phosphorus, dominated by sewage treatment works, have a highly important influence on its level in the water column through the growing season. It is important to tackle point sources comprehensively so that reductions in nutrients concentrations are maximised during this critical time of year. Diffuse sources, particularly from agriculture, are a major contributor to nutrient levels in riverine sedi-

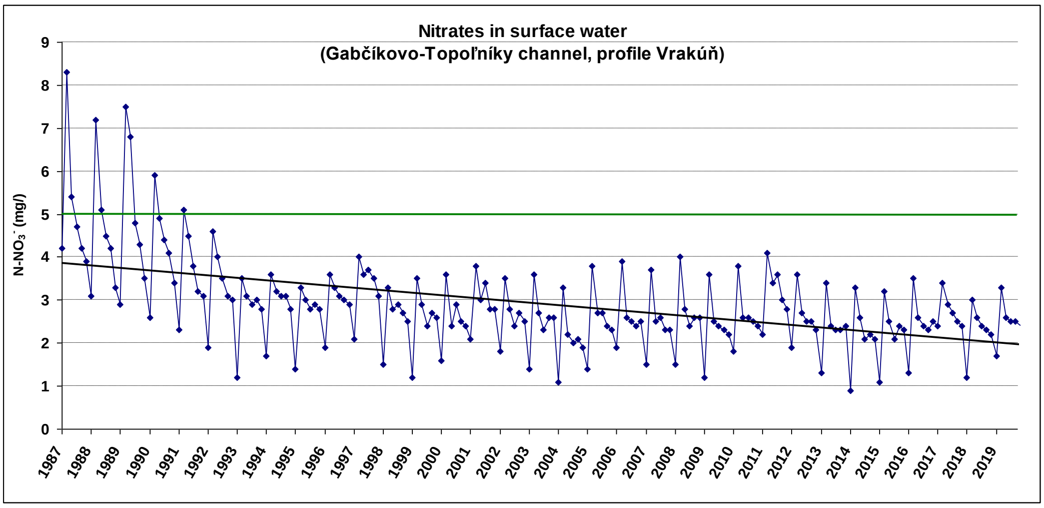

Fig. 1. Nitrates in surface water – Gabčíkovo-Topoľníky channel.

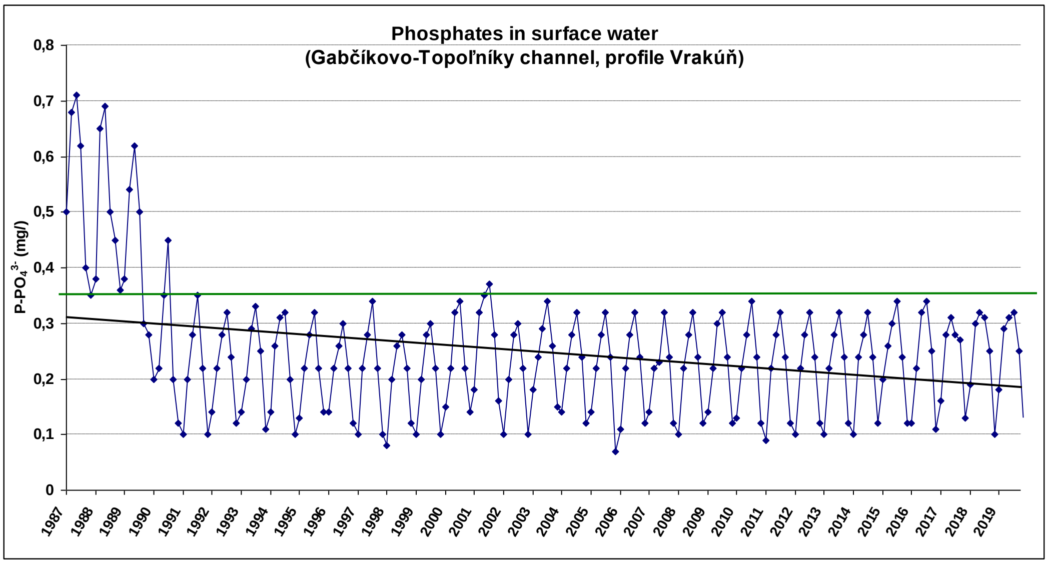

Fig. 2. Phosphates in surface water – Gabčíkovo-Topoľníky channel.

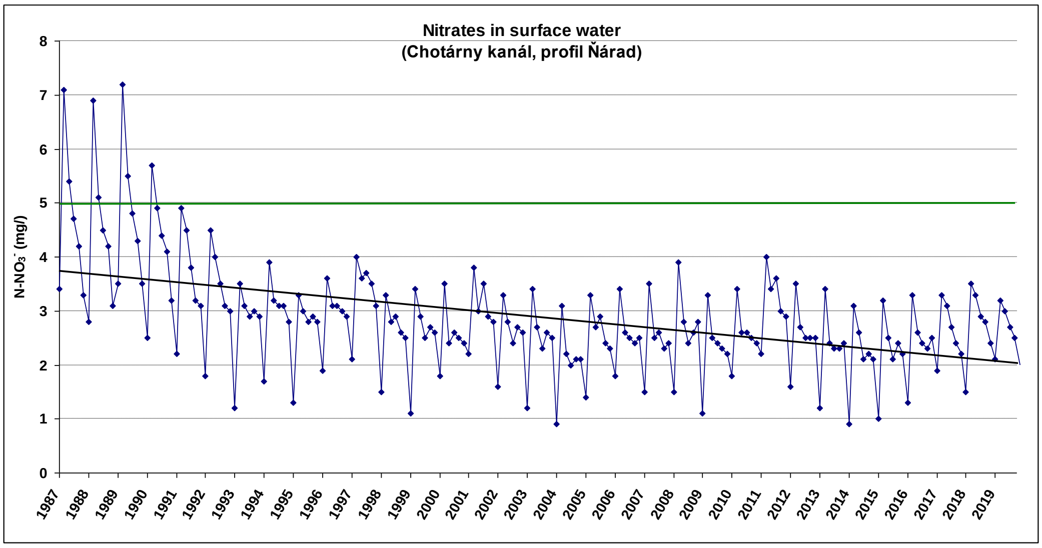

Fig. 3. Nitrates in surface water – Chotárny channel.

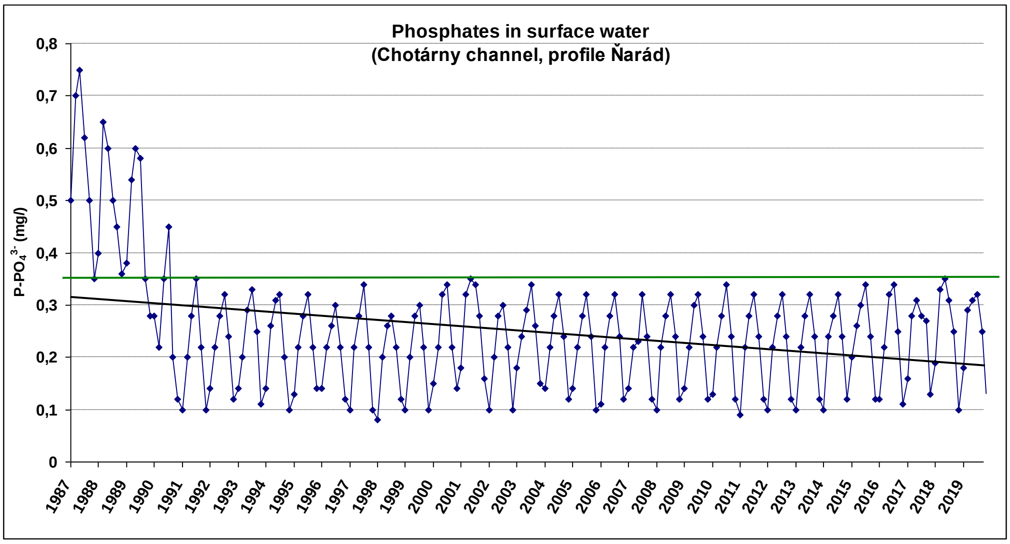

Fig. 4. Phosphates in surface water – Chotárny channel.

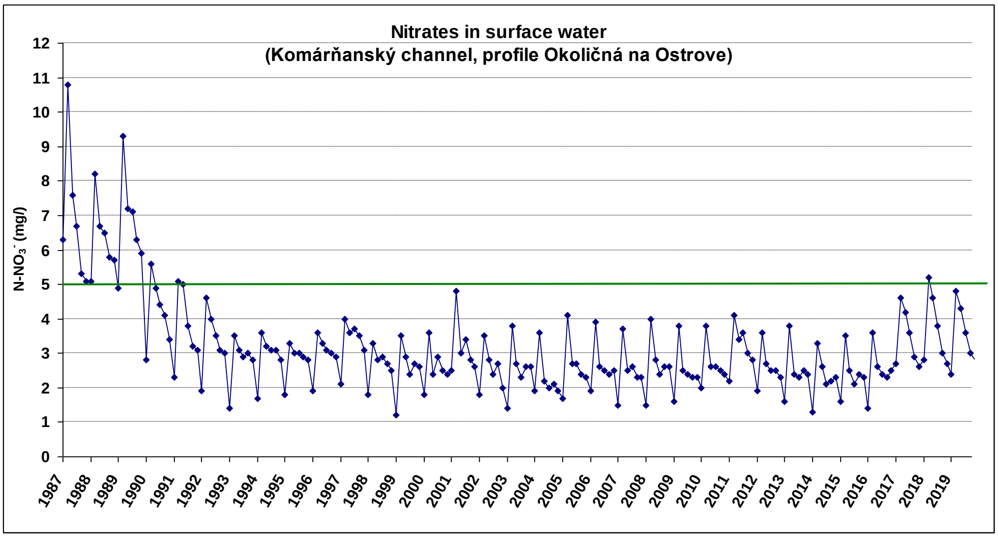

Fig. 5. Nitrates in surface water – Komárňanský channel.

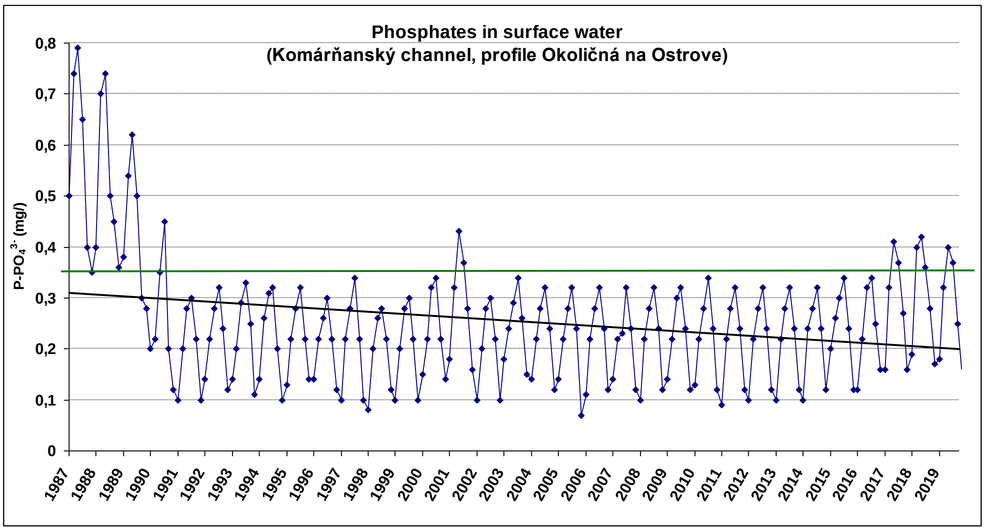

Fig. 6. Phosphates in surface water – Komárňanský channel.

Fig. 7. State of surface water eutrophication – Komárňanský channel (2019).

ments, where it can be utilised by benthic algae and rooted plants. This nutrients can also be released into the water column by a variety of processes. As point sources are brought under control, the relative contribution from diffuse sources becomes increasingly important.

The study is focused on identification of the long-term trends in the surface water quality in channel network at Žitný ostrov region. The paper shows changes in measured values of nitrates and phosphates in particular channels in years 1987–2019. It was shown the channel water quality has been changed significantly during the period 1987–1990, after 1990 is slightly decreased. However we observe slight increasing in some profiles of Komárňanský kanál with major agricultural activities during last few years.

Acknowledgement

This contribution was supported by project VEGA 2/0025/19 and project VEGA 1/0085/20.

References

Devlin, M., Bricker, S., Painting, S. (2011): Comparison of five methods for assessing impacts of nutrient enrichment using estuarine case studies. Biogeochemistry 106, 177–205.

Directive of Government SR No. 269/2010 for accomplish suitable state of water.

Directive 91/271/EHS regard cleaning urban waste-water.

Directive 91/676 EHS regard nitrate agricultural source pollution (preventing nitrates from agricultural sources polluting ground and surface waters and by promoting the use of good farming practices).

Directive (WFD) 2000/60/ES Water Framework Directive

Dulovičová, R., Velísková, Y., Schügerl, R. (2016): Modification of Silts Hydraulic Conductivity along the Lowland Channel Gabčíkovo-Topoľníky (Slovakia). In 16th International Multidisciplinary Scientific GeoConference SGEM 2016: Conference proceedings. Book 3, vol. 1. Hydrology and Water Resources. – Sofia, 521–528. ISBN 978-619-7105-61-2.

Dzuro, T., Králiková, R. (2016): Effective patented method in the process of eutrophication of surface waters. Environmental Policy tools. Conference proceeding VI. Internat. Scientific Conference, Bratislava, 36–42.

Fiala, D. (2016): Boj o fosfor, aneb pracují všichni vodohospodáři na plný výkon? Vodní hospodářství, 5, 2016.

Harper, D. (1992): Eutrophication of Freshwaters : Principles, problems and restoration. Chapman & Hall 1992, ISBN 978-94-011-3082-0, https://doi.org/10.1007/978-94-011-3082-0

Hessen, D. O. (1999): Catchment properties and the transport of major elements. In: Nedwell, D. B., Raffaelli, D. G. (Eds.), Estuaries. Adv. Ecol. Res. vol. 29, 1–41.

Hucko, P., Štetina, M., Luther, S. (2013): Národný prístup hodnotenia povrchových vôd v SR. Vodárenská biologie, Praha, 1–21.

Cheng, X. Y., Li, S. J. (2006): An analysis on the evolvement processes of lake eutrophication and their characteristics of the typical lakes in the middle and lower reaches of Yangtze River. Chinese Science Bulletin, 51(13): 1603–1613. doi:10.1007/s11434-006-2005-4.

Jickells, T. (2005): External inputs as a contributor to eutro-

phication problems. J. Sea Res. 54, 58–69.
Khan, F. A., Ansari, A. A., (2005): Eutrophication: An ecological vision. The Botanical Review, 71(4): 449–482.
Kobza, J., Gáborík, Š. (2008): Súčasný stav a vývoj obsahu makro a mikroelementov v poľnohospodárskych pôdach Slovenska. VÚPOP Bratislava, 57 s.
Mainstone, C. P., Parr, W., (2002): Phosphorus in rivers-ecology and management. The Science of the Total Environment, 282–283.
Makovinská, J. a kol. (2015): Metodika monitorovania a hodnotenia vodných útvarov povrchových vôd Slovenska. VÚVH, 179 s., ISBN 978–80-89740–02–4.
Nedwell, D. B., Dong, L. F., Sage, A., Underwood, G. J. C. (2001): Variations of the nutrient loads to the mainland UK estuaries: correlations with catchment areas, urbanisation and coastal eutrophication. Est. Coast. Shelf Sci. 56, 951–970.
Newman, J. R., Anderson, N. J., Bennion, H., Bowes, M. J., Luckes, S., Winder, J., (2005): Eutrophication in rivers : an ecological perspective. Centre for Ecology and Hydrology, 37 pp., DOI: 10.13140/2.1.3711.5208
Pavlidou, A., Simboura, N., Rousselaki, E., Tsapakis, M., Pagou, K., Drakopoulou, P., Assimakopoulou, G., Kontoyiannis, H., Panayotidis, P. (2015): Methods of eutrophication assessment in the context of the water framework directive: Examples from the Eastern Mediterranean coastal areas. Continental Shelf Research, 108, 156–168.
Pärn, J., Pinay, G., Mander, Ű. (2012): Indicators of nutrients transport from agricultural catchments under temperature climate: A review. Ecological Indicators, 22, 2012, 4–15.
Pärn, J., Henided, H., Kasaka, K., Kauere, K., Sohara, K., Tournebozed, J., Uema, E., Välik, K., Mander, U. (2018): Nitrogen and phosphorus discharge from small agricultural catchments predicted from land use and hydroclimate. Land Use Policy, 75, 260–268.
Schneider, S., Melzer, A. (2003): The Trophic Index of Macrophytes (TIM) – a new tool for indicating the trophic state of running waters. Hydrobiology, vol. 88, 1, 49–67, doi.org/10.1002/iroh.200390005.
Schneider, S., Melzer, A. (2004): Sediment and Water Nutrient Characteristics in Patches of Submerged Macrophytes in Running Waters, Hydrobiologia, 527, 195–207.
Schügerl, R., Velísková, Y., Dulovičová, R. (2018): Identifikácia zmien prietokových pomerov a rýchlostného profilu pri prúdení s voľnou hladinou. Hydrologkcký výskum v podmienkach prebiehajúcej klimatickej zmeny. Monografia ÚH SAV. Veda, Bratislava, 391 s.
Smith, V. H., Tilman, G. D., Nekola, J. C. (1999): Eutrophication: impacts of excess nutrient inputs on freshwater, marine, and terrestrial ecosystems. Environmental Pollution, 100, 179–196.
Tlučáková, A., Cibulka, R. (2016): Sledovanie časového vývoja priestorového rozšírenia dusičnanov v povrchových vodách Slovenska. Vodní hospod. 3, 2016.
Velísková, Y., Dulovičová R., Schügerl, R. (2017): Impact of vegetation on flow in a lowland stream during the growing season. Biologia 72/8, 840–846, DOI: 10.1515/biolog-2017-0095
Wang, J., Fu, B., Qiu, Y., Chen, L., (2001): Soil nutrients in relation to land use and landscape position in the semi-arid small catchment on the loess plateau in China. Journal of Arid Environments, 48, 537–550.
Western, D., 2001. Human-modified ecosystems and future evolution. Proceedings of the National Academy of Sciences of the United States of America, 98(10):5458–5465. [doi:10.1073/pnas.101093598]
Yang, X., Wu, X., Hao, H., He, Z. (2008): Mechanisms and assessment of water eutrophication. J. of Zhejjang Univ. Sci., 9 (3), 197–209.

Ing. Viera Kováčová (*corresponding author, e-mail: kovacova@uh.savba.sk)
Institute of Hydrology, SAS
Dúbravská cesta 9
841 04 Bratislava
Slovak Republic

DOI: 10.31577/ahs-2020-0021.01.0009

ACTA HYDROLOGICA SLOVACA

Volume 21, No. 1, 2020, 74 – 81

RELATIONSHIP OF NITRATES AND NITRITES IN THE WATER ENVIRONMENT WITH HUMANS AND THEIR ACTIVITY

Lucia Balejčíková*, Andrej Tall, Branislav Kandra, Dana Pavelková

Nitrates and nitrites in water pose a health and environmental hazards, in particular when exceeding limits defined in the European Union, i.e. max. 50 mg l^{-1} of nitrates. It is not recommended to exceed the limit of 10 mg l^{-1} of nitrates for infants and children. The maximum concentration of nitrites is 0.5 mg l^{-1} for adults and infants less than 0.1 mg l^{-1}. Our work offers a review of the water quality concerning the relationship between nitrates/nitrites and humans. Basic properties and forms of nitrates, their use for human activities, importance and risks to human health and possibilities of their physicochemical determination are summarized. Our study demonstrates also the novel approaches to the nitrates decontamination in a water environment using various nanomaterials. We aimed at a collection of records from the monitoring of nitrates in selected areas in Slovakia to show good quality of water in various water sources, which over time improves due to the increasingly low fertilization intensity and thus of agriculture production, which is gradually being replaced by imports.

KEY WORDS: nitrates/nitrites, importance/risk, determination, decontamination, monitoring

Introduction

A rapidly developed life trend because of its close association with an environment can lead to depreciation of sources, especially water sources. Water as a still extensive part of Earth is irreplaceable for life in any form. Unfortunately, some inadequate human activity can lead to water pollution. Widespread nitrates and nitrites are still considered as prominent sources of water pollution, especially in countries where their use exceeds organizational recommendations for protection against damage of human health. Therefore it is necessary to monitor them continuously. The basic difference between nitrates and nitrites comes from different atoms of oxygen (Fig. 1). They will differ in physicochemical properties, depending on a compounds type they will form.

It is generally known, that nitrates form stable crystalline solids salts of nitric acid. Nitrate anions can be found naturally in every water, atmosphere or on the earth in a form of various mineral as nitratine, nitrocalcite or nitromagnesite (Onac, 2012; Orel and Seinfeld, 1977). Usually, nitrates are prepared in the lab by dissolving metals in nitric acid or by reacting with metal hydroxides, oxides or carbonates. They are soluble in water and stable under aerobic conditions. Nitrites occur in water, where oxygen is absent, as a product of nitrate reduction (denitrification). Nitrite contains nitrogen in a relatively unstable oxidation state. In a natural nitrogen cycle, nitrifying bacteria produce nitrites followed by their oxidation back to nitrates. Nitrites are salts of nitrous acid. They can be prepared by thermal decomposition of alkali metal nitrates or by reduction of their melt e.g. lead. All nitrites are well soluble in water except yellow silver nitrite (Laue et al., 2006). Nitrates and nitrites cause danger in the environment, mainly in groundwater and sources of drinking water, due to an effect of fertilization ("area pollution"), or wastewater leaks ("spot pollution"), which often exceeds maximum concentrations in water sources for a human consumption.

Nitrates dissolve easily in a soil solution, i.e. nitrate salts dissociate in an aqueous medium to very mobile nitrate anions, and due to a low sorptivity on soil particles caused by their negative charge can be washed out of the soil into groundwater that can contaminate or flow into surface sources and rivers. From there it gets into plants and food (Šalgovičová and Krížová, 2006). Nitrates in increased concentrations occur in the soil as a result of agricultural activities (natural and synthetic fertilization), from the animal and industrial waste (from dye productions or engineering plants) (Lenghartová et al., 2015). Nitrate compounds for commercial applications are products of the chemical industry. The most used nitrates are sodium nitrate ($NaNO_3$), ammonium nitrate (NH_4NO_3), silver nitrate ($AgNO_3$) and potassium nitrate (KNO_3). They are widely used as a fertilizer component in agriculture, in glass productions, as an oxidizing agent in pyrotechnics, in a food preserving industry and as a stabilizer of a meat products colour, in medicine (Honikel, 2008; Nakayama et al., 2010; Nujić and Habuda-Stanić, 2017). Nitrites added to meat product causes a red colour, which is a result of many compli-cated reactions related to an oxidation state change of an iron ion in myoglobin localized in muscles. The use of sodium and potassium salts of nitrates and nitrites in the food industry is regulated and limited by laws that take into account their toxicity. The most used food additives are sodium nitrite and potassium nitrite (marked as E250, E249) and sodium nitrate and potassium nitrate (E251, E252). Positive effects of mentioned agents include antioxidant activity, prevention against microbial growth and finally a pleasant flavour of meat (Honikel, 2008).

Importance and risks of nitrates and nitrites to human health

The most important reason, why to study and monitor nitrates and nitrites in water sources and food is their effect on human health. Nitrates and nitrites are the normal part of the nitrogen cycle in nature. Living organisms including plants accept them for their needs. They occur in the environment, air, food (especially vegetables and fruits) and in water sources (Nujić and Habuda-Stanić, 2017).

The health benefit of nitrates includes their antibacterial activity in the stomach against microbes as Salmonella or Escherichia coli that cause gastroenteritis. First, nitrates are rapidly reduced by microbes on the tongue in mouth saliva to nitrites, which produce nitrous acid when it reaches a normal human stomach. Nitrates act against dental caries and even on our skin against fungal pathogens. When a human body is exposed to a nitrate-free diet, nitrate can be produced endogenously via nitric oxide synthase that acts on the amino acid L-arginine to produce nitric oxide (NO), from which nitrates are formed under the influence of superoxide or oxidized haemoglobin (Addiscott and Benjamin, 2006). Many studies have shown, that nitrates and nitrites positively affect biological activities of some substances necessary for normal physiological (mainly cardiovascular) functions in the human body (Larsen et al., 2006; Machha and Schechter, 2011; Bondonno et al., 2018). In detail, nitrites and nitrates improve endothelial function, cause vasodilation, inhibit platelet aggregation and play a significant role in NO (nitric oxide) biosynthesis and bioavailability, which improves blood circulation. The nitrite and nitrate application is usually suggested for the treatment and prevention of cardiovascular diseases (Machha and Schechter, 2011).

Despite the many health benefits of nitrates and nitrites it is necessary to take into account that positive biological effects of nitrite and nitrate depend on their systemic concentration from endogenous and exogenous sources (Dejam et al., 2004; Kapil et al., 2010; Lundberg and Weitzberg, 2009). Normal plasma concentrations of nitrites are between 0.01 and 0.6 μM and for nitrates is range 20–40 μM (Machha and Schechter, 2011). As it was in the case of common substances or drugs, also nitrates and nitrites after standard verified concentration limit exceeds will become toxic for humans. This situation may occur most often as a result of incorrect (excessive) fertilization with nitrogen fertilizers, which can get into groundwater through natural transport processes in nature, or excessive consumption of nitrate-containing meat. Contamination can come from food, water sources and wells near the industrial plants or drainage. The main health risk of nitrates comes from their conversion to nitrosamines that belong reportedly to carcinogenic substances acting on nucleic acids causes tumours (Lin, 1990; Gushgari and Halden, 2018). However, despite many epidemiological and experimental studies, there are no direct correlations between cancer development and nitrates and nitrites intake (Knight et al., 1990; Eichholzer and Gutzwiller, 1998). On the other hand, some other works show associations between nitrites and nitrates in meats with an increased risk of cancer formation (Cross et al., 2010; Ferrucci et al., 2010). Intoxication with nitrates and nitrites shows in 3 phases. Nitrate phase starts 3–7 hours after receiving a toxic substance. Symptoms are bloody diarrhoea, colic, cramps, palsy, eventually death. The nitrite phase includes the primary toxic effect of nitrites on the central nervous system and vessels. Tachycardia and hypotension are the main symptoms. This phase of intoxication ends with collapse, eventually death. The last phase is the methemoglobin phase. Haemoglobin is a protein in red blood cells which helps to distribute oxygen in the body. Absorbed nitrates are rapidly reduced to nitrites, which react with haemoglobin followed by the loss of its ability to transport oxygen. Nitrites in the bloodstream cause the oxidation of heamo-

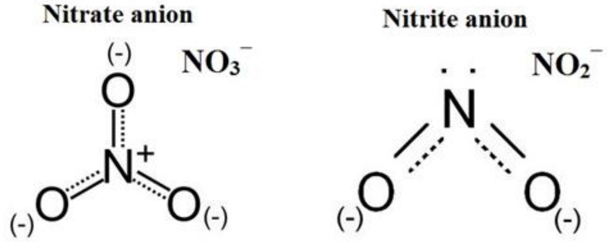

Fig. 1. Structural and chemical formula of nitrate and nitrite anion.

globin to methemoglobin. The Fe^{2+} ion present in the heme group is oxidized to its Fe^{3+} form, and the remaining nitrites bind strongly to heme, which does not allow oxygen transport. Hypoxemia is initialized. The skin turns blue and the blood turns brown. The health condition is called methemoglobinemia and can lead to cyanosis as a result of tissue suffocation. Abortions occur in pregnant women, and this phase can also end in death. In generally, methemoglobinemia represents a different degree of oxygen transport deficiency and poses a great risk especially to infants and children, which have increased oxidability of haemoglobin and relatively low methemoglobin reductase activity. Methylene blue or toluidine blue, ascorbic acid (vitamin C), O_2 treatment, exsanguination transfusion, hemodialysis etc. are usually used to relieve symptoms and treat methemoglobinemia (Ali Mansouri, 1985; Greer and Shannon, 2005; Králinský and Mečiaková, 2014). The most important is early diagnosis of this disorder.

Methods for nitrates and nitrites determination

Nitrates and nitrites monitoring in the human body, food, objects or areas should be performed by use preferred method for their determination. As much as possible it should be the available, inexpensive and time-saving method. Determination of nitrates and nitrites concentration or their presence in an aqueous medium can be performed using various methods, which have been developed over time. Basic principles, detection limits, advantages and disadvantages concerning various methods were processed in some detailed works (Lenghartová et al., 2015; Wang et al., 2017; Singh et al., 2019). Spectroscopic methods, as ultraviolet and visible (UV-VIS), spectrofluorimetric, Raman, infrared, Fourier-transform infrared, atomic absorption, chemiluminescence, mass spectroscopy, electron paramagnetic spectroscopy or nuclear resonance spectroscopy, are the most frequently applied for detection. UV-VIS spectroscopy as basic equipment of each chemical laboratory is usually used. Physical UV-VIS principle allow use catalytic, nitrosation, enzymatic, reduction or Griess assays. Also, nitrates and nitrites can be analyzed by titration methods (acidimetry, manganometry, indirect iodometry, etc.), electrochemical, separation methods (ion chromatography, electrophoresis) (Lenghartová et al., 2015; Wang et al., 2017) or colourimetrically (Woollard and Indyk, 2014). We would like to highlight, the suitability of selected method towards interferences (presence of other ions) and analyte concentration range should be verified before analytic determination (Singh et al., 2019).

Possibilities and new approaches of nitrates decontamination from the water environment

Requirements for high water quality are steadily increasing due to the continued widespread biological and chemical contamination as a result of the population growth over time. Unequal distribution of people in the surrounding environment led to the accumulation of contaminants in endangered areas, where natural flora and fauna have been eliminated in favour of the rapid development of humanity, technology and society.

One way to remove increased amounts of contaminants may be the development of separation technology. As we mentioned above in our paper, nitrites occur in unstable oxidation state and they are transformed back to nitrates in the natural nitrogen cycle, therefore separation technology is aimed at nitrates removal only. Usually, for reducing of nitrates, as durable and soluble ions, separation methods like adsorption, reversal osmosis, ion exchange, electrodialysis and biological, chemical or catalytic denitrification have been used (Kapoor and Viraraghavan, 1997; Soares, 2000; Shrimali and Singh, 2001; Bhatnagar and Sillanpää, 2011; Archna et al., 2012). Currently, the foremost challenge not only for scientists and engineers worldwide is focused on the development of innovative, effective and low-cost water treatments technologies. Highly popular nanotechnological systems could be a promising tool for water treatment and improving the water quality thanks to numerous laboratory studies. Application possibilities of nanotechnology involve membrane filtration, adsorptive elimination of micropollutants, nanocatalysis degradation and microbial decontamination (Li et al., 2008a, b). Madhura in the latest review refers to the interesting physicochemical properties of various nanomaterials characterized by an excellent adsorption capacity, enhanced photocatalysis, and high reactivity useful in separation processes such as reverse osmosis, microfiltration, and nanofiltration (Madhura et al., 2019). The most interesting and intensively studied material – graphene represents a highly promising system for environmental applications in water treatment. Also, low production cost raises the importance of the separation technologies development based on graphene. The one layer of carbon atoms in graphene nanostructure provides extreme thinness, mechanical strength, chemical stability, and inherent impermeability useful as a suitable two-dimensional separation nano-membrane (Celebi et al., 2014). Such application requires functionalization of graphene to achieve permeability, while holes for the transport of small molecules can be created (Hosseini et al., 2018; Shi et al., 2018). Then, nanopores, formed on the functionalized graphene sheet, can be used for nanofiltration of nitrates from contaminated water (Li et al., 2017; Anand et al., 2018). Jahanshahi and co-autors (2018) has used molecular dynamics simulation method to show how water molecules crossed through the fluorinated and hydrogenated graphene pores with different size localized in graphene sheets. Graphene membranes can be applied to nitrate ions elimination from water under various amounts of external pressures. We would like to emphasize that functionalization of graphene nano-membrane by specific chemical substances or groups, molecules or biomacromolecules with enzymatic activity can improve, accelerate, decelerate various ions and acting as a selective, controlled and time-regulated membrane. Also during transport, the chemical composition of holes can change properties of contaminant to more or less toxic. Chemical adjustment of nano-membrane can simply release ions or molecules according to properties of each contaminant, including charge, size and reactivity. The important role in transport processes can play diffusion and electrostatic gradient in the medium. Many researchers of various field of science are intensively engaged to the development of cost-effective synthesis technology for graphene-modified using various elements (e.g. oxygen, hydrogen or metals ions), molecules (e.g. epoxy, hydroxyl, carbonyl, carboxylic groups, or chelates) and magnetic nanoparticles, what continuously increased the popularity for proposing the ability of graphene-based systems to purify water from nitrates contamination by the separation or adsorption methods (Ghadiri et al., 2017; Ma et al., 2018; Jilani et al., 2018). Magnetic nanoparticles (most often of magnetite – Fe_3O_4) size in the range from 1–100 nm provide high surface energy and reactivity, what is the major cause of their different physical properties compared to macroscopic systems with the same chemical composition. Thanks to the unique properties and availability, their application possibilities constantly expand from the medical science, technology and industry to the environmental scope. Magnetic nanoparticles are commonly used to remove hazardous contaminants from wastewaters. Nanomagnetite thanks to the high specific surface area can be used as a nano-adsorbent. Superparamagnetic properties allow magnetic separation under external magnetic fields and after the treatment process, magnetic nanoparticles can be effortlessly retained and reused (Mayo et al., 2007). Similarly, magnetite nanoparticles, modified by 3- aminopropyl-triethoxysilane, were used to enhance the removal of nitrate ions from contaminated groundwater. The proposed system with good adsorption selectivity for nitrate ions can provide fast and efficient decontamination and rapid separation by using just an external magnetic field (Poursaberi et al., 2013). Another experiment has shown, that Fe_3O_4-based magnetic nanoparticles coated on powder activated carbon can be applied for the spontaneous and endothermic adsorption of nitrate from aqueous solutions (Rezaei Kalantary et al., 2014). Besides the absorption capacity of magnetic nanoparticles, their next advantage is catalytic activity allowing oxidative or reductive degradation of pollutants. Many studies on magnetic nanoparticles of magnetite coated by various surfactants have shown degradation activity of such durable materials as lysozyme amyloid fibrils (Bellova et al., 2010; Kopcansky et al., 2015). Despite that the precise mechanism of magnetic nanoparticles effects on various objects is still not fully understood, the catalytic effect is highly expected also in interaction with nitrates in the water environment. We assume, that the effectiveness of the remediation process of nitrates will dependent on the reaction time, the concentration of the catalytic agent (magnetic nanoparticles), the properties and composition of the surfactant (surface charge – zeta potential) and surrounding medium (pH). Interesting material for NO_3^- degradation seems to be intensively studied magnetoferritin, a semi-biological nanomaterial consisting of apoferritin cage with the size of 10–12 nm, which surrounds magnetic nanoparticles. The study of application possibilities of magnetoferritin was focused especially on the medical field of science. Magnetoferritin can be used as standard in diagnosis of various diseases, contrast agent in MRI, drug delivery system for targeted anti-cancer therapy, catalytic agent (peroxidase-like activity: protective agent against oxidative stress, destruction activity on fibrils responsible for amyloid disorders), etc. (Koralewski et al., 2012; Melnikova et al., 2014; Kopcansky et al., 2015; Strbak et al., 2017; Xue et al., 2019). According to the fact that magnetoferritin is expensive material related to the apoferritin origin, which is isolated from the biological organism (horse spleen), its use is limited to a large extent against surface water, groundwater and wastewater treatment. Application of magnetoferritin with catalytic activity is again directed to medical use, where exsanguination transfusion or hemodialysis for NO_3^- removal could be equipped e.g. by modified graphene nanostructured membrane functionnalized by magnetoferritin nanoparticles, which could serve as nano-adsorbent for NO_3^- anions. Magnetoferritin due to the catalytic activity under specific conditions of medium can provide chemical adsorption, while NO_3^- could be catalytically destructed. Next benefit of magnetoferrritin comes from its biogenic form, which was confirmed in various works. "Biogenic" magnetoferritin occurs in patients with neurodegenerative or cancer diseases (Kirschvink et al., 1992; Kobayashi et al., 1997; Dobson, 2001; Brem et al., 2006) and there are indications that it could be the part of healthy organisms similarly. In that case, magnetoferritin could play thanks to its catalytic activity a protective role against intoxication by nitrates. However, further experimental evidence is needed for these hypotheses.

Assessment of water quality from nitrates monitoring in various water sources in Slovakia

The concentration of nitrates in selected areas in Slovakia depends on anthropogenic, agricultural, industrial, urban activities and complex of meteorological (seasonal changes), hydrological, hydropedological and soil-chemical processes (e.g. precipitation and its transport together with fertilizers over and through the surface soil to streamflows). Nitrates can contaminate surface water, groundwater and rainwater. The greatest danger is the pollution of drinking water sources. The requirement for the drinking water quality and its control is defined by the law of the Ministry of Health in Slovakia, monitoring microbiological, biological, physical, chemical and radiological indicators. Drinking water treatment technologies are different. Various filtering equipment is used to remove nitrates and nitrites. Water quality control in surface and underground sources is provided by water companies or municipalities. The public health authority and regional public health authorities monitor the quality of drinking water within the framework of monitoring. Monitoring is carried out continuously and permanently, and sampling points are collected in premises or buildings where water flows out of taps normally used for human consumption. Determination of nitrates in various water sources (in surface, subsurface and rainwater) is carried out in Slovakia in the framework of the national monitoring program by the Slovak Hydrometeorological Institute or by scientific institutes to determine the suitability of studied water as a drinking water source. Pekárová and Miklánek evaluated nitrate concentration trends in five sub-basins of the Ondava River between 1968–93 taking into account the hydrometeorological elements (discharge, temperature, precipitation). A rapid decrease of nitrate concentration after 1989 was observed, most probably caused by a lower intensity of agricultural production and fertilization in Slovakia as a result of economic changes. Daily sampling in 1989 was compared also to those derived by Slovak Hydrometeorological Institute. The 25-years time series of monthly nitrate concentrations of the Ondava river area in 1968/69–1989/90 was analyzed. The mean annual concentrations increased from 2.9 mg l^{-1} in 1968/69 to 12.8 mg l^{-1} in 1988/89. After 1988/89 the mean annual nitrate concentration decreased to 5.3 mg l^{-1} in 1992/93 (Pekárová and Miklánek, 1993). Decreasing of nitrate concentration in surface water since 1989 was mentioned also in the next study (Pekárová and Pekár, 1996), where the environmental impact of forestry, agriculture and urban activities on the quality of water over short and long time-scaled was analyzed. The annual nitrate specific load varied from 5.90 to 110 kg ha^{-1}.$year^{-1}$, while the highest average annual nitrate concentration (47.4 mg l^{-1}) was determined in micro basin Rybárik and the lowest in the mountainous catchments Jalovecký Potok (2.02 mg l^{-1}), Bystrá (2.37 mg l^{-1}), forested micro basins Manelo (1.76 mg l^{-1}) and Lesný (2.78 mg l^{-1}) (Pekárová and Pekár, 1996). Another study was aimed at assessment of monthly time series of nitrate-nitrogen concentration monitoring in Ondava River by Slovak Hydrometeorological Institute (period 1987–1991) compared with daily time series of nitrate-nitrogen concentration monitoring by the Institute of Hydrology Slovak Academy of Sciences. The long-term development of nitrates content in Ondava River for the period 1967–2002 and trend analysis shows decreasing of nitrates amount and a further decline is expected (Pekárová et al., 2006). A long-term hydrological and water chemistry research was performed in three experimental micro basins: Rybarik, Lesny, and Cingelova within the larger Mostenik basin, differing in land cover. Nitrate concentration was investigated for a period of 3 years (1991–1993). Comparison of the net imported/ exported loads has shown that the nitrate content leached from the agricultural micro basin is ~3.7 times higher than that from the trees covered micro basin. These analyses justify that land cover land-use practices (fertilization in agriculture) may actively affect the retention and export of nitrates from the micro basins, and have a pronounce impact on the quality of stream-water. Agriculture and the use of natural or synthetic nitrogen fertilizers are the main anthropogenic source of nitrates. The number of nitrogen fertilizers applied in Slovakia between 1950 and 2005 has shown a decreased trend (Onderka et al., 2010). The continuous decrease in fertilization is caused by reduction of agricultural activity, increased fertilizer prices and lower number of farm animals. The evaluation of the content of nitrate-nitrogen ($N\text{-}NO_3^-$) in the surface waters and the monitoring of the qualitative characteristics of drainage canals in the East Slovakian lowlands was carried out at the Institute of Hydrology of the Slovak Academy of Sciences in 1999 and 2000 (Ivančo and Pavelková, 1999; Pavelková and Ivančo, 1999; Pavelková, 2000). Pavelková and Petrík in 2011 realized the analysis of nitrate content in water from house wells in 1997–2010 in districts Michalovce and Sobrance (Pavelková and Petrík, 2011). The recent study of Pavelková and Petrík was aimed at the monitoring of nitrate levels in house wells in the villages of Michalovce and Sobrance district (Pavelková and Petrík, 2016). Qualitatively and quantitatively determination of specific parameters in water environment can help better assesses the suitability of surface or subsurface water for human consumption in specific localities. Also, the scientific organization can prove the negative effects of specific contaminants in water and study various interaction processes and numerical modelling of dynamic processes of pollutants flow in water supplies. Due to the decreasing fertilization and agricultural activity in Slovakia, lower limits of nitrates in the last decades was observed. Slovakia still belongs to the states with a good quality of water. Nevertheless, there are endangered areas in Slovakia with over-limit concentrations of nitrates, therefore it is necessary to deal with monitoring and possibilities of their elimination.

Conclusion

This review aimed to summarize information about the relationship between nitrates and nitrites in the water environment with humans and their activity. Our assessment rises from the terms of environmentalism, biology, chemistry and nanotechnology. Unfortunately, higher nitrate levels in the soil and water worldwide are the result of the human inadequate activity. It is necessary to constantly monitor these pollutants, particularly in areas with increasing populations. Just as tons of waste is produced by humans, including agriculture, urbanism and industry, in the same way, humans can eliminate the number of contaminants from the environment with the help of nature or using synthetic nanomaterials as still popular graphene or magnetic nanoparticles. We would like to highlight that the improved situation was observed in Slovakia from hydrological monitoring after reducing agricultural activity. Finally, we would like to emphasize that it is necessary still to develop greenways to produce new separation materials for various pollutant reduction and removal following environmentally friendly approaches and technologies, that ensure good efficiency, rapidity and low cost.

Acknowledgement

The work was supported by the project VEGA Grant Agency No. 2/0044/20.

References

Addiscott, T. M., Benjamin, N. (2006): Nitrate and human health. Soil Use and Management, vol. 20, 98–104.

Anand, A., Unnikrishnan, B., Mao, J.-Y., Lin, H.-J., Huang, C.-C. (2018): Graphene-based nanofiltration membranes for improving salt rejection, water flux and antifouling–A review. Desalination, vol. 429, 119–133.

Archna, Sharma, S. K., Sobti, R. C. (2012): Nitrate Removal from Ground Water: A Review. E-J Chem, vol. 9, no. 4, 1667–1675.

Ali Mansouri, M. D. (1985): Methemoglobinemia. The American Journal of the Medical Sciences, vol. 289, 200–209.

Bellova, A., Bystrenova, E., Koneracka, M., Kopcansky, P., Valle, F., Tomasovicova, N., Timko, M., Bagelova, J., Biscarini, F., Gazova, Z. (2010): Effect of Fe_3O_4 magnetic nanoparticles on lysozyme amyloid aggregation. Nanotechnology, vol. 21, 065103–065109.

Bhatnagar, A., Sillanpää, M. (2011): A review of emerging adsorbents for nitrate removal from water. Chemical Engineering Journal, vol. 168, 493–504.

Bondonno, C. P., Blekkenhorst, L. C., Liu, A. H., Bondonno, N. P., Ward, N. C., Croft, K. D., Hodgson, J. M. (2018): Vegetable-derived bioactive nitrate and cardiovascular health. Molecular Aspects of Medicine, vol. 61, 83–91.

Brem, F., Hirt, A. M., Winklhofer, M., Frei, K. P., Yonekawa, Y., Wieser, H. X., Dobson, J. (2006): Magnetic iron compounds in the human brain: a comparison of tumour and hippocampal tissue. Journal of The Royal Society Interface, vol. 3, 833–841.

Celebi, K., Buchheim, J., Wyss, R. M., Droudian, A., Gasser, P., Shorubalko, I., Kye, J.-I., Lee, C., Park, H. G. (2014): Ultimate Permeation Across Atomically Thin Porous Graphene. Science, vol. 344, 289–292.

Cross, A. J., Ferrucci, L. M., Risch, A., Graubard, B. I., Ward, M. H., Park, Y., Hollenbeck, A. R., Schatzkin, A., Sinha, R. (2010): A large prospective study of meat consumption and colorectal cancer risk: an investigation of potential mechanisms underlying this association. Cancer Research, vol. 70, 2406–2414.

Dejam, A., Hunter, C. J., Schechter, A. N., Gladwin, M. T. (2004): Emerging role of nitrite in human biology. Blood Cells, Molecules and Diseases, vol. 32, 423–429.

Dobson, J. (2001): Nanoscale biogenic iron oxides and neurodegenerative disease. FEBS Letters, vol. 496, 1–5.

Eichholzer, M., Gutzwiller, F. (1998): Dietary nitrates, nitrites, and N-nitroso compounds and cancer risk: a review of the epidemiologic evidence. Nutrition Reviews, vol. 56, 95–105.

Ferrucci, L. M., Sinha, R., Ward, M. H., Graubard, B. I., Hollenbeck, A. R., Kilfoy, B. A., Schatzkin, A., Michaud, D. S., Cross, A. J. (2010): Meat and components of meat and the risk of bladder cancer in the NIH-AARP diet and health study. Cancer, vol. 116, 4345–4353.

Ghadiri, S. K., Nasseri, S., Nabizadeh, R., Khoobi, M., Nazmara, S., Mahvi, A. H. (2017): Adsorption of nitrate onto anionic bio-graphene nanosheet from aqueous solutions: Isotherm and kinetic study. Journal of Molecular Liquids, vol. 242, 1111–1117.

Greer, F. R., Shannon, M. (2005): Infant methemoglobinemia: the role of dietary nitrate in food and water. Pediatrics, vol. 116, 784–786.

Gushgari, A. J., Halden, R. U. (2018): Critical review of major sources of human exposure to N-nitrosamines. Chemosphere, vol. 210, 1124–1136.

Honikel, K.-O. (2008): The use and control of nitrate and nitrite for the processing of meat products. Meat Sci, vol. 78, 68–76.

Hosseini, M., Azamat, J., Erfan-Niya, H. (2018): Improving the performance of water desalination through ultrapermeable functionalized nanoporous graphene oxide membrane. Applied Surface Science, vol. 427, 1000–1008.

Ivančo, J., Pavelková, D. (1999): Zhodnotenie obsahu dusičnanoveho dusíka ($N\text{-}NO_3^-$) v povrchových vodách Východoslovenskej nížiny. Journal of Hydrology and Hydromechanics, vol. 47, 132–147.

Jahanshahi, D., Vahid, B., Azamat, J. (2018): Computational study on the ability of functionalized graphene nanosheet for nitrate removal from water. Chemical Physics, vol. 511, 20–26.

Jilani, A., Othman, M. H. D., Ansari, M. O., Hussain, S. Z., Ismail, A. F., Khan, I. U., Inamuddin (2018): Graphene and its derivatives: synthesis, modifications, and applications in wastewater treatment. Environmental Chemistry Letterss, vol. 16, 1301–1323.

Kapil, V., Webb, A. J., Ahluwalia, A. (2010): Inorganic nitrate and the cardiovascular system. Heart, vol. 96, 1703–1709.

Kapoor, A., Viraraghavan, T. (1997): Nitrate Removal From Drinking Water—Review. Journal of Environmental Engineering, vol. 123, 371–380.

Kirschvink, J. L., Kobayashi-Kirschvink, A., Woodford, B. J. (1992): Magnetite biomineralization in the human brain. Proceedings of the National Academy of Sciences of the United States of America, vol. 89, 7683–7687.

Knight, T. M., Forman, D., Pirastu, R., Comba, P., Iannarilli, R., Cocco, P. L., Angotzi, G., Ninu, E., Schierano, S. (1990): Nitrate and nitrite exposure in Italian populations with different gastric cancer rates. Interntional Journal of Epidemiology, vol. 19, 510–515.

Kobayashi, A., Yamamoto, N., Kirschvink, J. (1997): Studies of Inorganic Crystals in Biological Tissue: Magnetite in Human Tumor. Journal of the Japan Society of Powder and Powder Metallurgy, vol. 44, 294–300.

Kopcansky, P., Siposova, K., Melnikova, L., Bednarikova, Z., Timko, M., Mitroova, Z., Antosova, A., Garamus, V. M., Petrenko V. I., Avdeev, M. V., Gazova, Z. (2015): Destroying activity of magnetoferritin on lysozyme amyloid fibrils. Journal of Magnetism and Magnetic Materiaals, vol. 377, 267–271.

Koralewski, M., Kłos, J. W., Baranowski, M., Mitróová, Z., Kopčanský, P., Melníková, L., Okuda, M., Schwarzacher, W. (2012): The Faraday effect of natural and artificial ferritins. Nanotechnology, vol. 23, 355704–355713.

Králinský, K., Mečiaková, M. (2014): Alimentary methaemoglobinemia. Pediatrie pro praxi, vol. 15, 33–36.

Larsen, F. J., Ekblom, B., Sahlin, K. (2006): Effects of Dietary Nitrate on Blood Pressure in Healthy Volunteers. The New England Journal of Medicine, vol. 355, 2792–2793.

Laue, W., Thiemann, M., Scheibler, E., Wiegand, K. W. (2006): Nitrates and Nitrites. Ullmann's Encyclopedia of Industrial Chemistry. Weinheim: Wiley-VCH. ISBN 978-3527306732.

Lenghartová, K., Lauko, L., Beinrohr, E. (2015): Analytické metódy na stanovenie dusitanov. Chemické Listy, vol. 109, 191–197.

Li, J., Zhao, X., Shi, Y., Cai, Y., Mou, S., Jiang, G. (2008a): Mixed hemimicelles solid-phase extraction based on cetyltrimethylammonium bromide-coated nano-magnets Fe_3O_4 for the determination of chlorophenols in environmental water samples coupled with liquid chromategraphy/spectrophotometry detection. Journal of Chromatography A, vol. 1180, 24–31.

Li, Q., Mahendra, S., Lyon, D. Y., Brunet, L., Liga, M. V., Li, D., Alvarez, P. J. (2008b): Antimicrobial nanomaterials for water disinfection and microbial control: potential applications and implications. Water Research, vol. 42, 4591–4602.

Li, W., Wang, W., Zheng, X., Dong, Z., Yan, Y., Zhang, J. (2017): Molecular dynamics simulations of water flow enhancement in carbon nanochannels. Computational Materials Science, vol. 136, 60–66.

Lin, J. K. (1990): Nitrosamines as potential environmental carcinogens in man. Clinical Biochemistry, vol. 23, 67– 71.

Lundberg, J. O., Weitzberg, E. (2009): NO generation from inorganic nitrate and nitrite: role in physiology, nutrition and therapeutics. Archives of Pharmacal Research, vol. 32, 1119–1126.

Ma, X., Li, M., Liu, X., Wang, L., Chen, N., Li, J., Feng, C. (2018): A graphene oxide nanosheet-modified Ti nanocomposite electrode with enhanced electrochemical property and stability for nitrate reduction. Chemical Engineering Journal, vol. 348, 171–179.

Machha, A., Schechter, A.N. (2011): Dietary nitrite and nitrate: a review of potential mechanisms of cardiovascular benefits. European Journal of Nutrition, vol. 50, 293–303.

Madhura, L., Singh, S., Kanchi, S., Sabela, M., Bisetty, K., Inamuddin (2019): Nanotechnology-based water quality management for wastewater Treatment. Environmental Chemistry Letters, vol. 17, 65–121.

Mayo, J., Yavuz, C., Yean, S., Cong, L., Shipley, H., Yu, W., Falkner, J., Kan, A., Tomson, M., Colvin, V. (2007): The effect of nanocrystalline magnetite size on arsenic removal. Science and Technology of Advanced Materials, vol. 8, 71–75.

Melnikova, L., Pospiskova, K., Mitroova, Z., Kopcansky, P., Safarik, I. (2014): Peroxidase-like activity of magnetoferritin. Microchim Acta, vol. 181, 295–301.

Nakayama, H., Miyashita, T., Hashino, S., Yoshitake, N., Orita, R. (2010): An approximate theory of laser-induced ignition of boron/potassium nitrate pyrotechnic. Science and Technology of Energetic Materials, vol. 71, 31–38.

Nujić, M., Habuda-Stanić, M. (2017): Nitrates and nitrites, metabolism and toxicity. Food in Health and Disease, vol. 6, 48–89.

Onac, B. P. (2012): Minerals. Encyclopedia of Caves (Second Edition), USA, 499–508, ISBN 978-0-12-383832-2.

Onderka, M., Pekarova, P., Miklanek, P., Halmova, D., Pekar, J. (2010): Examination of the Dissolved Inorganic Nitrogen Budget in Three Experimental Microbasins with Contrasting Land Cover–A Mass Balance Approach. Water, Air, & Soil Pollution, vol. 210, 221–230.

Orel, A. E., Seinfeld, J. H. (1977): Nitrate formation in atmospheric aerosols. Environmental Science & Technology, vol. 11, 1000–1007.

Pavelková, D. (2000): Monitorovanie kvalitatívnych charakteristík odvodňovacích kanálov na Východoslovenskej nížine. Acta Hydrologica Slovaca, vol. 1, 197–205.

Pavelková, D., Ivančo, J. (1999): Zmeny niektorých kvalitatívnych charakteristík povrchových vôd na VSN. Acta horticulturae et regiotecturae : vedecký časopis pre záhradníctvo, krajinné inžinierstvo, architektúru a ekológiu, vol. 2, 12–15.

Pavelková, D., Petrík, O. (2011): Analýza obsahu dusičnanov vo vode z domových studní v rokoch 1997–2010 v okresoch Michalovce a Sobrance. Okresné dni vody : zborník referátov. Milan Gomboš (ed.). – Michalovce: ÚH SAV: VVSK, 75–78. ISBN 978-80-89139-22-4.

Pavelková, D., Petrík, O. (2016): Monitoring nitrate levels in house wells in the villages of Michalovce and Sobrance district. In XX. Okresné dni vody: Recenzovaný zborník referátov. – Bratislava; Michalovce; Košice: ÚH SAV: Výskumná hydrologická základňa: Východoslovenská vodárenská spoločnosť a. s., 93-96. ISBN 978-80-89139-37-8.

Pekárová, P., Miklánek, P. (1993): Spatial distribution and trend change of nitrate in Slovakia during 1968–1993. Acta Geologica Hispanica, vol. 28, 55–63.

Pekárová, P., Pekár, J. (1996): The impact of land use on stream water quality in Slovakia. Journal of Hydrology, vol. 180, 333–350.

Pekárová, P., Pekár, J., Miklánek, P. (2006): Impact of water sampling frequency on estimating water quality status in the Ondava River. Ecohydrology and Hydrobiology, vol. 6, 105–113.

Poursaberi, T., Karimi, M., Hassanisadi, M., Sereshti, H. (2013): Magnetic removal of nitrate ions from aqueous solution using amino-silica coated magnetic nanoparticles modified by oxovanadium(IV) porphyrin. Journal of Porphyrins and Phthalocyanines, vol. 17, 359–366.

Rezaei Kalantary, R., Dehghanifard, E., Mohseni-Bandpi, A., Rezaei, L., Esrafili, A., Kakavandi, B., Azari, A. (2014): Nitrate adsorption by synthetic activated carbon magnetic nanoparticles: kinetics, isotherms and thermodynamic studies. Desalination and Water Treatment, vol. 57, 16445–16455.

Shi, Q., Gao, H., Zhang, Y., Meng, Z., Rao, D., Su, J., Liu, Y., Wang, Y., Lu, R. (2018): Bilayer graphene with ripples for reverse osmosis desalination. Carbon, vol. 136, 21–27.

Shrimali, M., Singh, K. (2001): New methods of nitrate removal from water. Environmental Pollution, vol. 112, 351–359.

Singh, P., Singh, M. K., Bega, Y. R., Nishad, G. R. (2019): A review on spectroscopic methods for determination of nitrite and nitrate in environmental samples. Talanta vol. 191, 364–381.

Soares, M. (2000): Biological Denitrification of Groundwater. Water, Air, & Soil Pollution, vol. 123, 183–193.

Strbak, O., Balejcikova, L., Baciak, L., Kovac, J., Masarova-Kozelova, M., Krafcik, A., Dobrota, D., Kopcansky, P. (2017): Low-field and high-field magnetic resonance contrast imaging of magnetoferritin as a pathological model system of iron accumulation. Journal of Physics D: Applied Physics, vol. 50, 365401–365410.

Šalgovičová, D., Krížová, S. (2006): Exposure of the population of the Slovak Republic to nitrates. Journal of Food and Nutrition Research, vol. 45, 89–95.

Wang, Q. H., Yu, L. J., Liu, Y., Lin, L., Lu, R., Zhu, J. P., He, L., Lu, Z. L. (2017): Methods for the detection and determination of nitrite and nitrate: a review. Talanta, vol. 165, 709–720.

Woollard, D. C., Indyk, H. E. (2014): Colorimetric determination of nitrate and nitrite in milk and milk powders – Use of Vanadium (III) reduction. International Dairy Journal, vol. 35, 88–94.

Xue, L., Deng, D., Sun, J. (2019): Magnetoferritin: Process, Prospects, and Their Biomedical Applications. International Journal of Molecular Sciences, vol. 20, 2426–2443.

RNDr. Lucia Balejčíková, PhD. (*corresponding author, e-mail: balejcikova@uh.savba.sk)
RNDr. Andrej Tall, PhD.
Ing. Branislav Kandra, PhD.
Ing. Dana Pavelková, PhD.
Institute of Hydrology SAS
Dúbravská cesta 9
841 04 Bratislava
Slovak Republic

DOI: 10.31577/ahs-2020-0021.01.0010

ACTA HYDROLOGICA SLOVACA

Volume 21, No. 1, 2020, 82 – 88

METHOD OF WETLANDS WATER REGIMEN DIAGNOSIS

Štefan Rehák*, Peter Stradiot, Karol Kňava, Ľubica Kopčová, Viliam Novák

Wetlands are territories, permanently or temporary waterlogged; temporary waterlogging must cover majority of the season. Wetlands are ecosystems typical by maximum (potential) evapotranspiration with high solar energy consumption; therefore, they are important as local climate stabilizers. In this paper, method of wetland water regimen diagnosis is described, applicable to wetlands with so called autonomous water regimen. It means, that wetland water regimen is formed mostly by precipitation and (potential) evapotranspiration; such wetlands are hydrodynamically isolated from its neighbourhood. This is typical for majority of wetlands in Slovakia. Method of diagnosis is based on evaluation of water fluxes to and out of the wetland and is illustrated on three typical wetlands.

KEY WORDS: waterlogging, precipitation, potential evapotranspiration, wetland management

Introduction

Wetland is permanently or temporary inundated (wet) territory, with characteristic ecosystem. Another definetion is „wetland is a territory in which water is basic factor influencing living organisms of the territory". They occurred where water table is on the surface, close to the soil surface or soil surface is covered by thin water layer (The Ramsar Convention Manual, 1994). In the past, wetlands were taken as unusable water bodies and were frequently drained.

It was shown that wetlands are home of specific plants and animals; this knowledge led to their conservation. The principles of wetlands conservation as well as the list of the most important wetlands was accepted at Ramsar – a city in Iran; therefore this list is often notified as „Ramsars list of wetlands ". It was shown that wetlands are not important for their biotopes only; but their area on the Earth is so huge, that it can basically influence Earth's climate.

Results of measurements (from the satellites mostly) have shown that the area of wetlands covers about 5 percent of the Earth's surface, i.e. at about 7.5 million of square kilometre ($7.5x10^6$ km^2). Natural freshwater wetlands area is $5.7x10^6$ km^2; even rice fields are wetlands with area $1.3x10^6$ km^2; the rest are saline wetlands. As it follows from this analysis, wetlands ($7.5x10^6$ km^2) together with tropical rainforests ($12x10^6$ km^2) are the basic ecosystems influencing not microclimate only, but even macroclimate of the Earth. This strong effect on climate is based on the fact, that majority of rainforests and wetlands are in tropical areas, where observed precipitation totals are in the range 3000–6000 mm per year. High incoming fluxes of solar energy allows to evaporate in average about 2500 mm of water layer annually, thus consuming the huge quantity of energy as latent heat of evaporation at about $6.5x10^9$ J m^{-2} year^{-1}. Corresponding ratio of biomass production (2.2 kg m^{-2} year^{-1}), represents about four times of boreal forests production. From point of climate change, important is high portion of energy consumption by evaporation and only relatively small part of it (about 10 percent) is heating environment. High rate of photosynthesis absorbs high quantity of carbon dioxide and thus decreases its concentration in an atmosphere and weakens so called „greenhouse effect".

In Slovakia, the effect of wetlands on water regimen and climate is not so profound as it can be expected in tropical or subtropical areas. The total area of wetlands in Slovakia is 45 km^2, which represents about one thousand of its territory. From 1049 wetlands registered over Slovakia, 21 wetlands are listed in so called „Ramsars list", among them wetland Devínske Jazero which will be analysed.

In this contribution the method of wetlands water regimen diagnosis is presented. Water deficits are quantified and needed compensating water fluxes to wetlands can be estimated to optimize their water regimen.

Material and methods

The water regimen of wetlands is characterized by typical pattern of water fluxes to and from wetland as a part of their water balance during the season. To evaluate the type of wetland water regimen, it is necessary to quantify water fluxes between wetland and its environment and to estimate the most important ones which are determining retention of water in wetland. Therefore, to perform wetland water regimen diagnosis, the basic meteorological, hydrological and soil characteristics are needed, the basic ones should be measured at site. Methods of measurement description as well as results of measurement can be found in publications by Holubová et al., (2014 M3; M4).

Three typical wetlands were studied: wetland at Devínske Jazero, (site Šrek), another called Čiližska wetland at Žitný ostrov (Rye Island) nearby village Čiližska Radvaň and wetland at inundation Stará Nitra river (Martovce). All the three wetlands are typical for Slovakia. The method of wetlands water regimen identification will be demonstrated in detail on wetland Devínske Jazero (site Šrek) but results of water regimen analysis of all three wetlands will be presented. Devínske Jazero wetland is so called "Ramsar wetland", i.e. it is listed in the Ramsar list of important wetlands (Fig. 1).

The most important source of water in wetland Devínske Jazero is precipitation (precipitation was measured at site), the most important outflow component is evapotranspiration. The wetlands surface is usually water table with wetlands vegetation, or vegetation grown in wet environment, evapotranspiration of such surfaces can be indicated as potential evapotranspiration, i.e. evapotranspiration is not limited by lack of water, the limiting factors are parameters of atmosphere only. Then, biomass production in such conditions is maximum too. Because evapotranspiration of wetland is technically difficult to measure, its quantification was done by mathematical simulation model HYDRUS-1D (Šimůnek et al., 1997; 2008; Radcliffe and Šimůnek, 2010).

Results and discussion

The basic measured meteorological, hydrological and soil characteristics at wetland Devínske Jazero, site Šrek were measured to be used as input data to the simulation model model to perform diagnosis of wetland water regimen.

Results of water tables measurement of wetland Devínske Jazero and river Morava are in Fig. 2. Water table courses of wetland (1), and river Morava (2), during the wet year 2014 are shown. As it can be seen, inundation surface (3) is usually above the wetlands water table. Precipitation daily totals expressed in mm are also shown.

As it follows from Fig. 2, water table in the river Morava (with exception of short high-water table periods), is below the water table monitored in nearby wetland. Exceptions are periods of high precipitation, and corresponding high-water table level in which Morava river flooded inundation. During the wet year 2014 it was observed in May/June, in August and October. During the dry seasons such inundation is rare. Except of those short periods of inundating, there were not observed interactions between river and wetland. Due to extremely low hydraulic conductivity of soils at the bottom of the wetlands (estimated by measurements) it is assumed low wetland interaction with surrounding water bodies and therefore, analysed wetlands water regimen type can be indicated as autonomous. It means, that wetlands water regimen is formed preferentially by precipitation and evapotranspiration. Particularly, wetland Šrek can be influenced by short time inundation during the wet periods.

Results of analysis have shown:

Significant relationship between water table in the river Morava and water table in wetland (Blato Morava), was not identified during dry periods, because water table in wetland was higher, than water table in the river Morava. Wetland was inundated during the periods of high precipitation totals in catchment of river Morava, which can improve function of wetland.

Because water table in wetland nearby river Morava is not significantly influenced by the river Morava during dry (precipitation free) period, water delivery to the wetland to keep their expected function is necessary. Because Morava river water table is usually below the wetlands water table, it is necessary to manage water pumping from the river to wetland. The necessary fluxes to preserve this wetland function will be evaluated by wetland water regimen modelling.

Quantitative diagnosis of wetland Devínske Jazero water regimen

Quantitative diagnosis of wetland water regimen is evaluation of wetland water fluxes, which significantly influence its water balance and retention. As it was shown previously, the most important water fluxes to and from wetland (Devínske Jazero) are precipitation and evapotranspiration. Infiltration of water from river Morava to wetland is not expected, because water table in the river is below the water level in wetland, (with exception of short intervals of extreme water levels due to high precipitation) as it is demonstrated in Fig. 2, for wet year 2014.

Water fluxes from wetland to river Morava during the vegetation period are negligible, because hydraulic conductivity of wetland bead is extremely low. Hydraulic conductivity of bottom sediments is about K=1x10^{-7} m s^{-1}, (0.1 cm d^{-1}), it is about three orders lower than hydraulic conductivities of neighbouring soils. Low values of hydraulic conductivities of fine particle sediments of wetlands beads is primary reason of wetlands occurrence. Using other words, wetlands were formed in depressions secondary colmated by fine washload transported by nearby river. The natural depression and nearby river occasional flooding its inundation is the condition of such type wetland occurrence. Wetlands at Záhorska lowland (like Zelienka nearby Šaštín) in similar soil conditions (sandy soils), but beads (bottom) sediments of extremely low hydraulic conductivity are the reason of low rate of water infiltration from wetland to groundwater and thus wetlands water regimen are autonomous.

To evaluate wetlands water deficit, water flow to the wetland (measured precipitation) and outflows (potential evapotranspiration), calculated by simulation model will be compared.

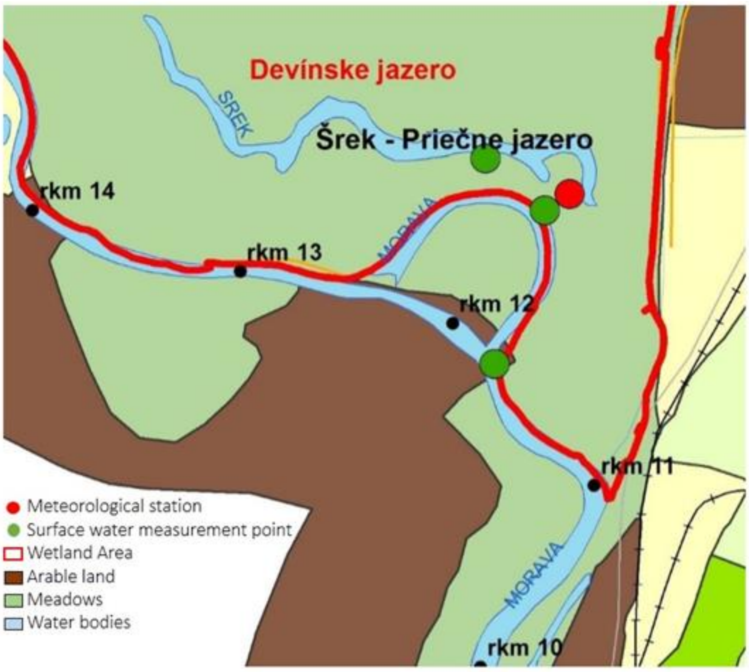

Fig. 1. The wetland Devínske Jazero locality and sites of measurement.

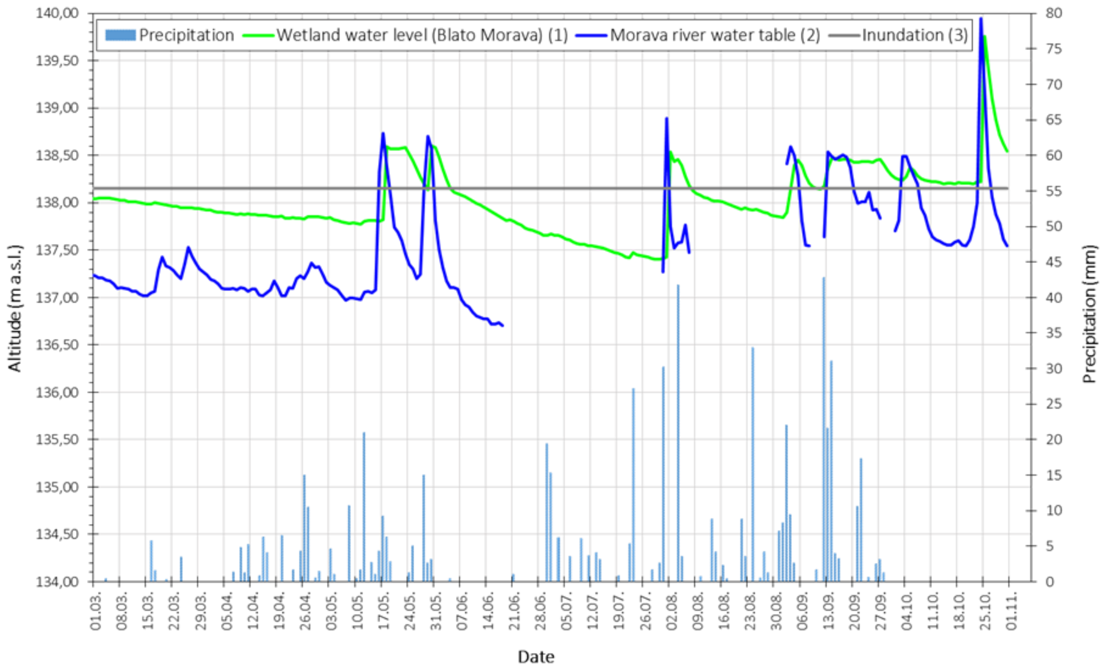

Fig. 2. Measured water table level of wetland Devínske Jazero (1), and water level in river Morava (2). Level of inundation at measurement site is also shown (3). Wet season 2014. Daily precipitation totals are expressed in mm.

Two contrast seasons (wet and dry) were evaluated. The seasonal courses of water deficits (or surplus) of water in wetlands will be estimated and thus water fluxes to wetlands can be managed, to preserve their optimal function.
To calculate water fluxes from a nd to wetlands, mathematical simulation model HYDRUS–1D, was applied to calculate daily totals of potential evapotranspiration of wetlands. Meteorological characteristics as well as soils hydrophysical characteristics measured at site and laboratory (Polák et al., 2014; Holubová et al., 2014, M4) were used as input data.

Simulation model HYDRUS

Model HYDRUS (Šimůnek et al., 1997; Šimůnek et al., 2008; Radcliffe and Šimůnek, 2010; Novák and Hlaváčiková, 2016) is mathematical, deterministic model simulating transport of water, heat and dissolved compounds in porous media (soil). It is used worldwide. Typical for this model is friendly interface, which is continuously improved. Detailed description of the model can be found in the above-mentioned literature.
Richards partial differential equation is the governing equation of the model. Its one dimensional form is used in the model HYDRUS-1D and can be used to simulate transport of water (solute) in one dimension to all directions (vertical, horizontal or in various angle).
To solve Richards equation, initial conditions must be known (initial distribution of soil water content or soil water matric potential) as well as boundary conditions, i.e. conditions at the boundary of the area to be solved. Typical boundary conditions is free drainage at the bottom boundary and precipitation and evapotranspiration at the upper (atmospheric) boundary. Evapotranspiration calculation is a part of the model HYDRUS 1D; in the case of wetlands it is potential evapotranspiration.

Wetland potential evapotranspiration calculation

Modified Penman–Monteith method called FAO method (Allen et al, 2006; Novák, 2012) was used to calculate wetland potential evapotranspiration. Potential evapotranspiration calculated by this method is known as „reference“ evapotranspiration. It is potential evapotranspiration of „reference“ grass canopy, albedo of which is 0.23. Because wetlands plant canopy grows in wet (and often flooded) environment, its albedo is lower, than albedo of grassland. Albedo a=0.13 was used as typical for wetland with appropriate plant canopy, for evaporating surface strongly influenced by water table. Therefore, lower albedo was used accounting for water table as a part of evaporating surface.
FAO Penman–Monteith equation for reference evapotranspiration surface was modified for wetlands, with defined properties of grass and water table. It can be written as (Allen et al., 2006):

$$ET_p = \frac{0.408\,\Delta(R_n - G) + \gamma\frac{900}{T+273}u_2(e_o - e)}{\Delta + \gamma[1 + 0.34\,u_2]} \qquad (1)$$

where
ET_p – is reference evapotranspiration [mm day^{-1}];
R_n – is the net radiation at evapotranspiration surface level [MJ m^{-2} day^{-1}];
G – is the heat flux to or from the wetland [MJ m^{-2} day^{-1}];
T – is the mean daily air temperature at standard height 2 m above evaporating surface [°C];
u_2 – is the wind velocity at standard height 2 m above evaporating surface [m s^{-1}];
e_o, e – is the saturated water vapor pressure at actual air temperature and actually measured water vapor pressure [kPa];
Δ – is the slope of the water vapor pressure curve [kPa K^{-1}];
γ – is the psychrometric constant [kPa K^{-1}].

Results of wetlands water regimen modelling

Daily totals of wetland potential evapotranspiration were calculated by the model. Positive differences between precipitation daily totals (P) and daily totals of potential evapotranspiration (E_p) indicate ideal hydric situation covering potential evapotranspiration. Negative differences between them can indicate higher potential evapotranspiration, than can be covered by current precipitation. Then, water table of wetland decreases. It can be noted, that evapotranspiration of wetland can be potential even when the negative difference of precipitation totals and precipitation is observed, it depends on evaporative demand of an atmosphere (Novák, 2012).
Sums of precipitation daily totals (P) and calculated potential evapotranspiration (E_p), of wetland Devínske Jazero of wet year 2014 and dry year 2015 expressed in mm are in Figs. 3 and 4.
The difference of precipitation daily totals (P) and calculated potential evapotranspiration (E_p), represents the surplus (or deficit) of water in wetland to cover potential evapotranspiration. The water deficit in wetland (negative difference between precipitation daily totals and potential evapotranspiration during the season) means suboptimal function of wetland, because there are not established conditions for potential evapotranspiration and thus for maximum biomass production. The sums of differences between daily precipitation totals (P) and daily potential evapotranspiration totals (E_p), expressed in mm of both wet season 2014 and dry season 2015 are presented in Fig. 5. The basic wetlands characteristics were calculated using seasonal courses of differences (P - E_p).
From results of water regimen wetland Devínske Jazero modelling (1308 hectares) it follows necessary water inflow to cover its potential evapotranspiration during time interval of water deficit increase up to 306 l s^{-1} (dry year) and 144 l s^{-1} (wet year). Data for all the three wetlands are in Table 1.

Conclusions

In this contribution the method of wetlands water regimen diagnosis is presented, quantified and quantities of water needed to manage their favourable water regimen are evaluated.
Water regimen of three typical wetlands of Slovakia (Devínske Jazero, Čiližska Radvaň and Martovce) were analysed, based on long – term measurements of their environmental characteristics. As it follows from analysis, their water regimen can be characterized as „autonomous“ which means, that precipitation and evapotranspiration are dominant processes of wetland water regiment formation; water fluxes between wetlands and their nearby water bodies (rivers, groundwater) are not significant. This „isolation“ is due to extremely low hydraulic conductivities of wetlands beads, located in terrain depressions. Specific situation can be observed at

site Devínske Jazero, where at high water level of Morava river water can inundate wetland.
Quantification of wetlands water regimen was conducted assuming autonomous water regimen, i.e. their water regimen is formed by precipitation and evapotranspiration only. The water balance of wetland was performed for two types of seasons (Table 1): for wet season (2014) and dry season (2015). For the wet season

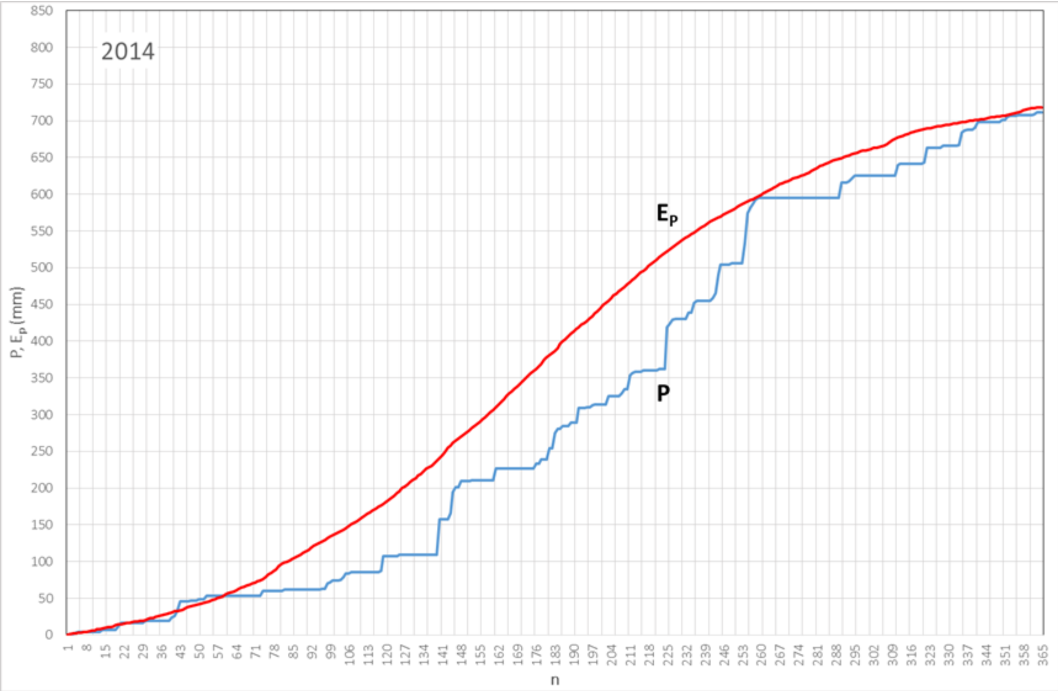

Fig. 3. Sums of precipitation daily totals (P) as well as sums potential evapotranspiration daily totals (Ep), expressed in mm, n is number of the day during the current year. Wetland Devínske Jazero, wet season 2014.

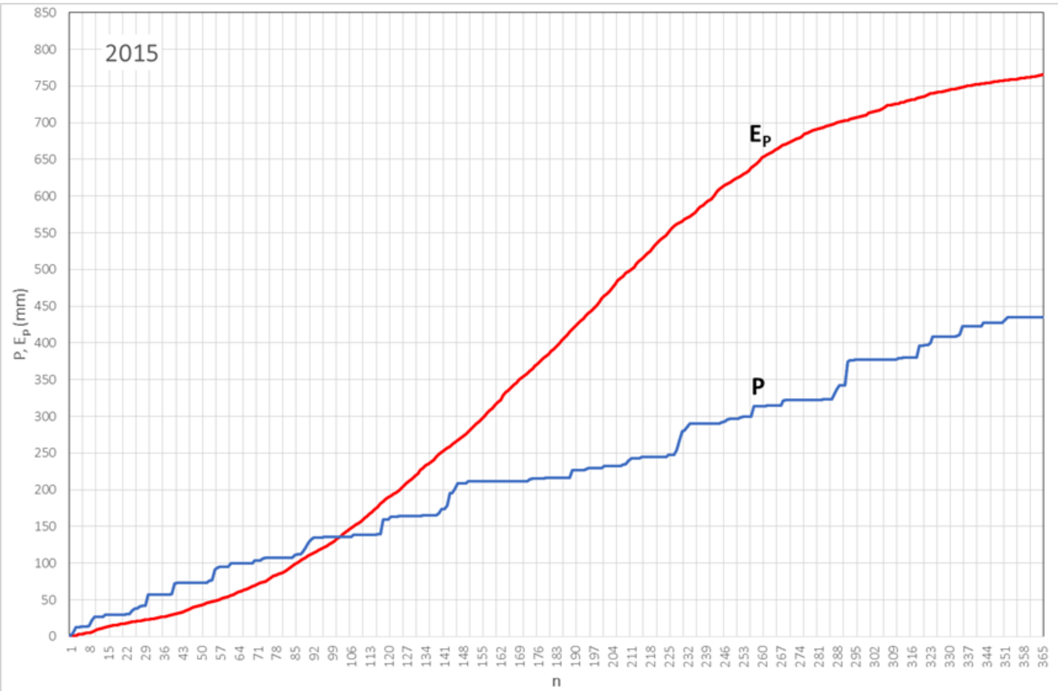

Fig. 4. Sums of precipitation daily totals (P) as well as sums potential evapotranspiration daily totals (Ep), expressed in mm, n is number of the day during the current year. Wetland Devínske Jazero, dry season 2015.

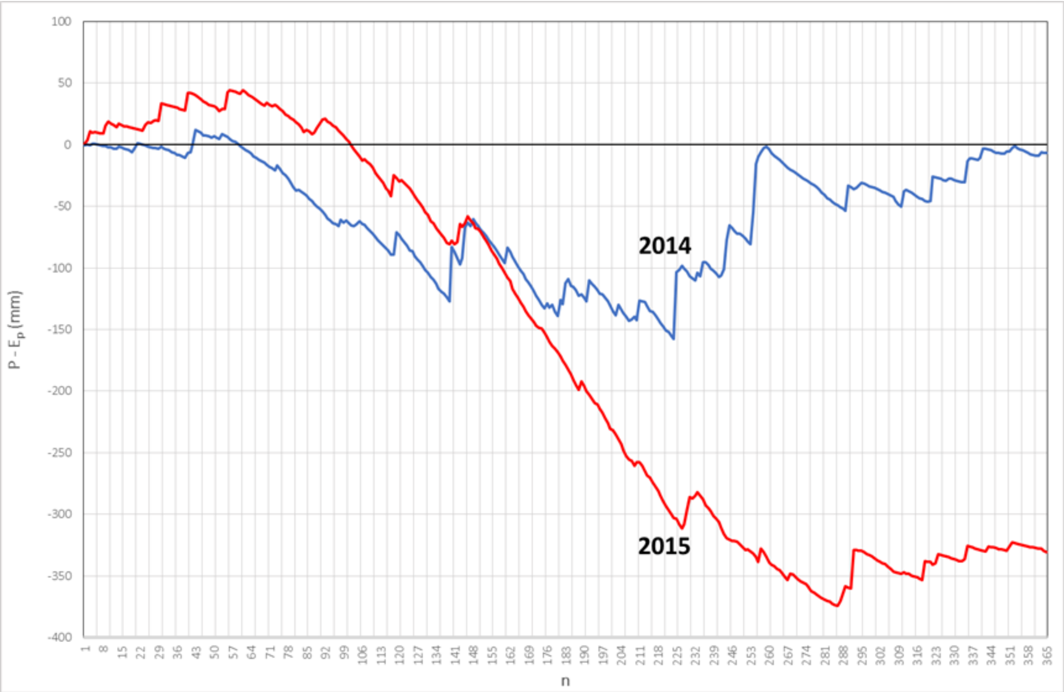

Fig. 5. Sums of differences between precipitation daily totals (P) and potential evapotranspiration daily totals (E_p), expressed in mm, n is number of the day during the current year. Wetland Devínske Jazero, wet season 2014 and dry season 2015.

Table 1. Wetlands water regimen characteristics (Devínske Jazero, Čiližska Radvaň, Martovce) calculated by the model HYDRUS-1D

	D. Jazero	Č. Radvaň	Martovce	Dimensions
n_w	201	174	185	-
n_d	264	275	218	-
D_w	-158	-145	-138	mm
D_d	-374	-282	-244	mm
n_{wd}	166	120	142	-
n_{dd}	185	141	80	-
Q_w	144	2.1	44	$l\ s^{-1}$
Q_d	306	3.8	141	$l\ s^{-1}$
A	1308	15.6	400	ha
P_w	711	800	787	mm
P_d	435	500	548	mm
E_{pw}	719	720	720	mm
E_{pd}	763	750	750	mm
P_w/E_{pw}	0.98	1.11	1.09	-
P_d/E_{pd}	0.57	0.66	0.73	-

Where: n_w, n_d number of days in wetlands with water deficit during wet (w) and dry year (d); D_w, D_d are total (integral) wetlands water deficits expressed in mm water layer; n_{wd}, n_{dd} are number of days with increasing water deficit during wet (w) and dry year (d); Q_w, Q_d are calculated water inflow needed to cover water deficits during wet (w) and dry year (d) expressed in litres per second; A is the area of wetland in hectares, P_w, P_d are annual precipitation totals during wet (m) and dry year (d); E_{pw}, E_{pd} are annual potential evapotranspiration totals during wet (w) and dry year (d); P_w/E_{pw} and P_d/E_{pd} are relative values of annual precipitation totals and annual potential evapotranspiration during wet (w) and dry year (d).

was not found critical water deficit, (Devínske Jazero, 157, Čiližska Radvaň, 145 and Martovce, 138 mm layer of water) and delivery of water to wetlands is not needed. During the dry season deficits of water are significant (Devínske Jazero, 375, Čiližska Radvaň, 282 and Martovce, 244 mm layer of water) and delivery of water is needed, when some „critical“ water deficit (which must be evaluated on site) will be reached.
This approach to the wetlands water regimen type identification and quantification can be applied for wide variety of wetlands with autonomous water regimen. It can be used to manage their water regimen by water delivery to wetlands according to the estimated fluxes and volumes of needed water.

Acknowledgement

Authors are grateful to the Slovak grant agency APVV for financial support of the Project APVV-14-0735 and APVV-16-0278.

References

Allen, R. G. et al. (2006): A recommendation on standardized surface resistance for hourly calculation of reference ET_0 by the FAO56 Penman-Monteith method. Agric. Water Manag. 82, 1–22.
Holubová, K. et al. (2014, M3): Revitalizačné postupy – možnosti obnovy narušenej dynamiky vody v mokradiach. Záverečná správa, VÚVH Bratislava
Holubová, K., et al. (2014, M4): Syntéza najdôležitejších výsledkov a poznatkov. Záverečná správa, VÚVH Bratislava.
Novák, V. (2012): Evapotranspiration in the Soil Plant Atmosphere System. Springer Science + Business Media, Doordrecht, pp. 253.
Novák,V., Hlaváčikova, H. (2016): Hydrológia pôdy. VEDA, Vydavateľstvo SAV, Bratislava, s. 347.
Polák, et al. (2014) (M1). Abioticko – fyzikálne procesy: Komplexná analýzy vodného režimu mokradí. Záverečná správa, VÚVH Bratislava
Radcliffe, D.E., Šimůnek, J. (2010): Soil Physics with HYDRUS. Modeling and Applications, CRC Press, Taylor and Francis Group, LLC, USA
Rejmers, N. F. (1985): Mikroenciklopedija biosfery, Znanie, Moskva.
Šimůnek, J., Huang, K., Šejna, M., van Genuchten, M. Th., Majerčák, J., Novák, V., Šutor, J. (1997): The HYDRUS-ET software package for simulating one dimensional movement of water, heat and multiple solutes in variably saturated media. Institute of Hydrology, SAS, Bratislava, pp. 184.
Šimůnek, J., Saito, H., Sakai, M., van Genuchten, M. Th. (2008): The HYDRUS-1D software package for simulating one dimensional movement of water, heat and multiple solutes in variably saturated media. Version 4., Hydrus Series 3. Dept. of Environmental Sciences, Univ. of California Riverside. Riverside, CA, USA.
The Ramsar Convention Manual (1994): The Ramsar Convention Secretariat, Mauverny.

doc. RNDr. Štefan Rehák, PhD. (*corresponding author, e-mail: rehak@vuvh.sk)
RNDr. Peter Stradiot, PhD.
Ing. Karol Kňava, PhD.
Ing. Ľubica Kopčová, PhD.
Institute of Water Resources Research
Nábrežie arm. gen. L. Svobodu 5
812 49 Bratislava 1
Slovak Republic

Ing. Viliam Novák, DrSc.
Institute of Hydrology SAS
Dúbravská cesta 9
84104 Bratislava
Slovak Republic

DOI: 10.31577/ahs-2020-0021.01.0011

ACTA HYDROLOGICA SLOVACA

Volume 21, No. 1, 2020, 89 – 97

RECONSTRUCTION OF ELECTRIC IMPEDANCE FIELD OF SOIL WITH CLAY ANOMALY

Zuzana Műnsterová*, Jana Pařílková, Jan Mikulka, Jan Dušek

Electrical impedance characterizes the properties of the examined environment when passing through an alternating electric current. The paper is based on the dependence of the course of real and imaginary components of electrical impedance on the humidity of the porous environment. Different soil environments have various water retention capacities under the same hydrometeorological conditions. This hydrophysical characteristic is used in the presented paper to study the inhomogeneity of the porous environment. The contribution is beneficial in that it proposes a method which, based on simple measurements, allows to evaluate the homogeneity of the porous environment. The method is widely used in water management (e.g. determination of failures of sealing cores in earth dams and dams) but also in hydrological survey and monitoring (e.g. determination of volume humidity).

KEY WORDS: clay, soil, probe, electrical impedance, Z-meter device

Introduction

Electrical impedance (EI) extends the concept of electrical resistance to situations where alternating electrical current passes through the environment. It is a quantity whose value depends on many factors of which is used in various fields of science and applications (Barbiero and Miracapillo, 2008). The EI of the measured environment can be detected across the frequency spectrum. Therefore it can provide a broader picture of its layout – impedance spectrometry (IS). It is consequently used to characterize or detect solid, liquid and gaseous substances and their properties. IS has become a relatively convenient method in the research and development of materials because it requires relatively simple electrical measurements, in most cases, non-destructive, which can be easily automated. Generally, three basic measurement methods are used in IS, namely transient phenomenon measurement, measurement response at white noise and EI measurement on each frequency of the required spectrum separately (Barsoukov and MacDonald, 2005).
In practical terms, the most commonly used method of measuring EI at each frequency of the desired spectrum is separately. Generally speaking, a harmonic signal of constant frequency and amplitude is input, and the phase shift and amplitude in the desired frequency range are monitored. The advantage of this measurement principle over the other two approaches is a good signal-to-noise ratio and the ability to measure (depending on the meter's instrumentation) in the frequency range from mHz to MHz. However, since it is necessary to perform measurements in the selected frequency spectrum for each frequency separately, it is required to take into account the time consuming of the measure, which may be a limiting factor when monitoring dynamic phenomena.
Because of their predictive ability, electrical resistance or electrical impedance methods have been included. They are also used as geoelectric research methods (Gruntorád, 1985; Karous, 1989; Vogelsang, 1994) or in hydrogeology (Mareš, 1983). The most common field electrical geophysical methods used for monitoring processes occurring in bodies of earth dams due to their hydrodynamic loading include methods using conductivity, capacitance, microwave and resistive measurement principles. Their basis is the dependence of parameters that characterize soil in an electric field on the change of water content in soil.
In the paper, a modified third EI measurement method was chosen for the measurement of electrical impedance for the detection of anomalies occurring in the ground environment. An alternating electric field was used to assess the soils. The EI measurement method was implemented by implementing the multi-electrode resistance method (MRM) IS with extension to electrical impedance tomography (EIT). The physical principle of the electrical resistive method using direct current, which is based on Ohm's relationship, has been known and used in archaeology and geology since the early 20th century. In this case, the modification of the IS measurement

method and the EI measurement method is based on the fact that an initial measurement is performed in the selected frequency spectrum. From the measured characteristics of the measured ground environment (output that monitors the EI components), one measurement frequency is chosen for the experiment at which the most positive signal response was detected in both EI components measured.

The experiment aimed to verify whether the above mentioned EIT diagnostic method and the apparatus with the Z-meter device can be used for the detection and mapping of soil failure sites, respectively places with anomalies. In practice, this involves revealing layers of deposits, gravel, the level of the bedrock, places saturated with water, cracks or larger veins in rocks. MRM has excellent results in searching for underground cavities, galleries, buried wells or excavations for utilities. In the field of water management, from the stability of the building structure and the safety of its operation, it is primarily the detection and monitoring of sites with higher water content.

Because of the water load, it is seepage through the dam can be detected, including possible catastrophic consequences leading to its total destruction (Cunningham, 1986; Dean et al., 1987).

The detection of anomalies occurring in the earth environment (subsoil of hydro-technical structures, earth dams, etc.) by electric impedance tomography (EIT) is, therefore, a topical topic.

Electrical impedance spectrometry and Z-meter device

The method of electrical impedance spectrometry belongs to a group of indirect measurement methods (Barbiero and Miracapillo, 2008), which represents a sensitive instrument and an experimental technique designed to determine the parameters of the observed hydrodynamic effect. It is based on a periodic harmonic signal of a small amplitude providing minimal concentration changes at the surface of the electrode associated with the measured environment (Pařílková, 2010).

The basic principle of the electrical impedance spectrometry method is the measuring of the frequency characteristic of the electrical impedance Z of the environment. Electrical impedance is a complex quantity that describes the apparent resistance of a porous medium and the phase shift of an electric voltage against an electric current when a harmonic alternating electric current of a given frequency passes through the environment. In the DC circuit, the electrical resistance R [Ω] of the resistor characterizes the soil properties (water content, porosity, humidity, ion content, temperature, etc.). The electrical impedance $\mathbf{Z}$ [Ω] characterizes the features of the soils in the AC circuits (the characteristics of the soils, which can be described above by the apparent resistance X [Ω], such as texture, grain size, ease, etc.).

The frequency response of the electrical impedance of the soils $\mathbf{Z}$ can be expressed in the form

$$\mathbf{Z} = R + \mathrm{j} \cdot X \tag{1}$$

where R [Ω] is the resistance forming the real part of the electrical impedance (generally independent of frequency) and X [Ω] is the reactance forming the imaginary part of the electrical impedance (varies with frequency).

When expressing the reactance, which is predominantly capacitive in the case of soils, the angular velocity ω [Hz], which is given by

$$\omega = 2 \cdot \pi \cdot f_M, \tag{2}$$

where f_M [Hz] is the measuring frequency.

The EI measurement of soils is based on the consideration that two electrodes, which form one EIS sensor, are installed in the distance L [m]. The electrically defined monitored space of the soil will always have the character of a resistor, that is, there will always be a real part R of the EI of the soil and the capacitor represented by the resistance X_C [Ω]

$$X_C = \frac{1}{\omega \cdot C} = \frac{1}{2 \cdot \pi \cdot f \cdot C}. \tag{3}$$

The electric conductor delimited in this way may have the shape of a cylinder or a prism with a cross-sectional area A [m^2] and a length l [m]. Therefore, it is possible to express the resistance value (resistivity) ρ [Ω m] resp. conductivity (specific conductivity)

$$\sigma = \rho^{-1} \tag{4}$$

which are used most frequently to describe the electrical properties of soil, as they are closely dependent on hydrogeological parameters of soil and rock environment.

$$\rho = R \frac{A}{l} \tag{5}$$

The complexity of monitoring the environment is documented by the nomogram of electrical resistances (Fig. 1), resp. the conductivity of the earth (Pande, 1975). For electrical impedance of soil measurement was used apparatus with Z-meter IV device. The apparatus consists of a Z-meter device, measuring probes with cables and an AC power source. The basic parameters of the used Z- meter IV device are given in Table 1.

Materials

For the experiment were used a sample of sand and three samples of clay. It is of sand (Fig. 2) mined near village Bratčice (designation sand Bratčice) was used.

The sand formed a homogeneous environment, so only a material with an effective grain size of 1.0 mm was used, which was separated by sieving through standard sieves.

As clay samples (Fig. 2) were used clays with different chemical composition (designation B01, GEM and GEP) were provided by LB Minerals. These samples were used to created inhomogeneity of the environment. The chemical composition of clays are given in Table 2.

A density test (Fig. 3), (ČSN EN ISO 14688-1, 2018), (ČSN EN ISO 14688-2, 2018) was used to characterize the clay samples. The result is a graph where the horizontal axe shows the grain diameters, and the vertical axe cumulatively show the weight percentages of soil particles. The results are shown in Fig. 4.

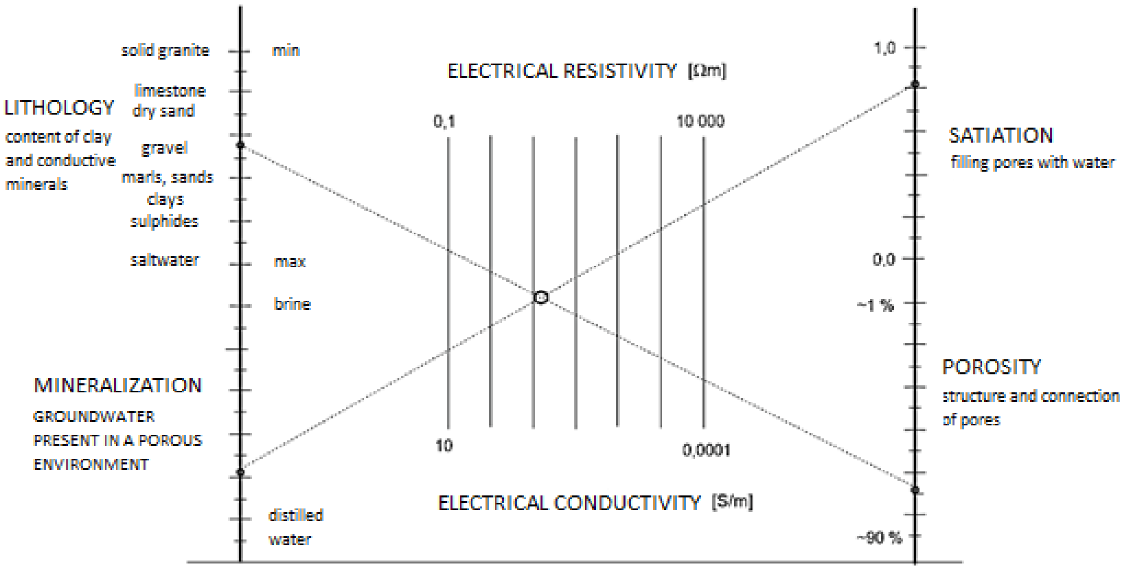

Fig. 1. Nomogram for estimating the impact of changes in basic factors on the resistivity assessment respectively conductivity of the natural environment.

Table 1. Parameters of the Z-meter IV device

Parameter	**Z-meter IV**
Impedance range	10 Ω - 1 MΩ
Frequency range	100 Hz – 200 kHz
Measuring Voltage	0.2 V and 1.0 V
Accuracy of module Z measurement	± 2 % from range
Accuracy of phase measurement	± 2 °
Communication interface	USB, SD card, Ethernet, Bluetooth
Numbere of measurement points	1, 8, 16, 32, 64, 128, 256
Switcher	internal, external
Power	battery, net

Table 2. Parameters of the Z-meter IV device

TITLE	SiO_2 [%]	Al_2O_3 [%]	Fe_2O_3 [%]	TiO_2 [%]	CaO [%]	MgO [%]	Na_2O [%]	K_2O [%]
B01	48 – 52	32.0 – 34.0	2.3 – 2.7	0.8 – 1.2	0.2 – 0.4	0.2 – 0.4	0.0 – 0.2	2.3 – 2.8
GEM	54 – 58	16.5 – 18.5	10.0 – 12.0	1.0 – 1.3	1.0 – 1.3	2.5 – 3.5	0.1 – 0.3	3.0 – 3.7
GEP	54 – 58	18.0 – 20.0	7.5 – 9.5	1.3 – 1.8	1.2 – 1.5	2.2 – 3.2	0.1 – 0.3	2.7 – 3.5

Fig. 2. Samples of soils (sand Bratčice, B01, GEM, GEP – designation from left to right).

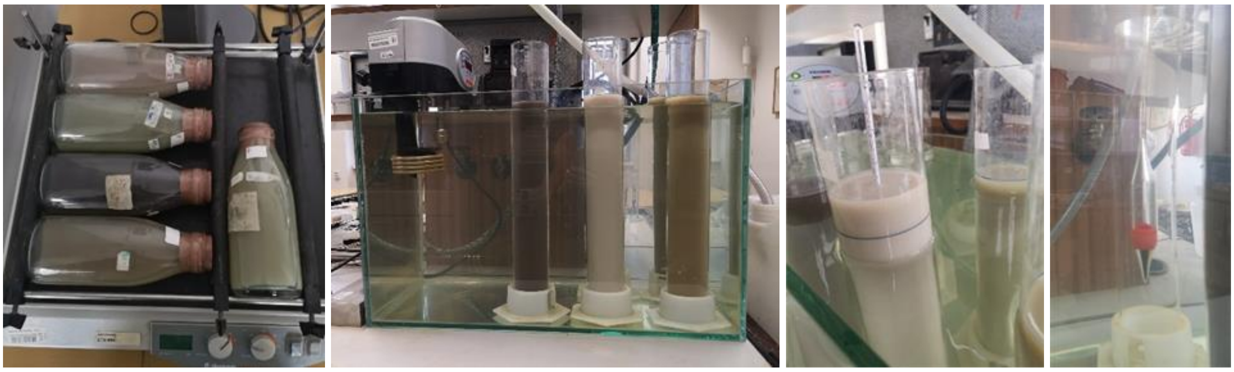

Fig. 3. Density test.

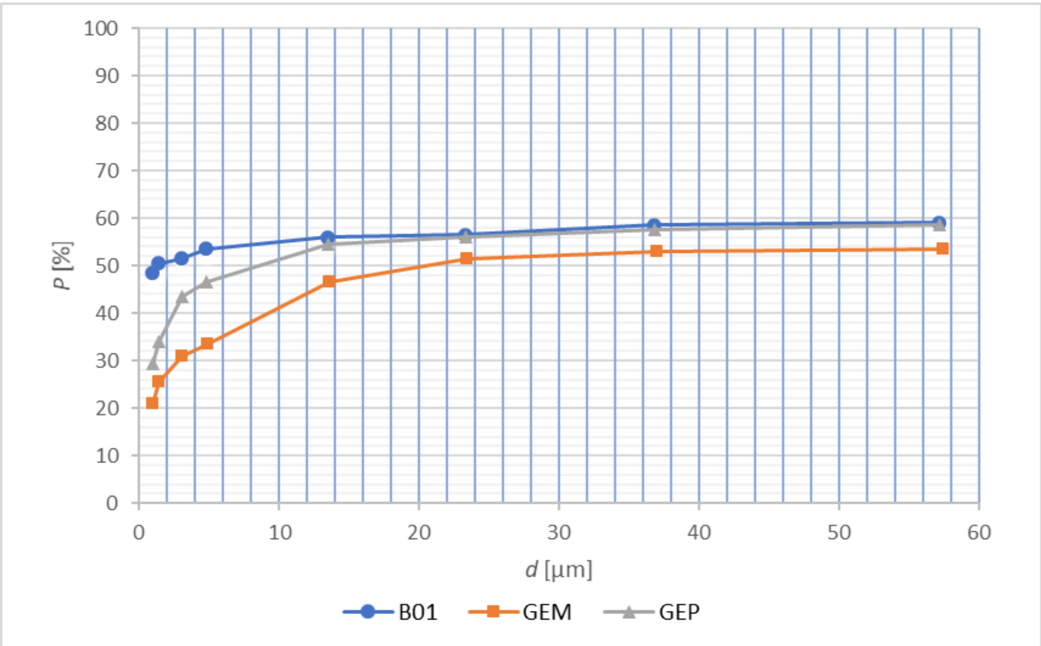

Fig. 4. Results of the density test.

Experiment

The experiment was carried out in laboratory conditions at the laboratory of Water Management Research at the Faculty of Civil engineering in Brno. It was based on the measurement of the components (real *R* and imaginary *X*) of the electrical impedance using the Z-meter IV device. (Pařílková and Radkovský, 2016). For the measurement of electrical impedance was used a model (Fig. 5 – left) consisting of a particular cylindrical organic glass container with an inner diameter D=0.19 m, a height h=0.29 m and a wall thickness t=0.004 m.

A carrier was placed in the model, which divided the model into a measurement space containing soil (upper part) and space for accumulating infiltrated water with an output outside the model (lower part). The measuring area of the cylindrical model was fitted with 16 stainless steel electrodes on the circumference at three „colours" levels (yellow, red and black) of the model (Fig. 5 – left). The electrodes were realized screws with a round head with a diameter of 0.01 m, whose mutual distance was constant L=0.037 m (Fig. 5 – left). Conductors with a constant length of 1.5 m were connected to the electrodes. To ensure stability and prevent leaching of fine particles of the soil sample in the modified cylindrical model, PE mesh-work was placed on the carrier (Fig. 5 – right). The mesh-work is inert to the adherence of possible impurity impurities of the salt type and has a mesh size sufficient to permeate water while preventing the elimination of soil particles.

The electrodes and the free conductor ends were numbered because of the gradual connection of the individual sensors to the Z-meter device. The EI measurement was carried out in such a way that each of the connection electrodes gradually formed a sensor with all the remaining electrodes in one surface section. Probes used in laboratory conditions were passive because they did not contain any active element (signal generator, voltage source, etc.) in their design. During the measurements, the sensed length of the examined environment was determined by the area of measuring electrode in contact with ground and distance between electrodes. The evaluated point of this conductor was placed in the geometric centre of the conductor for the further processing. The measurement of electrical characteristics (real R and imaginary X components) was realized with the Z-meter IV device. The device was connected to the measuring electrodes by cables. Switching of individual sensors (Fig. 6) was realized manually, since this is a static task, using KSS AC-3RD crocodile clips, which were equipped with insulating PVC material.

The experiments were designed in such a way that a sample of sand Bratčice's with an effective grain size of 0.001 m separated by sieving through standard sieves was gradually poured into the cylinder (Fig. 7 – right). The sample was compacted by shaking in layers and pierced. After the model was filled with a soil sample, the sample was loaded with distilled water 0.01 m above the soil sample level and was subsequently punctured again to eliminate air bubbles in the sample. Since free ions (e.g. Na +, Cl-) cause electrical conductivity in wet, porous soils, distilled water has been used to minimize the physicochemical properties of the water. At this time was done the first measurement of the field of electrical impedance. After the measurement, a portion of the soil was asymmetrically removed from the model, and a clay sample (Fig. 7 – left) was placed at this place, representing an anomaly in the ground environment. The anomaly was represented by a clay-shaped clay with a diameter of 0.04 m (Fig. 7 – in the middle). The clay sample was then backfilled with a sampled soil. The soil sample was again compacted with weights, pierced and loaded with water. Three samples of different clays were used in succession and were always placed in the same place.

The changes of ambient conditions were monitored during the whole experiments. The temperature and humidity of air in the room and the temperature and humidity of the environment were monitored. The changes in the measured ambient conditions during the experiments were negligible. In the place, the temperature was 22°C ± 0.2°C and air humidity was 60.0% with a deviation of ± 0.5%. The temperature of the soil samples measured varied by a maximum of 0.5°C.

Before starting the experiment, the parameters of the measuring device were set up (Table 3). The parameters of the measuring instrument were the same for all measured experiments. The location of the clay sample in the model is schematically shown on Fig. 8.

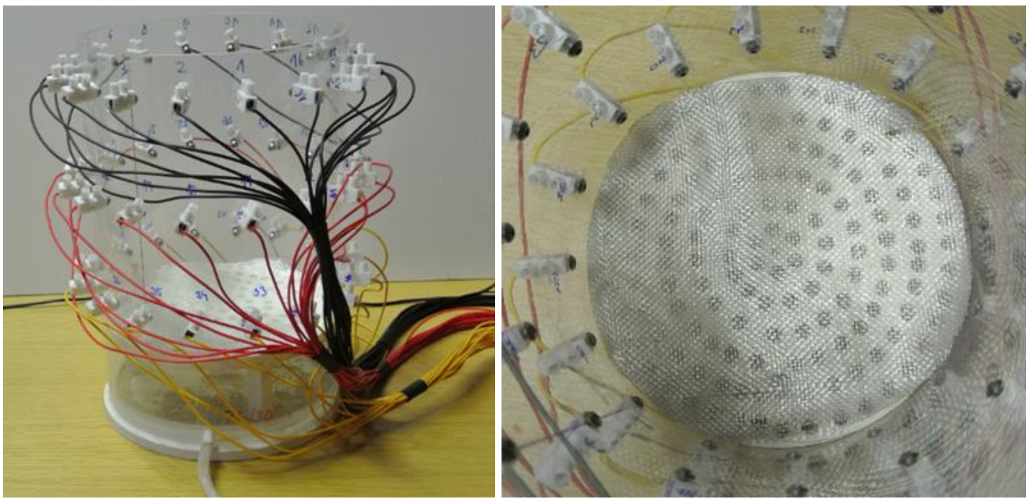

Fig. 5. A cylinder model – left, PE mesh-work – right.

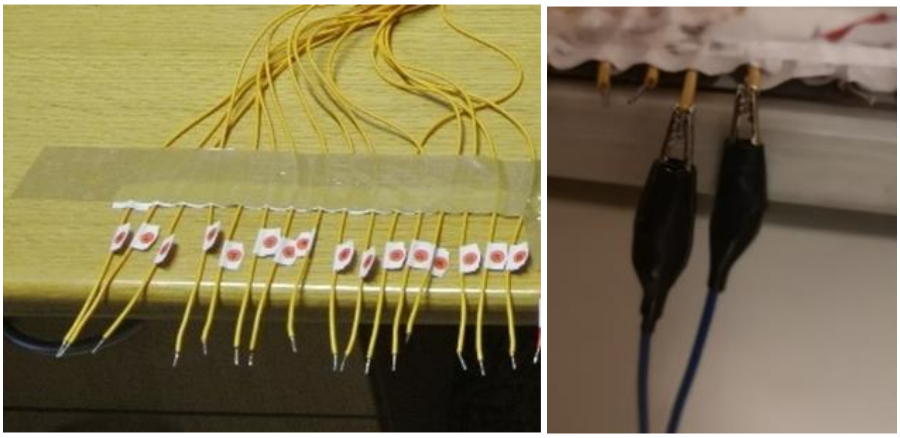

Fig. 6. Switching between individual sensors.

Fig. 7. A model with a sample of sand – left, a sample of clay – in the middle, sample of clay inside the environment – right.

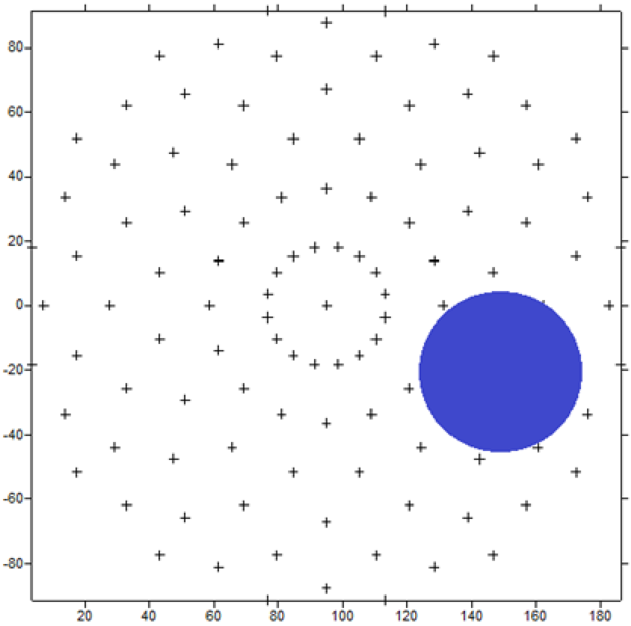

Fig. 8. Schematic design of the experiment (blue circuit presents clay position).

Table 3. Parameters of the Z-meter IV device

Measuring regime	1 probe pair	-	**Measuring frequency**	8 000	Hz
Number of channels	1	-	**Number of repetitions**	1	-
Sampling time (sensing the value)	100	ms	**Time lag between measurements**	10	ms

Results and discussion

Data were processed using an MS Excel program. Then the results were evaluated in the program Surfer 8 (Surfer, 2002). Triangulation with Linear interpolation was used for evaluation results.

This method uses the optimal Delaunay triangulation, which means that the algorithm creates triangles by drawing lines between data points. The original points are connected in such a way that no triangle edges are intersected by other triangles. The result is a patchwork of triangular faces over the extent of the grid. The accuracy of the method is determined by the positioning of the electrodes; it means the number of measured data (Surfer, 2002).

It was measured both components of the EI between each pair of electrodes total number of which is 16 in one level. After this measured was calculated model EI and phase shift. Resistance maps have been created from the EI model for better presentation of results. Resistivity was calculated according to formula (5). The implementation of resistivity values was done as relative. It means that was calculated and evaluated the difference of resistivity between the values of the initial environment and environment with an anomaly.

The results of the measured individual environments are shown in Fig. 9 – Fig. 11

From these results (Fig. 9 – Fig. 11) it is possible to detect the location of the "anomaly" in the given environment in individual experiments, resp. the changes of the monitored environment. However, the differences between the measurements are insignificant, as the clay samples used are very similar, which is also evident from the specified curves of grain size (Fig. 4).

The results also show the significant surrounding environmental changes near anomaly due to manipulation of the environment (removal, replacement and backfilling) between individual experiments.

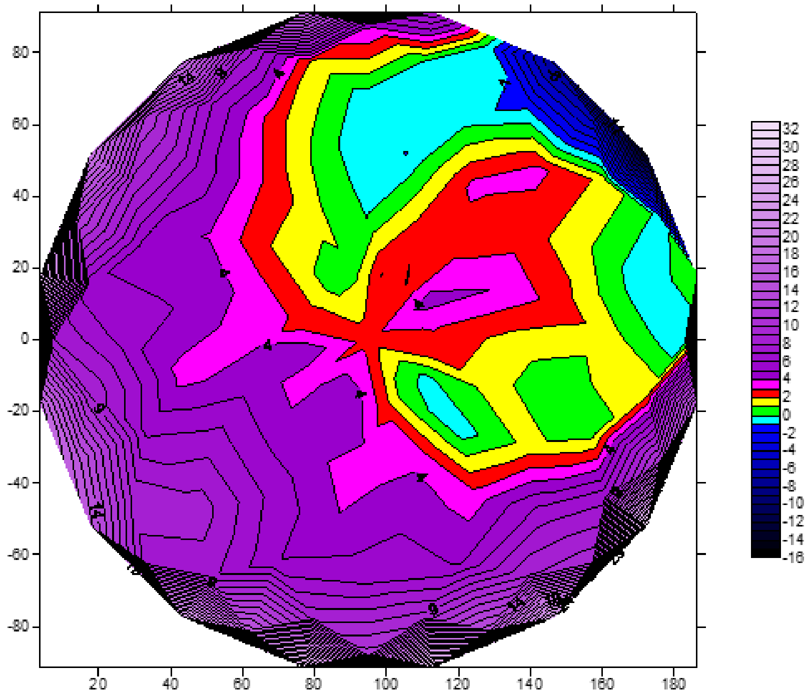

Fig. 9. Evaluation of resistivity in Surfer 8 for clay designation "B01".

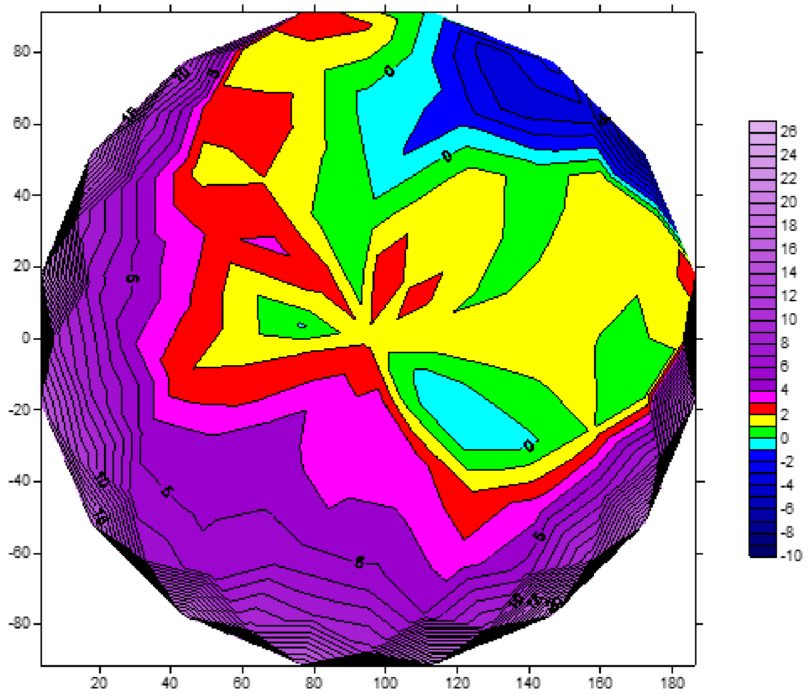

Fig. 10. Evaluation of resistivity in Surfer 8 for clay designation "GEM".

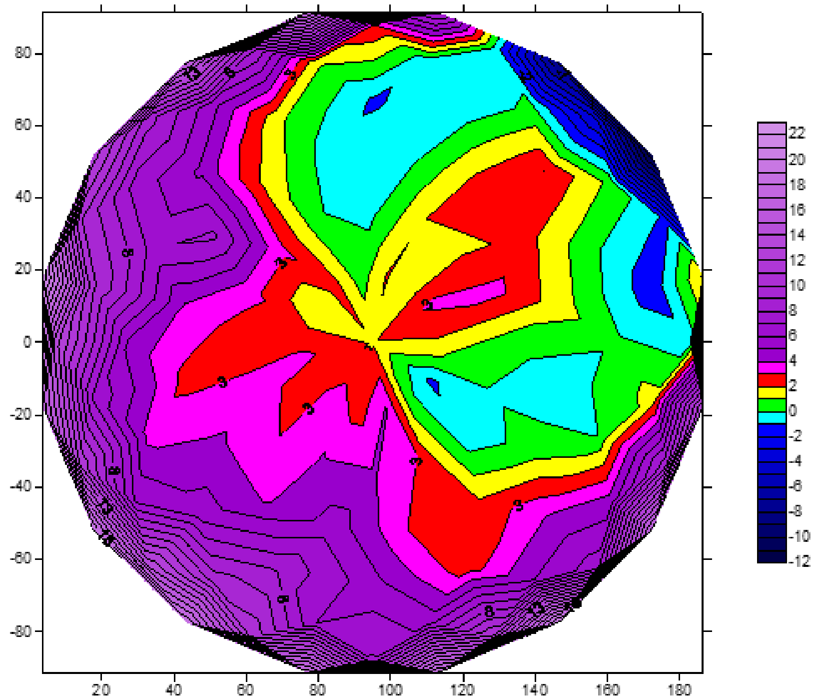

Fig. 11. Evaluation of resistivity in Surfer 8 for clay designation "GEP".

Conclusion

In laboratory conditions, experiments were performed using an apparatus with Z-meter device. The components of the electrical impedance of soils with an artificial clay anomaly were measured.

The results shows that the given modified EIS method with measuring apparatus and Z-meter IV device can be used for measurement and EI image reconstruction. Using the technique of EIS, it is possible to detect the location of the anomaly in the examined environment. Experiments were done in laboratory conditions. The advantage of this method is the relatively simple measuring procedure and manipulation with the measuring apparatus. The disadvantage can be its interpretation of the measurement results should be carried out by an expert with knowledge and practical experience of the method used.

Acknowledgement

The paper was carried out under the support of the Brno University of Technology project No. FAST/FEKT-J-18-5385 – Detection of anomalies of the environment by electric impedance tomography and within the sustainability of project E!7614 solved in EUREKA program.

References

Barbiero, G., Miracapillo, C. (2008): International application of EIS method (electrical impedance spectrometry) for soil humidity measuring. Results of Automated Bibliographical Search with ISI WEB of Knowledge – Report N.1, technical report R/160. ISSN 0392-967).

Barsoukov, E., Macdonald, J. (2005): Impedance spectroscopy: theory, experiment, and applications. 2nd ed. Hoboken, N. J.: Wiley-Interscience, p. 595. ISBN 04-716-4749-7

Cunningham, M. J. (1986): Automatic data logging timber moisture contents over the range 10% – 50% w/w. ISA Trans. 73–80

ČSN EN ISO 14688-1 (2018): Geotechnický průzkum a zkoušení – Pojmenování a zatřiďování zemin – Část 1: Pojmenování a popis.

ČSN EN ISO 14688-2 (2018): Geotechnický průzkum a zkoušení – Pojmenování a zatřiďování zemin – Část 2: Zásady pro zatřiďování.

Dean, T. J., Bell, J. P., Baty, A. J. B. (1987): Soil moisture measurement by an improved capacitane technique. J. Hydrol. 67–90

Gruntorád, J. (1985): Principy metod užité geofyziky. SNTL Praha, Alfa Bratislava.

Karous, M (1989): Geoelektrické metody průzkumu. SNTL Praha, Alfa Bratislava.

Mareš, S. (1983): Geofyzikální metody v hydrologii a inženýrské geologii. SNTL Praha.

Pande, A. (1975): Handbook of moisture determination and control. 1st ed. New York, Dekker.

Pařílková, J. (2010): Monitorování proudění vody zeminou a možnosti jeho využití u ochranných hrází. Teze habilitační práce. Brno: VUTIUM. ISBN 978-80-214-4068-5.

Pařílková, J., Radkovský, K. (2016). Z-meter IV, user's manual. Brno.

SURFER (2002): Surfer 8, user's manual.

Vogelsang, D. (1994): Environmental geophysics. A practical guide, Springer Verlag.

Ing. Zuzana Műnsterová (*corresponding author, e-mail: munsterova.z@fce.vutbr.cz)
doc. Ing. Jana Pařílková, CSc.
Brno University of Technology
Faculty of Civil Engineering, Institute of Water Structures
Veveří 95
602 00 Brno
Czech Republic

Ing. Jan Dušek
doc. Ing. Jan Mikulka, Ph.D.
Brno University of Technology
Faculty of Electrical Engineering and Communication
Department of Theoretical and Experimental Electrical Engineering
Technická 3082/12
616 00 Brno
Czech Republic

DOI: 10.31577/ahs-2020-0021.01.0012

ACTA HYDROLOGICA SLOVACA

Volume 21, No. 1, 2020, 98 – 105

ACTUAL VALUES OF SATURATED HYDRAULIC CONDUCTIVITY OF CHANNEL BED SILT AND ITS DISTRIBUTION ALONG KOMÁRŇANSKÝ CHANNEL

Renáta Dulovičová*, Radoslav Schügerl, Yvetta Velísková

This contribution deals with the evaluation of channel bed silt permeability along the Komárňanský channel based on the measurements during the year 2019. Komárňanský channel is the largest one from three great channels of channel network at Žitný ostrov area. The channel bed silt permeability is expressed by parameter of its saturated hydraulic conductivity. This paper describes the current state of channel bed silt distribution along this channel during the year 2019 and simultaneously brings the values of saturated hydraulic conductivity of channel bed silt. The channel bed silts were extracted and obtained by two ways, as a disturbed samples and as an undisturbed samples. The samples were taken in each selected profiles of channel in three layers – top, middle and bottom layer of channel bed silt. The selection of sampling was made in dependency on channel bed silt thickness in the measured profile. The values of channel bed silt saturated hydraulic conductivity from disturbed samples K_d were calculated according to empirical formulas of Bayer-Schweiger and Špaček. The valid values K_d reached from 1.09 x 10^{-08} – 1.98 x 10^{-04} m s^{-1}. The values of channel bed silt saturated hydraulic conductivity from undisturbed samples K_u were determined by the laboratory falling head method. The acquired values K_u for Komárňanský channel reached from 3.73 x 10^{-08} – 2.01 x 10^{-05} m s^{-1}. The current state of longitudinal distribution of channel bed silt along this channel was demonstrated in the paper graphically and values of saturated hydraulic conductivity were demonstrated numerically.

KEY WORDS: Žitný ostrov channel network, channel bed silt, grain size analysis, silt permeability, saturated hydraulic conductivity

Introduction

The channel network at Žitný ostrov (ŽO) area was built already in the late 19th century with primary aim to drain the wet places of this area. Thereafter its utilization began also to surface irrigation during dry periods and also to groundwater resources regulation in some ŽO localities. ŽO area is a flat plain with only small differences in altitude and that's why the flowing velocities in channels are very low. Just these slow velocities cause the silting up on the bottom of channels. It is very important to observe the development of this channel bed silt aggradation continuously, forasmuch as the channel network is in close interaction with groundwater. The silting up of channel bed by sediments has impact to bed permeability in time and by this way to interact with surrounding groundwater. The permeability is expressed by value of saturated hydraulic conductivity. This parameter can be determined from granularity analysis of extracted bed silt samples. This paper is adressed to results of field measurements along the Komárňanský channel in 2019 with aim to find out the current state of silting up at this channel and the influence of bottom aggradation degree to interaction between channel and its surrounding groundwater. The values of saturated hydraulic conductivity were determined on the base of two ways of channel bed silt extraction (disturbed and undisturbed channel bed silt samples).

Material and methods

Channel network at the ŽO area is created by several main channels – e.g. channel Gabčíkovo-Topoľníky, Chotárny channel (Aszód), Komárňanský channel, channel Čalovo-Holiare-Kosihy, channel Aszód-Čergov, channel Čergov-Komárno, channel Dudváh and by thus network of smaller channels – see Fig. 1. Our research of channels silting up has been concentrated since 1993 to three main channels of this network: channel Gabčíkovo-Topoľníky, Chotárny channel and Komárňanský channel (KCH). The localization of KCH is shown in more details – see Fig. 2.

Mutual interaction between channel network and groundwater of ŽO is influenced not only by general conditions of groundwater flow at ŽO area, but also by water level regime of its channel network. For this reason, many Slovak researchers were interested in solution of groundwater regime at this specific area

(Kosorin, K. 1997; Burger and Čelková, 2004; Čelková, 2014; Mucha et al., 2006; Štekauerová et al., 2009; Baroková and Šoltész, 2014; etc.).

The regulation of water level in channel network should be able to affect the groundwater level in its surrounding. Channels, manipulating objects and pumping stations as basic elements of channel network enable to control water level in channels and by this way to achieve optimal position of groundwater table mainly during growing season. But on the other hand, during this season the aquatic vegetation affects flow conditions in channels and also the thickness and structure of channel bed silts significantly influence the interaction between surface water in channel network and groundwater in surrounding area of the ŽO.

Komárňanský channel (KCH) is the largest one of three main channels of ŽO channel network. This channel, primary built for drainage, is now used also for irrigation

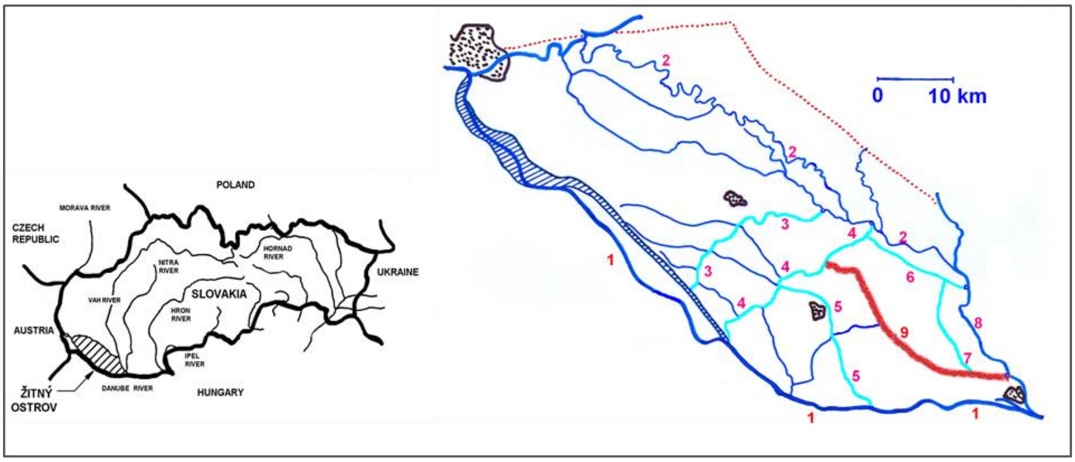

Fig. 1. Schematic map of channel network at ŽO area: left – ŽO situation, right - scheme of channel network: 1 – Danube; 2 – Small Danube; 3 – channel Gabčíkovo-Topoľníky; 4 – Chotárny channel; 5 – channel Čalovo-Holiare-Kosihy; 6 – channel Aszód-Čergov; 7 – channel Čergov-Komárno; 8 – channel Dudváh; ***9 – Komárňanský channel.***

Fig. 2. Localization of Komárňanský channel in the territory of channel network at ŽO area.

function. KCH is supplemented from the Váh river over pumping station Komárno – Nová Osada and it connects with Chotárny channel (in rkm 9.1 of Chotárny channel) through a manipulating objects northwest of the Okoč village. The last measured length of the KCH is about 28 km. The channel width during the measurements was in range 10–29 m, the measurements of channel depth registered maximal values up to 2.7 m (according to located cross-section profiles). The values of saturated hydraulic conductivity in aquifers nearby this channel K_{fs} were 0.40–3.4 x 10^{-3} m s^{-1} (Mišigová, 1988).

The measurements of channel bed silt thickness along the KCH were performed in 2019 from the displaceable inflatable dinghy by simple drill hole – see Fig. 3. The measurements were realized along the whole length of the KCH. The distance of cross-section profiles along the channel varied between 1.0–1.5 km. In all channel cross-section profiles there was measured the water depth and channel bed silt thickness with step 1.0–2.0 m along the channel width. Besides of channels silting up also the velocity profiles and discharges were measured during field measurements in 2019. The RiverSurveyor S5/M9 from SONTEK was used – see Fig. 4. The logged files from these measurements confirmed that the velocities in every channel cross-section profile are very low. In some profiles, the channel was overgrown by very dense aquatic vegetation inside the channel (under water level) and also by bank vegetation, so there was impossible to measure velocity profiles and discharges. In 2019 the samples of channel bed silt were taken in these selected KCH cross-section profiles where the largest channel bed silt thickness was noticed. The extraction of samples was done by equipment (see Fig. 5) which is so-called sediment beeker sampler. There was possible to take undisturbed samples with this equipment and from each whole sample there was extracted a part from top, middle and bottom layer of channel bed silt. After experimental determination of saturated hydraulic conductivity for each layer of sample from one cross-section profile, the sample was broken and changed to disturbed sample. Next, for each disturbed sample it was done the granularity analysis and determined the saturated hydrau-lic conductivity value.

Saturated hydraulic conductivity of channel bed silt

The values of saturated hydraulic conductivity of channel bed silt was determined from undisturbed samples and also from disturbed samples for the same localities.

The values of saturated hydraulic conductivity from disturbed samples were calculated by empirical formulas coming out from granularity curves. The several empirical relationships for determination of SHC from granularity exist, but their validity is limited and for that reason we should apply them very carefully. In case of disturbed samples sampling we used the relationships by Beyer-Schweiger and Špaček (Špaček, 1987). These relationships are functions of d_{10} – particle diameter in 10% of soil mass [m] and d_{60} – particle diameter in 60% of soil mass [m]. Both of them were determined from

Fig. 3. Equipment for measurement of silt thickness – drill hole probe at channel field measurement.

Fig. 4. Equipment for measurement of the velocity profiles and discharges in the channel – RiverSurveyor S5/M9.

Fig. 5. Measuring equipment for silt samples extraction in 2019 – the Beeker sampler.

granularity curves of extracted samples of channel bed silt. The formulas of Beyer-Schweiger and Špaček (Špaček, 1987) were used for determination of saturated hydraulic conductivity from disturbed samples from KCH – K_d. The equations for Bayer-Schweiger, Špaček I., Špaček II. formulas and for calculation of saturated hydraulic conductivity values have been already cited in previous published papers (e.g. Dulovičová et al., 2016, Dulovičová et al., 2018). The values of saturated hydraulic conductivity from disturbed samples K_d along the KCH are summarized in Table 1.

In case of undisturbed samples the values of saturated hydraulic conductivity were assessed by falling head method – direct measurement in laboratory. There was used simplified equipment for measuring of saturated hydraulic conductivity from undisturbed samples

(Kutílek, 1978; Rožnovský et al., 2013) – see Fig. 6 (methodology of measurement and calculation described e.g. Šurda et al., 2013; Dulovičová, 2014; Dulovičová et al., 2016; 2018; etc.).
The relation for calculation of average value of saturated hydraulic conductivity K_u according to scheme on Fig. 6 (Šurda et al., 2013) is:

$$K_u = \frac{l}{\Delta t} \ln \frac{h2}{h1} \tag{1}$$

where
K_u – is the saturated hydraulic conductivity of undisturbed samples [cm s^{-1}],
l – is a sample height [cm],
h_1, h_2 – variable static head [cm] – see Fig. 6.

The values of saturated hydraulic conductivity from undisturbed samples K_u, extracted from selected cross-section profiles of the KCH, were calculated by the relationship (1) according to scheme on Fig. 6. The values of K_u along the KCH are summarized in Table 2.

Results and discussion

As was mentioned before, flow velocity in the channels is very slow by low slope condition of whole area of ŽO, which is very flat. The low flow velocity caused the deposition of silt in the channel bottom. The distribution of channel bed silt along the channel depends also on flow conditions in channels junction. We supposed the smaller amounts of the silt deposition in the upstream and downstream parts of KCH (caused manipulating with pumping station) and larger amounts in the middle part. Also we supposed that this increase to be gradual and linear. Ours expectations were confirmed partially. The silt thicknesses along KCH during monitored period 2019 showed moderately increasing trend with rising stream log, but in middle part was noticed the decrease of silt thicknesses – see Fig. 7. Globally, the KCH aggradation gradually enlarged with rising stream log (excepting local parts with small amount of deposits) and the channel bed silt thicknesses increased.

Values of saturated hydraulic conductivity from disturbed samples

The value of saturated hydraulic conductivity, as the indicator of channel bed silt permeability, was calculated for disturbed samples by Beyer-Schweiger and Špaček

Table 1. Komárňanský channel – valid values of *Kp* from disturbed samples of silts in year 2019

Channel	**Komárňanský**				
Year	**2019**				
Channel distance [km]	**Sampling way**	**Silt layer**	**Saturated hydraulic conductivity K_p [m s^{-1}]**		
			Bayer-Schweiger	***Špaček I.***	***Špaček II.***
2.0	disturbed sample	top	-	$5.33x10^{-07}$	-
		middle	-	$2.53x10^{-07}$	-
		bottom	-	$2.60x10^{-07}$	-
7.0		top	-	$4.10x10^{-07}$	$1.68x10^{-06}$
		middle	-	-	$2.92x10^{-05}$
		bottom	-	-	$2.45x10^{-05}$
9.0		top	$2.56.10^{-08}$	$5.00x10^{-07}$	-
		middle	-	$4.13x10^{-07}$	-
		bottom	-	$1.01x10^{-06}$	-
12.0		top	-	$8.07x10^{-07}$	-
		middle	-	$5.18x10^{-07}$	-
		bottom	-	$6.37x10^{-07}$	-
20.0		top	-	$1.19x10^{-06}$	-
		middle	-	-	$1.24x10^{-05}$
		bottom	$8.20.10^{-05}$	-	$1.98x10^{-04}$
23.0		top	-	$4.44x10^{-07}$	-
		middle	-	$7.35x10^{-07}$	-
		bottom	-	$5.70x10^{-07}$	-
25.0		top	$5.04.10^{-08}$	$6.94x10^{-07}$	-
		middle	-	$2.52x10^{-07}$	-
		bottom	-	$8.66x10^{-07}$	-
28.0		top	-	$2.40x10^{-07}$	-
		middle	$1.09.10^{-08}$	$3.34x10^{-07}$	-
		bottom	-	$5.06x10^{-07}$	-

– unkept conditions of validity for aplication of Beyer-Schweiger and Špaček formulas

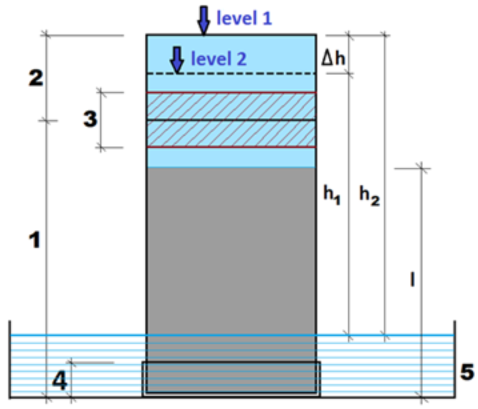

Fig. 6. Simplified equipment for measuring saturated hydraulic conductivity of undisturbed sample: 1 – sampling tube height, 2 – Kopecky´s roller, 3 rubber ring, 4 – filter paper and wire strainer, 5 – Petri dish.

Table 2. Komárňanský channel – valid values of K_n from undisturbed samples of silts in year 2019

Channel	Komárňanský		
Year	2019		
Channel distance [km]	Sampling way	Silt layer	Saturated hydraulic conductivity K_n [m s^{-1}]
2.0	undisturbed sample	top	7.47 x 10^{-06}
		middle	3.84 x 10^{-06}
		bottom	1.34 x 10^{-07}
7.0		top	1.31 x 10^{-07}
		middle	2.54 x 10^{-06}
		bottom	1.32 x 10^{-06}
9.0		top	1.03 x 10^{-06}
		middle	3.76 x 10^{-07}
		bottom	1.05 x 10^{-06}
12.0		top	5.90 x 10^{-07}
		middle	1.06 x 10^{-07}
		bottom	1.24 x 10^{-06}
20.0		top	6.81 x 10^{-07}
		middle	1.24 x 10^{-05}
		bottom	2.01 x 10^{-05}
23.0		top	2.60 x 10^{-06}
		middle	2.43 x 10^{-07}
		bottom	2.48 x 10^{-07}
25.0		top	1.39 x 10^{-07}
		middle	7.07 x 10^{-08}
		bottom	1.65 x 10^{-06}
28.0		top	3.00 x 10^{-07}
		middle	3.73 x 10^{-08}
		bottom	5.63 x 10^{-08}

relationships, which are the function of d_{10} (particle diameter in 10% of soil mass) and d_{60} (particle diameter in 60% of soil mass). The characteristics d_{10} and d_{60} were determined separately for top, middle and bottom layer of extracted samples.

The valid values of channel bed silt saturated hydraulic conductivity in KCH reached to 1.09 x 10^{-08} – 1.98 x 10^{-04} m s^{-1}. In comparison with values of saturated hydraulic conductivity in aquifers nearby this channel K_{fs} (Mišigová, 1988), the values K_d are severalfold lower. Detailed distribution of K_d values along the KCH shows Table 1.

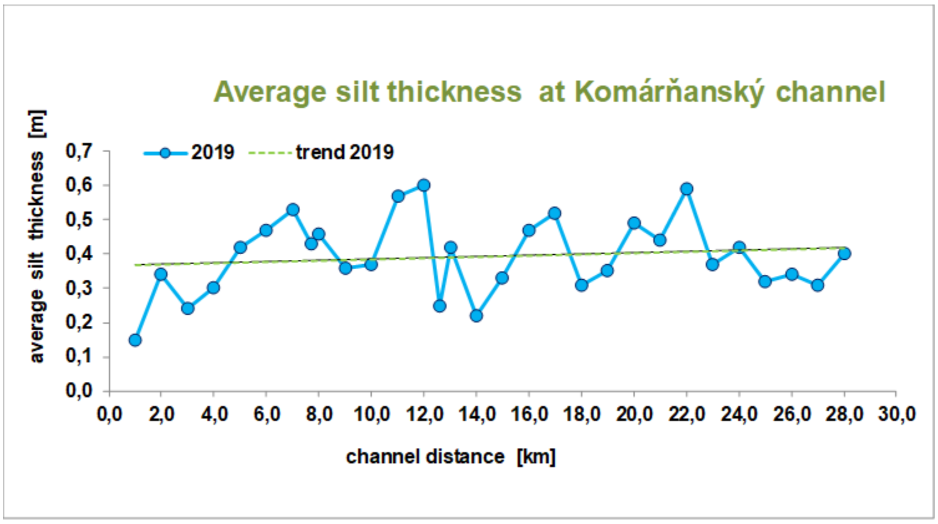

Fig. 7. Average silt thicknesses along Komárňanský channel in 2019.

Values of saturated hydraulic conductivity from undisturbed samples

The values of saturated hydraulic conductivity from undisturbed samples K_u extracted from selected cross-section profiles along the KCH during 2019 were determined by equation (1) in correspondence to scheme on Fig. 6. The valid values of K_u reached to 3.73 x 10^{-08} – 2.01 x 10^{-05} m s^{-1}. In comparison with values of saturated hydraulic conductivity in aquifers nearby this channel K_{fs} (Mišigová, 1988), the values of K_u are also severalfold lower. Detailed distribution of K_n values along the KCH shows Table 2.

We also compared the values of saturated hydraulic conductivity obtained from disturbed and undisturbed samples of channel bed silt.

As it is obvious from Table 1, the values of K_d from disturbed samples run into 10^{-08} to 10^{-04}, whereby the values 10^{-07} predominated. Likewise the values of K_u from undisturbed samples run into 10^{-08} to 10^{-05} (Table 2), predominant values were 10^{-07}–10^{-06}. This fact only partly confirmed our assumption that the values from undisturbed samples K_u will be lower then the values from disturbed samples $K_{d.}$ The differences betwen them were practically irrelevant.

At comparison of single layers of channel bed silt, extracted as disturbed samples, we detected that between top, middle and bottom layers were little differences, maximally tenfold.

In case of comparison of undisturbed samples in its single layers the differences between top, middle and bottom layer were tenfold up-to hundredfold.

The interesting results were obtained from mutual comparison of single layers of silt for disturbed and undisturbed samples. As it is obvious from comparison Table 1 and Table 2, along whole KCH the majority of the values K_d and K_u were nearly equal (10^{-07}) in all layers (top, middle, bottom). The assumption of decrease of K_u values opposite K_d values was endorsed only for middle and bottom layer in km 7.0; for top layer in km 20.0 and for bottom layer in km 28.0; evently in several cases were K_u values larger than K_d values (tenfold for top and middle layer in km 1.0; tenfold up to hundredfold for top layer in km 9.0; tenfold for bottom layer in km 12.0; tenfold for top layer in km 23.0 and tenfold for bottom layer in km 28.0). This fact is in contradiction with results from measurements in 2016, when obtained K_u values were tenfold lower than K_d values (Dulovičová et al., 2018). The reason of discrepancies between results of K_u and K_d values (the increase of K_u values in 2019 by comparison with 2016) could be caused probably by breaking or elimination of top layer or evently mutual mixing of all layers during running maintenance processes in the period between 2016 to 2019. In this way could occur the change of channel bed silt permeability expressed by tenfold up to hundredfold different values of channel bed silt saturated hydraulic conductivity.

Conclusion

This paper deals with the evaluation of bed silt permeability along the Komárňanský channel (KCH) on base of field measurements performed during the year 2019. The channel bed silt permeability and the thickness of bed silt determine the rate of mutual interaction between surface water of KCH and nearby groundwater in its surroundings. For this reason it is important to know actual state of channel bed aggradation. The permeability of channel bed silt is expressed by its saturated hydraulic conductivity.

According to results of distribution of average bed silt thickness along the KCH from 2019 it is visible that silting up of this channel has been changed, it gently increased with ascendant stream log, but in middle part there was noticed the local and also global decrease of silt thicknesses – see Fig. 7.

The values of saturated hydraulic conductivity of channel bed silt were determined by two ways: as channel bed silt extracted and obtained as disturbed samples and as undisturbed samples from top, middle and bottom layer of silt. From disturbed samples the values of saturated hydraulic conductivity of channel bed silt were calculated according to Bayer-Schweiger and Špaček formulas and they are presented in Table 1, the valid values K_d reach from 1.09 x 10^{-08} – 1.98 x 10^{-04} m s^{-1}. From undisturbed samples of channel bed silt there were determined values K_u by falling head method and they are summarized in Table 2. The values K_u reached values from 3.73 x 10^{-08} – 2.01 x 10^{-05} m s^{-1}.

Some discrepancies in distribution and values of saturated hydraulic conductivity obtained in 2019 and from previous study period exist. For this reason, it is necessary to put these results under the more detailed analysis in the next step in the future.

As it was mentioned, the aggradation along KCH enlarged in 2019, the channel bed silt thicknesses increased. Because the mutual interaction between surface water in channel and groundwater in its surroundings depends on channel bed permeability, which is mainly determined by the channel bed silt thickness and permeability, it is necessary to know these parameters for correct evaluation of the mutual exchange of water amounts between surface water in channel and groundwater in its surroundings. All obtained information about actual state of silting up of KCH, supplemented by values of saturated hydraulic conductivity channel bed silt, will be helpful for numerical simulation models, also for any way of regulation of groundwater level in surroundings of this channel and water source management at ŽO area.

Acknowledgement

This work was supported by the contract VEGA-02/0025/19 and APVV-14-0735.

References

Baroková, D., Šoltész, A. (2014): Analysis of surface and groundwater interaction in the Danube river branch system, SGEM Conference Proceedings, 14th SGEM Geo-Conference on Water Resources. Forest, Marine And Ocean Ecosystems, Vol. I., www.sgem.org, ISBN 978-619-7105-13-1/ ISSN 1314-2704, 51–58

Burger, F., Čelková, A. (2004): Simulation of aquifer feeding processes during dry period. Acta Hydrologica Slovaca, Vol.5, No.2, 348-357, (in Slovak)

Čelková, A. (2014): The influence of groundwater on soil salinization in the alluvium in the left bank side of Danube river between Komárno and Štúrovo. Acta Hydrologica Slovaca, Vol. 15, No. 2, 413–423, (in Slovak)

Dóša, M., Holko, L., Martincová, M., Danko, M., Kostka, Z., Gomboš, M. (2012): Determination of soil hydraulic conductivity in the mountain catchment by soil texture and field measurements. Acta Hydrologica Slovaca, Vol. 13, č. 2, 2012, 350–357

Dulovičová, R. (2014): Aggradation changes at Komárňanský channel during period 1993–2013, Acta Hydrologica Slovaca, Vol. 15, Temat. No., 2014, 103–111, (in Slovak)

Dulovičová, R., Velísková, Y., Schűgerl, R. (2016): Hydraulic conductivity of silts in Chotárny channel at Žitný ostrov, Acta Hydrologica Slovaca, Vol. 17, No. 2, 149–156, ISSN 1335-6291, (in Slovak)

Dulovičová, R., Velísková, Y., Schűgerl, R. (2018): Hydraulic conductivity of bed silts in Komárňanský channel – Žitný ostrov, Acta Hydrol. Slovaca, Vol. 19, No. 1, p. 117–125, ISSN 1335-6291, (in Slovak)

Kosorin, K. (1997): Spatial groundwater dynamics of the Rye Island aquifer, J.Hydrol.Hydromech., 45, 348–364

Kováčová, V. (2017): Trends of nitrate ions content in Žitný Ostrov channel network, Acta Hydrologica Slovaca, Vol. 18, No. 1, 57–67, (in Slovak)

Kutílek, M. (1978): Vodohospodářská pedologie, Alfa Bratislava, 296 s, SNTL 04-721-78, (in Czech)

Mucha, I., Banský, Ľ., Hlavatý, Z., Rodák, D. (2006): Impact of riverbed clogging colmatation on ground water, Riverbank Filtration Hydrology: Impacts on System Capacity and Water Quality, 43–72. NATO Science Series: IV. Earth and Environmental Sciences – Vol. 60. Springer, Printed in the Netherlands

Mišigová I. (1988): Methods of regional assessment of hydraulic properties of the rocks on the Žitný Ostrov, Report IHH SAS, (in Slovak)

Rožnovský, J., Litschmann, T. Středová, H., Středa, T. (eds). (2013): Zborník abstraktú z medzinár. konference Voda, půda a rostliny, Křtiny, 29.–30.5. 2013, ISBN 978-80-87577-17-2 http://www.cbks.cz/sbornikKrtiny13/surda.pdf

Špaček, J. (1987): Determination of filtration coefficient from total grain-size curves, J. Meliorace, 23, No.1, 1–13, (in Czech)

Šurda, P., Štekauerová, V., Nagy, V. (2013 a): Variability of the saturated hydraulic conductivity of the individual soil types in the area of the Hron catchment, Nővénytermelés, Vol. 62, supplement, 323-326, ISSN 0546-8191

Štekauerová, V., Nagy, V., Šútor, J., Milics, G., Neményi, M. (2009): Influence of groundwater level on soil water regime of Žitný ostrov. In V. Növénytermesztési Tudományos Nap – Növénytermesztés: Gazdálkodás – Klíma-változás – Társadalom, Akadémiai Kiadó, Budapest, 197–200.

Ing. Renáta Dulovičová (*corresponding author, e-mail: dulovicova@uh.savba.sk)
Mgr. Radoslav Schügerl, PhD.
Ing. Yvetta Velísková, PhD.
Institute of Hydrology, SAS
Dúbravská cesta 9
841 04 Bratislava
Slovak Republic

DOI: 10.31577/ahs-2020-0021.01.0013

ACTA HYDROLOGICA SLOVACA

Volume 21, No. 1, 2020, 106 – 112

THE MEASUREMENTS OF SATURATED HYDRAULIC CONDUCTIVITY OF THE FOREST FLOOR UNDER DECIDUOUS FOREST

Anton Zvala*, Tomáš Orfánus, Anežka Čelková

The aim of the paper is to present and evaluate the measured values of saturated hydraulic conductivity of organic soil horizons under deciduous forest at the examined locality Zelezna studienka. For determination of saturated hydraulic conductivity the single ring method, the falling head method and Guelph infiltrometer were used. The organic matters of forest floor come from dead plant material at various degrees of decomposition and aggregation and significantly influence the initiation processes of infiltration and outflow. The organic soil horizons of forest floor have extremely high porosity, very low bulk density, peculiar texture and structure, are changed according to the degree of mechanical and biochemical decomposition. The average values of saturated hydraulic conductivity were measured in the range from 153.39 cm h^{-1} for the falling head method up to 392.1 cm h^{-1} for the single ring method.

KEY WORDS: infiltration measurements, saturated hydraulic conductivity, forest floor, organic soil horizons

Introduction

The saturated hydraulic conductivity (K_s) is a quantitative characteristic of the ability to transfer water in a water saturated soil or other porous medium. It is a constant for a certain soil, but its value is different for different soils. This value depends mainly on the structure and texture of the soil. Hydraulic conductivity measurements are significantly influenced by the heterogeneity of the soil composition. The rate of water flow through the soil is strongly influenced by the presence of preferred soil paths through which the water flows faster as through the soil matrix. The value of saturated hydraulic conductivity is most influenced by the presence of preferred soil paths. The K_s value measured in soil that does not contain preferred soil paths directly characterizes the hydraulic conductivity of the matrix. Under natural conditions, the occurrence of preferred soil paths is frequent and natural, and therefore in many cases the measured K_s value characterizes the conductivity of the preferred soil paths rather than the conductivity of the matrix (Stekauerova et al., 2010). Most natural soils are neither homogeneous nor isotropic nor equally conductive in all directions. The soils are spatially variable natural units, which is caused by their genesis. Each soil type is characterized by a characteristic soil profile, thickness and development of its individual horizons. Among the other factors influencing the values of hydraulic conductivity in the forest floor are two very important characteristics: the vegetation cover and the pedogenic substrates resp. the maternal rocks from which the soil cover was evolved (Orfanus et al., 2018). Significantly, saturated hydraulic conductivity is higher in the organic horizon of forest floor, indicating that soil water fluxes are enhanced by natural vegetation cover (Pavao et al., 2019; Feng et al., 2019; Gonzales-Sosa et al., 2010).

The differences in the mother substrate, but also in vegetation on the surface of the soil, influence the existence of spatial variability of the soil, even at habitats relatively remote from each other. For this reason, the hydrophysical characteristics are also variable from one sampling point to another one (Hendrayanto et al., 2000). The spatial variability of hydraulic conductivity is manifested in both horizontal and vertical directions. The higher values of hydraulic conductivity in the vertical direction than in the horizontal direction is reflected in the structural soils, horizontal conductivity is observed in layers and oppressed soils (e.g. forest roads) (Surda et al., 2013). In addition to the mentioned spatial and temporal variability, in the case of hydraulic conductivity, there is a very high variability of values due to the methods used for its measurement and calculation, as stated Fodor et al., 2011, who found out on the scale of research areas (10 m^2) methodological variability of hydraulic conductivity which was equals or exceeds spatial variability. This implies a difficult interpretability and comparability of the determined hydraulic conductivities between different studies as well as in relation to the ongoing process of infiltration and redistribution of rainwater in the soil profile.

Forest soil is a complex dynamic natural formation, constantly evolving and changing. Developed and thus optimally structured forest soils have a high organic content and a developed network of soil macropores as a result of decomposition of dead plant and animal residues and activity of soil fauna. The presence of forest litter can alter the quantities of water available for soil infiltration and runoff (Guevara-Escobar et al., 2007). Undisturbed forest soils have high infiltration capacity, reduce surface runoff, risk of erosion and retain moisture needed for vegetation (Alaoui et al., 2011).

The aim of the paper is to present the results of measurements of saturated hydraulic conductivity by various field methods in the forest floor of deciduous forest. Interpretation of these results should contribute to the explanation of the impact of organic horizon of forest floor on partial hydrological processes in forested river basins. As despite their frequent occurrence there are very few hydrological studies considering hydrophysical properties of forest floor predominantly created by plant litter, naturally stratified by varying degrees of mechanical and biochemical degradation.

Material and methods

The research site of the forest floor was Zelezna studienka in Bratislava with a species-mixed deciduous forest. The research locality is part of the Bratislava Forest Park at the end of Mlynska dolina in the Male Karpaty Mountains. The coordinates of the research site are 48° 11' 21" northern latitude and 17° 04' 55" eastern longitude. The altitude is 228 m above sea level. The average annual temperature of the area is 8–9°C and the average rainfall is in the range of 600–700 mm (Lapin et al., 2002). The measurements of saturated hydraulic conductivity were carried out in the year 2017.

On this research site, we found places on a slope with a sufficiently deep forest floor below the broadleaf (beech, maple, hazel). The measuring research points were placed along the way, from the recreational area to the rising spring Zelezna studienka, near to pond II. The soil cover of the immediate surroundings of these sites is made up of Dystric Cambisols, Cambi-Dystric Leptosols and Fluvisols near the Vydrica Stream (WRB, 2014). The Loess clays and sand walls occur locally as part of the slope system. The measurement sites were chosen to capture the variability of the organic horizons of forest floor in terms of their structural composition. Three measuring points (1, 2 and 3) were located near the rising spring and pond II. (a system of artificial ponds on the Vydrica Stream). This place is covered with deciduous forest dominated by beech, maple and hazel. The soil at these sites is Dystric Cambisols, acidic, loamy sand to sandy. Other measuring points (4, 5 and 6) were near the recreational facility Zelezna studienka (Fig. 1). These measuring points are characterized by a very deep forest floor with a very mixed in terms of species of plant litter. Due to gravity, the plant litter accumulates here faster than decomposition. Below this forest floor there is a thick layer organomineral A horizon of an acidic to very acidic soil reaction (pH=5.07, determined in H_2O) reaching up to a depth of 100 cm or more below which is the weathered parent rock (granite, pegmatite). This soil we classified as Dystric Cambisols.

The saturated hydraulic conductivity of forest floor at the points described above was determined by three methods: by a single ring infiltration method, a falling head method and a Guelph infiltrometer.

At a single ring infiltration method the metal ring of the 30 cm diameter and 25 cm height was inserted into the soil down to the required depth (to the boundary between the forest floor and the A-horizon but not less than 7 cm). Perforated circular plate was inserted inside the ring, which prevented the forest floor material to be washed out during the water application onto the forest floor surface (Batkova et al., 2013). The water table (ponding) was set to 5 cm. The time intervals, at which the water level decreased by 2 cm (from water level of 5 to 3 cm), were recorded repeatedly until a steady flow

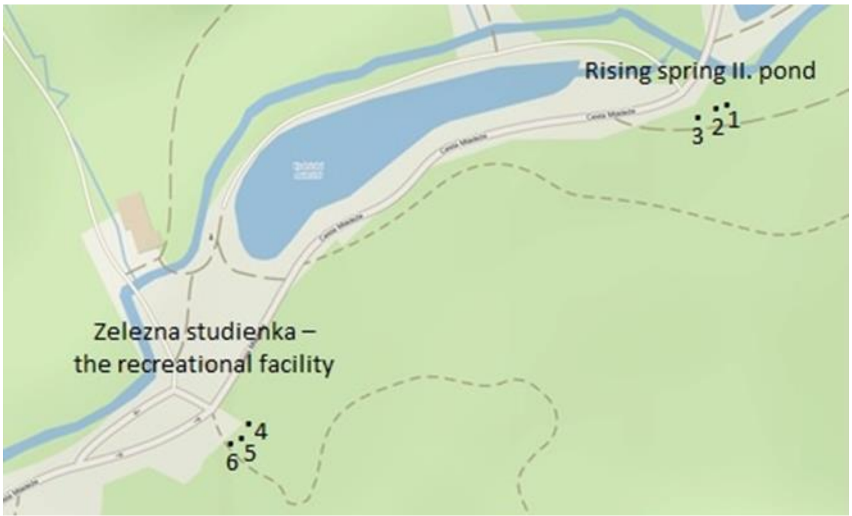

Fig. 1. Map of research site Zelezna studienka in Bratislava, Slovakia with marked measurement points.

was achieved. From the measured values of infiltrated water volume V and cumulative time t, the flow of water into the soil was calculated under conditions of steady state flow Q, which occurs after a longer period of infiltration. After insertion the value of depth of the ring in the soil d (L) and the radius of ring as to the following equation (1), the shape factor G was calculated:

$$G = 0.316\frac{d}{a} + 0.184 \tag{1}$$

where
G – the shape factor [L^3 T^{-1}],
d – the depth of the ring in the soil [L],
a – the radius of ring [L].

The saturated hydraulic conductivity K_s (Elrick and Reynolds, 1989), was calculated by insertion of Q, G, the height of water level in the ring H and α – the texture and structure dependent parameter, α=0.36 (the coarse and gravely sands; it may also include some highly structured soils with large and/or numerous cracks, macropores, etc.) into the equation:

$$K_s = \frac{QG}{aH + a^2 G\pi + \frac{a}{\alpha}} \tag{2}$$

where
K_s – the saturated hydraulic conductivity [L^3 T^{-1}],
Q – the steady state flow [L^3 T^{-1}],
G – the shape factor [L^3 T^{-1}],
a – the radius of ring [L],
H – the height of water level in the ring [L],
α – the texture and structure dependent parameter [-].

The falling head method was used to measure the saturated hydraulic conductivity K_s in a laboratory on 100 cm^3 soil samples taken in Kopecky cylinders. The different degrees of decomposed organic material litter Duff-1 and Duff-2 into the Kopecky cylinder were taken. The litter contains the proportion of unchanged, resp. a little altered dead uncrushed organic residues. Duff-1 is composed from decay organic residues of recognizable origin; the content of amorphous matter is below 50%. Duff-2 is composed from a biochemically degraded organic residues; the content of amorphous organic matter is over 50% (Saly et al., 2014). The soil samples were taken into Kopecky cylinder, whose inner side was coated with vaseline to prevent the wall effect on infiltration measurements. The saturation of all samples was performed by gradually raising of water level in the vessel. The measurement of K_s was realized on a device consisting of a Kopecky cylinder with a sample of soil on which we tightly attached the extension tube in form of Kopecky cylinder. Kopecky cylinder was inserted in the Petri dish with water. The extension tube was filled with water and the decrease of water level in the extension tube was repeatedly measured from the water level at the beginning of the measurement h_2 to the water level at the end of the measurement h_1. To calculate K_s by applying this method the following equation was used:

$$K_s = \frac{l}{t} ln\frac{h_2}{h_1} \tag{3}$$

where
l – the height of the sample in the Kopecky cylinder [L],
t – the time of the water level decrease from level h_2 to h_1 [T],
h_2 – the water level at the beginning of the measurement [L],
h_1 – the water level at the end of the measurement [L].

The saturated hydraulic conductivity of the upper soil layer, which consisted mostly of the organic horizon of forest floor and partially encroached into the organic-mineral A-horizon at the selected places, was measured by a Guelph infiltrometer. This is an experimental field method applying the principle of Marriott vessel which was inserted into the borehole with adjustable level of pond (Matula et al., 1989). The measured values of K_s express the integrally vertical and horizontal hydraulic conductivity of saturated soil (Stekauerová et al., 2010). The measurements were realized in 6 cm and 11cm deep of boreholes for each of the six measurement sites at the research locality. The depth of ponding was set to 5 cm and 10 cm. To calculate the steady water discharge (Q) and consequently the K_s, the equations 4–10 were used (Elrick and Reynolds, 1992). The parameter α was determined according to soil structure and then inserted into the equations together with the values of water head height H_1=5 cm and H_2=10 cm and then the shape factors C_1 and C_2 were calculated as follows:

$$C_1 = \left(\frac{\frac{H_1}{\alpha}}{2.074 + 0.093\left(\frac{H_1}{\alpha}\right)} \right)^{0.754} \tag{4}$$

$$C_2 = \left(\frac{\frac{H_2}{\alpha}}{2.074 + 0.093\left(\frac{H_2}{\alpha}\right)} \right)^{0.754} \tag{5}$$

where
C_1, C_2 – the shape factor [L^3 T^{-1}],
H_1, H_2 – the water head height [L],
α – the radius of borehole into soil [L].

After inserting C_1 and C_2 into equations (3) and (4), we calculate G_1 and G_2.

$$G_1 = \frac{H_2 C_1}{\pi\left(2H_1 H_2 (H_2 - H_1) + \alpha^2 (H_1 C_2 - H_2 C_1)\right)} \tag{6}$$

$$G_2 = \frac{H_1 C_2}{\pi\left(2H_1 H_2 (H_2 - H_1) + \alpha^2 (H_1 C_2 - H_2 C_1)\right)} \tag{7}$$

where
G_1, G_2 – the two head, combined reservoir,
H_1, H_2 – the water head height [L],
π – the constant (Ludolf′ s number, 3.14),
α – the radius of borehole into soil [L].

The measurement data of steady flow rate R_1 and R_2 obtained from the Guelph infiltrometer were inserted into equations Q_1 and Q_2:

$$Q_1 = R_1\, 35.22 \tag{8}$$

$$Q_2 = R_2\, 35.22 \tag{9}$$

where
Q_1 – the steady state infiltration flow rate [$L^3\, T^{-1}$] for setting water head height H_1,
Q_2 – the steady state infiltration flow rate [$L^3\, T^{-1}$] for setting water head height H_2,
R_1, R_2 – the steady flow rate from the Guelph infiltrometer [$L\, T^{-1}$].

The saturated hydraulic conductivity K_s was calculating by using Q_1, Q_2 and G_1, G_2 (10):

$$K_s = G_2\, Q_2 - G_1\, Q_1 \tag{10}$$

where
K_s – the saturated hydraulic conductivity [$L\, T^{-1}$].

Results and discussion

The saturated hydraulic conductivity measurements in the deciduous forest were performed at Zelezna studienka (Bratislava) in the Male Karpaty Mountain landscape. The measurements were carried out in the year 2017. The results of the measurements of K_s values of the forest floor under the deciduous vegetation at the research sites by a single ring infiltration method, a falling head method and by a Guelph infiltrometer, are presented in Table 1.

The graphical expression of K_s values which were found at all six measurement points by a single ring infiltration method, a falling head method and by a Guelph infiltrometer, are presented in Fig. 2.

The results of the measurements of the saturated hydraulic conductivity of the forest floor under the deciduous vegetation at the research site by various methods can be evaluated as follows:

At first glance, the forest floor in the deciduous forest differs from the coniferous forest. We can see higher variability of litter and much released structure of organic material, from which we can suppose higher number of soil macropores and preferred soil paths. The aggregation of litter is very weak. Using a single ring method, the values of saturated hydraulic conductivity from K_s=53.91 cm h^{-1} to 1018.73 cm h^{-1} were observed. This indicates a higher variability of forest floor in deciduous forest. Using by this method, the average value of K_s of 392.1 cm h^{-1} was detected. The results of K_s measurements by using a single ring method for the organic horizon of the deciduous forest are given in Table 1.

The average value of K_s which was measured by the falling head method was K_s=153.39 cm h^{-1}. As in the coniferous also in the deciduous forest, it has been confirmed that the litter had the highest hydraulic conductivity, the lower values had Duff-1 and the lowest values of K_s we have measured for the Duf-2 (Zvala et al., 2017). For example, for the measurement point 1, the saturated hydraulic conductivity values for litter K_s=227.48 cm h^{-1} were found, for Duff-1 K_s=25.89 cm h^{-1}, and for Duff-2 K_s=6.49 cm h^{-1}. In the research of Duff-2, we determined significantly lower values of saturated hydraulic conductivity compared to litter. During the measurement it was seen that the leaf structure of the litter can fill the inner diameter of the Kopecky cylinder and thus prevent the infiltration. We consider the falling head method the least suitable for measuring the saturated hydraulic conductivity of forest floor in deciduous forest. Significant deceleration of the infiltration of the Duff-2 layer (due to decomposed organic matter and water repellency of substances contained in the organic horizon), can cause shallow subsurface runoff that has natural character and normally does not have harmful effects. This component of the runoff causes a significant transport (wash) of the organic horizon of forest floor during heavy floods, which can be observed in the forest after extreme rainfall events In conjunction with slope failures (such as forest roads) probably also it contributes to the overall acceleration runoff process during floods.

The average value of K_s observed in six measuring points by using the Guelph infiltrometer, was K_s=217.8 cm h^{-1}. The variability of the texture and structure of the forest floor environment influence the measurement results. It can be stated that, when we measured the value of K_s=20.4 cm h^{-1}, in one case of measurement by the Guelph infiltrometer, the litter created a continuous compressed layer of leaves, which inhibit water infiltration to the forest soil. This phenomenon can even cause surface runoff in nature, as reported in the paper (Capuliak et al., 2008). The thickness of the litter layer is very different and it is exposed to natural conditions of wind, rain and accumulation at various places. Large differences in the measured results of K_s from K_s=20.4 cm h^{-1} to 449.4 cm h^{-1} are due to the uneven thickness of the forest floor, the different composition and degree of decomposition of litter in deciduous forest. The organo-mineral A-horizon also has water repellency in seconds to tens of seconds, and the material is not quite rigid either.

The measured average values of saturated hydraulic conductivity of the organic forest floor horizon for various measurement methods are significantly higher compared to values of saturated hydraulic conductivity of mineral soils (sandy, loam, clay). For illustration, the values of saturated hydraulic conductivity for mineral soils with different textures are presented in Table 2.

The measurement of unsaturated hydraulic conductivity using the disk infiltrometer method used in the coniferous forest (Zvala et al., 2017) is suitable for imitating the natural weather conditions under rain, with a relatively saturated soil profile but without forming a surface deposit. However, the method is quite unsuitable for measurements in deciduous litter, since, due to the structure of the deciduous litter, it is technically impossible to ensure surface contact of the infiltration disk with this material.

Table 1. The results of measurements of saturated hydraulic conductivity Ks by various methods at six measuring points at the research site (Fig. 1)

Measuring point	Single ring method	Falling head method		Guelph infiltrometer
	K_s [cm h^{-1}]	K_s [cm h^{-1}]		K_s [cm h^{-1}]
1	53.91	L	227.48	211.81
		D1	25.89	
		D2	6.49	
2	1018.73	L	176.16	180.47
		D1	30	
		D2	7.06	
3	447.19	L	463.86	20.40
		D1	53.22	
		D2	18.95	
4	348.73	L	675.66	267.61
		D1	123.07	
		D2	104.11	
5	179.21	L	178.54	177.63
		D1	66.52	
		D2	8.03	
6*	304.76	L	60.77	449.45
The average value of K_s [cm h^{-1}]	392.1	139.12		217.91

L – Litter, D1 – Duff-1, D2 – Duff-2

**The layers D1 and D2 at measurement point 6 were not developed at the organic horizon. There was already mineral soil under the L–layer.*

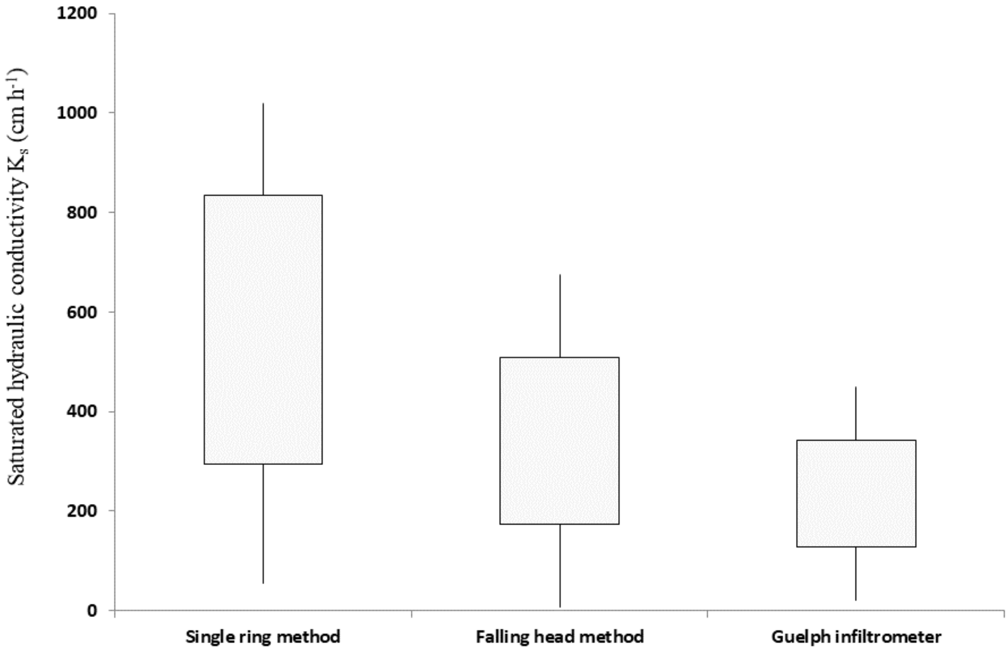

Fig. 2. Graphical display of saturated hydraulic conductivity Ks values measured by different methods (Zelezna studienka, 2017).

Table 2. **The characteristic values of saturated hydraulic conductivity *Ks* for mineral soils with different grain composition (Novák and Hlaváčiková, 2016)**

Soil texture	K_s [cm h^{-1}]
Sandy soil	4.16 – 20.83
Sandy – loam soil	1.25 – 4.16
Loam soil	0.42 – 2.08
Clay – loam soil	0.21 – 1.25
Clay soil	0.01 – 0.42

Conclusion

The observed values of saturated hydraulic conductivity of the forest floor determine important facts in terms of studying hydrological processes in forested river basins.

The measuring by using the falling head method is influenced by the large area of the leaf structure, which can slow down the saturated hydraulic conductivity measured in the Kopecky cylinder. The representativeness of the saturated hydraulic conductivity value of the 100 cm^3 soil sample in the Kopecky cylinder and the generalization to the entire organic horizon of forest soil is questionable. For the organic horizons we recommend to use rather a method that uses undisturbed samples of larger volume. From different measured values of hydraulic conductivity by variable hydraulic slope for different layers of organic horizon in deciduous forest, it can be stated that hydraulic conductivity is not the same throughout the organic horizon but decreases from top to bottom so how the degree of decomposition and aggregation of organic material (litter, Duff-1, Duff- 2) increases.

The measurements of K_s using the single ring method and the Guelph infiltrometer, show the high variability of the measured values of the saturated hydraulic conductivity of the forest floor of the deciduous forest. These differences in the measured values of saturated hydraulic conductivity can be justified by the interaction of several factors with different influences in the individual measurement methods such as specific texture and structure of the organic horizon, high porosity, continuous compressed the leaf structure, different soil moisture, different hydrophobicity of organic horizon and organo-mineral A-horizon, different installation depths for the Guelph infiltrometer method and the single ring method.

In addition, it can be stated that in the organic horizons in the research site, a substantial part of the water flows through the macropores and the preferred paths than through the soil matrix, which theoretically can help replenish the ground water reservoirs.

Forest floor of deciduous forest is of great importance for rainwater distribution between infiltration, evaporation (including interception), water retention and runoff processes. Combination of saturated hydraulic conductivity determination by several methods enables to identify possibilities of implementation of initiation processes on the surface of forest soil during transformation of precipitation into infiltration and runoff.

Acknowledgement

This publication is the result of the project implementation ITMS 26210120009 Infrastructure completion of hydrological research stations, supported by the Research & Development Operational Programme funded by the ERDF. Authors would like to express thanks to the Grant VEGA for the financial support from project VEGA 2/0096/19.

References

Alaoui, A., Caduff, U., Gerke, H. H., Weingartner, R. (2011): Preferential Flow Effects on Infiltration and Runoff in Grassland and Forest Soils. Vadose Zone Journal, Vol. 10, Issue 1, 367–377, DOI: 10.2136/vzj2010.0076.

Batkova, K., Matula, S., Mihalikova, M. (2013): Multimedial Study Guide of Field Hydropedological Measurements. 2nd revised edition [on-line]. English version. Czech University of Life Sciences Prague. Prague, Czech Republic. No pagination. Available at: http://hydropedologie.agrobiologie.cz. ISBN: 978-80-213-2434-3.

Capuliak, J., Homolák, M., Ascherbrenner, Š., Ahmed, Y. A. R., Královič, R. (2008): Influence of litter on initial water transport in soil under forest stand. In: Hydrology of small catchment 2008. Institute of Hydrodynamics, AVČR, 57–64.

Elrick, D. E., Reynolds, W. D. (1989): Water Flux Components and their measurements. Proc. App. Soil Physics in Stress Enviroments. Jan 22–26 NARC. Islamabad, Pakistan. p. 183.

Elrick, D. E., Reynolds, W. D. (1992): Methods for analysing constant head well permeameter data. Soil Science Society of America Journal, 56, 309–312.

Feng, G., Adeli, A., Read, J., McCarty, J., Jenkins, J. (2019): Consequences of pelletized poultry litter applications on soil physical and hydraulic properties in reduced tillage, continuous cotton system. Soil&Tillage research, Vol. 194, Article Number: 104309, 974–983 DOI: 10.1016/j.still.2019.104309.

Fodor, N., Sándor, R., Orfánus, T., Lichner, L., Rajkai, K. (2011): Evaluation method dependency of measured saturated hydraulic conductivity. Geoderma, 2011, Vol. 165, No. 1, 60–68.

Gonzales-Sosa, E., Braud, I., Dehotin, J., Lassabatère, L., Angulo-Jaramillo, R., Lagouy, M., Branger, F., Jacqueminet, C., Kermadi, S., Michel, K. (2010): Impact of land use on the hydraulic properties of the topsoil in a small French catchment. Hydrological Processes, Vol 24, Issue 17, 2382–2399, DOI: 10.1002/hyp.7640.

Guevara-Escobar, A., Gonzalez-Sosa, E., Ramos-Salinas, M., Hernandez-Delgado, G. D. (2007): Experimental analysis of drainage and water storage of litter layers. Hydrology and earth system sciences. Vol. 11, Issue 5, 1703–1716,

DOI: 10.5194/hess-11-1703-2007.
Hendrayanto, D., Kosugi, K., Mizuyama, T. (2000): Scaling hydraulic properties of forest soils. Hydrological Processes. Vol. 14, Issue 3, 521–538, DOI: 10.1002/(SICI)1099-1085(20000228)14:3<521:AID-HYP952> 3.0.CO;2-C.
Matula, S., Semotan, J., Vesela, J. (1989): Hydropedology – practice. Czech Technical University in Prague, Faculty of Civil Engineering, ČVUT, Publishing Center, ISBN 80-01-00031-1, p. 147. (In Czech)
Novák, V., Hlaváčiková, H., (2016): Soil hydrology. Institute of Hydrology SAS. VEDA, publischers Slovak Academy of Sciencies, 2016, ISBN 978-80-224-1529-3, p. 350.
Orfánus, T., Zvala, A., Nagy, V., (2018): Water infiltration into forest soil - what do the measurements signal? Current problems of the soil aeration zone under conditions of ongoing climate change. Science, Bratislava 2018, 54–79. ISBN 978-80-224-1690-0
Pavao, L. L., Sanchez, L., Pinto, O. O., Spolador, J. (2019): The influence of litter on soil hydrophysical characteristics in an area of Acuri palm in the Brazilian Pantanal. Ecohydrology&Hydrobiology, Vol. 19, Issue 4, 642–650, DOI: 10.1016/j.ecohyd.2019.04.004.
Saly, R., Bedrna, Z., Bublinec, E., Curlik, J., Fulajtar, E., Gregor, J., Hanes, J., Jurani, B., Kukla, J., Račko, J., Sobocka, J., Surina, B. (2014): Morphogenetic soil classification system of Slovakia. Basal reference taxonomy. Research Institute of Soil Science and Soil Protection. Bratislava, ISBN 978-80-8163-005-7, p. 96
Stekauerova, V., Sutor, J., Nagy, V., Brezianska, K. (2010): Measurement of saturated hydraulic conductivity by Guelph permeameter. Acta Hydrologica Slovaca 2010, vol. 11, no. 2, 349–352.
Surda, P., Stekauerova, V., Nagy, V. (2013): Statistical analysis of soil hydraulic conductivity in the Hron river basin. In: Rožnovský, J., Litschmann, T., Středová, H., Středa, T. (eds): Water, soil and plants, Křtiny. ISBN 978-80-87577-17-2. 1–17
WRB, 2014. World Reference Base for Soil Resources (2014): World Soil Resources Reports No. 106. Rome, 192 p.
Zvala, A., Orfanus, T., Stojkovova, D., Nagy, V. (2017): Hydraulic conductivity of superimposed organic horizons. Acta Hydrologica Slovaca, vol. 18., no. 1, 112–119, ISSN 1335-6291.

Mgr. Anton Zvala PhD. (*corresponding author, e-mail: zvala@uh.savba.sk)
RNDr. Tomáš Orfánus PhD.
Ing. Anežka Čelková
Institute of Hydrology SAS
Dúbravská cesta 9
84104 Bratislava
Slovak Republic

DOI: 10.31577/ahs-2020-0021.01.0014

ACTA HYDROLOGICA
SLOVACA

Volume 21, No. 1, 2020, 113 – 122

ASSESSMENT OF THE IMPACT OF PROPOSED CUT-OFF WALLS ON GROUND-WATER LEVEL REGIME DURING EXTREME HYDROLOGICAL CONDITIONS

Dana Baroková*, Michaela Červeňanská, Andrej Šoltész

The capacity of rivers Váh, Small Danube and the deviation of river Nitra, located in Slovakia, is sufficient in terms of transferring flood flow rates, however defects occur during long-lasting flood situations. If the problem is ignored, different processes may eventually endanger the adjacent territory or may lead to contamination of water and soil as a result of flooding a nearby sewage treatment plant. For these reasons an additional sealing of dykes was proposed. The article deals with the impacts of suspended cut-off walls on groundwater flow and level regime in a wider area for both steady and unsteady scenarios.

KEY WORDS: cut-off wall, numerical simulation, groundwater, flood, TRIWACO

Introduction

During long-lasting flood situations in Slovakia (e. g. in years 2006 and 2010) there were defects repeatedly seen on the downstream slopes of the flood protective dykes along rivers Váh, Small Danube and the deviation of river Nitra (Fig. 1, Fig. 2). These defects are mainly followed by leakage and seepage of water and waterlogging accompanied by leaching of fine-grained particles from the subsoil of the protective dykes. Seepage through dyke bodies can significantly reduce the stability of the dykes. At the same time, there were signs of lifting of the cover layers with the risk of breaking. The geological composition of the area as well as the occurrence of these phenomena indicates that there should probably be some preferred routes through the dyke bodies and also in the subsoil. If the problem is ignored, different processes may eventually endanger the adjacent territory with residential houses, infrastructure and agricultural land. Other negative impact (Julínek et al. 2020) could be the contamination of water and soil as a result of flooding a nearby wastewater treatment plant (WTP) located in Zemné (Fig. 2). For these reasons an additional sealing of the dykes using suspended cut-off walls (CW) was proposed (Šoltész at al., 2017). Cut-off walls, built from the top of the dykes, will eliminate the risk of suffosion and minimize the risk of breakage of the cover layers caused by buoyancy. These protective measures extend the leakage path and thereby greatly reduce the hydraulic gradient and, accordingly, leaching quantities (Krempa, et al., 2016; Hnidiak et al., 2016; Chládek and Kováčiková, 2016).

Before the application of proposed measures, it is necessary to verify the functionality of such a solution using the method of mathematical modelling. That is why the numerical simulation of the groundwater flow and groundwater level regime at a relatively steady state (steady flow model) as well as during flood event (transient flow model created for the flood wave based on Q_{100}) was elaborated (Gramblíčková et al., 2017). It also includes the impacts of the suspended cut-off walls on the groundwater flow and level regime in a wider area. The numerical model of the area of interest was created using Triwaco-Flairs software (Velstra, et al., 2014) simulating the groundwater flow using finite element method.

Material and methods

Creation of a numerical model requires knowledge of the area of interest. Therefore, it was necessary to conduct a field survey before the modelling process itself. It is also needed for subjective decision making during the phase of modelling. During the data preparation phase, all available data, information or background materials on geomorphology, geology, hydrogeology, hydrology as well as anthropogenic activity were collected, processed and evaluated. These data served to determine the parameters of the filtration area such as the hydraulic conductivity, storage coefficient, porosity and thickness of aquifers, aquifer interface, effective precipitation, etc. Based on collected data, it was possible to determine boundary conditions needed for steady and also initial conditions for unsteady flow simulations.

Fig. 1. *The location of the area of interest (source: mapy.atlas.sk).*

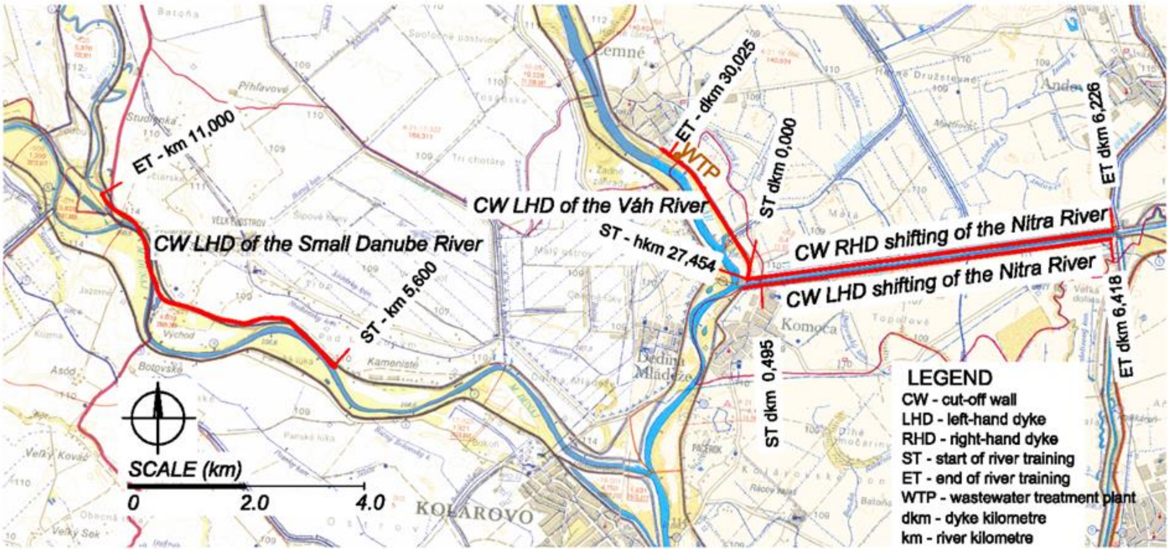

Fig. 2. *The situation of proposed cut-off walls (background: Water management map, 2003).*

Description of the area of interest

The area of the proposed activity is a plane with a slope of less than 1°. The average altitude in the wider area is around 107–115 m a. s. l. (Miklos, 2002).

The geological structure of the area has led to the formation of two hydrogeological units – a neogene and a quaternary. Neogene sediments (neogene clay) arepractically impermeable (Pristaš et al., 1992).

There are two genetic types of quaternary sediments – fluvial represented by gravel, sandy gravel or sand with a thickness about 10–30 m (rarely 70–80 m) and eolian represented by silt and fine sands with a thickness about 2–6 m. Fluvial sediments form the first aquifer with phreatic conditions that is in interaction with surface water. In some places, the groundwater level may be moderately stressed (Pristaš et al., 1992).

From a hydrogeological point of view, the area of interest

is influenced by the hydrogeological conditions of the Rye Island (the area between the rivers Danube, Small Danube and Váh) which is one of the most important areas, both in terms of quantity and quality of groundwater. The hydraulic conductivity of Quaternary sediments varies from $k_f=10^{-4}$ to 10^{-5} m.s^{-1} (Pristaš et al., 1992).
For the simulation of groundwater flow it was necessary to determine:

- the surface water level course in the rivers Váh, Small Danube and in the deviation of river Nitra (Fig. 3) using 4 gauging stations of the Slovak Hydrometeorological Institute (SHMI) [SHMI];
- the surface water level course in adjacent drainage channels (Fig. 4) using measurements at 3 pumping stations (PS) of the Slovak Water Management Enterprise, state enterprise (SWME, s. e.) (PS Komoča, PS Kolárovo and PS Kráľov Brod) [SWME]; all drainage channels can be seen in Fig. 7;
- the groundwater level regime (Fig. 5) [SHMI];
- and the total precipitation in the location (Fig. 5) [SHMI].

Data used for calibration of the model and also for the prediction were from hydrological years 2009–2013. The reason is the fact that years 2010 and 2013 were rich in rainfall and therefore extreme flood situations occurred. These extreme flood situations were also the reason for designing the cut-off walls.

Developing a conceptual model of the system

The purpose of building a conceptual model is to simplify the field problem and organize the associated field data so that the system can be analysed. Simplification is necessary because a complete reconstruction of the field system is not feasible (Anderson and Woessner, 2002). The first step in formulating the conceptual model is to define the area of interest, i.e. to identify boundaries of the model (Fig. 6).
Numerical models also require inner and outer boundary conditions. Correct selection of boundary conditions is a critical step in model design (Anderson and Woessner, 2002). Along the whole outer boundary the Dirichlet boundary condition was used using the measurements of the groundwater level in monitoring boreholes [SHMI]. To simulate water level course in rivers and drainage channels (Dušek and Velísková, 2017) within the interior of the grid, the internal boundary condition was inserted (Fig. 7). This step was based on data described above.

Calibration of the numerical model

The purpose of calibration is to establish that the model can reproduce field-measured heads and flows. During calibration, a set of values for aquifer parameters and stresses that approximates field-measured heads and flows, was found (Anderson and Woessner, 2002). Calibration was performed under steady-state conditions and

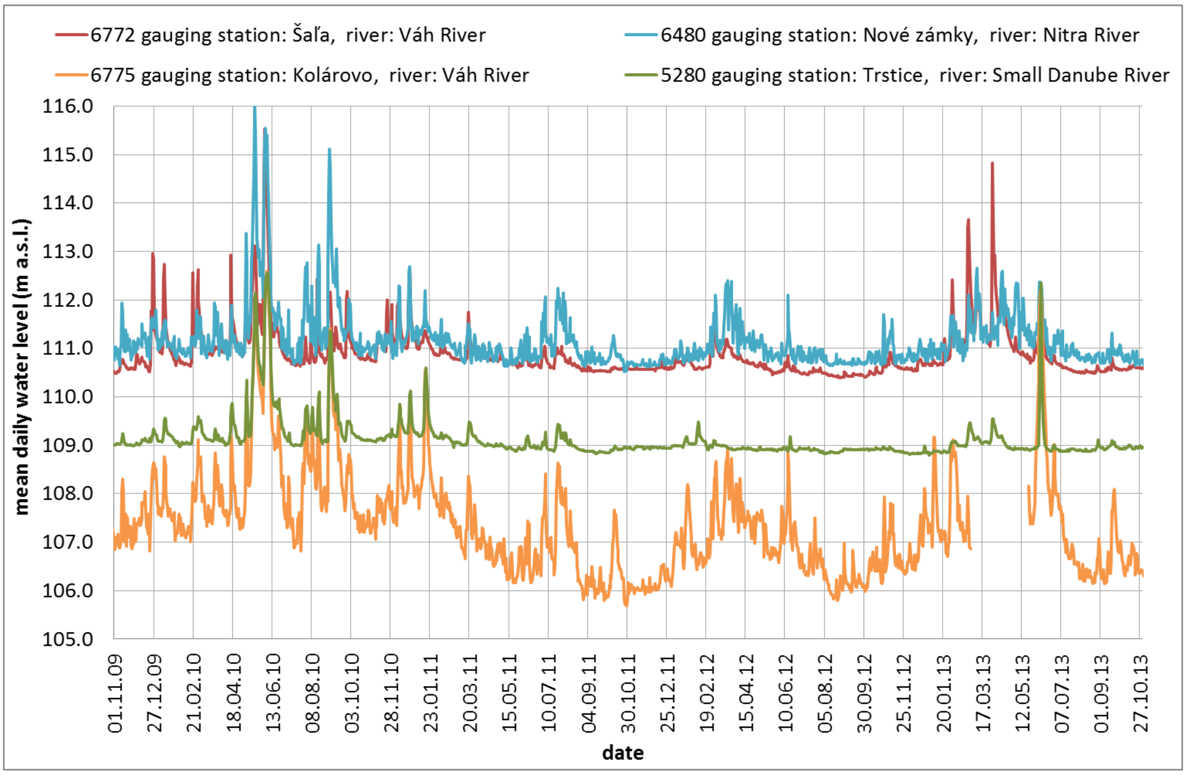

Fig. 3. Water level course in gauging stations Šaľa, Kolárovo, Nové Zámky and Trstice [SHMI].

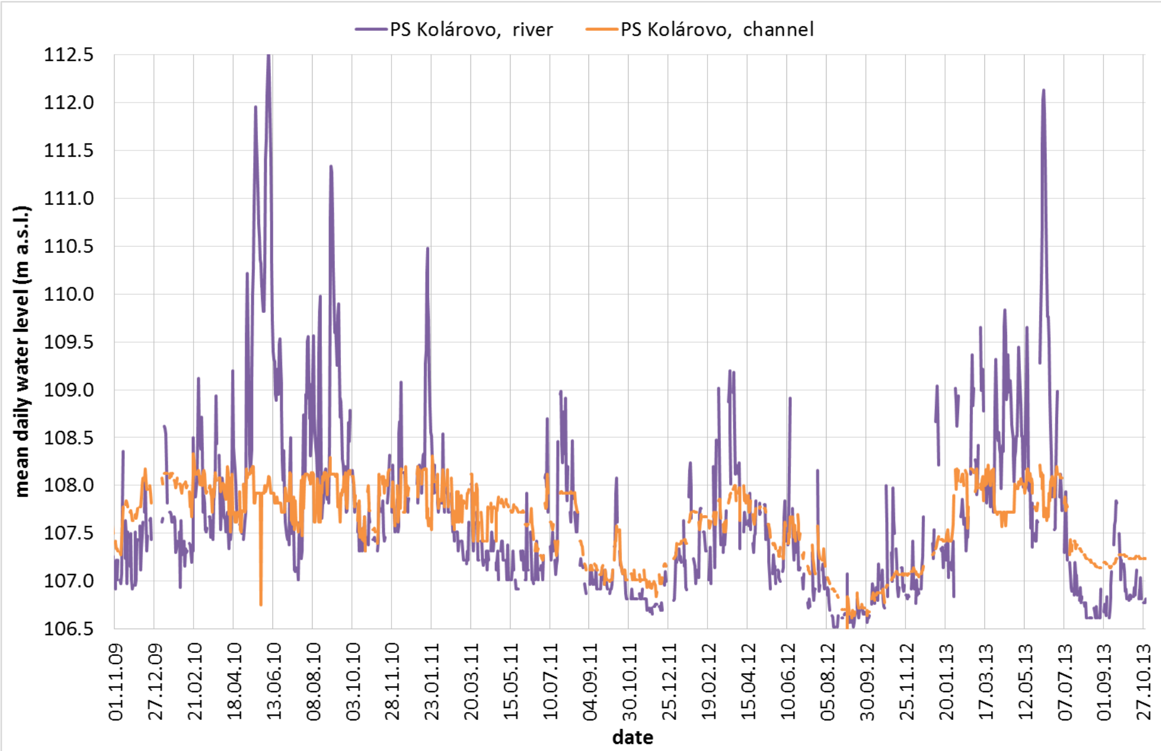

Fig. 4. Water level course at the pumping station Kolárovo – channel and river [SWME].

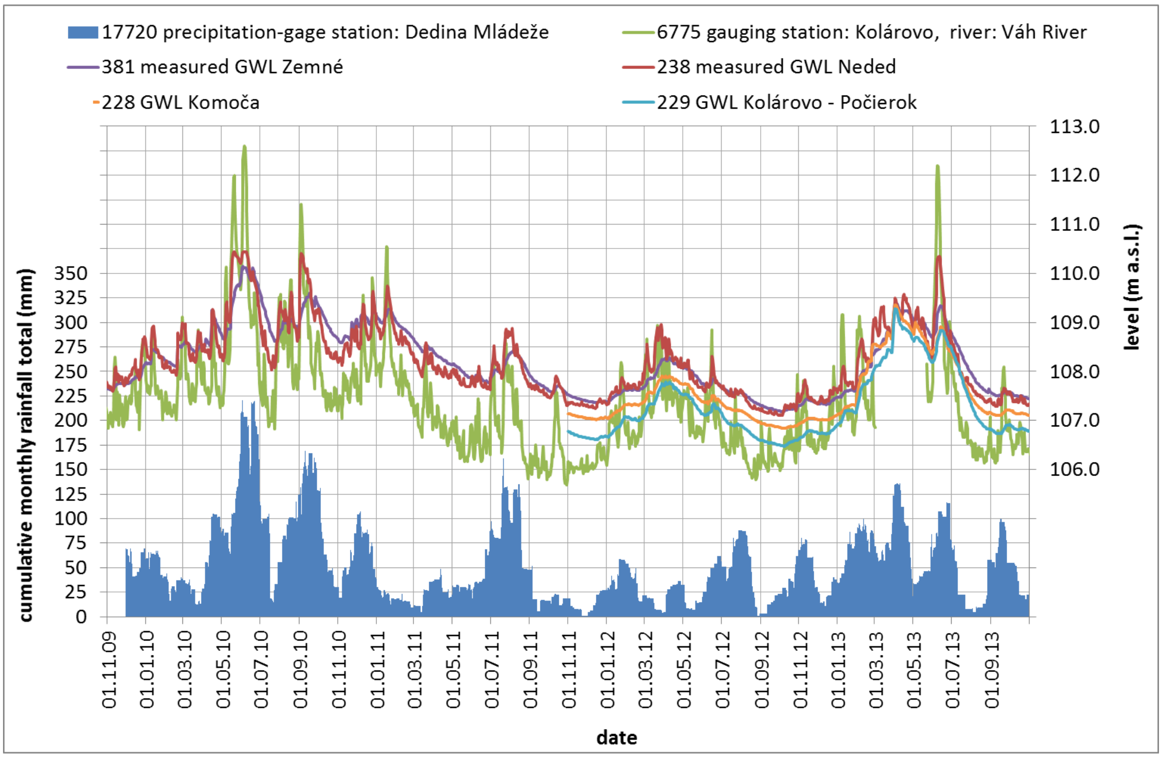

Fig. 5. Groundwater levels in selected measuring stations (381, 238, 228, 229), water level course in gauging station Kolárovo and cumulative monthly rainfall total in precipitation-gage station Dedina Mládeže [SHMI].

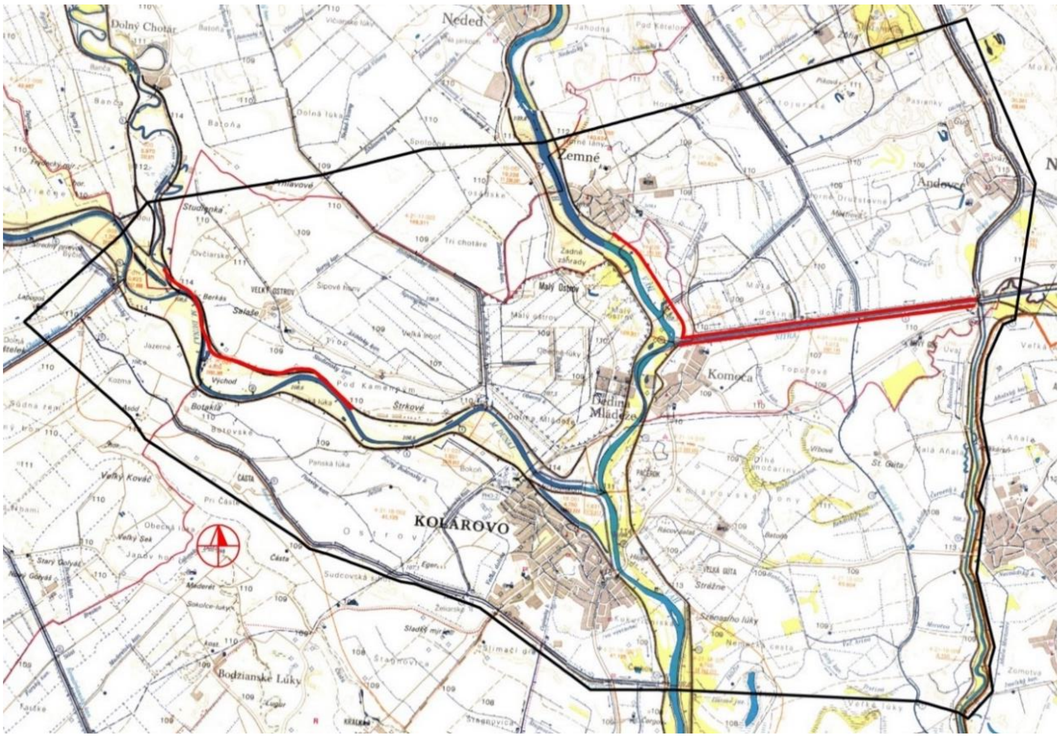

Fig. 6. The area of interest with the model boundary and proposed cut-off walls (legend: red – cut-off walls, blue – rivers and drainage channels, black – boundary of the model).

Fig. 7. Location of rivers and drainage channels. The inner boundary conditions – surface water elevation (m a. s. l.).

was done by trial-and-error adjustment of parameters such as hydraulic conductivity, storage coefficient, effective rainfalls and drainage and infiltration resistance (Dulovičová, 2013).

The calculated values of groundwater levels, respectively piezometric heads, were compared with existing field measurements in observation points (Fig. 8). Fig. 8 shows the differences between the simulated and measured piezometric heads in groundwater monitoring boreholes of SHMI. The value on the right is determined assuming zero effective rainfall, the value on the left assuming the average value of effective rainfall (Švasta and Malík, 2006).

The effective rainfall is the part of precipitation totals, which is able to infiltrate into the soil. There are no strict and clear rules ensuring good calibration, except this one: the difference between the calculated and measured values considering the total piezometric head in observation points should be small. Assuming the groundwater levels fluctuation in monito-ring boreholes between 2 to 3 m, the results are sufficient for the prognosis of the development of piezometric heads after realization of underground sealing walls.

The results of simulation of the current state after calibration of the model taking into account effective rainfall can be seen in Figure 9.

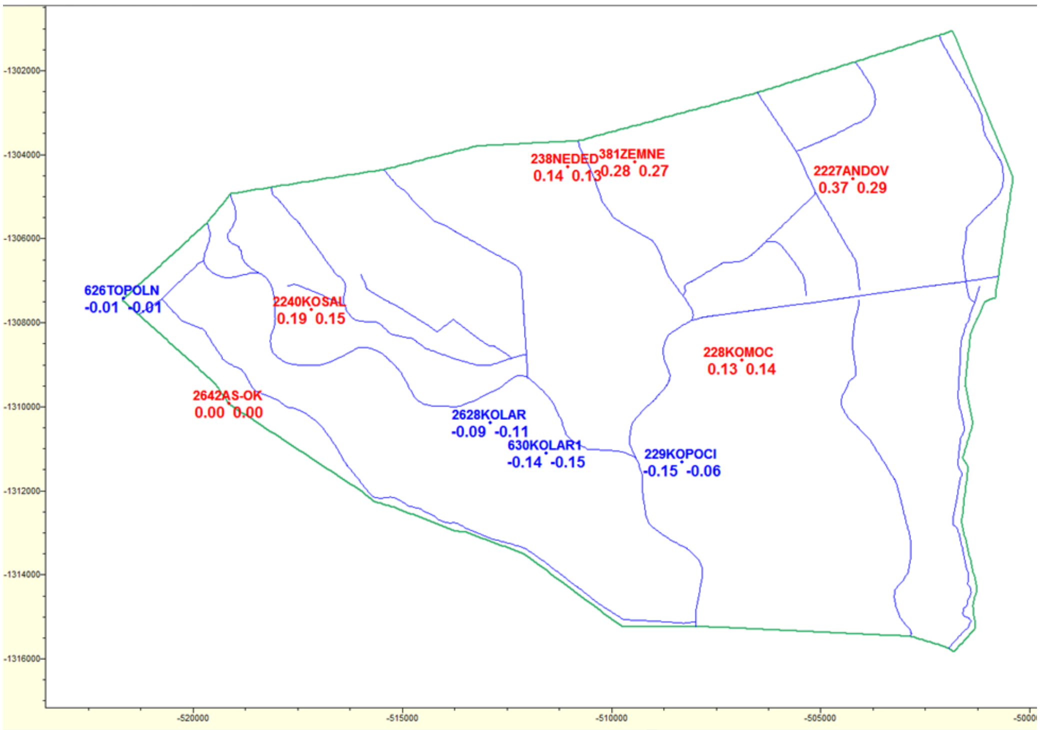

Fig. 8. The differences between calculated and measured values of piezometric heads in observation points assuming zero effective rainfall (on the right) and also the average value of effective rainfall (on the left).

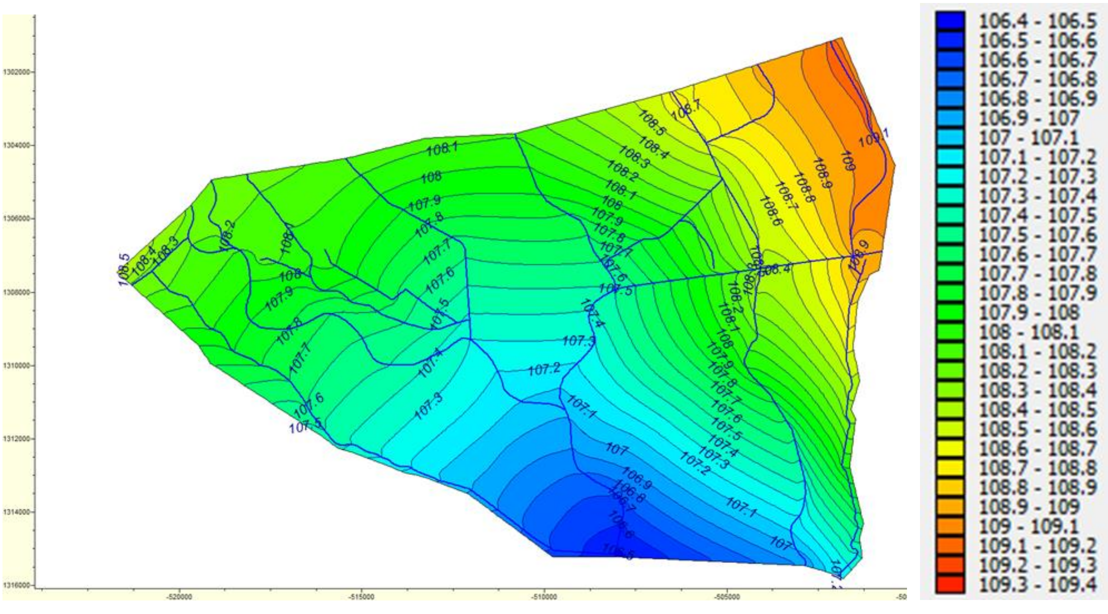

Fig. 9. The contour map of the calculated piezometric head taking into account effective rainfall.

Results and discussion

Prediction using steady-state model

The aim of modelling is a simulation of the future events. However, if the prognosis serves for answering questions about changes due to anthropogenic interventions, i.e. to determine the effect of cut-off walls (CW) on the piezometric heads after realization of a wall embedded to a depth of 15 m from the dam crest, it is necessary to proceed to a modification of the model. The modification consists in the input of CW by a parameter expressing the permeability of the aquifer, i.e. by changing the values of the hydraulic conductivity, but only in certain parts of the aquifer.
For this purpose, it was necessary to divide the aquifer into two parts as shown in Fig. 10. The individual aquifers are separated by a fictitious semi-permeable layer. In the upper aquifer, it is then possible to enter the CW as a region of a very low permeability, i.e. as the area with hydraulic conductivity around 10^{-9} to 10^{-11} m s^{-1}. The lower part of the aquifer has the same properties as before.

The steady-state prognosis, created using the long-time mean values of hydrological conditions, shows that the situation after realization of CWs will not change in the future. In Fig. 11, you can see the vertical cross section of the model with the influence of the cut-off walls on the groundwater flow.

Predictions using unsteady-state model

The steady-state model is also an initial condition for the transient model simulation. In order to determine the impact of CWs on groundwater level regime, the most extreme three months from hydrological point of view, were selected for simulation. The 122-day period was characterized by high water level conditions in all rivers as well as by high precipitation. Such a situation occurred in the period from 1st April 2010 to 31st July 2010. For simulation of an unsteady flow it was necessary to specify time-dependent water level in rivers (Velísková et al, 2015).
This parameter was entered through a relative value, i.e. through a daily change in water levels (Fig. 12). This is a change considering the mean value of water levels

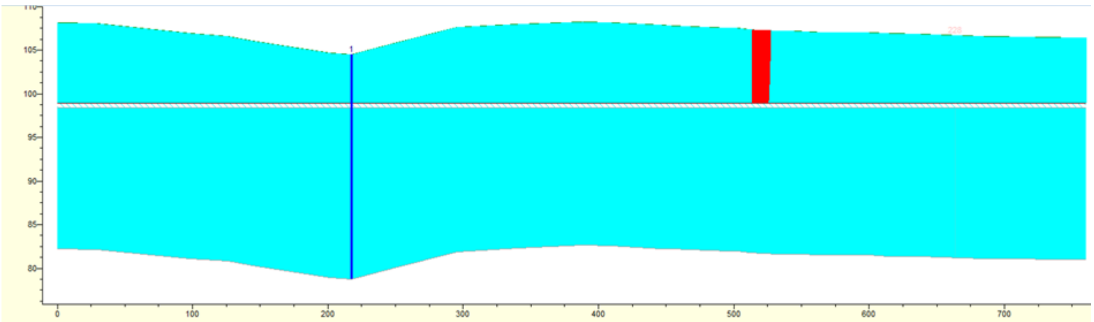

Fig. 10. Division of the aquifer using fictitious semi-permeable layer (white). Section at km 29.400 of the left-hand side of the river Váh – (red) CW is embedded to a depth of 98.8 m a. s. l.

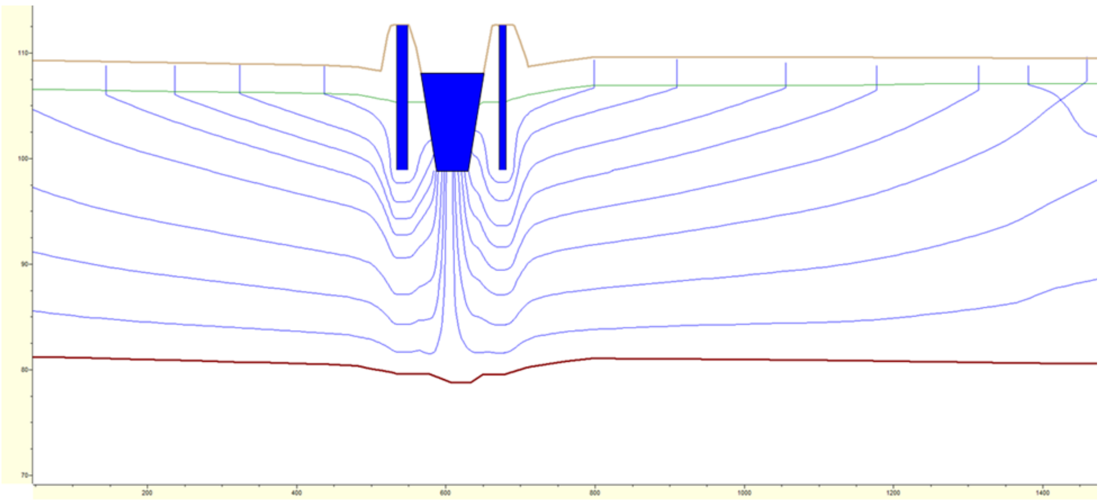

Fig. 11. Influence of the cut-off walls on the groundwater flow – vertical cross section.

(increase or decrease of water levels related to the mean value).

The results of the simulation of the unsteady flow is the difference in piezometric heads between the current state and the future scenario (assuming after realization of CWs) in specific days of the simulation:

- 20th May 2010 – 50th simulation day,
- 21st May 2010 – 51st simulation day,
- 4th Jun 2010 – 65th simulation day,
- 21st July 2010 – 112th simulation day.

Fig. 13 shows the calculated and also measured groundwater levels in two monitoring boreholes as well as total daily precipitation.

During extreme hydrological conditions the piezometric head in the wider area of interest may slightly change (in certain part it may drop by max. 0.6 m and rise by max. 0.4 m) (Fig. 14).

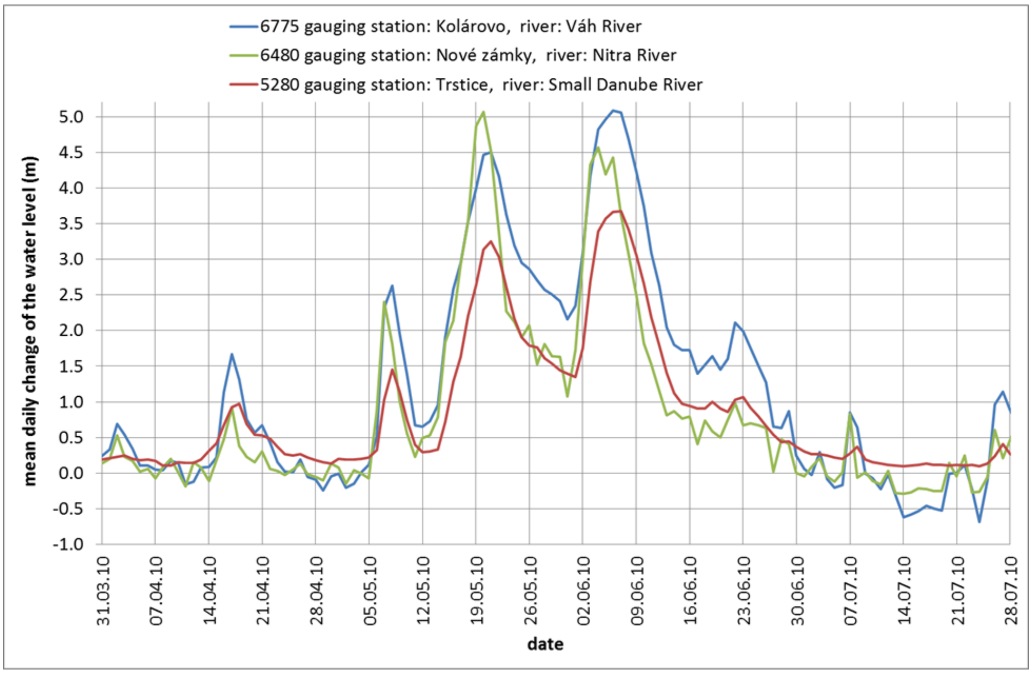

Fig. 12. The daily change of water levels in rivers Váh, Small Danube and Nitra.

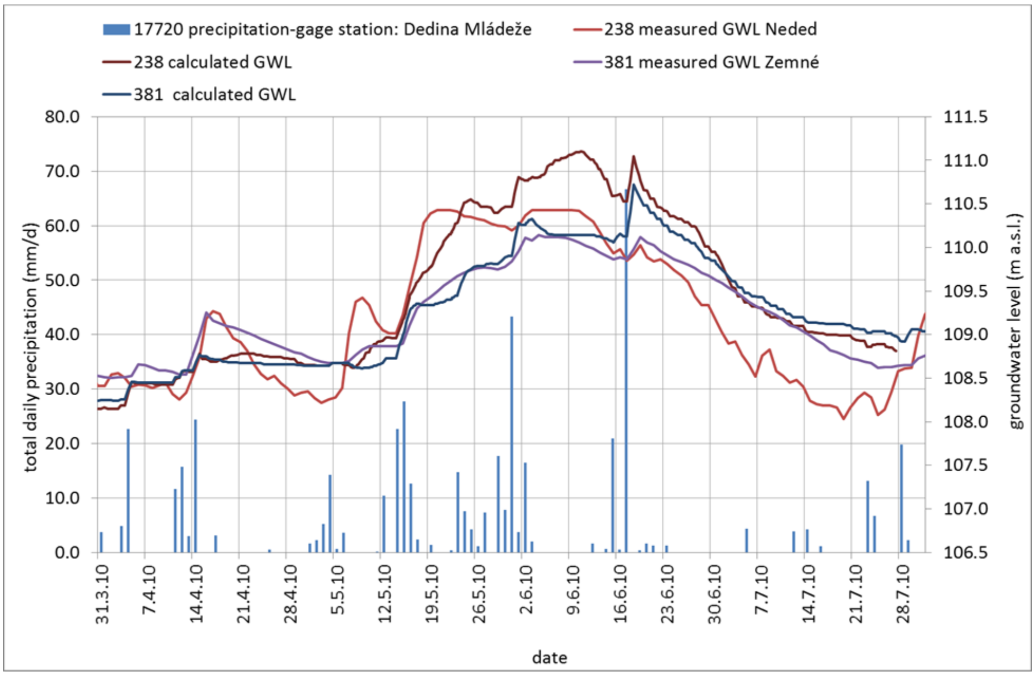

Fig. 13. Groundwater levels (calculated and measured) in two monitoring boreholes.

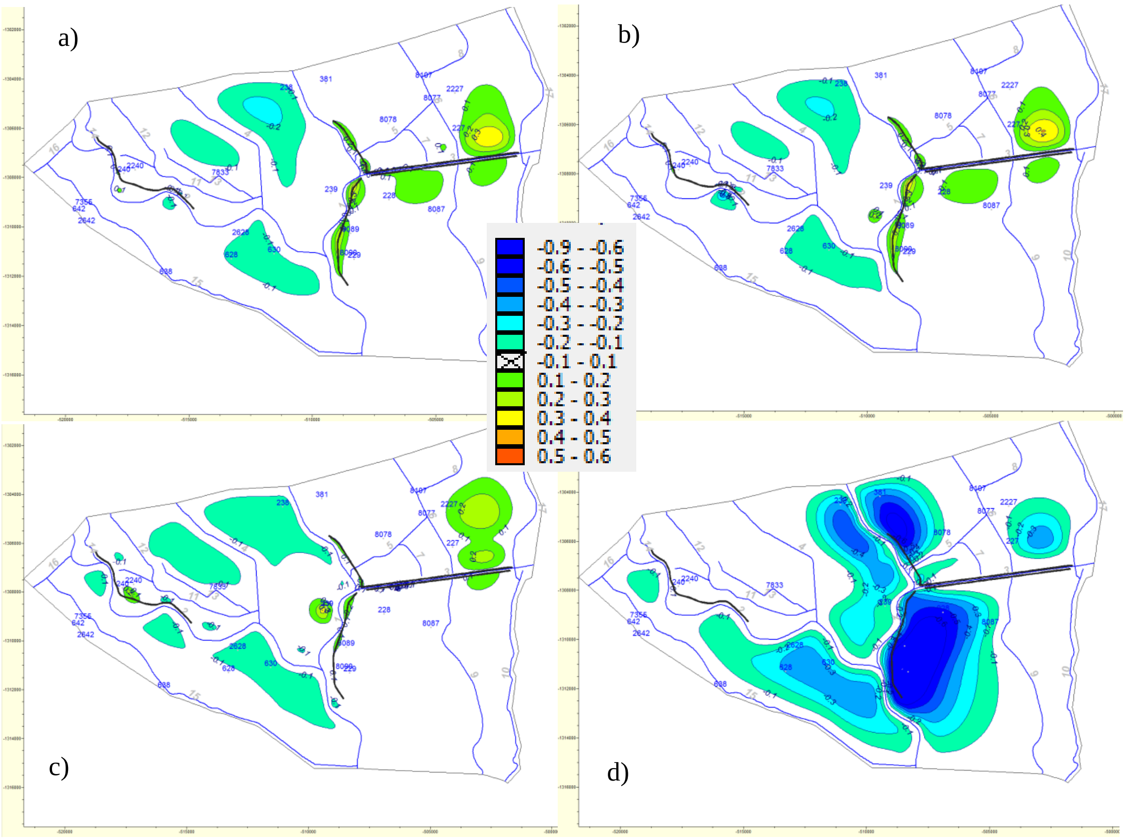

Fig. 14. Prognosis of the difference in piezometric heads after and before the realization of CWs [m] – a) 50th, b) 51st, c) 65th day and d) 112th day of the simulation.

Conclusion

There were defects repeatedly seen on the downstream sides of the flood protective dykes along rivers Váh, Small Danube and the deviation of river Nitra. These defects can significantly reduce the stability of the dykes, which may lead to endangerment of the adjacent territory with residential houses, infrastructure and agricultural land, or to the contamination of water and soil as a result of flooding a nearby sewage treatment plant. Therefore, the additional sealing of dykes using suspended cut-off walls was proposed.

The aim of the paper was the verification of the functionality of the proposed cut-off walls using the method of mathematical modelling. The numerical simulation of the groundwater flow and groundwater level regime at steady state as well as during flood event was created. It includes also the impacts of the suspended cut-off walls on the groundwater flow and level regime in a wider area. The steady-state prediction, created using the long-time mean values of hydrological conditions, shows that the situation after realization of cut-off walls will not change after the realization of such a measure. The primary purpose of the cut-off walls is the elimination of the risk of suffusion and minimization of the risk of breakage of the cover layers caused by buoyancy. These protective measures extend the leakage path and thereby greatly reduce the hydraulic gradient and, accordingly, leaching quantities.

On the other hand, the piezometric head in the wider area of interest may slightly change during extreme hydrological conditions – in certain parts it may drop by max. 0.6 m and rise by max. 0.4 m.

Acknowledgements

This work was supported by the Slovak Research and Development Agency under Contract No. APVV-15-0489, APVV-16-0278 and Research Grant Agency VEGA 1/0800/17.

References

Anderson, M. P., Woessner, W. W. (2002): Applied Groundwater Modeling. Simulation of Flow and Advective Transport, First Edition, Academic Press, California.

Dušek, P., Velísková, Y. (2017): Interaction Between Groundwater and Surface Water of Channel Network at Žitný Ostrov Area. In: Negm A., Zeleňáková M. (eds) Water Resources in Slovakia: Part I. The Handbook of Environmental Chemistry, vol 69. Springer, Cham.

Dulovičová, R., Velísková, Y, Koczka Bara, M., Schűgerl, R. (2013): Impact of silts distribution along the Chotárny channel on seepage water amounts. Acta Hydrologica Slovaca 14(1):126–134. (in Slovak).

Gramblíčková, D., Bednárová, E., Škvarka, J., Chrobák, V. (2017): Design, assessment and remediation of the left flood protectoin dike of the river Váh in km 23,040 – 27,075, Acta Hydrologica Slovaca, 18(1) 31–38.
Hnidiak, L., Rabatin, T., Farkaš, S. (2016): Project documenttation Komoča – the Nitra River, additional sealing of the right-hand side rkm 0.000-6.260 and left-hand side rkm 0.490-6.490 of the deviation of the Nitra River. Building intention (in Slovak), Enviroline Ltd., Košice.
Chládek, P., Kováčiková, K. (2016): Flood protective cut-off wall of the left-hand side dyke on the Váh River in rkm 27.450-29.860. Building intention of public works (in Slovak), Cabex Ltd., Bratislava.
Julínek, T., Duchan, D., Říha, J. (2020): Mapping of uplift hazard due to rising groundwater level during floods, Journal of Flood Risk Management, Special Issue.
Krempa, P., Halamová, D., Kvetko, S. (2016): Flood protecttive cut-off wall of the left-hand side dyke on the Little Danube River in rkm 5.600-11.000 (in Slovak), Hydrotrajekt Ltd., Banská Bystrica.
mapa.sk accessible to: https://mapa.zoznam.sk/?search=mapy +atlas+sk
Miklos, L. et al. (2002): Atlas of the country of the Slovak republic, Ministry of Environment of the Slovak Republic, Slovak Environmental Agency Banska Bystrica; Bratislava, Banska Bystrica (Slovakia), 344 p. (in Slovak).
Pristaš, J., Horniš, J., Halouzka, R., Maglay, J., Konečný, V., Lexa, J., Nagy, A., Vass, D., Vozár, J. (1992): Povrchová geologická mapa podunajska M 1:50 000 (DANREG), Manuskript – archív ŠGÚDŠ In: Káčer, Š., Antalík, M., Lexa, J., Zvara, I., Fritzman, R., Vlachovič, J., Bystrická, G., Brodianska, M., Potfaj, M., Madarás, J., Nagy, A., Maglay, J., Ivanička, J., Gross, P., Rakús, M., Vozárová, A., Buček. S., Boorová, D., Šimon, L., Mello, J., Polák, M., Bezák, V., Hók, J., Teťák, F., Konečný, V., Kučera, M., Žec, B., Elečko, M., Hraško, Ľ., Kováčik, M., Pristaš, J. (2005): Digitálna geologická mapa Slovenskej republiky v M 1:50 000 a 1:500 000, SGÚDŠ, dostupné na http://apl.geology.sk/gm50js/
Šoltész, A., Baroková, D., Červeňanská, M., Šille, A. (2017): Assessment of the impact of the proposed cut-off walls on the groundwater regime in the adjacent area of the protective dikes of the Little Danube, Váh and Nitra relocation (in Slovak: Posúdenie vplyvu navrhovaných podzemných tesniacich stien na režim podzemných vôd v priľahlej oblasti ochranných hrádzí tokov Malý Dunaj, Váh a preložka Nitry), Final research report, Slovak University of Technology in Bratislava, Bratislava, 48 p.
Švasta, J., Malík, P. (2006): Spatial distribution of mean effective precipitation over Slovakia (in Slovak), Podzemná voda, vol. XII/, No. 1, 65–77.
Velísková, Y., Dulovičová, R., Schügerl, R. (2015): Assessment of hydraulic conductivity values of bed sediments along Komárňanský channel, International Multidisciplinary Scientific GeoConference Surveying Geology and Mining Ecology Management, SGEM.
Velstra, J., Kleinendorst, T., Niemeijer, A., Zaadnoordijk, W. J., van der Wal, B., Swierstra, W. (2014): Integrated Model Environment Water Management TRIWACO 4.0., Report Royal Haskoning DHV, Netherlands, www. triwaco.nl
Water management map (2003): 1:50000: Map sheets 45–32, 45-41,45-23, 45-14, 3. waiver, Geodetical and cartografic institute, Bratislava.
[SHMI] Source data from the Slovak Hydrometeorological Institute in electronic form.
[SWME] Source data from the Slovak Water Management Enterprise, s. e. in electronic form.

Assoc. prof. Ing. Dana Baroková, PhD. (*corresponding author, e-mail: dana.barokova@stuba.sk)
Ing. Michaela Červeňanská
prof. Ing. Andrej Šoltész, PhD.
Department of Hydraulic Engineering
Faculty of Civil Engineering
Slovak University of Technology in Bratislava
Radlinského 11
810 05 Bratislava
Slovak Republic

DOI: 10.31577/ahs-2020-0021.01.0015

ACTA HYDROLOGICA SLOVACA

Volume 21, No. 1, 2020, 123 – 129

EFFECT OF AQUATIC VEGETATION ON MANNING´S ROUGHNESS COEFFICIENT VALUE – CASE STUDY AT THE ŠÚRSKY CHANNEL

Radoslav Schügerl*, Yvetta Velísková, Valentin Sočuvka, Renáta Dulovičová

Vegetation growing in the water along watercourses has been the subject of several studies since it was recognized that it could have a significant impact on the water flowIncreased bed roughness caused by aquatic vegetation is a very often phenomenon in case of flow in natural open channel during the growing season. Vegetation impedes the water flow and may increase flood risks. Thus, determining the effect of aquatic vegetation on flow conditions in streams is very important for estimation of hydrodynamics in natural streams. Occurance of aquatic vegetation is more often in case of lowland streams. The purpose of this paper is to investigate and determine how aquatic vegetation influences flow resistance, water depth and discharge in the Šúrsky channel at the Podunajská lowland area. Measurements performed during three various times of year 2019 at this stream were used for an evaluation of vegetation impact on flow conditions in this stream. The Manning´s coefficient was used as one way of quantifying this impact. The results show variation of this parameter during the winter and summer season.

KEY WORDS: aquatic vegetation, water-level, discharge, Manning´s roughness coefficient

Introduction

Vegetation affects flow processes and by this way it affects hydraulics of streams and river management. Advances in understanding the behaviour of flow over vegetation allow us to improve both the knowledge of flow-velocity profiles and flow resistance (James et al., 2004; Cheng, 2011; Nehal et al., 2013; Nikora et al., 2008).

In natural streams conditions, the complexity is increased due to many factors: heterogeneity of plant species, difficulty in parameterization of plant characteristics, plant distribution within sections, three-dimensional effects due to side walls, seasonal variations etc. In natural environments, studies of the effect of vegetation have mainly focused on the influence on resistance (Green, 2005; 2006), which can be related to the blockage factor defined as the ratio of total frontal area of a vegetation to total area in the cross section profile.

Artificial water conveyance systems may be considered as intermediate media between laboratory flumes and natural streams as they generally have a regular shape (similar to laboratory flumes), but also present some of the complexity of natural stream, with the presence of natural and non-uniform vegetation. This vegetation may be composed of macrophytes, but smaller-size colonies present in open-channels, such as algal biofilms, may also affect velocity profiles.

For correct design or computation of discharge and water level in an open channel, it is necessary to evaluate the channel resistance to flow, which is typically represented by a roughness parameter, such as Manning's *n* (Velísková et al., 2017). Its determination is not easy for natural streams, because the characteristics of channels and the factors that affect channel capacity can vary greatly; furthermore, the combinations of these factors are numerous. Therefore, the selection of roughness for natural and constructed channels is often based on field judgment and personal skill, which are acquired mainly through experience. Determination of the roughness coefficient *n*, according to a seasonal variation, is an important tool in hydraulic modelling (De Doncker et al. 2009; Korichi and Hazzab 2012).

The aim of this contribution is to demonstrate, on the basis of results from experimental field measurements along the Šúrsky channel (Slovakia), how overgrowthing of the stream by aquatic vegetation affects the flow conditions and capacity of the stream.

Theoretical background

Resistance accounts for the (boundary) turbulence caused by surface properties, geometrical boundaries, obstructions and other factors causing energy losses. Therefore, a resistance coefficient reflects the dynamic behaviour in terms of momentum or energy losses in resisting the flow of the water.

Roughness reflects the influence of the surface on the momentum and energy dissipation in resisting the flow of the water. Therefore, with a roughness factor the actual or effective unevenness of the boundary surface is meant.

We know several ways how to describe the resistance of vegetation - ranging from simple roughness descriptions to descriptions that take into account various vegetation characteristics. In addition we know new approaches for describing the resistance of vegetation, mainly for flexible submerged vegetation (Kutija and Hong, 1996; Stone and Shen, 2002; Wilson, 2007).

In general, hydraulic models for open channel flow are based on the Saint-Venant equations. These equations (continuity equation and momentum equation) are the one dimensional simplification of the Navier Stokes equations, which describe fluid flow in three dimensions. In simple general form, the discharge in a stream cross section is given as discharge cross-sectional area multiplied by mean flow velocity.

Relationships for determination of mean flow velocity in natural open channels can be found in literature as:

Chézy´s equation: $$v = C\sqrt{Ri_o} \quad (1)$$

Darcy-Weisbach´s equation: $$v = \sqrt{\frac{8g}{f}}\sqrt{Ri_o} \quad (2)$$

Manning´s equation: $$v = \frac{1}{n}R^{2/3}\, i_o^{1/2} \quad (3)$$

or other ones, where

v – mean flow velocity [m s^{-1}],
R – hydraulic radius [m],
i_o – water level slope,
C – Chézy´s coefficient [m$^{1/2}$ s^{-1}], $C=(1/n).R^y$,
n – Manning´s roughness coefficient [xm$^{-1/3}$ s],
f – Darsy-Weisbach´s friction factor,
g – gravity acceleration [m s^{-2}].

Manning's equation is the limit form of the Chézy´s formula and it is the most widely used equation among these. Although it expresses the resistance at the reach scale and reflects only the influence of the boundary shear on flow depth and averaged velocity, Manning's coefficient n is often used as a summarizing parameter accounting for all the various influences in a river reach. Theoretical calculation of the Manning coefficient n is difficult. It is commonly estimated through experience from simple verbal or photograph descriptions of channels and their table values. In case of natural channel bed with various roughness parts (sand, gravel, grass, brushwood, etc.) in a cross-section profile, there is used following the relation:

$$\bar{n} = \frac{\sum_{i=1}^{k}(n_i P_i)}{P} \quad (4)$$

where

P – wetted perimeter [m].

It might also be determined by empirical formula, which spitted channel resistance into several parts, including the bed material, presence of vegetation in the river, meandering, etc.:

$$n = (n_0 + n_1 + n_2 + n_3 + n_4).m \quad (5)$$

where

n_0 – basic value, for a straight, uniform channel,
n_1 – irregularities of the bottom,
n_2 – variations in the geometry of the channel,
n_3 – obstacles,
n_4 – vegetation,
m – correction factor for meandering.

The determination of spatial parameters of a stream, such as the discharge area, stream bed slope, wetted perimeter and hydraulic radius, is quite easy, but the stream bed roughness assessment could be a problem. During a year, the various degrees of in-channel sprouting could be found and usually the different kinds of water plants grow up in stream cross-section profiles. The extension of aquatic vegetation depends mainly on flow velocities, longitudinal slope, but also on the water temperature and nutrient content. The height of the vegetation with respect to the water level is important in describing vegetation resistance, because it influences the flow velocity profile (Velísková et al., 2017).

There are many vegetation characteristics that affect the hydraulic resistance in overgrown channels. The first important vegetation characteristic that affects the flow resistance is the geometry of the vegetation itself, concerning the taxonomy of the species as the branching index, the density of the shoots, the maximum level of growth that each species can reach in a cross section and the seasonal presence of the plant. In addition to this, there is a hydraulic parameter which considers the characteristic dimension of the vegetation in relation to flow conditions.

So, it is clear that determination of correct value of the Manning´s roughness coefficient in natural open channel is not easy. Determination of n value is very complex task, but by calculation from the discharge and the water levels along the river reach with steady uniform flow condition and with applying of the Saint-Venant equations, it is possible to calibrate the roughness of the channel (expressed by the roughness coefficient or friction factor) by comparing with field measured data:

$$n = \frac{A.R^{2/3}\, i_0^{0,5}}{Q} \quad (6)$$

where

A – discharge area [m^2],
Q – discharge [m^3 s^{-1}].

Material and methods

Field measurements, related to the investigation of aquatic vegetation impact on flow in a lowland stream, were performed along the Šúrsky channel at the Podunajská lowland. The Šúrsky channel flows through the territory of the Pezinok and the Senec town district. It is a left tributary of the Malý Dunaj river and it is 16.95 km long.

Four observing cross-section profiles were selected along the Šúrsky channel, their locations are shown in Fig. 1. Measurements were carried out in two sections: the first section with distance 3620 meters (from bridge profile to Račiansky stream profile / upstream) and the second section with distance 2150 meters (from Račiansky stream profile / downstream to speedway profile). Cross-section profiles parameters – channel width, distribution of water depth along the width of a cross-section profile (by levelling device), discharges and velocity distribution along the width of cross-section profile (by ADV – Acoustic Doppler Velocimeter device Flow Tracker) were measured. Measurements were performed in the channel segments with steady uniform flow conditions. Field measurements were done in February and during summer time (June and August), thereby we try to detect if any changes occur in these different periods of the growing season.

Results and discussion

As it was mentioned, there exists a number of ways how to evaluate the influence of aquatic vegetation on flow in lowland streams. Quantification of the impact of aquatic vegetation through the calibration of roughness coefficient on base of field measurement data is one of the practically suitable methods. This roughness coefficient represents an actual parameter influencing discharge capacity of streams. Ranges of measured data from each measurement campaign are summarized in Table 1 (for section 1 from the bridge profile to the Račiansky stream profile/upstream) and Table 2 (for section 2 from the Račiansky stream profile/downstream to the speedway profile). Tables contain data on the mean flow velocity (v), discharge area (A), wetted perimeter (P), hydraulic radius (R), water level change (Δh), water level slope (i_o) and determined Manning´s roughness coefficient (n).

The roughness coefficient value in the sprouted stream bed is changing during the growing season depending on aquatic vegetation growth. In consequence of raised roughness, the velocity profile is changing and thereafter the discharge capacities are also changed. For example, in the season of observation, the differences of n values along the channel varied in the most extensive range (0.051–0.203) for the first section, for the second section the differences of n values along the channel varied in the most extensive range (0.055–0.300).

Aquatic vegetation recording by means of camera during the year 2019 (February vs. June vs. August) are shown in Fig. 4, 5 and 6 (the bridge profile and the Račiansky stream profile/downstream). The mean flow velocity values decrease with increasing roughness coefficient and there are lower during the summer season than during winter for the same discharge sub-range.

By Chow (1959), the values of the Manning´s roughness coefficient for overgrown - not maintained channel with dense aquatic vegetation higher than flow depth is from 0.050 to 0.120 or with shrubby vegetation is from 0.080 to 0.140. In our case the calculated values of n are higher, mainly during the summer season.

Changes of discharge and water-level during the experimental time in 2019 for section 1 (from the bridge profile to the Račiansky stream profile / upstream) and section 2 (from the Račiansky stream profile / downstream to the speedway profile) are shown in Fig. 2 and Fig. 3 and Table 3. The results show, that when there is recorded the biggest discharge value, the water-level value is the smallest one (for all measured cross-section profile). On the other side, when the discharge value is the smallest one, water-level value is not the biggest.

Fig. 4, Fig. 5 and Fig. 6 illustrate aquatic vegetation growing situation in the Šúrsky channel during the experiments time in 2019 (for the bridge profile and the Račiansky stream profile / upstream).

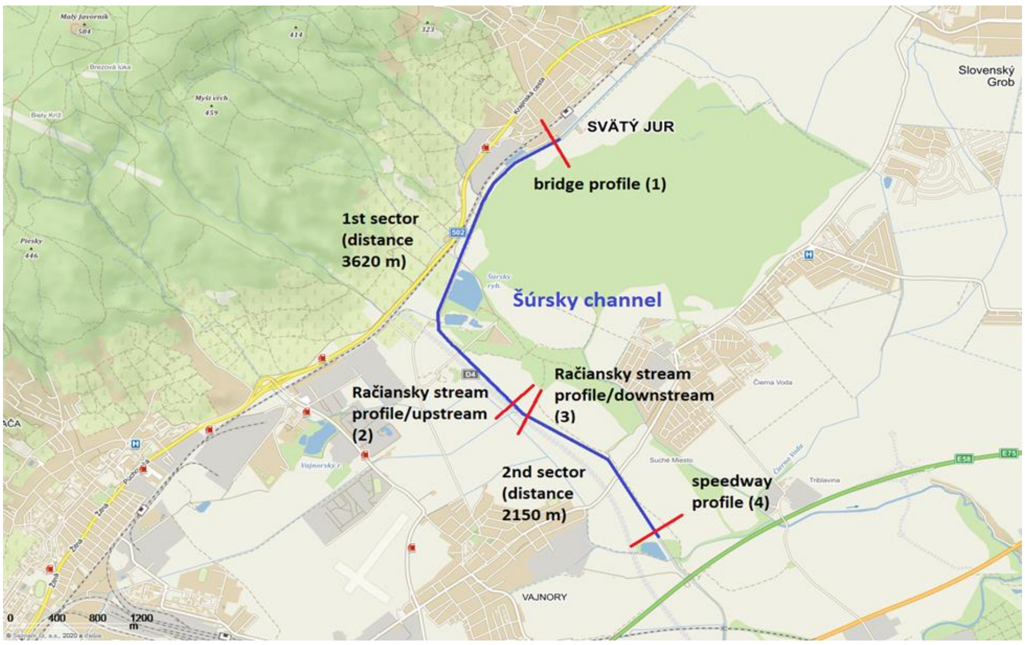

Fig. 1. Location of observing cross-section profiles along the Šúrsky channel.

Table 1. Summary of measured and calculated data of the first experiment section (from the bridge profile to the Račiansky stream profile/upstream)

Date of measur.	bridge profile				Račiansky stream profile (upstream)				Δh [m]	i_o	n
	v[m s^{-1}]	A[m^2]	P [m]	R [m]	v[m s^{-1}]	A[m^2]	P [m]	R [m]			
02/2019	0.317	0.608	4.75	0.129	0.212	1.805	5.15	0.350	1.749	0.000483	0.051
06/2019	0.198	0.432	4.50	0.096	0.050	1.955	5.60	0.349	1.520	0.000419	0.203
08/2019	0.105	0.58	4.40	0.131	0.064	2.335	5.75	0.355	1.594	0.000441	0.179

Table 2. Summary of measured and calculated data of the second experiment section [from the Račiansky stream profile/downstream to the speedway profile)

Date of measur.	Račiansky stream profile (downstream)				speedway profile				Δh [m]	i_o	n
	v[m s^{-1}]	A[m^2]	P [m]	R [m]	v[m s^{-1}]	A[m^2]	P [m]	R [m]			
02/2019	0.208	1.563	5.15	0.304	0.136	2.715	9.20	0.295	0.633	0.000294	0.055
06/2019	0.037	2.578	5.90	0.436	0.029	3.127	9.85	0.317	0.707	0.000328	0.300
08/2019	0.054	1.618	6.55	0.247	0.046	3.042	10.10	0.301	0.770	0.000351	0.223

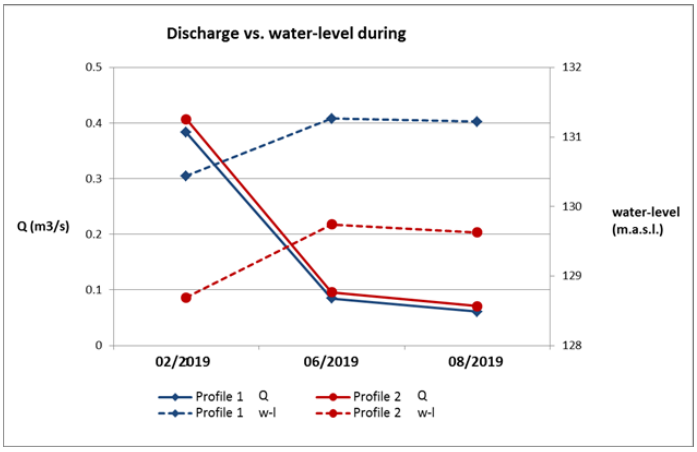

Fig. 2. Changes of discharge and water-level in the Šúrsky channel during the experiment time – section 1.

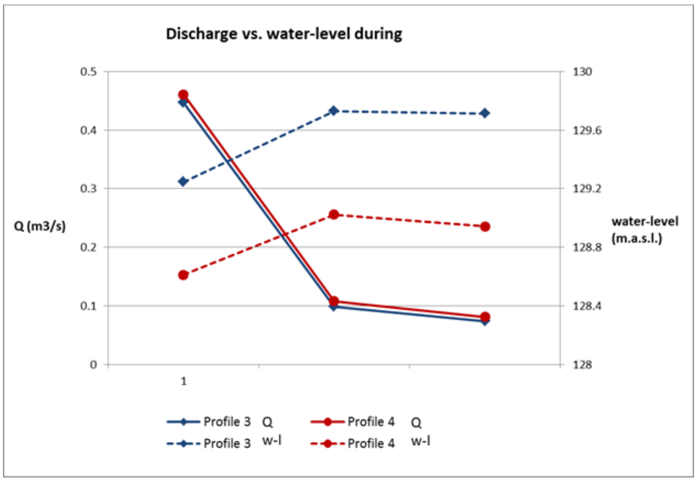

Fig. 3. Changes of discharge and water-level in the Šúrsky channel during the experiment time – section 2.

Table 3. **Summary of measured data on the discharge and water-level in four cross-section profiles** (profile 1 – the bridge profile, profile 2 – the Račiansky stream profile / upstream, profile 3 – the Račiansky stream profile / downstream, profile 4 – the speedway profile)

Date of measur.	profile 1		profile 2		profile 3		profile 4	
	Q [m^3 s^{-1}]	w-l [m a.s.l.]	Q [m^3 s^{-1}]	w-l [m a.s.l.]	Q [m^3 s^{-1}]	w-l [m a.s.l.]	Q [m^3 s^{-1}]	w-l [m a.s.l.]
02/2019	0.383	130.439	0.407	128.690	0.477	129.246	0.461	128.613
06/2019	0.085	131.265	0.096	129.745	0.099	129.730	0.108	129.023
08/2019	0.061	131.222	0.071	129.628	0.072	129.713	0.081	128.943

Fig. 4. Aquatic vegetation in the Šúrsky channel during February 2019 – profile (1) and profile (3).

Fig. 5. Aquatic vegetation in the Šúrsky channel during February 2019 – profile (1) and profile (3).

Fig. 6. Aquatic vegetation in the Šúrsky channel during August 2019 – profile (1) and profile (3).

Conclusions

Vegetation in natural streams influences the flow field and related characteristics and phenomena, such as discharge capacity, velocity profile, roughness, but also erosion and sedimentation, pollutant transport and water biota. The aim of this paper was to investigate and determine the impact rate of aquatic vegetation on flow conditions, based on field measurements along the Šúrsky channel during the year 2019. The roughness coefficient *n* was used as a way of quantifying this impact.

An analysis of the obtained data revealed that the roughness coefficient value changes mainly during the growing season. Results of measurements showed and confirmed that consequence of vegetation growth in the channel is the change of velocity profile and water level in comparison with discharge amount. The analyses of measured data showed and confirmed the complexity of the impact of in-channel vegetation on stream flow and despite obtaining important database of roughness coefficient value for the Šúrsky channel the necessity to continue investigation of this problem.

Acknowledgement

This paper was prepared with the support of the project No. VEGA 2/0025/19.

References

Cheng, N. (2011): Hydraulic radius for evaluating resistance induced by simulated emergent vegetation in open-channel flows. Journal of Hydraulic Engineering, vol. 137, 2011, 995–1004.

Chow, V. T. (1959): Open channel hydraulics. McGraw-Hill, 1959.

De Doncker, L., Verhoeven, R., Bal, K., Meire, P., Quintelier, J. (2009): Determination of the Manning roughness coefficient influenced by vegetation in the river Aa and Biebrza river. Environmental Fluid Mechanics, vol. 9, no. 5, 2009, 549–567. https://doi.org/10.1007/s10652-009-9149-0

Green, J. C. (2005): Modelling flow resistance in vegetated streams: review and development of new theory. Hydrological processes, vol. 19, no. 6, 2005, 1245–1259.

Green, J. C. (2006). "Effect of macrophyte spatial variability on channel resis tance." Advances in Water Resources, 29(3), 26–438.

James, C. S., Birkhead, A. L., Jordanova, A. A., O'Sullivan, J. J. (2004): Flow resistance of emergent vegetation. Journal of Hydraulic Research, vol. 42, no. 4, 2004, 390–398.

Korichi, K., Hazzab, A. (2012). Hydrodynamic investigation and numerical simulation of intermittent and ephemeral flows in semi-arid regions: Wadi Mekerra, Algeria. Journal of Hydrology and Hydromechanics, vol. 60, no. 2, 2012, 125–142.

Kutija, V., Hong, H. T. M. (1996): A numerical model for assessing the additional resistance to flow introduced by flexible vegetation. Journal of Hydraulic Research, vol. 34, no. 1, 1996, 99–114.

Nehal, L., Hamimed, A., Khaldi, A. (2013): Experimental study on the impact of emergent vegetation on flow, p. 6. In: Proc. 7th International Water Technology Conference, IWTC17, Istanbul, (http://iwtc.info/wp-content/uploads/2013/11/94.pdf).

Nikora, V., Larned, S., Nikora, N., Debnath, K., Cooper, G., Reid, M. (2008): Hydraulic resistance due to aquatic vegetation in small streams: Field study. Journal of Hydraulic Engineering, vol. 134, no. 9, 2008, 1326–1332. ISSN 0733-9429.

Stone, M. B., Shen, H. T., (2002): Hydraulic resistance of flow in channels with cylindrical roughness. Journal of

Hydraulic Engineering, vol. 128, no. 5, 2002, 500–506.

Velísková, Y., Dulovičová, R., Schügerl, R. (2017): Impact of vegetation on flow in a lowland stream during the growing season. Biologia, vol. 72, no. 8, 2017, 840–846. DOI: 10.1515/biolog-2017-0095

Wilson, C. A., Hoyt, J., Schnauder, I. (2007): Flow resistance models for flexible submerged vegetation. Journal of Hydrology, vol. 134, no. 7, 2007, 213–222.

Mgr. Radoslav Schügerl, PhD. (*corresponding author, e-mail: schugerl@uh.savba.sk)
Ing. Yvetta Velísková, PhD.
Ing. Valentin Sočuvka, PhD.
Ing. Renáta Dulovičová
Institute of Hydrology, SAS
Dúbravská cesta 9
841 04 Bratislava
Slovak Republic